Polymeric delivery of miRNA therapeutics

By Annette Kargaard

Dissertation presented in partial fulfilment of the requirements for the degree of PhD (Polymer Science)

Promoters: Prof Dr Bert Klumperman & Prof Joost Sluijter

University of Stellenbosch

Department of Chemistry and Polymer Science

March 2018

Declaration

By submitting this dissertation electronically, I declare the entirety of the work contained therein is my own, original work, that I am the owner of the copyright thereof (unless to the extent explicitly otherwise stated) and that I have not previously in its entirety or in part submitted it for obtaining any qualification.

Annette Kargaard December 2017

For my parents, Jens and Jill.

Table of Contents

Table of Figures

Table of Schemes

Table of Tables

List of Abbreviations

PEG	poly(ethylene glycol)
PVP	poly(*N*-vinyl pyrrolidone)
pDMAEMA	poly(dimethylamino)ethyl methacrylate
pDMAEA	poly(dimethylamine)ethyl acrylate
SMA	poly(styrene-*co*-maleic anhydride)
PMMA	poly(methyl methacrylate)
PHPMA	poly(hydroxypropyl methacrylate)
BMA	butyl methacrylate
MMA	methyl methacrylate
*n*BA	*n*-butyl acrylate
PAA	poly(acrylic acid)
PLGA	poly(lactic acid-*co*-glycolic acid)
PTEA	poly(triethyl-(4-vinylbenzyl)ammonium chloride
PTBA	poly(tributyl-(4-vinylbenzyl)phosphonium chloride
PTEP	poly(tributyl-(4-vinylbenzyl)ammonium chloride
TBP	4-vinylbenzyltributylphosphonium chloride
MPC	2-(methacryloxy)ethyl phosphorylcholine
OEGMA	oligo(ethylene glycol)$_9$ methyl ether methacrylate
PEGMA	Poly(ethylene glycol) methyl ether methacrylate
TEGMA	triethylene glycol methacrylate
TTMA	2,4,6-trimethoxybenzylidene-1,1,1-tris(hydroxymethyl) ethane methacrylate
PVIM	poly(1-vinyl-imidazole)
PEI	poly(ethylenimine)
RDRP	reverse deactivation radical polymerization

RAFT	reversible addition-fragmentation chain transfer
ATRP	atom-transfer radical polymerization
M_n	number average molecular weight
M_W	weight average molecular weight
CTA	chain transfer agent
Đ	dispersity
FT-IR	Fourier transform infrared
^{1}H NMR	Proton nuclear magnetic resonance
^{13}C NMR	Carbon-13 nuclear magnetic resonance
SEC	size exclusion chromatography
ppm	parts-per-million
NTA	Nanoparticle tracking analysis
ζ-potential	zeta potential
ACVA	4,4'-azobis(4-cyanovaleric acid)
AIBN	2,2'-azobis(isobutyronitrile)
EDC	1-ethyl-3-(3-dimethylaminopropyl)carbodiimide
DMSO	dimethyl sulfoxide
DCC	*N,N'*-dicyclohexylcarbodiimide
DMAPA	3-(*N*,*N*-dimethylamino)propyl-1-amine
EtOAc	ethyl acetate
RNAi	RNA interference
miRNA	microRNA
anti-miRNA	anti-microRNA
mRNA	messenger RNA
siRNA	short interfering RNA
shRNA	short hairpin RNA

AONs	antisense oligonucleotides
oligo-DNA	oligonucleotide DNA
N/P ratio	Nitrogen-to-Phosphorus charge ratio
FDA	Food and drug administration
RISC	RNA-induced silencing complex
CardioTL	CSTSMLKAC peptide sequence
RGD	ACDCRGDCFGG peptide sequence
QKI	Quaking
RES	reticulo-endothelial system
FBS	fetal bovine serum
CMPCs	cardiomyocyte progenitor cells
HMECs	human microvascular endothelial cells
FaDu Fluc	human epithelial firefly luciferase cells
EGM-2	endothelial cell growth medium-2
NEAA	non-essential amino acids
DMEM	Dulbecco's modified Eagle's medium (DMEM)
P/S	penicillin streptomycin solution
M199	Medium 199
MEK	Methyl ethyl ketone
SDS	Sodium dodecyl sulfate

Abstract

RNA interference therapeutics are regarded as having a crucial role in gene regulation and play an integral role in diseases, *e.g.* cancer, neurological diseases and heart disease. However, the lack of success in using non-coding RNAs as therapeutics lies in the absence of efficient, safe and reliable tools for targeted delivery. Although polymeric vectors have yielded some success in gene delivery, there are still major downfalls related to toxicity, endosomal escape and cytoplasmic delivery.

Herein, two classes of novel delivery vehicles have been synthesized and their gene regulation efficiency tested, in an effort to address the difficulties in endosomal escape and cytoplasmic release. The first type of system is a diblock-copolymer conjugated via a pH-labile linker to enhance endosomal escape. The first block is poly(*N*-vinylpyrrolidone) (PVP) which was synthesized via RAFT–mediated polymerization. The second block is composed of either hydrolysable poly(2-(*N*,*N*-dimethylamino)ethyl acrylate-*co*-butylmethacrylate) (p(DMAEA-*co*-BMA)) or non-hydrolysable poly(2-(*N*,*N*-dimethylamino)ethyl methacrylate-*co*-butylmethacrylate) (p(DMAEMA-*co*-BMA)), which are both capable of RNA complexation. The hydrolysable properties of the p(DMAEA-*co*-BMA) causes decationization, releasing the RNA within the cytoplasm. Neither of the diblock-copolymer conjugates caused significant cytotoxicity. Although gene regulation for both systems was greater than or equivalent to poly(ethylamine), the gold standard in gene regulation, they do not effectively escape the endosome. Interestingly, p(DMAEMA-*co*-BMA)-*b*-PVP is more efficient at regulating gene expression than p(DMAEA-*co*-BMA)-*b*-PVP.

Ring opened and closed DMAPA-modified poly(styrene-*co*-maleic anhydride) derivatives were synthesized as the second class of zwitterionic polymer vectors. Although the ring-closed derivative was more efficient in condensing the RNAs, the ring-open analogue is more effective at delivering gene regulation. Both systems cause no cytotoxicity, erythrocyte aggregation or hemolysis. The ring-opened analogue, in particular, provides a platform from which potentially effective and safe gene delivery vectors can be designed.

Opsomming

RNA-obtrusieterapeutiesemiddels speel 'n belangrike rol in geenregulering asook in behandeling van siektes soos bv. kanker, neurologiesesiektes en hartsiektes. Die gebrek aan sukses in die gebruik van nie-koderende-RNAs as terapeutiese middels lê egter in die afwesigheid van doeltreffende, veilige en betroubare sisteme vir geteikende-aflewering. Alhoewel polimeriesevektore 'n mate van sukses behaal het in geenaflewering, is daar steeds groot tekortkominge wat verband hou met toksisiteit, endosomale ontsnappings en sitoplasmiese aflewering.

Hierin is twee klasse nuwe afleweringsvoertuie gesintetiseer en hulle geenregulasie doeltreffend getoets in 'n poging om die probleme in endosomale ontsnapping en sitoplasmiese vrystelling aan te spreek. Die eerste tipe stelsel is die van 'n diblok-kopolimeer wat via 'n pH-sensitiewekoppelaar verbind is om endosomale ontsnapping te verbeter. Die eerste blok bestaan uit poli(*N*-vinielpyrolidoon) (PVP) wat deur RAFT-gemedieerde polimerisasie gesintetiseer is. Die tweede blok is saamgestel uit óf hidroliseerbare poli(2-(*N*, *N*-dimetielamien)etielakrilaat-ko-butielmetakrilaat) (p(DMAEA-*ko*-BMA)) óf nie-hidroliseerbare poli(2-(*N,N*-dimetielamien)etielmetakrilaat-*ko*-butielmetakrilaat p(DMAEMA-*ko*-BMA)), wat beide in staat is tot RNA-kompleksasie. Die hidroliseerbare eienskappe van die p(DMAEA-*ko*-BMA) veroorsaak dekationisasie wat die RNA binne die sitoplasma vrystel. Nie een van die diblok-kopolimeergekonjugeerde sisteme het beduidende sitotoksisiteit veroorsaak nie. Alhoewel geenregulering vir beide stelsels groter is as of ekwivalent is aan poli(etielamien) (die goudstandaard in geenregulering) ontsnap hulle nie die endosoom effektief genoeg nie. Interessant genoeg is dat p(DMAEMA-*ko*-BMA)-b-PVP meer doeltreffend is om geenuitdrukking te reguleer as p(DMAEA-*ko*-BMA)-b-PVP.

Ring-oop en ringgeslote DMAPA-gemodifiseerde poli(stireen-*ko*-maleïenanhidried) afgeleides is gesintetiseer as die tweede klas van zwitterioniese polimeervektore. Alhoewel die ringgeslote afgeleide meer doeltreffend was om die RNAs te kondenseer, is die ring-oop vorm meer doeltreffend in geenregulering. Beide sisteme veroorsaak geen sitotoksisiteit, eritrosiete-aggregasie of hemolise nie. Die besondere analoog bied 'n platform waarvan potensiële, effektiewe en veilige geenafleweringsvektore ontwerp kan word.

Acknowledgements

I would like to begin by thanking my supervisors Bert Klumperman and Joost Sluijter. Bert, thank you for all that you have done in developing me into the scientist that I am today, and for teaching me to think critically and independently. Thank you for all of the opportunities that you have bestowed upon me, from conferences in South Africa and Australia, to my two research stays in the Netherlands.

Joost, thank you for providing me with the opportunity to come to Utrecht and for making me feel completely part of the group from the first moment. Thank you for your patience in teaching me the world of cells and biology, and for your support in the final stretch of my lab work and writing. I truly loved being at UMC Utrecht.

I would like to thank and acknowledge the researchers and post-doctoral fellows for their contribution to this project and to my development as a scientist. Firstly, thank you Rueben Pfukwa for your help and guidance. Pieter Vader, Zhiyong Lei, Alain van Mil and Saskia Eggers-de Jagger, without the four of you I would have been completely lost. Pieter your combined knowledge of chemistry and biology was indispensable. Thank you for your patience and help.

Thank you to the CAF staff as well as all the technical staff at both SU and UMC Utrecht. A special thank you to Calvin Maart. Thank you for always being willing to help, even out of store hours, and for always being such a happy constant in the Polymer Building. I would also like to warmly acknowledge Elsa Malherbe. You are so selfless. Thank you for always being so helpful and kind.

Thank you to the South African National Research Foundation, Stellenbosch University and UMC Utrecht for funding.

I have been blessed with two wonderful research groups. To the past and current members of the Free Radical Group, thank you for all the chats, coffees, lunches on the wall, laughs, beer and wine outings and friendships. To the Experimental Cardiology Group, thank you all for making me feel so at home in the Netherlands. For always including me and for teaching me all the naughty words in Dutch. Thank you for helping me to find my way around a

biology lab. On this note, a special thank you to Esther for showing me the biology ropes, from electrophoresis to cell culturing.

I would like to thank a few members of FR in particular: Elrika, thank you for being my desk buddy. For our back and forth work discussions, for allowing me to bounce ideas off you and for always being there. Most importantly, thank you for our friendship, our coffees and breakfasts. Thank you Lisa, firstly for your contribution in the PVP work, but most importantly for your ever positive and happy personality; for all your words of encouragements and all the laughs. Nelmarie, thank you for generously sharing your polymers with me, and for always being keen and ready for a beer. Elaine, I am delighted that you joined our group, it wasn't whole until you and Lisa came along. I had so much fun during your visit in Utrecht and am so happy to call you a friend. Nusrat, asanti sana my 'fellow' Kenyan. Your quiet strength is so encouraging. Thank you for being such a supportive friend. And for the ice cream – one must never forget the ice cream. Simba, el captain, it has been so fun watching you develop into the polymer scientist you have become. You are a seriously caring and fun guy, and I'm really grateful for our friendship. Bennie, you have enough energy to kick-start a rocket going to the moon. You lightened up our office with your silliness and genuine cheerfulness. I have never met anyone quite like you, and I am so happy that I did. Andre, thank you for being a really great friend, always there through thick and thin – and for the coffees.

There are also some particular members of Experimental Cardio that need to be mentioned: Robin and Judith, thank you for accepting this stranger into your office with open arms and making it feel like home. Robin, your singing and general tomfoolery, although not conducive of productivity, was super fun and the highlight of every day. Judith, you are amazing. Your supportive, encouraging and fun personality got me through my last stretch of PhD. Thank you for being a really great friend. Sandra, or Crinky, your warmth and slight idiosyncrasies make you who you are. We took to each other like glue, and I am so happy that I met you. Thank you for everything. Thank you to Patricia and Mariann for your friendship, support, wine and coffee. Thank you Mariann for never failing to sneak into the office for a quick laugh or encouraging hug. Patty, you are an absolute jewel and I have no doubt that we will be 80 years old, drinking wine and laughing together.

Thank you to my friends beyond science. Ené, Meagan, Michael, Zee, Marcel, Andy, Jaime, Aziza, Alley, Zaskia, Niels, Carla, Frank, Hein, Lee, Shaz, Jeff and Zanelle, thank you all for your friendships and support. Thank you for celebrating my lab wins and putting up with my sulks and moans when things didn't work. Every single one of you is so special to me, and my life wouldn't be the same without you.

And lastly, I would like to take a moment to acknowledge the most important people in my life, my family. We are quite an odd bunch, but I wouldn't have it any other way. Thank you for your never-ending love and support. Lise, Nina, Kim, Kiki and Martin, thank you for being the best older siblings a kid could ask for. You have all shaped me into who I am, and I love you every single one of you. Nick, Carla and Dave, I am so glad that you joined our crazy family. Thank you for your love and support. Lebohang, thank you for all that you do for me. I can't have done this without your help and endless encouragement. I cannot wait for our next adventure together. Kea leboha! I love you. And last but not least, mom and dad. No words can describe how thankful I am for everything that you have done for me. Your support, encouragement and love have no bounds. Thank you sounds so small and insignificant in return for what you have done, but all the same – thank you.

Chapter 1: Prologue

1.1 Introduction

Within the field of gene therapy, there is a considerable need for the development of non-viral vectors that are able to compete with the efficiency obtained by viral vectors, while maintaining a good toxicity profile and not inducing an immune response within the body. While there have been many reports of possible delivery systems, (1-5) few have made it from the bench to a clinical setting due to toxicity, systemic instability or gene regulation inefficiency. (6) Figure 1.1 depicts the journey of a delivery system from complexation with the nucleotide to gene regulation.

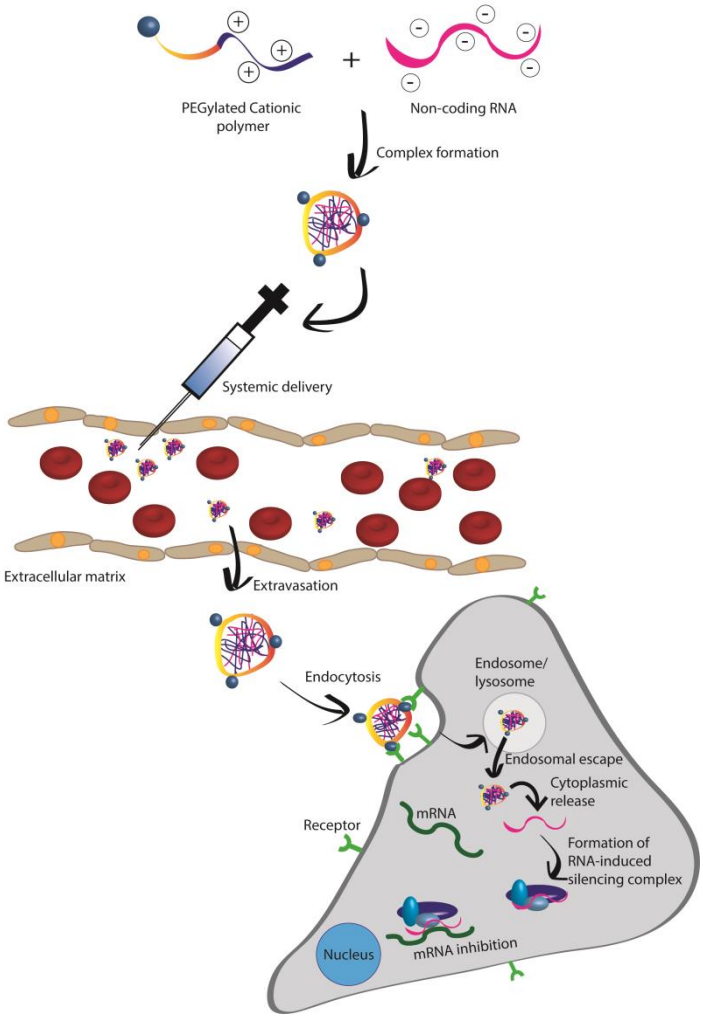

Figure 1.1 The journey of polycationic gene delivery systems, from complexation, to systemic delivery and extravasation, endocytosis and cytoplasmic release to the final steps of the formation of the RNA-induced silencing complex and mRNA inhibition/degradation

There are a number of hurdles a delivery system must conquer on route to delivering its payload. Firstly, the polymeric delivery system must be able to condense the gene therapeutic. Due to the nucleotide's negative charge, this has been achieved in the past through electrostatic interactions with polycations, such as polyethylenimine (PEI). (7, 8) These complexed polymer-nucleotide systems are referred to as polyplexes. During systemic delivery, these polyplexes should not interact aspecifically with blood components, or cause erythrocyte aggregation or hemolysis. The polymer system should increase the half-life of the therapeutic, and allow for passive targeting. Polycations fail in a number of these aspects, (9) but all of these issues have been seen to be improved by the addition of a hydrophilic polymer, such as poly(ethylene glycol) (PEG). (10-13)

After extravasation from the blood vessels/capillaries into the extracellular matrix, the polyplexes must enter the cell through endocytosis via interactions with the cell membrane. (14, 15) This has been reported to be enhanced by the addition of targeting ligands/antibodies, *i.e*. through active targeting. (6, 16) One of the biggest hurdles comes next: the polyplex's endosomal escape. (6, 17) It has been seen that the PEGylation which enhances stability and half-life, decreases endosomal escape. (18, 19) Reports have shown that by incorporating a pH-labile linker between the PEG group and the polycation, it is possible to exploit the decrease in pH within the endosome/lysosome to enhance endosomal escape. (19, 20)

The next obstacle has to do with cytoplasmic release of the RNA therapeutic from the complex. Due to the high complexation efficiency of the polycationic systems, this seems to be the biggest bottleneck for delivery. (21) The use of decationizing systems, *i.e.* systems which lose their cationic charge by breaking the bond between the cationic moiety and the polymer backbone via for example hydrolysis or reduction of disulfides, have been reported to enhance this payload release, which in turn allows for the gene regulation to occur. (22, 23)

In this dissertation, two types of polymeric delivery systems were designed and investigated. The first is a diblock conjugate containing an acid-labile linker to enhance endosomal escape. Two different hydrophobic polymers were employed, a non-hydrolysable p(DMAEMA-*co*-BMA) system and a hydrolysable, de-cationizing p(DMAEA-*co*-

BMA) system. The issues pertaining to the immune response caused by PEG (24) was addressed through the alternative use of poly(*N*-vinylpyrrolidone) (PVP). Targeting ligands were attached to facilitate active targeting. These two systems were analysed *in vitro* and their efficiency was compared.

The second polymeric delivery system investigated was a zwitterionic poly(styrene-*co*-maleic anhydride) derivative, functionalized with 3-(*N*,*N*-dimethylamino)propyl-1-amine. This novel system was assessed for its complexation efficiency and *in vitro* application. It was compared to its ring-closed (maleimide) analogue, which does not possess the zwitterionic properties.

1.2 Objectives

The objectives of this study are summarized as follows:

1. To develop an easy route of obtaining α,ω-heterotelechelic PVP with high chain end fidelity.
2. To design and synthesize a pH-responsive, polymeric gene delivery system by conjugating a hydrophobic, cationic block to hydrophilic PVP functionalized with targeting ligands.
3. To test the physiological application of the abovementioned conjugates in terms of complexation efficiency, cytotoxicity, cellular uptake and gene regulation efficiency.
4. To additionally study the use of a zwitterionic copolymer for use as a gene delivery vector, including synthesis, characterization, gene complexation efficiency, cytotoxicity, cellular uptake and its mechanism, as well as gene regulation efficiency. Futhermore, to compare this zwitterionic copolymer to its ring-closed, cationic analogue.

1.3 Layout of dissertation

The dissertation comprises 7 chapters.

Chapter 1: Prologue

Chapter 1 gives a brief introduction to previous research within the field of gene therapy, as well as an overview of the aims and objectives of the study.

Chapter 2: Literature Review

Chapter 2 presents a comprehensive literature review in which the focus is on previous polymeric systems designed to improve gene delivery. The overview summarizes what has been learned from the original gene delivery systems, such as PEI, and how the field has developed into the use of "smart" polymeric delivery systems.

Chapter 3: Facile routes to telechelic poly(*N*-vinylpyrrolidone) with high chain end fidelity

Chapter 3 reports a route for synthesizing PVP via RAFT-mediated polymerization with chain transfer agents that were previously termed unsuitable. The method offers polymers with high chain end fidelity and α,ω-heterotelechelic functionality.

Chapter 4: Polymer synthesis, characterization and diblock conjugation

Chapter 4 describes the design, polymerization, conjugation and characterization of pH-labile polymeric vectors, with both non-hydrolysable and hydrolysable moieties for RNA complexation.

Chapter 5: Packaging of anti-miR-214 for targeted cardiovascular delivery

Chapter 5 investigates the *in vitro* use of the conjugates synthesized in Chapter 4 as gene delivery vectors. It describes their RNA complexation efficiency, toxicity profiles, cellular uptake and gene regulation efficiency.

Chapter 6: Zwitterionic poly(styrene-*co*-maleic anhydride) derivatives for application in gene therapy

Chapter 6 describes the synthesis of a zwitterionic poly(styrene-*co*-maleic anhydride) derivative for application as a non-viral vector in gene delivery, and compares the system to its cationic analogue. The chapter further addresses the polymer systems' abilities to condense anti-miRNA and their combined cytotoxicity, cellular uptake, uptake mechanism and gene regulation efficiency.

Chapter 7: Epilogue

Chapter 7 provides a brief overview of the results discussed within the dissertation, as well as giving some recommendations for future improvements and development of gene delivery systems.

1.4 References

1. Al-Dosari MS, Gao X. Nonviral gene delivery: principle, limitations, and recent progress. AAPS J. 2009;11(4):671-3.
2. Nayerossadat N, Maedeh T, Ali PA. Viral and nonviral delivery systems for gene delivery. Adv Biomed Res. 2012;1:27.
3. Pack DW, Hoffman AS, Pun S, Stayton PS. Design and development of polymers for gene delivery. Nat Rev Drug Discov. 2005;4(7):581-93.
4. Ramamoorth M, Narvekar A. Non viral vectors in gene therapy- an overview. J Clin Diagn Res. 2015;9(1):GE01-GE6.
5. Mastrobattista E, van der Aa MAEM, Hennink WE, Crommelin DJA. Artificial viruses: a nanotechnological approach to gene delivery. Nat Rev Drug Discov. 2006;5:115-21.
6. Dominska M, Dykxhoorn DM. Breaking down the barriers: siRNA delivery and endosome escape. J Cell Sci. 2010;123(8):1183-9.
7. Xiaoli S, Na Z. Cationic polymer optimization for efficient gene delivery. Mini-Rev Med Chem. 2010;10(2):108-25.
8. Garnett MC. Gene-delivery systems using cationic polymers. Crit Rev Ther Drug Carrier Syst. 1999;16(2):147-207.
9. Lv H, Zhang S, Wang B, Cui S, Yan J. Toxicity of cationic lipids and cationic polymers in gene delivery. J Control Release. 2006;114(1):100-9.
10. Uchida S, Itaka K, Chen Q, Osada K, Ishii T, Shibata M-A, Harada-Shiba M, Kataoka K. PEGylated polyplex with optimized PEG shielding enhances gene introduction in lungs by minimizing inflammatory responses. Mol Ther. 2012;20(6):1196-203.
11. Vader P, van der Aa LJ, Engbersen JFJ, Storm G, Schiffelers RM. Physicochemical and biological evaluation of siRNA polyplexes based on PEGylated poly(amido amine)s. Pharm Res. 2012;29(2):352-61.
12. Kooijmans SAA, Fliervoet LAL, van der Meel R, Fens MHAM, Heijnen HFG, van Bergen en Henegouwen PMP, Vader P, Schiffelers RM. PEGylated and targeted extracellular vesicles display enhanced cell specificity and circulation time. J Control Release. 2016;224(Supplement C):77-85.
13. Liu Z, Zhang Z, Zhou C, Jiao Y. Hydrophobic modifications of cationic polymers for gene delivery. Prog Polym Sci. 2010;35(9):1144-62.

14. Rejman J, Bragonzi A, Conese M. Role of clathrin- and caveolae-mediated endocytosis in gene transfer mediated by lipo- and polyplexes. Mol Ther. 2005;12(3):468-74.
15. Elouahabi A, Ruysschaert J-M. Formation and intracellular trafficking of lipoplexes and polyplexes. Mol Ther. 2005;11(3):336-47.
16. Schätzlein AG. Targeting of synthetic gene delivery systems. J Biomed Biotechnol. 2003;2003(2):149-58.
17. Blanco E, Shen H, Ferrari M. Principles of nanoparticle design for overcoming biological barriers to drug delivery. Nat Biotechnol. 2015;33(9):941-51.
18. Majzoub RN, Chan C-L, Ewert KK, Silva BFB, Liang KS, Jacovetty EL, Carragher B, Potter CS, Safinya CR. Uptake and transfection efficiency of PEGylated cationic liposome–DNA complexes with and without RGD-tagging. Biomaterials. 2014;35(18):4996-5005.
19. Chan C-L, Majzoub RN, Shirazi RS, Ewert KK, Chen Y-J, Liang KS, Safinya CR. Endosomal escape and transfection efficiency of PEGylated cationic lipid–DNA complexes prepared with an acid-labile PEG-lipid. Biomaterials. 2012;33(19):4928-35.
20. Park I-K, Singha K, Arote RB, Choi Y-J, Kim WJ, Cho C-S. pH-responsive polymers as gene carriers. Macromol Rapid Commun. 2010;31(13):1122-33.
21. Dinçer S, Türk M, Pişkin E. Intelligent polymers as nonviral vectors. Gene Ther. 2005;12:S139-S45.
22. Convertine AJ, Diab C, Prieve M, Paschal A, Hoffman AS, Johnson PH, Stayton PS. pH-responsive polymeric micelle carriers for siRNA drugs. Biomacromolecules. 2010;11(11):2904-11.
23. Truong NP, Jia Z, Burges M, McMillan NAJ, Monteiro MJ. Self-catalyzed degradation of linear cationic poly(2-dimethylaminoethyl acrylate) in water. Biomacromolecules. 2011;12(5):1876-82.
24. Knop K, Hoogenboom R, Fischer D, Schubert US. Poly(ethylene glycol) in drug delivery: pros and cons as well as potential alternatives. Angew Chem Int Ed. 2010;49(36):6288-308.

Chapter 2: Literature Review

2.1 Gene delivery

Gene therapy is the delivery of genetic materials in order to modulate diseases. There are two approaches for gene therapy, where the first is to deliver a functional copy of a gene that is defective/absent, while the second is to deliver RNA interference (RNAi) therapeutics that can remove a pathological gene expression. RNAi therapeutics include the following nucleic acids: short interfering RNA (siRNA), microRNA (miRNA), short hairpin RNA (shRNA) and antisense oligonucleotides (AONs). The work presented in this thesis will focus specifically on the second approach.

RNAi was first discovered by Fire *et al.* (1), and the importance of RNAi has become a recognized fact over the past 20 years, with siRNA and miRNA becoming accepted as having a vital role in gene regulation. Their importance therein has been studied extensively and, as such, these nucleic acids have been linked, beyond healthy individuals, to playing an integral role in diseases such as cancer, neurological diseases and heart disease. (2) However, the lack of success in gene therapy, despite the large number of gene therapy-related clinical trials, can often be attributed to the absence of a safe, reliable and efficient tool for targeted delivery of these RNA molecules into their intracellular locations of diseased cells. This lack of success is also due to the RNA molecules' size, negative charge, instability and difficulty in cellular uptake. (3) Although there has been some success in local delivery of naked RNA molecules, especially siRNA, (4-6), complications arise when targeting tissue via systematic administration. Furthermore, local delivery falls short, as it is not appropriate for all diseases. Numerous studies have investigated diverse means of protecting these RNAs via delivery systems, with the intention of transporting the therapeutics to reach their site of action. Davis *et al.* reported the first in-human phase 1 clinical trial in 2010, in which they showed systemic administration of siRNA via a PEG-coated nanoparticle delivery system. (7) Since then, many delivery systems have been developed, including viral vectors, (8-10) liposomes, (11, 12) dendrimers, (13-16) peptides (17-19) and polymers (20-22). This chapter will focus specifically on polymeric delivery systems, known as polyplexes when the polymers are complexed with the gene therapeutic. Polymeric delivery systems do not cause an immune response like those seen for viral vectors (23, 24) and, due to the development of controlled polymerization techniques, the ease with which polymeric

delivery systems can be modified makes them a strong alternative as vectors within gene therapy.

There are a number of factors that are important when designing a polymeric gene delivery system, and these factors are based on the end function of the gene therapy vehicle. It is vital that the vector protects the pay load from degradation, which can be caused by the constituents within the extracellular fluid such as serum components and proteins, while not causing an immune response. Moreover, the system should not form non-specific aggregates or cause aggregation of blood components, as this can cause capillary occlusions. (25) It is also important that the vehicle facilitates cellular uptake, (26) usually through endocytosis, (26, 27) where a major obstacle remains the endosomal/lysosomal release of the polymeric delivery system into the cytoplasm. (28, 29) Thereafter, one further hurdle is the release of the payload from the polyplex in order for it to be able to perform its intended purpose of regulating gene expression. (30)

Thus far, no delivery vehicles have been able to address all of these requirements, but large strides have been made over the past decade. More research has been performed investigating the delivery of oligo-DNA with polymer vectors, and this knowledge, both positive and negative, can be directly applied to non-coding RNA delivery, although the system might need some slight refinement in order to achieve its new purpose. Therefore, this can be used as a type of shortcut when designing delivery vehicles for non-coding RNAs. This chapter will discuss a variety of different systems that have been designed for both non-coding RNAs and oligo-DNAs, with an emphasis on their positive and negative attributes.

2.2 Cationic polymeric delivery systems

Cationic polymers have emerged as highly attractive vehicles for gene therapy and are, by far, the most deliberated polymeric gene delivery vehicles for both non-coding RNAs and oligo-DNAs. Generally, these polymers are composed of amines that can be protonated, and which are thus capable of interacting with the non-coding RNAs and condensing them to form polyplexes. By condensing the nucleotides, the polycations protect them from degradation by decreasing their interactions with proteins and enzymes, as well as by minimizing systemic clearance, transporting them systemically, increasing their half-life, and

facilitating cellular uptake through increased interaction with cells. (31) However, the disadvantage of polycation systems is the inherent cytotoxicity that they cause due to their positive charge. (32)

The nitrogen to phosphorus charge (N/P) ratio is the ratio of positive charge on the polymer to the negative charge on the nucleic acid, and it is an important physicochemical factor to consider when forming polyplexes as it has an impact on the size, stability and net charge of the system. Higher N/P ratios have been seen to form smaller micelles and enhance gene expression *in vivo.* (33, 34) This enhanced gene expression is due to the presence of free polycations which increases intracellular delivery; however, when the charge neutral point is surpassed due to these free polycations, the cytotoxicity of the polyplexes increases due to non-specific aggregation with constituents within the extracellular fluid. (35) Fischer *et al.* (36) conducted an *in vitro* study that explored the structural effects of the polymer that influenced the polycation's influence on the cell viability and hemolysis. This study highlighted that the cytotoxicity of a polymer directly relates to the cationic charge density and the molecular weight. Thus, significance is placed on finding the correct N/P ratio for each system, *i.e*. the balance between transfection efficiency and the toxicity profile.

One way in which to improve the toxicity profile of polyplexes is to add a hydrophilic surface-coating polymer block, *e.g*. poly(ethylene glycol) (PEG). This also offers other advantages such as an increased circulation time *in vivo,* decreased aggregation, and more protection against blood components. (37-40) On the other hand, due to the shielding of the positive charge, the PEGylation has been seen to decrease the complexation efficiency (41) and cellular interactions, causing a decrease in cellular uptake. This issue has been addressed by actively targeting cells by adding targeting ligands or antibodies on the surface of the system. (28, 38, 42-46) PEGylation increases the passive targeting of the polyplexes, *i.e*. it increases the chance of polyplexes reaching their targeted site due to the increased circulation time. (47) The incorporation of targeting ligands and antibodies allows for active targeting by interacting with receptor proteins on specific cell types, which subsequently facilitates cellular uptake. (48) For example, Allen *et al*. (49) synthesized poly(1-vinyl-imidazole) (PVIM) quaternized with various *t*-Boc-protected bromoalkylamines (up to 30% quaternization) and then, after Boc-deprotection, was functionalized with folic acid. Although these polyplexes wholly underachieved in comparison with poly(ethylenimine)

(PEI) and SuperFect Transfection Reagent in terms of transfection efficiency, the results nevertheless underscore the remarkable impact that folic acid has on the cellular uptake of polyplexes. The folic acid functionality increased the luciferase expression up to 250 times compared to the unmodified analogues. Thus, this reiterates the importance of targeting ligands, such as folic acid, within gene therapy.

In addition, the transfection efficiency of PEGylated systems decreases due to insufficient intracellular release. It has been repeatedly observed that endosomal escape is of greater significance than cellular uptake when attempting to achieve efficient gene knockdown. (50-53) Some evidence shows that, through the use of pH labile, PEGylated polymer systems, it is possible to improve the endosomal escape of the delivery systems. (54-59) Depending on the delivery system, this enhancement can occur via the collapse of nanoparticles and, in the case of polycations, through an increased proton sponge effect that is caused by an elevation in osmotic pressure due to the number of products from the broken pH-labile bond. Consequently, this increases the pressure within endosomes, which in turn causes the swelling and rupture of the endosome. Therefore, the use of these pH-labile linkers can facilitate gene regulation through delivering the vector to the cytoplasm. (53, 60-62)

Because reversible deactivation radical polymerization (RDRP) techniques, such as ATRP and RAFT-mediated polymerizations, allow for the synthesis of polymers with predetermined molecular weights and architectures, it has been possible to elucidate the effect of polymers' molecular weight and architecture on polyplex transfection efficiency and toxicity. The results of numerous studies have shown that, by increasing the molecular weight of the polycation, or by increasing the molecular weight of the polycation block within a block copolymer, the oligonucleotide condensation capabilities and the transfection efficiency of the polyplex are also increased. However, these increases also cause a rise in the inherent cytotoxicity. (63-67) This increase in cytotoxicity has been linked to two causes: firstly, that the increased molecular weight causes an increase in the polyplex size, which thus increases their propensity to bind to negatively charged peptides. Secondly, that they interact more with the cell membrane, causing destabilization and, consequently, cell death. Hence, it is imperative to consider molecular weight when developing polymers for gene delivery applications.

Similarly, the polymer backbone architecture, *e.g.* homopolymers, block copolymers, statistical or random copolymers, graft copolymers, and star-shaped polymers, imparts important properties that influence gene delivery. Due to a lower charge density, random copolymers impart lower cytotoxicity than block copolymers. (68) Furthermore, polyplexes produced from grafted and branched copolymers display better toxicity profiles, as well as higher transfection efficacy, than those from linear homopolymers. (63, 69, 70) These grafted polymers display higher electrostatic interactions with the nucleic acids and cell membranes, subsequently improving membrane disruption and increasing uptake.

Ziebarth and Wang (71) used coarse-grained molecular dynamics simulations to investigate the effect of the polymer architecture, as well as the molecular weight of blocks, within copolymers on the polyplex structure. These theoretical models revealed that polyplexes that consist of longer, linear block copolymers were smaller and possess more well-defined core-coronas. This is due to their ability to better condense the RNA/DNA molecules than lower molecular weight blocks. Linear copolymers were reported to be homogeneously dispersed with RNA/DNA molecules whereas polyplexes, prepared from star-shaped polymers, form layered structures. Furthermore, experimental investigations have shown that polyplexes from star-shaped polymers display higher transfection efficacy. This is due to the enhanced condensation of polyanions than polyplexes from their equivalent linear or randomly branched polymers. (72-76)

Georgiou *et al.* established that, beyond the importance of the polymer's architecture, the positioning of monomers within the polymer is of equal significance, as the architecture impacts the transfection ability of the polyplex. (77, 78) Synatschke *et al*. (75) suggested that the ideal polyplexes are those prepared from branched polymers with intermediate molecular weight, as this would help researchers to discover the most optimal balance between transfection efficiency and cytotoxicity.

A number of different polycations have been investigated for use in gene delivery systems. A few of these systems will be discussed in more detail in the subsequent sections. The most well researched polycation is PEI, see Figure 2.1. (79, 80)

2.2.1 Polyethylenimine (PEI)

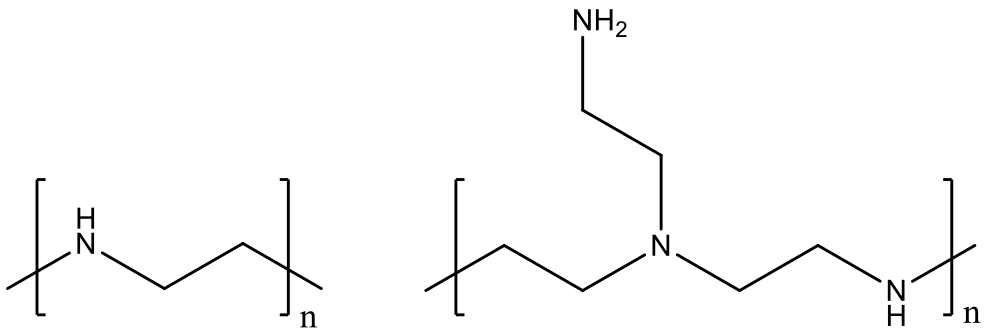

Figure 2.1 Structural representations of linear and branched polyethylenimine

PEI has been named the "gold standard" of non-viral based delivery systems and, due to this, there have been a tremendous number of studies that vary PEI's architectures, add modifications or conjugations, PEGylation and target different cell/tissue types. PEI's success as a gene delivery vehicle can be found in its ability to complex with non-coding RNAs and oligo-DNAs due to its amines that can be protonated to bear a strong positive charge.

However, this positive charge also causes its inherent cytotoxic nature. (35, 81) The levels of its cytotoxicity have been strongly correlated to the size and structure of PEI. (82) Thus, the charge ratio of PEI polyplexes is very important, with increased N/P ratios resulting in smaller particles with more positive charge, and hence allow for enhanced permeation into cells. (83) Of course, this leads to increased cytotoxicity. In an *in vivo* study conducted by Chollet *et al.,* a clear enhancement in the luciferase activity in the lung was noted with systemic injections when the concentration of linear PEI/DNA polyplexes was increased. However, an adverse reaction of this accumulation was necrosis in the liver and fatality. (84)

Fischer *et al*. (36) discovered that the nature of cell death caused by linear PEI and polyplexes was indicative of a nectrotic type of cell death due to the fact that cell apoptosis was not detected. Comparatively, a study by Kafil *et al*. (85) reported that branched PEI is capable of eliciting apoptosis in target cells. This study noted that branched PEI (25 kDa) caused higher levels of toxicity than linear PEI (25 kDa). The increased cytotoxicity was thought to be related to the higher zeta potential of branched PEI compared to linear PEI.

Interestingly, subsequent studies have revealed that linear PEI demonstrates higher efficiency than branched PEI. (86)

It has become a well-known phenomenon that, as the molecular weight of PEI increases, so too the cytotoxicity rises. However, the transfection efficiency of low molecular weight PEI is also notably lower. Therefore, studies have been conducted in which chains of low molecular weight PEI are connected via a reducible link, in order to obtain biodegradable high molecular weight PEI. (82, 87) This has proven to be effective in obtaining superior RNAi activity with lower cytotoxicity. Gosselin *et al*. incorporated a disulfide bond between two low molecular PEI molecules, using dithiobis(succinimidylpropionate) and dimethyl,3,3'-dithiobispropionimidate. These polymeric systems showed slightly lower transfection efficiencies compared to high molecular weight PEI; however, the cytotoxicity was also somewhat reduced via the inclusion of the disulfide bridge. (87) In comparison to this, Breunig *et al.* investigated the viability and efficacy of disulfide crosslinked, low molecular weight, linear PEI in numerous cell lines. They obtained a decrease in cytotoxicity (>90% viability across all cell lines), while improving the transfection efficacy. Nonetheless, the maximum efficacy of these reducible PEI polyplexes required higher N/P ratios relative to the non-reducible PEI polyplexes. Thus, one can deduce that, although the use of reducible bonds between low molecular weight PEI can somewhat decrease the cytotoxicity, the yielded transfection efficiency may be compromised when compared to non-reducible PEI of the same ultimate molecular weight. (88, 89)

As mentioned above, there can be no true RNA delivery without endosomal escape, and hence no gene regulation can occur, as the delivered RNA molecule must be able to enter the cytosol in order to interact with the targeted RNA. Understanding the mechanism of endosomal escape is pertinent in order to improve the actual delivery system; however, this mechanism is still rather elusive in terms of PEI. A number of theories abound regarding endosomal escape. The most accepted, and most widely debated, theory is the "proton sponge" effect. (90) This theory is based on the large buffering capacity of polycations, including PEI. It is believed that the endosome will eventually rupture due to an increase in osmotic pressure, caused by an uptake of chloride ions that are passively transported into the endosome due to the charge gradient. Although popular, this theory has also been greatly disputed. A study by Benjaminsen *et al*. (91) reported evidence that suggested that

no decrease in pH occurs within the lysosome, thus shedding doubt on the accuracy of the proton sponge effect. Yet, no concrete explanation exists to explain how PEI polyplex causes gene regulation, only that they do.

In elaboration to the abovementioned, PEGylation has become common practice in order to address the toxicity, stability and circulation time of PEI polyplexes. (92-94) Due to the disadvantages of PEGylation, studies have been conducted in order to investigate the PEG chain length, in hope of discovering the optimum architecture for the simultaneous protection and maintenance of cellular uptake and transfection efficiency. (92, 93, 95) However, due to the proof that a hydrophilic polymer on the external surface decreases cellular uptake transfection efficiency, (96, 97) many PEGylated PEI polyplexes have included different targeting ligands or antibodies on the surface, with the intent to promote active targeting. (98-100) As such, folic acid has become a popular targeting ligand in gene therapy due to its selectivity towards cancerous cells which over-express folate receptors, thus increasing its internalization efficiency. (99, 101)

Acid-labile linkers have also been incorporated in order to improve the endosomal escape, and consequently the transfection efficacy, of PEGylated PEI polyplexes. (54, 97, 102) Knorr *et al*. (54) synthesized novel PEG-acetal-PEI polyplexes, via a Michael addition, between a maleimide moiety on the PEG chain-end and the mercaptan-modified PEI. The resultant PEG-acetal-PEI was seen to break down after 3 minutes in pH 5.5 – the pH corresponding to that within the endosomal compartment. A 10-fold increase in transfection efficiency was obtained, which was notable in comparison to the PEGylated PEI with a stable linkage.

Other examples have incorporated disulfide links between the hydrophilic polymer and PEI, for example Carlisle *et al*. (103) connected PEI and hydroxypropyl methacrylate (HPMA) via a reducible, disulfide bond. They hypothesized that the increase obtained in terms of transfection efficiency was caused by the reducing environment in the late-endosome/lysosome, which thus caused the breakage of the disulfide linker. However, in more recent studies, the use of disulfide links has been rendered less effective than a pH-labile bond. This will be discussed further in Section 2.5.

Despite all of these investigations, the transfection efficiency of PEI still remains inadequate, especially when the toxicity profile is kept in check. Thus, although research on PEI

polyplexes remains active, there has been a boom of new research within gene delivery, as many no longer consider PEI to be the ultimate vector for these delivery systems. Instead, "smart" polymeric systems have become leaders in this field. Their "smart" nature can be attributed to a range of different factors, including biodegradability, responsiveness to stimulus such as pH, temperature, reducible linkers, etc. But all of these systems have one thing in common – they aim to enhance biodistribution, biocompatibility, cellular uptake, endosomal escape and cytoplasmic release – and ultimately their main function is the delivery of the RNA species in order to control gene expression. Accumulatively, this is an attempt to improve what PEI predecessors could not achieve. Few of these "smart" polymeric systems, if any, are able to fulfill all of these objectives. Many of them have utilized RDRP techniques, *e.g*. RAFT-mediated polymerization and ATRP, to obtain more sophisticated polymers and copolymers with better molecular architecture. A major advantage of RDRP techniques is that they enable the synthesis of polymers in a sequential manner and allow for facile means of incorporating functional modifications, such as linking targeting ligands, fluorescent markers or other imaging modalities, or even the RNA molecule itself.

2.2.2 Poly(2-(N,N-dimethylamino)ethyl methacrylate) (pDMAEMA)

The anionic nature of RNA remains a simple manner in which to form polyplexes. Poly(2-(*N*,*N*-dimethylamino)ethyl methacrylate (pDMAEMA) is a well-studied polymer for these sorts of delivery systems (104). Its complexation is also based on the protonation of amines, thus causing endosomal escape to be based on the hypothesis of the debated proton sponge effect. Owing to the sterically unhindered and free nature of the amines of pDMAEMA, they have a higher capacity of absorbing protons, and thus possess a higher proton sponge buffering potential. (89, 105) In a comparative study, pDMAEMA with tertiary amines was compared to those with quaternized amines. They found that, although the complexation with nucleic acids is higher for quaternized pDMAEMA, the toxicity also increases, while the transfection efficiency decreases. They hypothesized that this decrease in transfection efficiency is caused by the quaternized amines' inability to be further protonated, which then decreases the buffering capacity of the polymer. (63, 106)

Via controlled radical polymerization techniques, many investigations have been conducted on the effect of molecular weight on complexation efficiency, toxicity, cellular uptake and transfection efficiency of pDMAEMA. Like PEI, pDMAEMA is inherently cytotoxic due to its cationic nature, and this toxicity increases with an increase in the molecular weight. (90, 107) It has been observed that transfection efficiency rises with an increase in molecular weight, and that the only limiting factor is toxicity. It has been possible to study the effect of polymer architecture on the polyplex properties and, as such, linear, star-shaped, (66, 74, 75) grafted copolymers, (63, 69, 108) statistical copolymers (58, 59, 109-111) and block copolymers of pDMAEMA (64, 112) have all been investigated. Studies of pDMAEMA grafted onto poly(2-hydroxyethyl methacrylate), (69) hydroxypropyl cellulose, (63) dextran (106), and chitosan (70) have highlighted that these grafted or branched polymers have better toxicity profiles compared to their high molecular weight, linear pDMAEMA counterparts. Moreover, their transfection efficiency is also higher, even at lower cation incorporation. (63) This same phenomenon was also seen for hyperbranched pDMAEMA of the same molecular weight as linear pDMAEMA. (113) Synatschke *et al*. (75) investigated the effect of branched pDMAEMA on transfection efficiency and cytotoxicity by synthesizing linear, 3-arm and 5-arm pDMAEMA at different molecular weights. They found that a minimum threshold molecular weight is required in order to obtain cellular uptake which differs according to the polymer architecture. Moreover, in line with other studies, they reported that linear pDMAEMA is more cytotoxic than star-shaped polymers. However, they also specified that they noticed an upper limit of the dependency of N/P ratio on cellular uptake. This is more likely due to a stronger complexation of plasmid DNA to the polycation, which causes a shielding effect of the green fluorescent protein encoded in the plasmid, as described by Vader *et al*. (114)

PEG has been used profusely as a protective block for pDMAEMA in a similar manner to its use with PEI. However, as controlled polymerization techniques lend themselves to easy incorporation of other comonomers, there have also been investigations into the use of other hydrophilic protective blocks. For example, Song *et al.* (112) synthesized copolymers of poly(*N*-vinylpyrrolidone) (PVP) and pDMAEMA (PVP-*g*-pDMAEMA), as well as PVP-pDMAEMA with poly(methyl methacrylate) (PMMA) (PVP-*g*-pDMAEMA-*b*-PMMA) via ATRP. The PVP-*g*-pDMAEMA are able to form coils in aqueous medium, while the PVP-*g*-

pDMAEMA-*b*-PMMA form micelles with PMMA in the hydrophobic corona. The incorporation of PMMA allowed for better condensation of pDNA, a higher buffering capacity and subsequently a higher transfection efficiency. As such, both of these systems display an increased transfection efficiency when compared to PEI (25k) at low N/P ratios.

In order to tackle toxicity, and inspired by reducible PEI, You *et al.* (115) synthesized reducible high molecular weight pDMAEMA by coupling low molecular weight pDMAEMA via disulfide bonds. The use of RAFT-mediated polymerization makes synthesis of well-defined reducible pDMAEMA easier than reducible PEI. You *et al.* synthesized a bisfunctional RAFT agent and, post-polymerization, removed the trithiocarbonate-end groups in order to obtain α,ω-dithiol-pDMAEMA. Thereafter, this was oxidized to form the high molecular weight product. They obtained lower cytotoxicity than the non-reducible analogue, and equivalent transfections efficiency; however, the transfection of PEI remains significantly higher.

In order to further lessen the toxicity, studies have worked towards developing smarter pDMAEMA polymers that contain reduced charge, by incorporating a neutral comonomer. Methyl methacrylate (MMA), (112, 116) butyl methacrylate (BMA) (109, 117, 118) and butyl acrylate (*n*BA) (60) have all been copolymerized with DMAEMA in order to decrease the cytotoxicity and improve the transfection efficiency. Within this scope, they have exhibited a good ability to complex the nucleotides. Nonetheless, slightly higher N/P ratios are commonly necessary to achieve this. While the incorporation of *n*BA improves the stability and cytotoxicity of the polyplexes, it reduces their pH-dependent disruptive behavior. Thus, this leads to a decrease in RNAi activity, which may be due to endosomal entrapment. (109) Conversely, the copolymerization of DMAEMA and BMA produced pH tunable polymer micelles, with a pH directly related to the percentage of BMA incorporated in the polymer chain. In a study conducted by Nelson *et al.,* varied percentages of BMA were incorporated into PEGylated copolymers of DMAEMA and BMA. It was found that polymers with a content of 50% or more BMA form micelles at pH 7.4. As the pH is lowered, these micelles disassociate at a pH inversely proportional to the percentage of BMA. At 70% BMA, the micelles are stable – even at pH 4.0. This suggests that they do not gather enough positive charge to destabilize the BMA's increased hydrophobic interactions. (109) The investigation revealed that the cellular uptake of the polyplexes increases as the percentage of BMA

decreases; however, 50% BMA conveys the highest luciferase silencing relative to all other copolymers. This indicates that the polyplexes, based on the 50% BMA, show better endosomal release as a result of their pH dependent profile. Stayton *et al.* (111) incorporated propylacrylic acid (PAA) into this system, forming poly(DMAEMA-*b*-[DMAEMA-*s*-PAA-*s*-BMA]) via RAFT-mediated polymerization. This system enhances serum stability and, most importantly, the endosomal escape of the polyplex is enhanced due to the tuning of the polyplex's pH-dependent membrane disruptive behavior. They later incorporated a folate targeting ligand through a folate-containing RAFT agent. This system was reported to further facilitate specific cellular uptake through folate-receptor interaction. (110)

To improve the endosomal escape, pH-labile linkers have been incorporated between the hydrophilic surface polymer and pDMAEMA. Lin *et al.* (119) incorporated a pH labile, ortho-ester, linker between pDMAEMA and PEG. Unfortunately, they found that the ortho ester linker is not the ideal bond type for a gene therapy system as it is stable around pH 6.5. Thus, this means that the deshielding effect of PEG was not complete.

2.2.3 Poly(L-lysine)

Poly(L-lysine) was one of the first cationic polymers to be used for the complexation of nucleotides due to its biodegradable nature. (120, 121) Nevertheless, it was judged to be a second rate choice due to its poor transfection efficiency, which was caused by a lack of buffering capability, short circulatory half-life and high cytotoxicity. (122) In fact, it has been revealed to possess an equivalent toxicity to branched PEI. (36) Nonetheless, it has been possible to incorporate other polymer blocks with poly(L-lysine) in order to improve transfection efficiency and/or toxicity. (123, 124) One such example was investigated by Patil *et al*., (125) whereby they synthesized triblock poly((amido amine)-*b*-(ethylene glycol)-*b*-(L-lysine)) nanocarriers. The poly(L-lysine) provides the polycationic nature required for the condensation of RNAs, as well as encourages cellular uptake. Conversely, the poly(amido amine) enhances endosomal escape and cytosplasmic delivery of RNAs due to the presence of its tertiary amine groups, *i.e*. it functions as the proton sponge. The gene knockdown is substantially decreased when poly(amido amine) is not present in the nanocarrier, thus confirming its essential role in making the delivery system effective.

Another such example was the investigation into the use of PEG-*b*-poly(L-lysine)-*b*-(L-leucine) for gene delivery. (126) It was observed that, only by tuning the poly(L-lysine) and poly(L-leucine) segments, was it possible to obtain better transfection efficiency than poly(L-lysine). A similar study incorporated poly(aspartamide) derivatives into PEGylated poly(L-lysine). (124) The poly(aspartamide) was introduced with the intention of enhancing *in vivo* micelle stability, which was previously seen to be lacking in polyplexes that spontaneously assemble due to electrostatic interactions. The presence of both hydrophilic nucleotides and hydrophobic polycations is believed to cause some destabilization *in vivo*. (124, 127, 128) These stabilized polyanion micelles were compared to "randomly" hydrophobic control micelles, as well as non-PEGylated diblock copolymer micelles. They reported that the non–PEGylated micelles are more readily taken up by cells, while the "randomly" hydrophobic control micelles are taken up the least. But the cellular uptake did not tally with efficient gene silencing, as the non-PEGylated micelles' performance were the least successful. This was determined to be due to the fact that these micelles are unable to release the siRNA in the cells, whereas the triblock micelles release their payload more effectively. The triblock micelles also outperformed the "randomly" hydrophobic control micelles, which was correlated to their balance between serum stability and RNA release. (124)

Matsumoto *et al.* (129) developed environmentally responsive core shell-type polyion complex micelles containing PEG-*b*-poly(L-lysine) with iminothilane modification, in order cross-link the core with disulfide bonds. This crosslinking was utilized in an attempt to stabilize the structure of the micelles in physiological conditions, while also allowing for cytoplasmic release of RNAs due to the reductive nature within the cell. These responsive systems are able to achieve a 100-fold increase in siRNA activity compared to the unmodified PEG-*b*-poly(L-lysine).

Oishi *et al*. (130) conjugated siRNA and lactocylated PEG via a β-thiopropionate acid-labile linkage, and subsequently complexed it with poly(L-lysine), in order to infuse pH-sensitivity into their novel polyion complex micelles. Since the β-thiopropionate bond is stable at physiological pH, but readily cleaves at the pH of the intracellular endosomal compartment (pH = 5.5), the smart complexes are able to release the siRNA from the lactocylated PEG. This allowed them to achieve enhanced gene silencing in hepatoma cells at extremely low siRNA concentrations compared to Lac-PEI-siRNA complexes. In fact, they obtained almost a

100 times enhancement in RNAi activity for their pH sensitive PIC micelles when compared to the Lac-PEG-siRNA conjugate. Very notably, these PIC conjugates retained their RNAi activity even when incubated with 50% serum for 30 minutes prior to transfection. Oishi *et al.* (130) investigated the importance of the pH-labile linker to the RNAi activity by inhibiting the endosomal acidification. This was achieved by adding nifericin to their culture medium. As a result, they saw a significant decrease in the RNAi activity, while no change was seen in the RNAi activity for the Lac-PEG-siRNA conjugates. This suggests that the cleavage of the acid-labile linker indeed occurs within the intracellular endosomal compartment, and that it is probable that the free PEG increases the osmotic pressure within the endosomal compartment, which causes swelling and disruption within the compartment. Ultimately, this allows for the release of the siRNA into the cytoplasm.

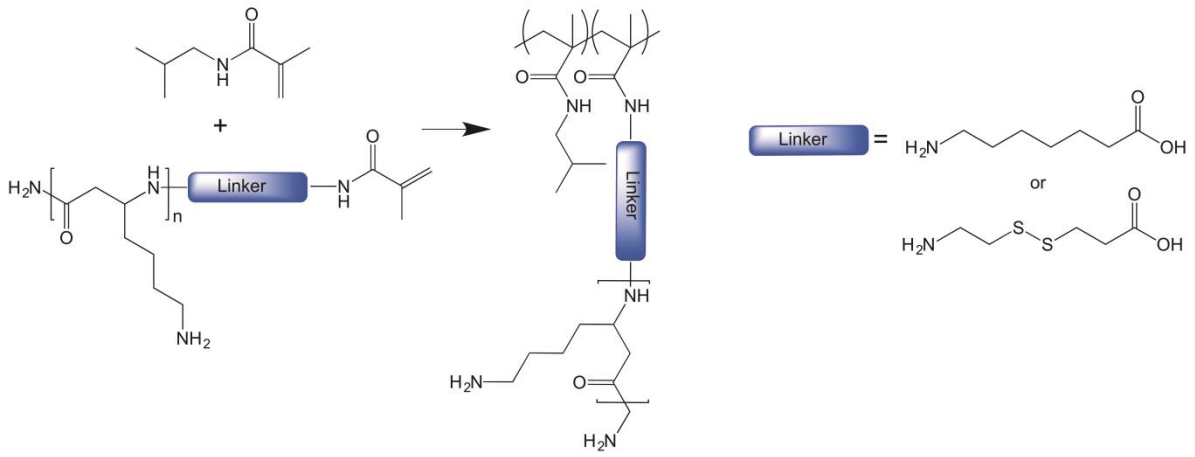

Scheme 2.1 A schematic illustration of the synthesis of HPMA-oligolysine polymers containing a reducible or non-reducible linker between the polymer backbone and the RNA-complexing, oligolysine side-chains

An interesting trend was observed when comparing HPMA-oligolysine polymers synthesized via RAFT-mediated polymerization and via conventional free radical polymerization, Scheme 2.1. (131) The transfection efficiency was seen to be similar in both systems; however, the IC_{50} values (the polymer concentration at which there is 50% cell survival) for the conventional free radical polymers were 10-fold lower than those of the RAFT-mediated

polymers, indicating that the conventional free radical polymers cause far greater cytotoxicity.

2.2.4 Polyester delivery systems

Poly(lactic acid-*co*-glycolic acid) (PLGA) is a biodegradable polyester synthesized through copolymerization of lactic acid and glycolic acid. It has found many applications within the medical field as its biodegradation time (depending on molecular weight and copolymer ratio) can be tailored, and also due to its biocompatibility and FDA approval. PLGA enhances the transfection efficiency because it is able to facilitate the continuous intracellular release of its payload. Within drug delivery, this has the ability to improve drug release from mere days to weeks. (132) Results indicated that this endosomal escape of PLGA nanoparticles is not due to the proton sponge mechanism, but rather due to a selective charge reversal, from anionic to cationic, on the surface of the nanoparticles within the acidic endosome/lysosome, causing the nanoparticles to adhere to the endo-lysosomal membranes. (133) The nanoparticles were reported to not adhere to membranes of early endosomal membranes, thus underscoring the need for a decrease in pH in order to facilitate endo-lysosomal escape. That said, the drawback of utilizing PLGA for gene therapy is that it cannot effectively condense nucleotides. Arora *et al.* (134) attempted to overcome this disadvantage by incorporating PEI into the PLGA delivery system. However, the zeta potential of the nanoparticles is not as high as expected, even with the incorporation of PEI. Although a slow, sustained release of the miRNA *in vitro* was reported, a very significant increase in the time of release in the presence of serum was also noted. This is most likely a result of inefficient complexation of the miRNA. Since then, similar studies have been performed with poly(L-lysine) (135); however, the necessity of using non-degradable polycations as copolymers reduces the allure of utilizing biodegradable polymers.

However, the hydrolytic degradability and biocompatibility of polyesters make them highly attractive polymers in biological applications – and certainly in gene delivery. (136-138) Although polyesters are very structurally diverse, there are synthetic challenges inherent in generating new monomers, such as linear step-growth polymerization necessitating monomers containing less than 1% impurity. Regardless of this obstacle, Nelson *et al.* (139) recently published their investigation into water soluble polyesters functionalized with

imidazolium groups as possible vehicles within gene delivery. Via catalyst and solvent free melt polycondensation reactions, they obtained a collection of cationic polyesters of imidazolium diol, neopentylglycol and adipic acid with tunable hydrophobicity and thermal transitions. The range of polymers acquired included polyesters with 10-75 mol% ionic content, imidazolium homopolyester and poly(neopentylene adipate) (neutral), which allowed them to investigate the role of charge content and structure on transfection efficiency. The polyplexes achieve DNA complexation at very low N/P ratios (N/P of 4 completely complexes DNA) and show insignificant toxicity in HeLa cells; however, the transfection efficiency of all of the polyester systems are orders of magnitude lower than PEI and Superfect. Although these results are seemingly disappointing, very few studies have investigated these sorts of polycations, compared to the tremendous number of studies that focus on polycations based on nitrogen ions, *e.g*. PEI. As these polymers are able to show transfection at low N/P ratios, by adjusting the cationic charge and structure, it is plausible that there is still some hope that these polyesters have potential applications in gene delivery.

Kozielski *et al.* (140) optimized the production of a bio-reducible, linear poly(β-amino ester) by incorporating disulfide bonds into the polymeric backbone. These polymers are capable of condensing the siRNA into nanoparticles, which subsequently release their payload into the cytoplasm of the cells within minutes. This is achieved due to the presence of glutathione in the cytosol. In comparison to their non-reducible counterparts, they are able to obtain efficient GFP knockdown with decreased cytotoxicity in human brain cancer cells. However, the bio-reducible nanoparticles display some instability. Thus, in their later work, (141) Kozielski *et al.* endeavored to address these issues by balancing the bioreducibility of the polymer backbone with the hydrophobicity from the poly(β-amino ester). A balance was found between the cytotoxicity (lowered by a higher level of bioreducibility and increased with a rise in hydrophobicity), and the enhanced delivery and stability of the nanoparticles affiliated with hydrophobicity. This was achieved while still maintaining the cytoplasmic targeting imparted by the bioreducible nature of the nanoparticles. They were able to obtain nanoparticles with enhanced properties and gene knockdown. The nanoparticles also display cell specific knockdown, whereby human primary glioblastomas show higher gene knockdown (97 ± 4%) than human primary non-cancer brain cells (27 ±9%).

2.2.5 Phosphonium-containing polymers

There has been some interest in polyplexes that are prepared from phosphonium-containing polymers. (142-144) Clément and coworkers were the first to investigate lipids containing phosphonium and arsenium, in comparison to ammonium, for use in gene therapy, with respect to the effect that the cationic core plays on structure and properties/function. (145-147) They discovered that by replacing the ammonium core with phosphonium or arsenium, they were able to achieve an improved toxicity profile, as well as higher levels of stability in the solution – both *in vitro* and *in vivo*.

Hemp *et al*. (143) used conventional free radical polymerization in order to synthesize styrenic-based ammonium and phosphonium containing polymers. They varied the length of the alkyl substituent attached to the cation in order to elucidate structure's impact on transfection efficiency. They synthesized poly(triethyl-(4-vinylbenzyl)ammonium chloride (PTEA), poly(tributyl-(4-vinylbenzyl)ammonium chloride (PTBA), poly(triethyl-(4-vinylbenzyl)phosphonium chloride (PTEP) and poly(tributyl-(4-vinylbenzyl)phosphonium chloride (PTBP). The transfection efficiency of the four polymers was compared to that of Superfect and Jet-PEI, and it was seen that PTBP has better transfection efficiency than Superfect. Moreover, they observed that PTBA's transfection efficiency is equivalent to that of Superfect. In comparison, the ethyl moiety seems to affect the transfection efficiency of the polyplexes, as both of these were inferior to Superfect. As cellular uptake of the ethyl containing polyplexes was seen via fluorescent markers on the polyplexes, it was hypothesized that the poor transfection efficiencies are due to intracellular mechanisms. The consideration was that perhaps the longer alkyl chain in the butyl derivatives aid in membrane disruption and endosomal escape, as has been reported in the past. (111, 148) Further hypothesizing led them to consider that the shorter alkyl chain may have caused stronger electrostatic interactions with the DNA, thus decreasing the release of the DNA and inhibiting the end function, as was reported by Song *et al*. (149) This study stresses that it is not only the type of cation used, but also the immediate structural environment around that cation that impacts the transfection efficiency of the polyplex delivery system. However, these polyplex systems are completely ineffective in serum. Therefore, Hemp *et al.* (144) have subsequently developed a phosphonium-containing diblock copolymer based on their previous work, containing a 4-vinylbenzyltributylphosphonium chloride (TBP) block and a

colloidal protecting block of either oligo(ethylene glycol)$_9$ methyl ether methacrylate (OEGMA) or 2-(methacryloxy)ethyl phosphorylcholine (MPC), all of which demonstrate steric shielding of nanoparticles that led to a resistance towards proteins and prolonged circulation times. (150, 151) Using RAFT-mediated polymerization, they synthesized their diblock copolymer from a macroCTA containing the stabilizing polymer, which then allowed them to target TBP with three different molecular weights (DP 25, 50, 75). This enabled them to determine the optimal AB block ratio for gene transfection for this system. In order to establish the effect of the protecting block, they also synthesized a homopolymer of TBP via RAFT-mediated polymerization, with a molecular weight equal to the intermediate diblock copolymers. As expected, all $MPC_{87}TBP_y$ and $OEG_{52}TBP_y$ polymers show an increased resistance towards serum proteins, as well as a heightened stability at physiological salt concentrations. The diblock copolymers exhibit cell specific uptake in HepaRG cells, with poor cellular uptake, and therefore low transfection, in COS-7 and HeLa cells. The transfection efficiency in HepaRG cells is equivalent to Jet-PEI; however, the phoshonium diblock copolymers cause lower cytotoxicity than the Jet-PEI polyplexes.

A study by Ornelas-Megiatto *et al.* (142) was published at around the same time as the abovementioned research by Hemp *et al.* (143, 144), and it showed similar results. In this study they synthesized poly(acrylic acid) modified with triethylene glycol monochlorohydrin via a hydrolyzable ester linkage. A second post-polymerization modification via a nucleophilic substitution of the chloride produced five different polycations containing triethylphosphine, tri(*tert*-butyl)phosphine, tris(3-hydroxy-propyl)phosphine, triphenylphosphine and triethylammonium, respectively. After eliminating the triphenylphosphine–containing polymer due to low aqueous solubility, the tri(*tert*-butyl)phosphine–containing polymer because of high cytotoxicity and the tris(3-hydroxy-propyl)phosphine–containing polymer for poor transfection efficiency (even though it was less cytotoxic than the triethylammonium–containing polymer), it was ascertained that the triethylphosphine–containing polymer exhibits lower cytotoxicity than the triethylammonium–containing polymer. In addition, it also displays a higher transfection efficiency. A notable result from this study was the superior transfection efficiency for the triethylphosphine–containing polymer in the presence of serum. Thus, this indicates that the polymer is more stable in physiological conditions than the ammonium analog.

2.2.6 Amphiphilic polymers

A few studies have investigated the use of amphiphilic polymers as vectors for gene delivery. (152, 153) Due to their amphiphilic nature, these polymers incorporate some liposome-like characteristics; however, as they are still synthetic polymers, they are also easily modified. Their dual-hydrophilic-hydrophobic nature suggests that they would be less cytotoxic than polycations, while still facilitating cellular uptake. (154)

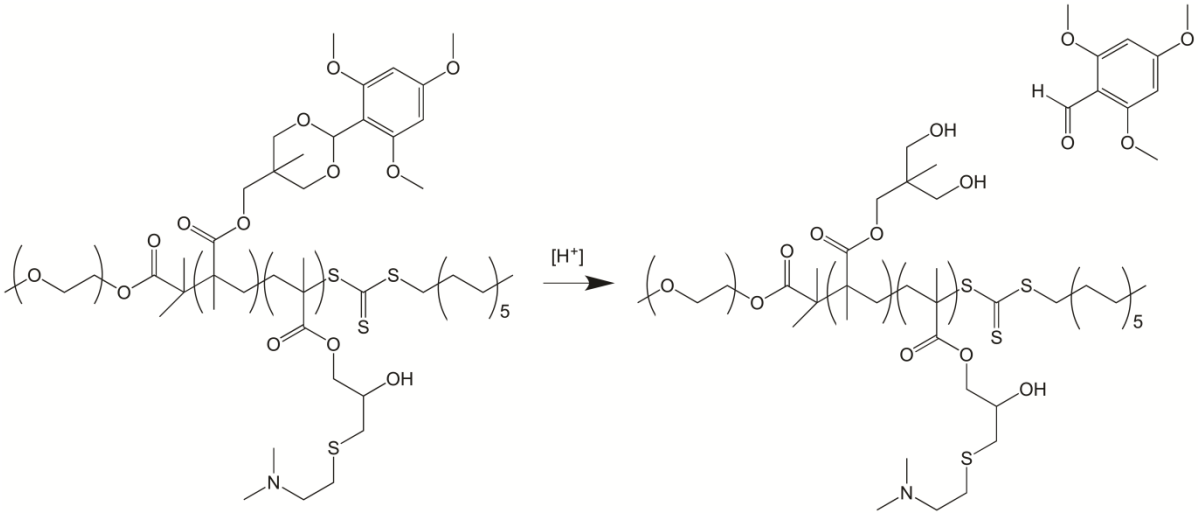

Scheme 2.2 A schematic representation of the pH-response hydrolysis causing a transition from hydrophobic to hydrophilic form, inducing a breakdown of the self-assembled structure.

Recently, Du *et al.* (53) developed pH responsive, amphiphilic nanomicelles from poly(ethylene glycol)-*b*-poly[(2,4,6-trimethoxybenzylidene-1,1,1-tris(hydroxymethyl)] ethane methacrylate-*b*-poly(dimethylamino glycidyl methacrylate). These are the first 2,4,6-trimethoxybenzylidene-1,1,1-tris(hydroxymethyl) ethane methacrylate (TTMA)-based siRNA delivery systems to be developed. The hydrolysis of the acetal group in acidic pH causes a hydrophobic to hydrophilic transition of the pTTMA, Scheme 2.2. Since the hydrophobicity induces self-assembly, this transition causes a breakdown of these self-assembled structures. Furthermore, there is evidence showing that this transition promotes endosomal escape; thus, this improves the gene knockdown efficiency of the delivery system (at N/P ratios ≥ 20) compared to Lipofectamine 2000. Importantly, they reported no significant cytotoxicity caused by the nanomicelles. By inhibiting the mechanisms of clathrin and

caveolae-mediated endocytosis, as well as micropinocytosis, they showed that nanomicelles enter the cell via both clathrin and caveolae-mediated endocytotic pathways. These results indicated that the nanomicelles exhibit improved half-life (30 min) in the body compared to naked siRNA (<5 minutes). They also investigated the biodistribution of the amphiphilic nanomicelles in mice and saw majority accumulation in the liver, spleen and lungs.

2.3 Decationizing polymers

The problems associated with the use of polycations are not limited to a systematic issue, *i.e.* the issues associated with systemic cytotoxicity, blood aggregation and hemolysis, as well as biodistribution and renal clearance, but also expand to the cellular level. Although, PEGylation addresses the systemic toxicity, the cellular toxicity remains a major limiting factor due to disturbances it presents to the cell membrane, (36, 81, 155) interferences with physiological polyanions, such as enzymes, cell receptors, non-targeted RNA or DNA, etc., (156) and their possible implications in cancer formation through the activation of oncogenes, which also induces apoptosis. (157) Therefore, there has been a redirect of research towards neutral RNAi delivery systems. One such system, developed by Hennink and co-workers, (158) employs a decationized polyplex system for the delivery of siRNA, Scheme 2.3. RAFT-mediated polymerization was employed to obtain poly(hydroxypropyl methacrylate-*N,N*'-dimethylaminoethanol-*b*-*N*-[2-(2-pyridyldithio)]ethyl methacrylamide)-*b*-PEG, with folic acid targeting functionality from a (folic acid-PEG_{5000})$_2$-(4,4'-azobis(4-cyanovaleric acid)) macroinitiator. Complexation with siRNA was attained by employing electrostatic interactions between the cationic polymer with the negatively charged nucleic acid, in the same manner as the polycationic systems mentioned above. However, post-complexation, crosslinking of the polyplexes was obtained via disulfide bonds causing a physical entrapment of the RNAs. The polycations were then decationized via cleavage of the carbonate ester group through hydrolysis, releasing the positively charged side chains from the poly(hydroxypropyl methacrylate) backbone. After cellular internalization of the decationized, reducibly cross-linked polyplexes, the disulfide bonds were reduced in the cytosol, due to the presence of glutathione, allowing for the payload to be deposited. These polyplexes impart lower cytotoxicity compared to their cationic counterparts.

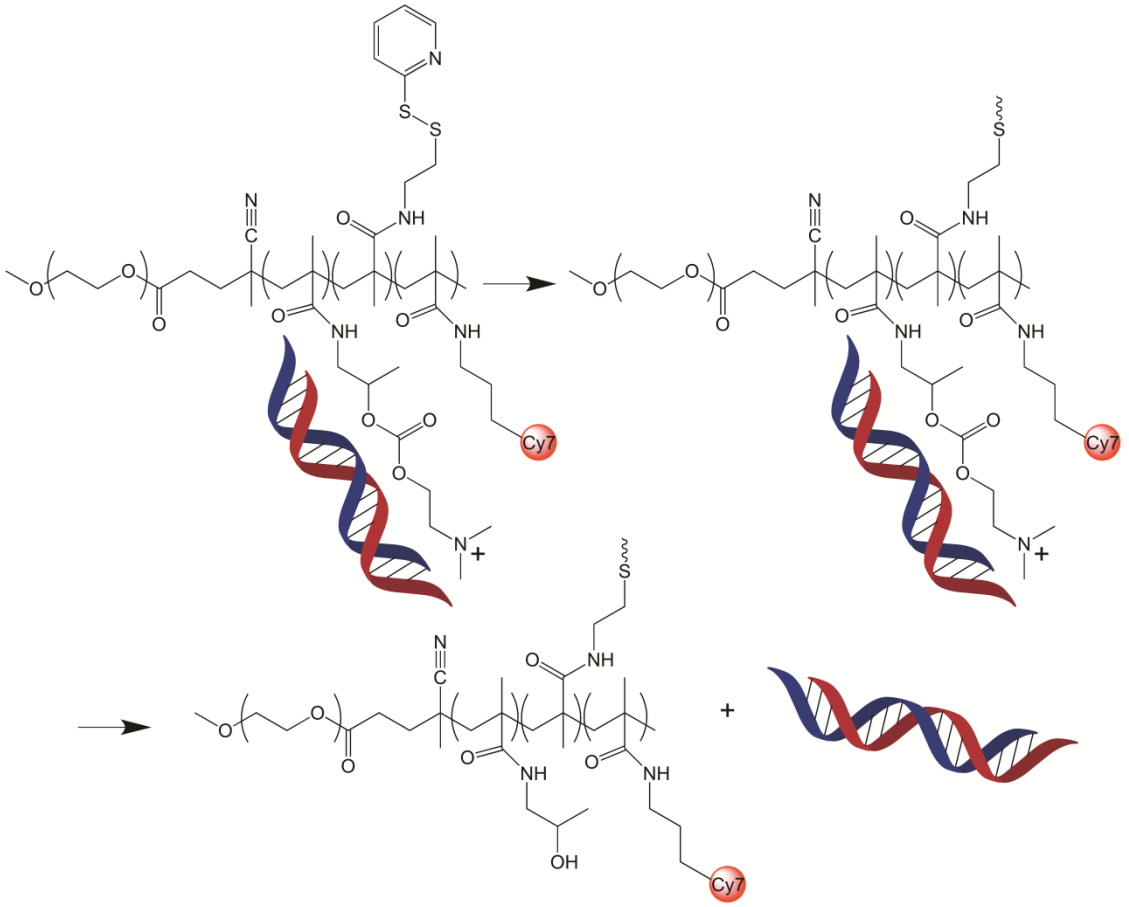

Scheme 2.3 Schematic illustration of the complexation of poly(hydroxypropyl methacrylate-*N,N'*-dimethylaminoethanol-*b*-N-[2-(2-pyridyldithio)]ethyl methacrylamide)-*b*-PEG via electrostatic interaction between the RNA and the hydroxypropyl methacrylate-*N,N'*-dimethylaminoethanol moiety, and crosslinking via disulfide formation. Subsequent de-complexation is also shown caused by hydrolysis-induced de-cationization

Monteiro and coworkers (159) developed poly(2-(*N*,*N*-dimethylamino)ethyl acrylate) which strongly resembles pDMAEMA; however, they were able to undergo self-catalyzed hydrolysis in aqueous medium into poly(acrylic acid) and 2-(*N*,*N*-dimethylamino)ethanol. This degradation occurs over 10 hours, but is independent of pH and other external cues. These de-cationizing polymers behave similarly to pDMAEMA, with the marked difference of being able to release their payload within the cytoplasm due to their degradative behavior. (111, 160) Werfel *et al*. (161) compared PEGylated copolymers of DMAEA and BMA to their DMAEMA analogue and noted an enhanced cytosol delivery of the degrading species. It is important to note that the hydrophilic protection, *e.g*. PEGylation, remains an important

component for polyplexes regardless of the charged nature of the polymer backbone. (162, 163)

2.4 Polymers directly bonded to RNA

There have been some attempts in connecting neutral polymers directly to nucleotides via labile linkers, *e.g*. disulfide (164) or pH-labile (102) bonds. This means that the nucleotide is modified, usually on the 5'-end, for this functionalization to be possible. Maynard and coworkers (164) synthesized RAFT-polymerized poly(PEG acrylate), a polymer similar to PEG, using a pyridyl disulfide (activated disulfide) RAFT agent. Poly(PEG acrylate) has been shown to facilitate passive targeting through increased circulation time. Post-polymerization, this polymer was conjugated to a thiol-modified siRNA. They obtained efficient binding, as well as reversibility of the bond. In a later publication, (165) they combined the polymer-siRNA conjugates with a fusogenic peptide KALA, which is able to facilitate endosplasmic escape, in order to assess the *in vitro* efficiency of the system. They reported that transfection efficiency was comparable, but slightly lower, than that of Lipofectamine complexed siRNA. Low and high molecular weight poly(PEG acrylate), 6000 and 17 400 $g \cdot mol^{-1}$, respectively, exhibited little impact on transfection efficiency, while the presence of both KALA and poly(PEG acrylate) components was of utmost importance, with transfection efficiency decreasing significantly with the absence of either of the components.

Recently, Lin and Maynard (166) described, for the first time, a study in which the polymer was grafted from siRNA, although the strategy had previously been used for DNA. (167) The ATRP initiator was attached to the siRNA via a disulfide bond, thus introducing a reducible link between the polymer and siRNA for later cleavage within the cytoplasm. Poly(ethylene glycol) methyl ether methacrylate (PEGMA) and di(ethylene glycol) methyl ether methacrylate (DEGMA) were grafted from the siRNA via AGET ATRP. These monomers were chosen based on having previously exhibited a nuclease stabilizing effect on siRNA. (165) They reported some low initiator efficiency, causing some siRNA to remain unreacted; however, they obtained good control over molar mass and its distribution. This technique represents a possible future alternative for the introduction of polymeric delivery. However, no *in vitro* or *in vivo* results have been published to date.

Perrier and coworkers (168) used surfactant-free emulsion polymerization to synthesize 2-(2-pyridyldithio)ethylamine modified, carboxyl-α-end HOOC-poly(acrylamide)-stabilized polystyrene latex particles. The disulfide ligand was then conjugated to a miRNA duplex via a reducible disulfide bond. Thereafter, they successfully characterized the conjugation as well as subsequent release of miRNA via incubation in glutathione. No *in vitro* results were shown, and therefore further investigation would be required in order to evaluate the true potential that these nanoparticles have within gene delivery, especially focusing on possible aggregation and serum stability.

The direct chemical modification of nucleotides can cause some difficulties, as possible side reactions may occur, and because stimulation of premature degradation of the nucleotide may take place. Furthermore, purification of a polymer-nucleotide can be challenging. To combat this, Averick *et al.* (169) reported the use of three covalently bonded, biocompatible polymers (PEG-methacrylate-pOEOMA; pOEOMA-co-MEO_2MA and pOEOMA-co-DMAEMA) to a passenger siRNA via click chemistry, in order to obtain a polymer-escort siRNA. The passenger siRNA was complementary to the guide siRNA (the biologically active therapeutic), enabling the guide strand to be annealed to the polymer-escort siRNA. This system allowed the polymers to provide nuclease resistance and facilitate cellular uptake, while the guide siRNA remained unmodified. Unfortunately, a limiting factor in this system remains, as the guide strand needs to dissociate from the passenger strand in order for it to form the RISC complex, and in so doing allowing the gene expression to be regulated. That said, *in vitro* experiments resulted in efficient luciferase knockdown for all three polymer escort systems.

2.5 Nanoparticles

As polyplex formation is dependent on electrostatic interactions, the polyplex's superstructure is thus reliant on its anionic payload, which, in this case, is the RNA/DNA molecule. Because siRNA and miRNAs are too small to guarantee stability resulting from charge, the polyplexes have an inherent flaw in their make-up. This also means that the ζ-potential of the polyplex is dependent on the siRNA and, subsequently, the aggregation behavior of the system differs depending on the payload. As mentioned before, polyplex aggregation is of grave concern. As the physiochemical properties of the superstructure are

conditional on the RNA payload, this competitive interaction with other polyanions in the physiological environment is also at the mercy of the payload. In a dynamic system, for example within the physiological environment, the polyplex's superstructure may be compromised or weakened due to this dependence on the payload. For this reason, some researchers have shifted their attention towards nanoparticles and nanogels (170) with a superstructure independent of their payloads. Nanoparticles and nanogels possess stable size and morphology, as well as stability that is independent of their load. The first siRNA clinical trial using nanoparticles as gene delivery tools was published in 2010. (7) The nanoparticles were formulated from PEG that had been conjugated to adamantine, making it able to form inclusion complexes with cyclodextrin. The nanoparticles were functionalized with transferrin protein targeting ligands in order to facilitate specific cellular uptake, due to the overexpression of transferrin protein receptors on cancer cells. Thereafter, the particles were administered intravenously and a gene knockdown effect was seen in tumor cells.

Siegwart *et al.* (171) developed a library of cationic core shell nanoparticles, with various hydrophilic surface polymers, to protrude from the nanoparticles and protect the shell. They used crosslinkers with secondary and tertiary amine functionalities in order for these nanoparticles to be able to complex with nucleotides, while still ensuring that the particle formation was not based on polymer-nucleotide interactions. Successful *in vivo* delivery of cholesterol-protected siRNA to liver hepatocytes in mice was reported, while naked siRNA was reported to be distributed to the liver, kidneys and lung.

Zentel and coworkers (172) developed cationic nanogels from amphiphilic ester precursor polymers, which show a tendency towards aggregation in polar aprotic solvents such as DMSO. They followed Siegwart's example (171) and cross-linked the hydrophobic inner core with amine functionalized cross-linkers, allowing them to obtain a cationic core for siRNA interaction. Due to a low knock-down efficiency of these nanogels, they then adapted these crosslinker molecules to contain disulfides or ketal (pH labile) linkers (173) in order to obtain second generation, degradable nanoparticles. This, in turn, produced stimuli responsive nanogels that can be destabilized under specific conditions, such as the reductive environment in the cytosol or acidic conditions in the endosome. The particle size and stability is independent of their payload. After *in vitro* analysis of these nanogels, it was ascertained that the disulfide containing cross-linker required relatively high N/P ratios

compared to the ketal-containing cross-linker. This corresponded to their previously published results. (174) This was due to the need for elevated concentrations of glutathione to be present in order for the disulfide bond to break. Such levels of glutathione are predominantly present within the cytoplasm; (175) thus, the nanogels had to be transported into the cytoplasm in order to disassemble. Predominantly, this does not seem to successfully occur. (51, 176) Therefore, they continued their *in vivo* work with the ketal-containing cross-linker and saw a significant improvement in knock-down compared to their previously unresponsive nanogels. In fact, the *in vitro* knockdown, caused by these nanoparticles being capable of effectively delivering their payload, was comparable to that of Lipofectamine. The nanoparticles were tested on different cell lines for cytotoxicity, and no significant toxicity was detected in cells after transfection with concentrations of up to 400 nM. Subsequently, Zentel and coworkers conducted consecutive injections in order to establish more information of the clearance capabilities of the degradable nanoparticles compared to the non-degradable, spermine crosslinked analogues. They discovered that the biodegradable ketal-modified particles reported superior clearance properties. The biodegradable property of these nanoparticles, as well as the high *in vitro* and *in vivo* transfection efficiency, make these nanoparticles stand out as true contenders in the race for gene therapeutic delivery systems. Of course, one area of concern is the fact that, although the particles themselves are degradable due to the cleavage of the crosslinker, their polymer components are not. This means that, while the nanoparticles degrade, the cationic polymers are still present within the cells post-degradation. These polycations may destabilize the endosomal membrane allowing for endosomal release; however, they are still able to interact with the RNA therapeutics and decrease the knockdown efficiency of the therapeutics. Furthermore, the presence of these polymers poses the same cytotoxic threat as the original polyplex systems.

Klinker *et al*. (177) recently published a study describing the formation of bio-responsive polypept(o)ide nanohydrogels synthesized from polypeptoid polysarcosine and *S*-alkylsulfonyl-protected cysteine *N*-carboxyanhydrides. The *S*-alkylsulfonyl cysteine promotes micelle self-assembly and provides a chemoselective reactivity towards thiols, allowing for reductive disulfide crosslinking. They demonstrated that these nanohydrogels are able to complex with cholesterol-modified siRNA, while still maintaining their size and morphology

and exhibiting an almost neutral ζ-potential. This provides an interesting new platform for gene therapy. However, they did not show any results describing the nanohydrogel's transfection efficiency. It is plausible that they will suffer the same challenges as Zentel's disulfide nanogels described above. Thus, further investigation is necessary in order to truly assess these nanohydrogel's future potential in the field of gene therapy.

2.6 Future outlooks

Extensive work has been conducted within the development of non-viral, polymeric delivery system for gene therapy. Nonetheless, despite all efforts, the challenges of the past decade remain prevalent. Although cationic polyplexes allow for efficient uptake, they lack biocompatibility and efficiency in knockdown effects. The issues of endosomal escape and cytosolic release are still very real and are, therefore, the limiting factor within any delivery system. Thus, they should remain the focal point when designing gene delivery systems in the future, while also keeping cytotoxicity in mind. It is probable that future research will see a marked shift towards vectors in the form of neutral or amphiphilic nanoparticles/nanogels or polymeric-RNA escort systems.

2.7 References

1. Fire A, Xu S, Montgomery MK, Kostas SA, Driver SE, Mello CC. Potent and specific genetic interference by double-stranded RNA in Caenorhabditis elegans. Nature. 1998;391:806-11.
2. Mintzer MA, Simanek EE. Nonviral vectors for gene delivery. Chem Rev. 2009;109(2):259-302.
3. de Fougerolles A, Vornlocher H-P, Maraganore J, Lieberman J. Interfering with disease: a progress report on siRNA-based therapeutics. Nature Rev Drug Discov. 2007;6:443-53.
4. DeVincenzo JP. Harnessing RNA interference to develop neonatal therapies: From Nobel Prize winning discovery to proof of concept clinical trials. Early Hum Dev. 2009;85(10, Supplement):S31-S5.
5. Vaishnaw AK, Gollob J, Gamba-Vitalo C, Hutabarat R, Sah D, Meyers R, de Fougerolles T, Maraganore J. A status report on RNAi therapeutics. Silence. 2010;1(14):1-13.
6. Dorn G, Patel S, Wotherspoon G, Hemmings-Mieszczak M, Barclay J, Natt FJC, Martin P, Bevan S, Fox A, Ganju P, Wishart W, Hall J. siRNA relieves chronic neuropathic pain. Nucleic Acids Res. 2004;32(5):e49.
7. Davis ME, Zuckerman JE, Choi CHJ, Seligson D, Tolcher A, Alabi CA, Yen Y, Heidel JD, Ribas A. Evidence of RNAi in humans from systemically administered siRNA via targeted nanoparticles. Nature. 2010;464:1067-70.
8. Sliva K, Schnierle BS. Selective gene silencing by viral delivery of short hairpin RNA. Virol J. 2010;7:248.
9. Tomar RS, Matta H, Chaudhary PM. Use of adeno-associated viral vector for delivery of small interfering RNA. Oncogene. 2003;22:5712-5.
10. Yin H, Kanasty RL, Eltoukhy AA, Vegas AJ, Dorkin JR, Anderson DG. Non-viral vectors for gene-based therapy. Nature Rev Genet. 2014;15:541-55.
11. Balazs DA, Godbey W. Liposomes for use in gene delivery. J Drug Deliv. 2011;2011:1-12.
12. Kikuchi H, Suzuki N, Ebihara K, Morita H, Ishii Y, Kikuchi A, Sugaya S, Serikawa T, Tanaka K. Gene delivery using liposome technology. J Controlled Release. 1999;62(1):269-77.

13. Santos SS, Gonzaga RV, Silva JV, Savino DF, Prieto D, Shikay JM, Silva RS, Paulo LHA, Ferreira EI, Giarolla J. Peptide dendrimers: drug/gene delivery and other approaches. Can J Chem. 2017;95(9):907-16.
14. Navarro G, Tros de Ilarduya C. Activated and non-activated PAMAM dendrimers for gene delivery in vitro and in vivo. Nanomed Nanotechnol Biol Med. 2009;5(3):287-97.
15. Hu J, Hu K, Cheng Y. Tailoring the dendrimer core for efficient gene delivery. Acta Biomater. 2016;35(Supplement C):1-11.
16. Yang J, Zhang Q, Chang H, Cheng Y. Surface-engineered dendrimers in gene delivery. Chem Rev. 2015;115(11):5274-300.
17. Prata CAH, Zhang X-X, Luo D, McIntosh TJ, Barthelemy P, Grinstaff MW. Lipophilic peptides for gene delivery. Bioconjugate Chem. 2008;19(2):418-20.
18. Martin ME, Rice KG. Peptide-guided gene delivery. AAPS Journal. 2007;9(1):E18-E29.
19. de Raad M, Teunissen EA, Mastrobattista E. Peptide vectors for gene delivery: from single peptides to multifunctional peptide nanocarriers. Nanomedicine. 2014;9(14):2217-32.
20. Zhang P, Wagner E. History of polymeric gene delivery systems. Top Curr Chem. 2017;375(2):26.
21. Park TG, Jeong JH, Kim SW. Current status of polymeric gene delivery systems. Adv Drug Del Rev. 2006;58(4):467-86.
22. Yue Y, Wu C. Progress and perspectives in developing polymeric vectors for in vitro gene delivery. Biomater Sci. 2013;1(2):152-70.
23. Bessis N, GarciaCozar FJ, Boissier MC. Immune responses to gene therapy vectors: influence on vector function and effector mechanisms. Gene Ther. 2004;11:S10-7.
24. Li S-D, Huang L. Non-viral is superior to viral gene delivery. J Controlled Release. 2007;123(3):181-3.
25. Boeckle S, von Gersdorff K, van der Piepen S, Culmsee C, Wagner E, Ogris M. Purification of polyethylenimine polyplexes highlights the role of free polycations in gene transfer. J Gene Med. 2004;6(10):1102-11.
26. Khalil IA, Kogure K, Akita H, Harashima H. Uptake pathways and subsequent intracellular trafficking in nonviral gene delivery. Pharmacol Rev. 2006;58(1):32-45.

27. Ziello JE, Huang Y, Jovin IS. Cellular endocytosis and gene delivery. Mol Med. 2010;16(5-6):222-9.

28. Jhaveri A, Torchilin V. Intracellular delivery of nanocarriers and targeting to subcellular organelles. Expert Opin Drug Discov. 2016;13(1):49-70.

29. Shete HK, Prabhu R, Patravale V. Endosomal rscape: A bottleneck in intracellular delivery. J Nanosci Nanotechnol. 2014;14(1):460-74.

30. Cho YW, Kim J-D, Park K. Polycation gene delivery systems: escape from endosomes to cytosol. J Pharm Pharmacol. 2003;55(6):721-34.

31. Modra K, Dai S, Zhang H, Shi B, Bi J. Polycation-mediated gene delivery: Challenges and considerations for the process of plasmid DNA transfection. Eng Life Sci. 2015;15(5):489-98.

32. Haladjova E, Halacheva S, Posheva V, Peycheva E, Moskova-Doumanova V, Topouzova-Hristova T, Doumanov J, Rangelov S. Comblike polyethylenimine-based polyplexes: balancing toxicity, Cell internalization, and transfection efficiency via polymer chain topology. Langmuir. 2015;31(36):10017-25.

33. Bragonzi A, Dina G, Villa A, Calori G, Biffi A, Bordignon C, Assael BM, Conese M. Biodistribution and transgene expression with nonviral cationic vector/DNA complexes in the lungs. Gene Ther. 2000;7:1753-560.

34. Di Gioia S, Rejman J, Carrabino S, De Fino I, Rudolph C, Doherty A, Hyndman L, Di Cicco M, Copreni E, Bragonzi A, Colombo C, Boyd AC, Conese M. Role of biophysical parameters on ex vivo and in vivo gene transfer to the airway epithelium by polyethylenimine/albumin complexes. Biomacromolecules. 2008;9(3):859-66.

35. Regnström K, Ragnarsson EGE, Köping-Höggård M, Torstensson E, Nyblom H, Artursson P. PEI – a potent, but not harmless, mucosal immuno-stimulator of mixed T-helper cell response and FasL-mediated cell death in mice. Gene Ther. 2003;10:1575-83.

36. Fischer D, Li Y, Ahlemeyer B, Krieglstein J, Kissel T. In vitro cytotoxicity testing of polycations: influence of polymer structure on cell viability and hemolysis. Biomaterials. 2003;24(7):1121-31.

37. Suk JS, Xu Q, Kim N, Hanes J, Ensign LM. PEGylation as a strategy for improving nanoparticle-based drug and gene delivery. Adv Drug Del Rev. 2016;99(Part A):28-51.

38. Kooijmans SAA, Fliervoet LAL, van der Meel R, Fens MHAM, Heijnen HFG, van Bergen en Henegouwen PMP, Vader P, Schiffelers RM. PEGylated and targeted extracellular vesicles display enhanced cell specificity and circulation time. J Controlled Release. 2016;224(Supplement C):77-85.

39. Ogris M, Brunner S, Schüller S, Kircheis R, Wagner E. PEGylated DNA/transferrin–PEI complexes: reduced interaction with blood components, extended circulation in blood and potential for systemic gene delivery. Gene Ther. 1999;6:595-605.

40. Liu Y, Samsonova O, Sproat B, Merkel O, Kissel T. Biophysical characterization of hyper-branched polyethylenimine-graft- polycaprolactone-block-mono-methoxyl-poly(ethylene glycol) copolymers (hy-PEI-PCL-mPEG) for siRNA delivery. J Controlled Release. 2011;153(3):262-8.

41. Tang MX, Szoka FC. The influence of polymer structure on the interactions of cationic polymers with DNA and morphology of the resulting complexes. Gene Ther. 1997;4:823-32.

42. Wadhwa MS, Collard WT, Adami RC, McKenzie DL, Rice KG. Peptide-mediated gene delivery: Influence of peptide structure on gene expression. Bioconjugate Chem. 1997;8(1):81-8.

43. Peer D, Lieberman J. Special delivery: targeted therapy with small RNAs. Gene Ther. 2011;18:1127-33.

44. Alexis F, Pridgen E, Molnar LK, Farokhzad OC. Factors affecting the clearance and biodistribution of polymeric nanoparticles. Mol Pharm. 2008;5(4):505-15.

45. York AW, Zhang Y, Holley AC, Guo Y, Huang F, McCormick CL. Facile synthesis of multivalent folate-block copolymer conjugates via aqueous RAFT polymerization: targeted delivery of siRNA and subsequent gene suppression. Biomacromolecules. 2009;10(4):936-43.

46. Dohmen C, Fröhlich T, Lächelt U, Röhl I, Vornlocher H-P, Hadwiger P, Wagner E. Defined folate-PEG-siRNA conjugates for receptor-specific gene silencing. Molecular therapy Nucleic acids. 2012;1(1):e7.

47. Mishra P, Nayak B, Dey RK. PEGylation in anti-cancer therapy: An overview. AJPS. 2016;11(3):337-48.

48. Upponi JR, Torchilin VP. Passive vs. active targeting: An update of the EPR role in drug delivery to tumors. In: Alonso MJ, Garcia-Fuentes M, editors. Nano-

Oncologicals: New Targeting and Delivery Approaches. Cham: Springer International Publishing; 2014. p. 3-45.

49. Allen MH, Day KN, Hemp ST, Long TE. Synthesis of folic acid-containing imidazolium copolymers for potential gene delivery applications. Macromol Chem Phys. 2013;214(7):797-805.

50. Sahay G, Querbes W, Alabi C, Eltoukhy A, Sarkar S, Zurenko C, Karagiannis E, Love K, Chen D, Zoncu R, Buganim Y, Schroeder A, Langer R, Anderson DG. Efficiency of siRNA delivery by lipid nanoparticles is limited by endocytic recycling. Nat Biotechnol. 2013;31:653-8.

51. Gilleron J, Querbes W, Zeigerer A, Borodovsky A, Marsico G, Schubert U, Manygoats K, Seifert S, Andree C, Stöter M, Epstein-Barash H, Zhang L, Koteliansky V, Fitzgerald K, Fava E, Bickle M, Kalaidzidis Y, Akinc A, Maier M, Zerial M. Image-based analysis of lipid nanoparticle–mediated siRNA delivery, intracellular trafficking and endosomal escape. Nat Biotechnol. 2013;31:638-46.

52. Blanco E, Shen H, Ferrari M. Principles of nanoparticle design for overcoming biological barriers to drug delivery. Nat Biotechnol. 2015;33(9):941-51.

53. Du L, Zhou J, Meng L, Wang X, Wang C, Huang Y, Zheng S, Deng L, Cao H, Liang Z, Dong A, Cheng Q. The pH-triggered triblock nanocarrier enabled highly efficient siRNA delivery for cancer therapy. Theranostics 2017;7(14):3432-45.

54. Knorr V, Allmendinger L, Walker GF, Paintner FF, Wagner E. An acetal-based PEGylation reagent for pH-sensitive shielding of DNA polyplexes. Bioconjugate Chem. 2007;18(4):1218-25.

55. Choi JS, MacKay JA, Szoka FC. Low-pH-sensitive PEG-stabilized plasmid–lipid nanoparticles: preparation and characterization. Bioconjugate Chem. 2003;14(2):420-9.

56. Li W, Huang Z, MacKay JA, Grube S, Szoka FC. Low-pH-sensitive poly(ethylene glycol) (PEG)-stabilized plasmid nanolipoparticles: effects of PEG chain length, lipid composition and assembly conditions on gene delivery. J Gene Med. 2005;7(1):67-79.

57. Walker GF, Fella C, Pelisek J, Fahrmeir J, Boeckle S, Ogris M, Wagner E. Toward synthetic viruses: Endosomal pH-triggered deshielding of targeted polyplexes greatly enhances gene transfer in vitro and in vivo. Mol Ther. 2005;11(3):418-25.

58. Murthy N, Campbell J, Fausto N, Hoffman AS, Stayton PS. Design and synthesis of pH-responsive polymeric carriers that target uptake and enhance the intracellular delivery of oligonucleotides. J Controlled Release. 2003;89(3):365-74.

59. Murthy N, Campbell J, Fausto N, Hoffman AS, Stayton PS. Bioinspired pH-responsive polymers for the intracellular delivery of biomolecular drugs. Bioconjugate Chem. 2003;14(2):412-9.

60. Gary DJ, Lee H, Sharma R, Lee J-S, Kim Y, Cui ZY, Jia D, Bowman VD, Chipman PR, Wan L, Zou Y, Mao G, Park K, Herbert B-S, Konieczny SF, Won Y-Y. Influence of nano-carrier architecture on in vitro siRNA delivery performance and in vivo biodistribution: polyplexes vs micelleplexes. ACS Nano. 2011;5(5):3493-505.

61. Xu X, Wu J, Liu Y, Yu M, Zhao L, Zhu X, Bhasin S, Li Q, Ha E, Shi J, Farokhzad OC. Ultra pH-responsive and tumor-penetrating nanoplatform for targeted siRNA delivery with robust anti-cancer efficacy. Angew Chem. 2016;55(25):7091-4.

62. Xu X, Wu J, Liu Y, Saw PE, Tao W, Yu M, Zope H, Si M, Victorious A, Rasmussen J, Ayyash D, Farokhzad OC, Shi J. Multifunctional envelope-type siRNA delivery nanoparticle platform for prostate cancer therapy. ACS Nano. 2017;11(3):2618-27.

63. Xu FJ, Ping Y, Ma J, Tang GP, Yang WT, Li J, Kang ET, Neoh KG. Comb-shaped copolymers composed of hydroxypropyl cellulose backbones and cationic poly((2-dimethyl amino)ethyl methacrylate) side chains for gene delivery. Bioconjugate Chem. 2009;20(8):1449-58.

64. Xu F-J, Li H, Li J, Zhang Z, Kang E-T, Neoh K-G. Pentablock copolymers of poly(ethylene glycol), poly((2-dimethyl amino)ethyl methacrylate) and poly(2-hydroxyethyl methacrylate) from consecutive atom transfer radical polymerizations for non-viral gene delivery. Biomaterials. 2008;29(20):3023-33.

65. Sun J, Luo T, Sheng R, Li H, Wang Z, Cao A. Intracellular plasmid DNA delivery by self-assembled nanoparticles of amphiphilic PHML-b-PLLA-b-PHML copolymers and the endocytosis pathway analysis. J Biomater Appl. 2016;31(4):606-21.

66. Xu FJ, Zhang ZX, Ping Y, Li J, Kang ET, Neoh KG. Star-shaped cationic polymers by atom transfer radical polymerization from β-cyclodextrin cores for nonviral gene delivery. Biomacromolecules. 2009;10(2):285-93.

67. Georgiou TK, Vamvakaki M, Patrickios CS, Yamasaki EN, Phylactou LA. Nanoscopic cationic methacrylate star homopolymers: synthesis by group transfer

polymerization, characterization and evaluation as transfection reagents. Biomacromolecules. 2004;5(6):2221-9.

68. Le Bon B, Van Craynest N, Boussif O, Vierling P. Polycationic Diblock and Random Polyethylene Glycol- or Tris(hydroxymethyl)methyl-Grafted (Co)telomers for Gene Transfer: Synthesis and Evaluation of Their in Vitro Transfection Efficiency. Bioconjugate Chem. 2002;13(6):1292-301.
69. Jiang X, Lok MC, Hennink WE. Degradable-brushed pHEMA–pDMAEMA synthesized via ATRP and click chemistry for gene delivery. Bioconjugate Chem. 2007;18(6):2077-84.
70. Ping Y, Liu C-D, Tang G-P, Li J-S, Li J, Yang W-T, Xu F-J. Functionalization of chitosan via atom transfer radical polymerization for gene delivery. Adv Funct Mater. 2010;20(18):3106-16.
71. Ziebarth J, Wang Y. Coarse-grained molecular dynamics simulations of DNA condensation by block copolymer and formation of core−corona structures. J Phys Chem B. 2010;114(19):6225-32.
72. Pafiti KS, Mastroyiannopoulos NP, Phylactou LA, Patrickios CS. Hydrophilic cationic star homopolymers based on a novel diethanol-N-methylamine dimethacrylate cross-linker for siRNA transfection: Synthesis, characterization, and evaluation. Biomacromolecules. 2011;12(5):1468-79.
73. Yasuhide N, Takeshi M, Makoto N, Michiko H, Moto O, Mariko H-S. High performance gene delivery polymeric vector: Nano-structured cationic star polymers (star vectors). Curr Drug Del. 2005;2(1):53-7.
74. Schallon A, Jérôme V, Walther A, Synatschke CV, Müller AHE, Freitag R. Performance of three PDMAEMA-based polycation architectures as gene delivery agents in comparison to linear and branched PEI. React Funct Polym. 2010;70(1):1-10.
75. Synatschke CV, Schallon A, Jérôme V, Freitag R, Müller AHE. Influence of polymer architecture and molecular weight of poly(2-(dimethylamino)ethyl methacrylate) polycations on transfection efficiency and cell viability in gene delivery. Biomacromolecules. 2011;12(12):4247-55.
76. Georgiou TK. Star polymers for gene delivery. Polym Int. 2014;63(7):1130-3.

77. Georgiou TK, Phylactou LA, Patrickios CS. Synthesis, characterization, and evaluation as transfection reagents of ampholytic star copolymers: effect of star architecture. Biomacromolecules. 2006;7(12):3505-12.

78. Georgiou TK, Vamvakaki M, Phylactou LA, Patrickios CS. Synthesis, characterization, and evaluation as transfection reagents of double-hydrophilic star copolymers: effect of star architecture. Biomacromolecules. 2005;6(6):2990-7.

79. Remant Bahadur KC, Uludağ H. Chapter 2: PEI and its derivatives for gene therapy. Polymers and nanomaterials for gene therapy. Alberta: Woodhead Publishing; 2016. p. 29-54.

80. Lai W-F. In vivo nucleic acid delivery with PEI and its derivatives: current status and perspectives. Expert Rev Med Devices. 2011;8(2):173-85.

81. Moghimi SM, Symonds P, Murray JC, Hunter AC, Debska G, Szewczyk A. A two-stage poly(ethylenimine)-mediated cytotoxicity: implications for gene transfer/therapy. Mol Ther. 2005;11(6):990-5.

82. Breunig M, Lungwitz U, Liebl R, Goepferich A. Breaking up the correlation between efficacy and toxicity for nonviral gene delivery. Proc Natl Acad Sci USA. 2007;104(36):14454-9.

83. Xie Q, Xinyong G, Xianjin C, Yayu W. PEI/DNA formation affects transient gene expression in suspension Chinese hamster ovary cells via a one-step transfection process. Cytotechnology. 2013;65(2):263-71.

84. Chollet P, Favrot MC, Hurbin A, Coll J-L. Side-effects of a systemic injection of linear polyethylenimine–DNA complexes. J Gene Med. 2002;4(1):84-91.

85. Kafil V, Omidi Y. Cytotoxic impacts of linear and branched polyethylenimine nanostructures in A431 cells. BioImpacts : BI. 2011;1(1):23-30.

86. Wightman L, Kircheis R, Rössler V, Carotta S, Ruzicka R, Kursa M, Wagner E. Different behavior of branched and linear polyethylenimine for gene delivery in vitro and in vivo. J Gene Med. 2001;3(4):362-72.

87. Gosselin MA, Guo W, Lee RJ. Efficient gene transfer using reversibly cross-linked low molecular weight polyethylenimine. Bioconjugate Chem. 2001;12(6):989-94.

88. Won Y-Y, Sharma R, Konieczny SF. Missing pieces in understanding the intracellular trafficking of polycation/DNA complexes. J Controlled Release. 2009;139(2):88-93.

89. Lee Y, Mo H, Koo H, Park J-Y, Cho MY, Jin G-w, Park J-S. Visualization of the degradation of a disulfide polymer, linear poly(ethylenimine sulfide), for gene delivery. Bioconjugate Chem. 2007;18(1):13-8.

90. Boussif O, Lezoualc'h F, Zanta MA, Mergny MD, Scherman D, Demeneix B, Behr JP. A versatile vector for gene and oligonucleotide transfer into cells in culture and in vivo: polyethylenimine. Proc Natl Acad Sci. 1995;92(16):7297-301.

91. Benjaminsen RV, Mattebjerg MA, Henriksen JR, Moghimi SM, Andresen TL. The possible proton sponge effect of polyethylenimine (PEI) does not include change in lysosomal pH. Mol Ther.21(1):149-57.

92. Glodde M, Sirsi SR, Lutz GJ. Physiochemical properties of low and high molecular weight poly(ethylene glycol)-grafted poly(ethylene imine) copolymers and their complexes with oligonucleotides. Biomacromolecules. 2006;7(1):347-56.

93. Merkel OM, Beyerle A, Librizzi D, Pfestroff A, Behr TM, Sproat B, Barth PJ, Kissel T. Nonviral siRNA delivery to the lung: investigation of PEG−PEI polyplexes and their in vivo performance. Mol Pharm. 2009;6(4):1246-60.

94. Liu Y, Liu Z, Wang Y, Liang Y-R, Wen X, Hu J, Yang X, Liu J, Xiao S, Cheng D. Investigation of the performance of PEG–PEI/ROCK-II-siRNA complexes for Alzheimer's disease in vitro. Brain Res. 2013;1490(Supplement C):43-51.

95. Mao S, Neu M, Germershaus O, Merkel O, Sitterberg J, Bakowsky U, Kissel T. Influence of polyethylene glycol chain length on the physicochemical and biological properties of poly(ethylene imine)-graft-poly(ethylene glycol) block copolymer/SiRNA polyplexes. Bioconjugate Chem. 2006;17(5):1209-18.

96. Nguyen HK, Lemieux P, Vinogradov SV, Gebhart CL, Guérin N, Paradis G, Bronich TK, Alakhov VY, Kabanov AV. Evaluation of polyether-polyethyleneimine graft copolymers as gene transfer agents. Gene Ther. 2000;7:126-38.

97. Chan C-L, Majzoub RN, Shirazi RS, Ewert KK, Chen Y-J, Liang KS, Safinya CR. Endosomal escape and transfection efficiency of PEGylated cationic lipid–DNA complexes prepared with an acid-labile PEG-lipid. Biomaterials. 2012;33(19):4928-35.

98. Höbel S, Appeldoorn CCM, Gaillard PJ, Aigner A. Targeted CRM197-PEG-PEI/siRNA complexes for therapeutic RNAi in glioblastoma. Pharmaceuticals. 2011;4(12):1591-606.

99. Biswal BK, Debata NB, Verma RS. Development of a targeted siRNA delivery system using FOL-PEG-PEI conjugate. Mol Biol Rep. 2010;37(6):2919-26.

100. Rudolph C, Sieverling N, Schillinger U, Lesina E, Plank C, Thünemann AF, Schönberger H, Rosenecker J. Thyroid hormone (T3)-modification of polyethyleneglycol (PEG)-polyethyleneimine (PEI) graft copolymers for improved gene delivery to hepatocytes. Biomaterials. 2007;28(10):1900-11.

101. Bahrami B, Mohammadnia-Afrouzi M, Bakhshaei P, Yazdani Y, Ghalamfarsa G, Yousefi M, Sadreddini S, Jadidi-Niaragh F, Hojjat-Farsangi M. Folate-conjugated nanoparticles as a potent therapeutic approach in targeted cancer therapy. Tumor Biol. 2015;36(8):5727-42.

102. Oishi M, Sasaki S, Nagasaki Y, Kataoka K. pH-responsive oligodeoxynucleotide (ODN)−poly(ethylene glycol) conjugate through acid-labile β-thiopropionate linkage: Preparation and polyion complex micelle formation. Biomacromolecules. 2003;4(5):1426-32.

103. Carlisle RC, Etrych T, Briggs SS, Preece JA, Ulbrich K, Seymour LW. Polymer-coated polyethylenimine/DNA complexes designed for triggered activation by intracellular reduction. J Gene Med. 2004;6(3):337-44.

104. Verbaan FJ, Oussoren C, Snel CJ, Crommelin DJA, Hennink WE, Storm G. Steric stabilization of poly(2-(dimethylamino)ethyl methacrylate)-based polyplexes mediates prolonged circulation and tumor targeting in mice. J Gene Med. 2004;6(1):64-75.

105. Lee H, Son SH, Sharma R, Won Y-Y. A discussion of the pH-dependent protonation behaviors of poly(2-(dimethylamino)ethyl methacrylate) (PDMAEMA) and poly(ethylenimine-ran-2-ethyl-2-oxazoline) (P(EI-r-EOz)). J Phys Chem B. 2011;115(5):844-60.

106. Wang ZH, Li WB, Ma J, Tang GP, Yang WT, Xu FJ. Functionalized nonionic dextran backbones by atom transfer radical polymerization for efficient gene delivery. Macromolecules. 2011;44(2):230-9.

107. Cai J, Yue Y, Rui D, Zhang Y, Liu S, Wu C. Effect of chain length on cytotoxicity and endocytosis of cationic polymers. Macromolecules. 2011;44(7):2050-7.

108. Guo S, Huang Y, Wei T, Zhang W, Wang W, Lin D, Zhang X, Kumar A, Du Q, Xing J, Deng L, Liang Z, Wang PC, Dong A, Liang X-J. Amphiphilic and biodegradable methoxy

polyethylene glycol-block-(polycaprolactone-graft-poly(2-(dimethylamino)ethyl methacrylate)) as an effective gene carrier. Biomaterials. 2011;32(3):879-89.

109. Nelson CE, Kintzing JR, Hanna A, Shannon JM, Gupta MK, Duvall CL. Balancing cationic and hydrophobic content of PEGylated siRNA polyplexes enhances endosome escape, stability, blood circulation time, and bioactivity in vivo. ACS Nano. 2013;7(10):8870-80.

110. Benoit DSW, Srinivasan S, Shubin AD, Stayton PS. Synthesis of folate-functionalized RAFT polymers for targeted siRNA delivery. Biomacromolecules. 2011;12(7):2708-14.

111. Convertine AJ, Diab C, Prieve M, Paschal A, Hoffman AS, Johnson PH, Stayton PS. pH-responsive polymeric micelle carriers for siRNA drugs. Biomacromolecules. 2010;11(11):2904-11.

112. Song Y, Zhang T, Song X, Zhang L, Zhang C, Xing J, Liang X-J. Polycations with excellent gene transfection ability based on PVP-g-PDMAEMA with random coil and micelle structures as non-viral gene vectors. J Mater Chem B. 2015;3(5):911-8.

113. Newland B, Tai H, Zheng Y, Velasco D, Di Luca A, Howdle SM, Alexander C, Wang W, Pandit A. A highly effective gene delivery vector - hyperbranched poly(2-(dimethylamino)ethyl methacrylate) from in situ deactivation enhanced ATRP. Chem Commun. 2010;46(26):4698-700.

114. Vader P, van der Aa LJ, Engbersen JFJ, Storm G, Schiffelers RM. A method for quantifying cellular uptake of fluorescently labeled siRNA. J Controlled Release. 2010;148(1):106-9.

115. You Y-Z, Manickam DS, Zhou Q-H, Oupický D. Reducible poly(2-dimethylaminoethyl methacrylate): Synthesis, cytotoxicity, and gene delivery activity. J Controlled Release. 2007;122(3):217-25.

116. Carlsson L, Fall A, Chaduc I, Wagberg L, Charleux B, Malmstrom E, D'Agosto F, Lansalot M, Carlmark A. Modification of cellulose model surfaces by cationic polymer latexes prepared by RAFT-mediated surfactant-free emulsion polymerization. Polym Chem. 2014;5(20):6076-86.

117. Gary DJ, Min JB, Kim Y, Park K, Won Y-Y. The Effect of N/P ratio on the in vitro and in vivo interaction properties of PEGylated poly(2-(dimethylamino)ethyl methacrylate)-based siRNA complexes. Macromol Biosci. 2013;13(8):1059-71.

118. Malcolm DW, Freeberg MAT, Wang Y, Sims KR, Awad HA, Benoit DSW. Diblock copolymer hydrophobicity facilitates efficient gene silencing and cytocompatible nanoparticle-mediated siRNA delivery to musculoskeletal cell types. Biomacromolecules. 2017;18(11):3753-65.

119. Lin S, Du F, Wang Y, Ji S, Liang D, Yu L, Li Z. An acid-labile block copolymer of PDMAEMA and PEG as potential carrier for intelligent gene delivery systems. Biomacromolecules. 2008;9(1):109-15.

120. Choi YH, Liu F, Kim J-S, Choi YK, Jong Sang P, Kim SW. Polyethylene glycol-grafted poly-l-lysine as polymeric gene carrier. J Controlled Release. 1998;54(1):39-48.

121. Harada-Shiba M, Yamauchi K, Harada A, Takamisawa I, Shimokado K, Kataoka K. Polyion complex micelles as vectors in gene therapy – pharmacokinetics and in vivo gene transfer. Gene Ther. 2002;9:407-14.

122. Navarro G, Pan J, Torchilin VP. Micelle-like nanoparticles as carriers for DNA and siRNA. Mol Pharm. 2015;12(2):301-13.

123. Jeong JH, Park TG. Poly(l-lysine)-g-poly(d,l-lactic-co-glycolic acid) micelles for low cytotoxic biodegradable gene delivery carriers. J Controlled Release. 2002;82(1):159-66.

124. Kim HJ, Miyata K, Nomoto T, Zheng M, Kim A, Liu X, Cabral H, Christie RJ, Nishiyama N, Kataoka K. siRNA delivery from triblock copolymer micelles with spatially-ordered compartments of PEG shell, siRNA-loaded intermediate layer, and hydrophobic core. Biomaterials. 2014;35(15):4548-56.

125. Patil ML, Zhang M, Minko T. Multifunctional triblock nanocarrier (PAMAM-PEG-PLL) for the efficient intracellular siRNA delivery and gene silencing. ACS Nano. 2011;5(3):1877-87.

126. Deng J, Gao N, Wang Y, Yi H, Fang S, Ma Y, Cai L. Self-assembled cationic micelles based on PEG-PLL-PLLeu hybrid polypeptides as highly effective gene vectors. Biomacromolecules. 2012;13(11):3795-804.

127. Bates FS, Hillmyer MA, Lodge TP, Bates CM, Delaney KT, Fredrickson GH. Multiblock polymers: panacea or pandora's box? Science. 2012;336(6080):434-40.

128. Moughton AO, Hillmyer MA, Lodge TP. Multicompartment block polymer micelles. Macromolecules. 2012;45(1):2-19.

129. Matsumoto S, Christie RJ, Nishiyama N, Miyata K, Ishii A, Oba M, Koyama H, Yamasaki Y, Kataoka K. Environment-responsive block copolymer micelles with a disulfide cross-linked core for enhanced siRNA delivery. Biomacromolecules. 2009;10(1):119-27.

130. Oishi M, Nagasaki Y, Itaka K, Nishiyama N, Kataoka K. Lactosylated poly(ethylene glycol)-siRNA conjugate through acid-labile β-thiopropionate linkage to construct pH-sensitive polyion complex micelles achieving enhanced gene silencing in hepatoma cells. J Am Chem Soc. 2005;127(6):1624-5.

131. Shi J, Johnson RN, Schellinger JG, Carlson PM, Pun SH. Reducible HPMA-co-oligolysine copolymers for nucleic acid delivery. Int J Pharm. 2012;427(1):113-22.

132. Zhou J, Patel TR, Fu M, Bertram JP, Saltzman WM. Octa-functional PLGA nanoparticles for targeted and efficient siRNA delivery to tumors. Biomaterials. 2012;33(2):583-91.

133. Panyam J, Zhou W-Z, Prabha S, Sahoo SK, Labhasetwar V. Rapid endo-lysosomal escape of poly(D,L-lactide-co-glycolide) nanoparticles: implications for drug and gene delivery. FASEB J. 2002;16(10):1217-26.

134. Pillai JJ, Thulasidasan AKT, Anto RJ, Devika NC, Ashwanikumar N, Kumar GSV. Curcumin entrapped folic acid conjugated PLGA-PEG nanoparticles exhibit enhanced anticancer activity by site specific delivery. RSC Advances. 2015;5(32):25518-24.

135. Arora S, Swaminathan SK, Kirtane A, Srivastava SK, Bhardwaj A, Singh S, Panyam J, Singh AP. Synthesis, characterization, and evaluation of poly (D,L-lactide-co-glycolide)-based nanoformulation of miRNA-150: potential implications for pancreatic cancer therapy. Int J Nanomedicine. 2014;9:2933-42.

136. Cameron DJA, Shaver MP. Aliphatic polyester polymer stars: synthesis, properties and applications in biomedicine and nanotechnology. Chem Soc Rev. 2011;40(3):1761-76.

137. Zhang C. Biodegradable polyesters: Synthesis, properties, applications. Biodegradable Polyesters. Weinheim: Wiley-VCH Verlag GmbH & Co. KGaA; 2015. p. 1-24.

138. Reul R, Nguyen J, Biela A, Marxer E, Bakowsky U, Klebe G, Kissel T. Biophysical and biological investigation of DNA nano-complexes with a non-toxic, biodegradable amine-modified hyperbranched polyester. Int J Pharm. 2012;436(1-2):97-105.

139. Nelson AM, Pekkanen AM, Forsythe NL, Herlihy JH, Zhang M, Long TE. Synthesis of water-soluble imidazolium polyesters as potential nonviral gene delivery vehicles. Biomacromolecules. 2017;18(1):68-76.

140. Kozielski KL, Tzeng SY, Green JJ. A bioreducible linear poly([small beta]-amino ester) for siRNA delivery. Chem Commun. 2013;49(46):5319-21.

141. Kozielski KL, Tzeng SY, Hurtado De Mendoza BA, Green JJ. Bioreducible cationic polymer-based nanoparticles for efficient and environmentally triggered cytoplasmic siRNA delivery to primary human brain cancer cells. ACS Nano. 2014;8(4):3232-41.

142. Ornelas-Megiatto C, Wich PR, Fréchet JMJ. Polyphosphonium polymers for siRNA delivery: An efficient and nontoxic alternative to polyammonium carriers. J Am Chem Soc. 2012;134(4):1902-5.

143. Hemp ST, Allen MH, Green MD, Long TE. Phosphonium-containing polyelectrolytes for nonviral gene delivery. Biomacromolecules. 2012;13(1):231-8.

144. Hemp ST, Smith AE, Bryson JM, Allen MH, Long TE. Phosphonium-containing diblock copolymers for enhanced colloidal stability and efficient nucleic acid delivery. Biomacromolecules. 2012;13(8):2439-45.

145. Picquet E, Le Ny K, Delépine P, Montier T, Yaouanc J-J, Cartier D, des Abbayes H, Férec C, Clément J-C. Cationic lipophosphoramidates and lipophosphoguanidines are very efficient for in vivo DNA delivery. Bioconjugate Chem. 2005;16(5):1051-3.

146. Floch V, Loisel S, Guenin E, Hervé AC, Clément JC, Yaouanc JJ, des Abbayes H, Férec C. Cation substitution in cationic phosphonolipids: a new concept to improve transfection activity and decrease cellular toxicity. J Med Chem. 2000;43(24):4617-28.

147. Guénin E, Hervé A-C, Floch V, Loisel S, Yaouanc J-J, Clément J-C, Férec C, des Abbayes H. Cationic phosphonolipids containing quaternary phosphonium and arsonium groups for DNA transfection with good efficiency and low cellular toxicity. Angew Chem Int Ed. 2000;39(3):629-31.

148. Convertine AJ, Benoit DSW, Duvall CL, Hoffman AS, Stayton PS. Development of a novel endosomolytic diblock copolymer for siRNA delivery. J Controlled Release. 2009;133(3):221-9.

149. Song Y, Wang H, Zeng X, Sun Y, Zhang X, Zhou J, Zhang L. Effect of molecular weight and degree of substitution of quaternized cellulose on the efficiency of gene transfection. Bioconjugate Chem. 2010;21(7):1271-9.

150. Monge S, Canniccioni B, Graillot A, Robin J-J. Phosphorus-containing polymers: A great opportunity for the biomedical field. Biomacromolecules. 2011;12(6):1973-82.

151. Knop K, Hoogenboom R, Fischer D, Schubert US. Poly(ethylene glycol) in drug delivery: pros and cons as well as potential alternatives. Angew Chem Int Ed. 2010;49(36):6288-308.

152. Aji Alex MR, Nagpal N, Kulshreshtha R, Koul V. Synthesis and evaluation of cationically modified poly(styrene-alt-maleic anhydride) nanocarriers for intracellular gene delivery. RSC Advances. 2015;5(28):21931-44.

153. Zhang Y-M, Huang Z, Zhang J, Wu W-X, Liu Y-H, Yu X-Q. Amphiphilic polymers formed from ring-opening polymerization: a strategy for the enhancement of gene delivery. Biomater Sci. 2017;5(4):718-29.

154. Duan X, Xiao J, Yin Q, Zhang Z, Mao S, Li Y. Amphiphilic graft copolymer based on poly(styrene-co-maleic anhydride) with low molecular weight polyethylenimine for efficient gene delivery. Int J Nanomedicine. 2012;7:4961-72.

155. Choksakulnimitr S, Masuda S, Tokuda H, Takakura Y, Hashida M. In vitro cytotoxicity of macromolecules in different cell culture systems. J Controlled Release. 1995;34(3):233-41.

156. Ballarín-González B, Howard KA. Polycation-based nanoparticle delivery of RNAi therapeutics: Adverse effects and solutions. Adv Drug Del Rev. 2012;64(15):1717-29.

157. Merkel OM, Beyerle A, Beckmann BM, Zheng M, Hartmann RK, Stöger T, Kissel TH. Polymer-related off-target effects in non-viral siRNA delivery. Biomaterials. 2011;32(9):2388-98.

158. Novo L, Rizzo LY, Golombek SK, Dakwar GR, Lou B, Remaut K, Mastrobattista E, van Nostrum CF, Jahnen-Dechent W, Kiessling F, Braeckmans K, Lammers T, Hennink WE. Decationized polyplexes as stable and safe carrier systems for improved biodistribution in systemic gene therapy. J Controlled Release. 2014;195-175:162-75.

159. Truong NP, Jia Z, Burges M, McMillan NAJ, Monteiro MJ. Self-catalyzed degradation of linear cationic poly(2-dimethylaminoethyl acrylate) in water. Biomacromolecules. 2011;12(5):1876-82.

160. Truong NP, Jia Z, Burgess M, Payne L, McMillan NAJ, Monteiro MJ. Self-catalyzed degradable cationic polymer for release of DNA. Biomacromolecules. 2011;12(10):3540-8.

161. Werfel TA, Swain C, Nelson CE, Kilchrist KV, Evans BC, Miteva M, Duvall CL. Hydrolytic charge-reversal of PEGylated polyplexes enhances intracellular un-packaging and activity of siRNA. J Biomed Mater Res Part A. 2016;104(4):917-27.

162. Walkey CD, Chan WCW. Understanding and controlling the interaction of nanomaterials with proteins in a physiological environment. Chem Soc Rev. 2012;41(7):2780-99.

163. Dakwar GR, Zagato E, Delanghe J, Hobel S, Aigner A, Denys H, Braeckmans K, Ceelen W, De Smedt SC, Remaut K. Colloidal stability of nano-sized particles in the peritoneal fluid: Towards optimizing drug delivery systems for intraperitoneal therapy. Acta Biomater. 2014;10(7):2965-75.

164. Heredia KL, Nguyen TH, Chang C-W, Bulmus V, Davis TP, Maynard HD. Reversible siRNA-polymer conjugates by RAFT polymerization. Chem Commun. 2008(28):3245-7.

165. Gunasekaran K, Nguyen TH, Maynard HD, Davis TP, Bulmus V. Conjugation of siRNA with comb-type PEG enhances serum stability and gene silencing efficiency. Macromol Rapid Commun. 2011;32(8):654-9.

166. Lin E-W, Maynard HD. Grafting from small interfering ribonucleic acid (siRNA) as an alternative synthesis route to siRNA–polymer conjugates. Macromolecules. 2015;48(16):5640-7.

167. Averick SE, Dey SK, Grahacharya D, Matyjaszewski K, Das SR. Solid-phase incorporation of an ATRP initiator for polymer–DNA biohybrids. Angew Chem Int Ed. 2014;53(10):2739-44.

168. Poon CK, Tang O, Chen X-M, Pham BTT, Gody G, Pollock CA, Hawkett BS, Perrier S. Preparation of inert polystyrene latex particles as microRNA delivery vectors by surfactant-free RAFT emulsion polymerization. Biomacromolecules. 2016;17(3):965-73.

169. Averick SE, Paredes E, Dey SK, Snyder KM, Tapinos N, Matyjaszewski K, Das SR. Autotransfecting short interfering RNA through facile covalent polymer escorts. J Am Chem Soc. 2013;135(34):12508-11.

170. Nuhn L, Tomcin S, Miyata K, Mailänder V, Landfester K, Kataoka K, Zentel R. Size-dependent knockdown potential of siRNA-loaded cationic nanohydrogel particles. Biomacromolecules. 2014;15(11):4111-21.

171. Siegwart DJ, Whitehead KA, Nuhn L, Sahay G, Cheng H, Jiang S, Ma M, Lytton-Jean A, Vegas A, Fenton P, Levins CG, Love KT, Lee H, Cortez C, Collins SP, Li YF, Jang J, Querbes W, Zurenko C, Novobrantseva T, Langer R, Anderson DG. Combinatorial synthesis of chemically diverse core-shell nanoparticles for intracellular delivery. Proc Natl Acad Sci. 2011;108(32):12996-3001.

172. Nuhn L, Hirsch M, Krieg B, Koynov K, Fischer K, Schmidt M, Helm M, Zentel R. Cationic nanohydrogel particles as potential siRNA carriers for cellular delivery. ACS Nano. 2012;6(3):2198-214.

173. Leber N, Kaps L, Aslam M, Schupp J, Brose A, Schäffel D, Fischer K, Diken M, Strand D, Koynov K, Tuettenberg A, Nuhn L, Zentel R, Schuppan D. SiRNA-mediated in vivo gene knockdown by acid-degradable cationic nanohydrogel particles. J Controlled Release. 2017;248(Supplement C):10-23.

174. Nuhn L, Braun L, Overhoff I, Kelsch A, Schaeffel D, Koynov K, Zentel R. Degradable cationic nanohydrogel particles for stimuli-responsive release of siRNA. Macromol Rapid Commun. 2014;35(24):2057-64.

175. Soboll S, Gründel S, Harris J, Kolb-Bachofen V, Ketterer B, Sies H. The content of glutathione and glutathione S-transferases and the glutathione peroxidase activity in rat liver nuclei determined by a non-aqueous technique of cell fractionation. Biochem J. 1995;311(3):889-94.

176. Sahay G, Querbes W, Alabi C, Eltoukhy A, Sarkar S, Zurenko C, Karagiannis E, Love K, Chen D, Zoncu R, Buganim Y, Schroeder A, Langer R, Anderson DG. Efficiency of siRNA delivery by lipid nanoparticles is limited by endocytic recycling. Nat Biotechnol. 2013;31(7):653-8.

177. Klinker K, Schäfer O, Huesmann D, Bauer T, Capelôa L, Braun L, Stergiou N, Schinnerer M, Dirisala A, Miyata K, Osada K, Cabral H, Kataoka K, Barz M. Secondary-structure-driven self-assembly of reactive polypept(o)ides: controlling size, shape, and function of core cross-linked nanostructures. Angew Chem Int Ed. 2017;56(32):9608-13.

Chapter 3: Facile routes to telechelic poly(N-vinylpyrrolidone) with high chain end fidelity

Synopsis

α,ω-Heterotelechelic vinyl polymers with high chain-end fidelity, and their block copolymers, have attracted much attention for applications in drug delivery. However, their synthesis requires multiple steps of protection, deprotection and/or activation. In this chapter, a facile route of obtaining poly(*N*-vinylpyrrolidone) using chain transfer agents (CTAs) that were previously believed to be 'unsuitable' was designed. This method resulted in difunctional PVP with high chain end fidelity, as well as PVP polymerized using a bromine functional xanthate CTA in order to produce PVP macroATRP initiators for later chain extension with activated monomers.

3.1 Introduction

Precision polymers have played an integral role in the advancement of drug delivery by providing a platform for targeted delivery of drugs, controlled release and increased circulation, leading to lowered overall dosages and reduced side-effects. (1-4) These polymeric drug delivery systems have developed into responsive structures with the not-so-improbable hope of tailor-making them for specific applications. As such, it can be very beneficial to couple bioactive compounds or biomacromolecules to telechelic polymers containing complementary functional end-groups. (5-10) Therefore, there is growing interest in producing α,ω-heterotelechelic polymers, whereby the end-groups can react orthogonally to produce "smarter" systems. The advancement of reversible deactivation radical polymerization techniques (RDRP), such as reversible addition–fragmentation chain transfer (RAFT) mediated polymerization (11-15) and atom–transfer radical polymerization (ATRP) (16, 17), has provided a simplistic route to obtain polymers with controlled molecular weight, narrow molecular weight distributions and defined end-groups available for bioconjugation. RAFT–mediated polymerization utilizes a chain transfer agent in order to control the polymerization. These chain transfer agents employed in RAFT–mediated polymerization are made up of a leaving (R–) group and a thiocarbonyl thio (Z–) group, which form the α– and ω–chain ends of the final polymer, respectively, Scheme 3.1 (12-15, 18) Therefore, through careful selection of functional R– and Z–groups, it is possible to impart desired α– and ω–end group functionalities.

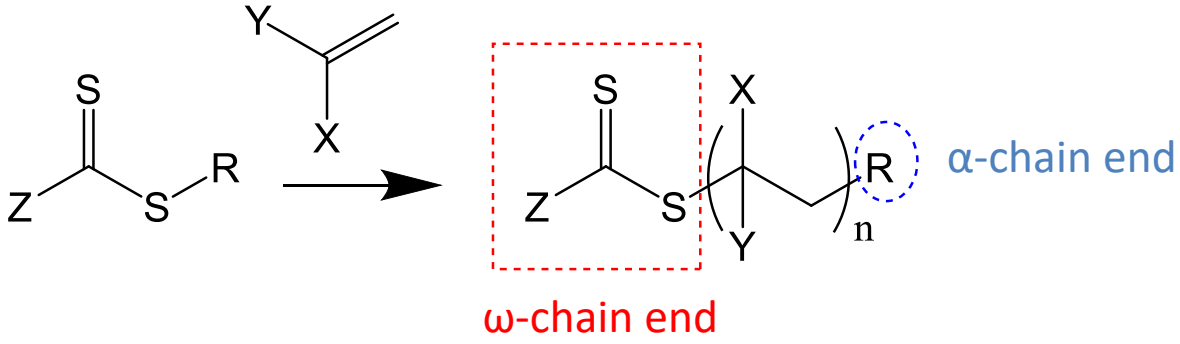

Scheme 3.1 General representation of a RAFT–mediated polymerization using chain transfer agents containing an R and Z group, resulting in polymers with α– and ω–chain ends, respectively

The instability of the Z–group to nucleophiles allows for a simple route in which the ω-chain end can be modified, post-polymerization, in order to obtain useful functional groups, including via aminolysis, hydrolysis, thermolysis, oxidation and reduction. (19, 20) The production of thiols and disulfides through aminolysis is particularly useful, since thiols readily react in a Michael addition with acrylate, vinylsulfone and maleimide functionalities (21-24), while disulfides are useful to produce biologically reducible bonds with peptides or proteins. (25)

Several studies imparted α-chain end functionality on polymers by designing RAFT agents with R-groups that contain functional groups such as activated disulfides (26), activated esters (27), biotin (6) or azides. (28) These can be used post-polymerization for further modification to yield α-end functional polymers. However, the use of reactive functional R–groups causes difficulties for the polymerization of many monomers, especially true for (less activated) vinyl monomers such as *N*VP. (29-32) It has previously been reported by our group that *N*VP can undergo many side reactions during xanthate–mediated polymerization, which negatively influence the control over the polymerization. (33) Pound *et al*. previously reported that the presence of certain functional groups on the RAFT agent enhances the formation of side products during the polymerization of *N*VP. This was especially true in the presence of xanthates containing *R*-groups with carboxylic acid and hydroxyl functionalities, which were shown to cause significant dimer formation of *N*VP. (33) Therefore, restrictions are placed on the type of functional groups that can be present during RAFT–mediated polymerization of *N*VP. Of course, this means that if any of these 'restricted' functionalities are desired, post-polymerization functionalization is necessary, which is not always straightforward or facile.

In order to obtain α,ω-heterotelechelic PVP, the restrictions caused by R-group functionality must be circumvented. Different RAFT agents have been designed whereby functional groups have been protected, and are subsequently deprotected post-polymerization, or altered post-polymerization. (34-36) Shimoni *et al*. (34), for example, polymerized *N*VP in the presence of *O*-ethyl *S*-(phthalimidomethyl) xanthate. Post-polymerization they used hydrazine, which aminolyzed the xanthate into a thiol and hydrazinolyzed the phthalamidomethyl R-group, in order to obtain a primary amine. Another such example has been described in our group, where Reader *et al*. (36) designed a linear acetal functionalized

RAFT agent, *O*-{1-[1-(3,3-diethoxypropyl)-1H-1,2,3-triazol-4-yl]ethyl} *O*-ethyl carbonodithioate, whereby a one-pot orthogonal end-group modification procedure was employed to obtain α,ω-heterotelechelic polymer. In this case, the linear acetal functional α-end group was converted into an aldehyde group and the xanthate ω-chain end was converted into a thiol. However, very high CTA:AIBN (4:1) ratios were necessary in order to achieve reasonable monomer conversion. This high ratio is known to lead to loss of end-groups, yielding lower functionality, which is defying the ultimate goal of using this RAFT agent.

The common method of xanthate–mediated polymerization of *N*VP is at 60 °C in bulk or in organic solvents. (29, 30, 32, 33, 37-47) Via this method, it is accepted that up to 10% of the polymer chain ends are unsaturated. (33) Anything above this temperature increases the formation of unsaturated chain ends. These unsaturated chain ends lead to a loss of ω-chain end functionality. Furthermore, water, as a rule, has been avoided as a solvent, as it is known to react with *N*VP, thus causing numerous side-reactions to occur. (33, 48-51) However, there are many advantages of using an aqueous medium in a polymerization process, the most important of these being that it is non-toxic and environmentally friendly. Due to the high viscosity within the reaction mixture that occurs during bulk polymerization, complications arise, such as increased dispersity, unsaturated chain ends, and ultimately decreased control over the polymerization. This is especially true at high monomer conversion. Destarac *et al*. (52, 53) successfully polymerized *N*VP in aqueous medium at low temperatures using redox initiators (ascorbic acid/t-BuOOH and Na_2SO_3/t-BuOOH) in the presence of a xanthate CTA. The byproducts of hydrolysis and dimer formation that are typically present during xanthate–mediated polymerizations of *N*VP at elevated temperature in organic media were shown to be absent under these conditions and, due to the low temperature, no formation of unsaturated chain ends seemed to occur.

Due to the low activity of *N*VP, it requires the use of a RAFT agent with a poorly stabilizing Z-group, such as a xanthate or dithiocarbamate. (14, 18, 30, 37) However, this presents challenges in preparing block copolymers containing PVP, since these Z-groups are unsuitable for more activated monomers. (14, 15) The idea of block copolymers containing PVP remains appealing; hence, several studies have investigated ways in which to obtain such block copolymers, including the use of ‘switchable’-CTAs. (43) Others have separately

synthesized homopolymers and conjugated the blocks through click chemistry. (54) More recently, there have been some studies investigating the use of dual RAFT/ATRP chloroxanthate CTAs. (44, 55) Matyjaszewski and coworkers (44) reported that the presence of small amounts of bromoxanthate polyfunctional initiator-transfer agents, or inifers, leads to almost quantitative dimerization of NVP, and therefore, they employed a chloroxanthate inifer with decreased electrophilicity compared to the bromoxanthate inifer. Despite the success of the polymerization using the chloroxanthate CTA, they faced problems when chain extending the PVP macroinitiators, possibly due to the single methyl substituent on the R-group of the CTA, but also possibly due to the chloro– rather than bromo– ATRP intiator. Employing a similar system containing two methyl substituents on the R-group, Jumeaux *et al*., (55) showed successful RAFT–mediated polymerization of *N*VP and ATRP–mediated chain extension of triethylene glycol methacrylate (TEGMA), Scheme 3.2. However, if it were conceivable to use bromoxanthate CTA, the possible applications of the block copolymers are endless.

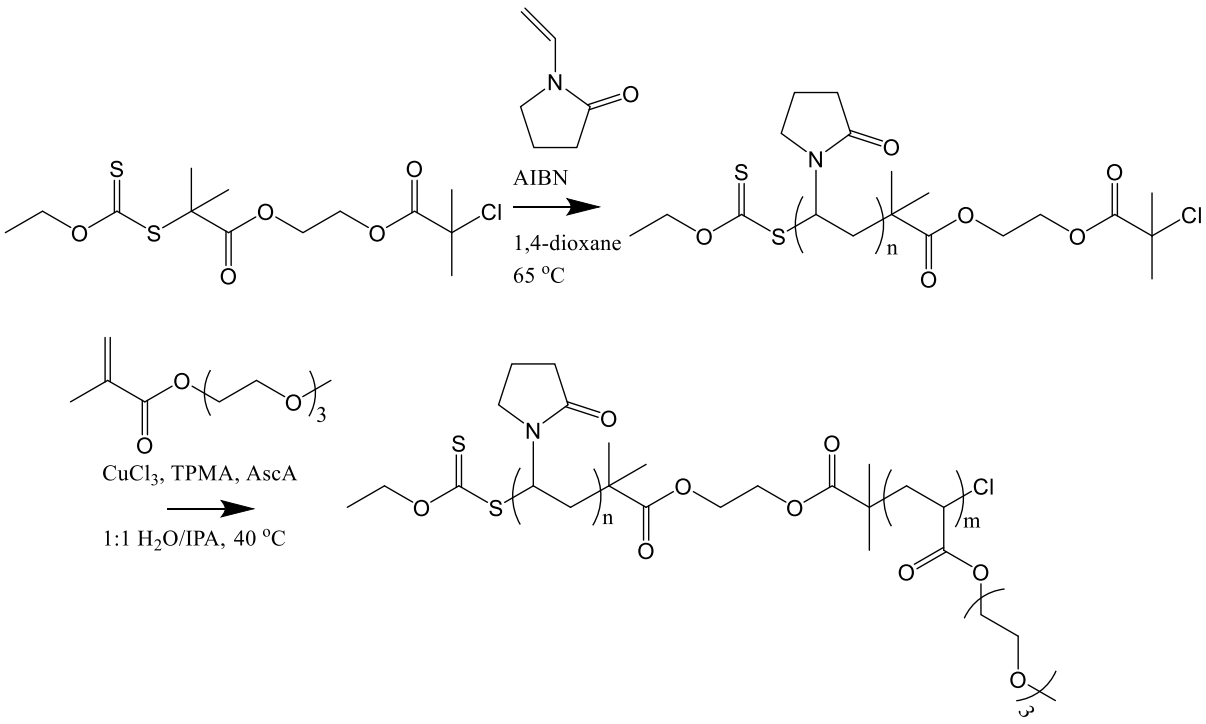

Scheme 3.2 RAFT-mediated polymerization of NVP using chloroxanthate chain transfer agent and further chain extention of the macroinitiator with triethylene glycol methacrylate, as described by Jumeaux *et al*. (55)

Since the commercial applications of functional PVP are widespread, the ideal polymerization method is one that allows for the facile production of α,ω-heterotelechelic polymers with high chain-end fidelity. Furthermore, simple preparation of block copolymers of PVP holds exciting possibilities. In this study, a method is presented whereby unpurified *N*VP is polymerized to high monomer conversion and with good control over molecular weight in the presence of CTAs containing functionalities that were previously deemed unsuitable. Through NMR spectroscopic analysis, high chain-end fidelity is illustrated. Furthermore, the ability of polymerizing *N*VP with a bromoxanthate CTA, previously reported to cause dimerization of *N*VP and thus cause retardation of the polymerization, is shown. (44) This allows for the formation of PVP macro-ATRP initiators for future chain extension with activated monomers.

3.2 Results and Discussion

3.2.1 Polymerization of NVP

The three CTAs (**R3.1-3**) seen in Figure 3.1 were synthesized for this study. CTAs R3.1 and R3.2 were synthesized according to protocols previously reported by Pound *et al*. (33) R3.2 has previously been used in the polymerization of *N*VP in our group; however, the results showed large fractions of unsaturated chain ends and poor monomer conversions. (56) Pound *et al*. (33) showed that the use of **R3.1** and **R3.2** as CTAs in the RAFT–mediated polymerization of *N*VP resulted in dimer formation, and retardation of conversion to PVP. **R3.3** is a novel CTA, where 1-ethyl-3-(3-dimethylaminopropyl)carbodiimide (EDC) was used to couple R3.1 and 2-hydroxybenzaldehyde via a carbodiimide coupling reaction. **R3.3**, the benzaldehyde functional CTA, provides a novel way to introduce a benzaldehyde functional group pre-polymerization. According to ^{1}H NMR spectrum, two isomers of **R3.3** are present in the final product; approximately 30% of the benzaldehyde group is in the meta-position while the rest is in the ortho-position, Figure 3.6 (a) in Section 3.2.2. The isomeric positioning of the benzaldehyde is of no consequence to the end-application as the importance simply lies in the presence of the functional group for end group conjugation. There is an unassigned quartet peak in the ^{1}H NMR spectrum at 9.91 ppm, possibly due to an impurity. However, purification via column chromatography was unsuccessful. **R3.3** was

used, as is, for the polymerization of *N*VP, discussed further in Section 3.2.2. The use of an aldehyde functional CTA has, to our knowledge, never been reported in literature.

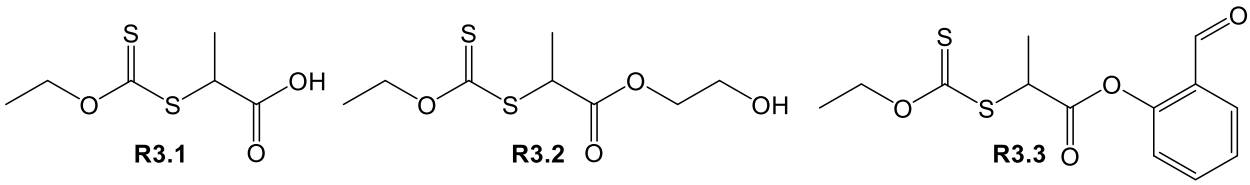

Figure 3.1 Chemical structures of chain transfer agents R3.1-3 used for the RAFT-mediated polymerization of *N*VP

Table 3.1 A summary of results from RAFT–mediated polymerization of NVP using R3.1-3

Entry	Solvent	Initiator	NVP	CTA	Temp (°C)	Time (h)	$\alpha^{\ddagger}$ (%)	$M_{n,\,theo}$ (g·mol^{-1})	$M_n^{\S}$ (g·mol^{-1})	$M_W^{\S}$ (g·mol^{-1})	$Đ^{\S}$
P3.1	water	$C_6H_8O_6$/ t-BuOOH	undistilled	R3.1	25	7	81	1700	1000	1300	1.2
P3.2	water	$C_6H_8O_6$/ t-BuOOH	undistilled	R3.1	25	4	95	4750	4100	4900	1.2
P3.3	water	$C_6H_8O_6$/ t-BuOOH	distilled	R3.1	25	15	93	4650	4500	5250	1.1
P3.4	water	$C_6H_8O_6$/ t-BuOOH	undistilled	R3.1	25	8	55	13750	12600	17400	1.4
P3.5	1,4-dioxane	AIBN	distilled	R3.1	60	24	48	2400	900	1700	1.9
P3.6	water	ACVA	distilled	R3.1	60	24	5	250	1300	3750	2.9
P3.7	water	$C_6H_8O_6$/ t-BuOOH	undistilled	R3.2	25	24	95	5700	3900	4900	1.2
P3.8	1,4-dioxane	AIBN	distilled	R3.2	60	24	33	3300	2500	3300	1.3
P3.9	water	$C_6H_8O_6$/ t-BuOOH	undistilled	R3.3	25	24	89	4450	4300	5400	1.3

§ - Determined by SEC in DMAc relative to PMMA standards.
‡ - Conversion obtained through gravimetric analysis.

Distilled and undistilled *N*VP was polymerized in the presence of R3.1-3 using different polymerization methods, including a slightly modified version of the redox initiated conditions described by Destarac *et al*. (52, 53) and standard thermally initiated RAFT–mediated polymerization at 60 °C, (**P3.1-9**, Table 3.1). The polymers were analyzed using SEC calibrated using PMMA standards, and the SEC chromatograms of polymers synthesized using R3.1-3 can be seen in Figure 3.2. As expected from literature, the polymerization of distilled *N*VP with R3.1 as CTA was retarded in organic solvent at 60 °C, and thus, relatively

low molar mass polymer was obtained with poor control (*Đ* = 1.90) (**P3.5**). (33) Under redox initiated polymerization conditions, it was possible to suppress the formation of dimers, previously attributed to the presence of carboxylic acid and hydroxyl R-group functionalities of CTAs, and thereby obtain polymers with predetermined molar masses and with relatively low dispersities (*Đ* < 1.3) (**P3.1-4**; **P3.7**). It can be noted that the use of distilled *N*VP compared to undistilled *N*VP yielded only slight improvements in the control over molecular weight and its distribution (**P3.2 and P3.3**). Thus, this method eliminates the need for tedious purification of *N*VP pre-polymerization. Often, during the distillation of *N*VP, hydration of the vinyl bond occurs to a large extent.(33,46) Although reversible, this retards the polymerization, which consequently leads to further problems due to the formation of unsaturated chain ends. Typically, vacuum distillation is employed during purification; however, the temperature required for efficient distillation can reach 60 °C, thus inducing oligomer formation. The process of distillation ultimately results in cost implications, and, as such, should preferably be avoided.

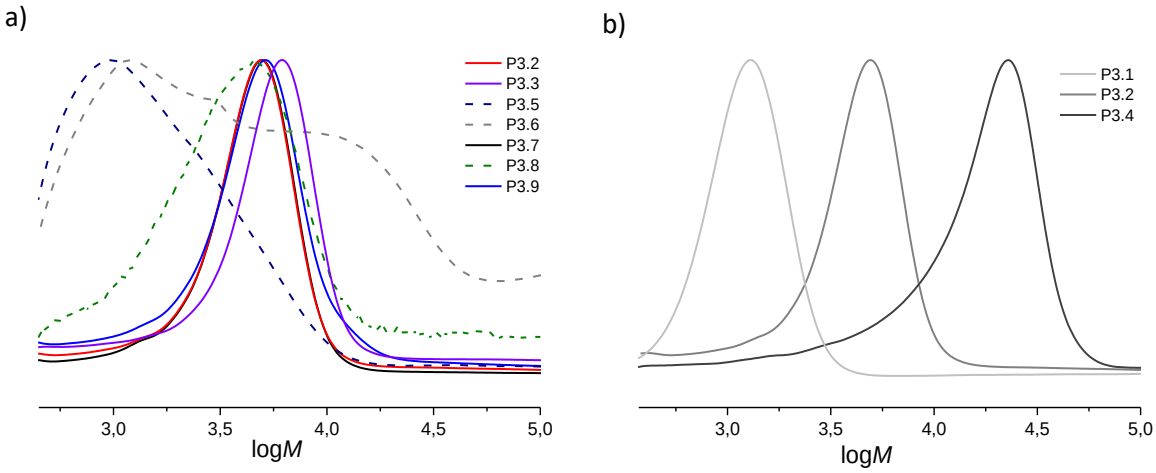

Figure 3.2 (a): Molar mass distribution for the RAFT–mediated polymerization of NVP with R3.1-3 using thermally initiated and redox initiated methods in water and 1,4-dioxane and (b): Molar mass distribution for the RAFT mediated polymerization of NVP with R3.1 using the redox method targeting different molar masses

The redox initiated and thermally initiated RAFT–mediated polymerization of *N*VP differ in two parameters: temperature and solvent (water). Thus, it is possible that either of these

parameters is responsible for the flexibility of this method towards CTAs with protic functionalities. It is possible that the lower temperature decreases the dimer formation, thus, allowing the polymerization to occur, or it is possible that the presence of water interferes with the interaction between *N*VP and the CTA containing protic functionalities, thus allowing for the polymerization to take place. In order to further understand this, polymerizations were conducted where only one of these parameters was varied, *i.e*. the solvent. Polymerization of undistilled *N*VP in water at 60 °C using a water soluble initiator, 4,4'-azobis(4-cyanovaleric acid) (ACVA) and R3.1 as CTA yielded no polymer. When the polymerization was performed with distilled NVP, 5% monomer conversion was achieved and polymer with high dispersity (*Đ* = 2.87) was obtained. These results lead us to believe that the temperature of the polymerization method plays a crucial role in the mechanism of the polymerization, allowing for use of previously believed to be unsuitable CTAs.

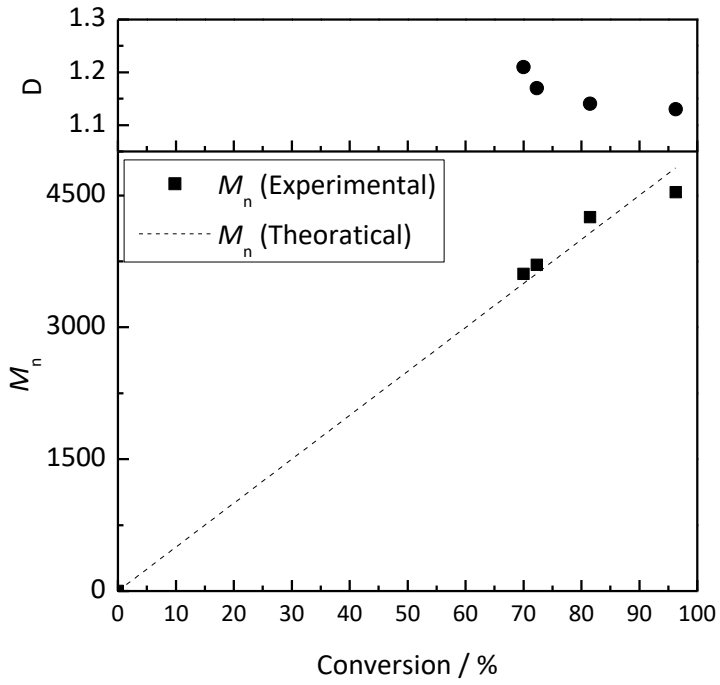

Figure 3.3 Molar mass as a function of conversion plot for the redox initiated polymerization of NVP using RAFT agent R3.1. Dotted lines represent the theoretical Mn curve

A kinetic study of the polymerization of *N*VP with R3.1 was performed using the redox initiated method in water. Samples were taken hourly, until the reaction mixture was too viscous to continue stirring (ca. 4 hours). The evolution of M_n and *Đ* as a function of

monomer conversion is depicted in Figure 3.3. From Figure 3.3, it is worth noting that 70% of the monomer is converted to PVP within a quarter of the reaction time. Figure 3.3 depicts a linear evolution of *M*n with monomer conversion up to about 80% conversion values, before slightly tapering off as would be expected at relatively high monomer conversion. Figure 3.3 is thus sufficient in exemplifying the level of control over *N*VP polymerization using R3.1.

3.2.2 End-group analysis and post-polymerization functionalization

As mentioned above, the formation of unsaturated chain ends is prevalent in thermally initiated RAFT–mediated polymerizations of *N*VP due to the thermally labile nature of the xanthate moiety adjacent to the terminal *N*VP unit. This unsaturation not only decreases the control over the polymerization, it also causes problems with post-polymerization functionalization, as the chain ends necessary for functionalization are no longer present. For certain applications of the polymer, especially for biological applications where telechelic polymers are desired, the significant loss of end groups may cause a noteworthy disadvantage. Pound *et al*. showed that ^{1}H NMR spectroscopy can be used to quantify the presence of these unsaturated chain-ends. (33) The signal representing protons attached to the unsaturated carbons **a** and **b** (Figure 3.4a) can be seen at approximately 4.7 ppm and 6.8 ppm, respectively. The polymers obtained from the thermally initiated conventional RAFT–mediated polymerization method with R3.2 (**P3.8**) shown in the NMR spectrum in Figure 3.4a exhibit a very high percentage of unsaturation, which is in agreement with the observation of a high dispersity. These signals are absent in the ^{1}H NMR spectrum of the PVP synthesized using the redox initiated method (**P3.7**), see Figure 3.4b, indicating that no unsaturated end groups are formed under these conditions. This lack of unsaturation is due to the polymerization taking place at a lower temperature, as was noted in the case for Destarac *et al.* (52,53) The absence of unsaturated chain ends makes this technique ideal for polymerization where chain end fidelity is important, such as in the production of telechelic polymers.

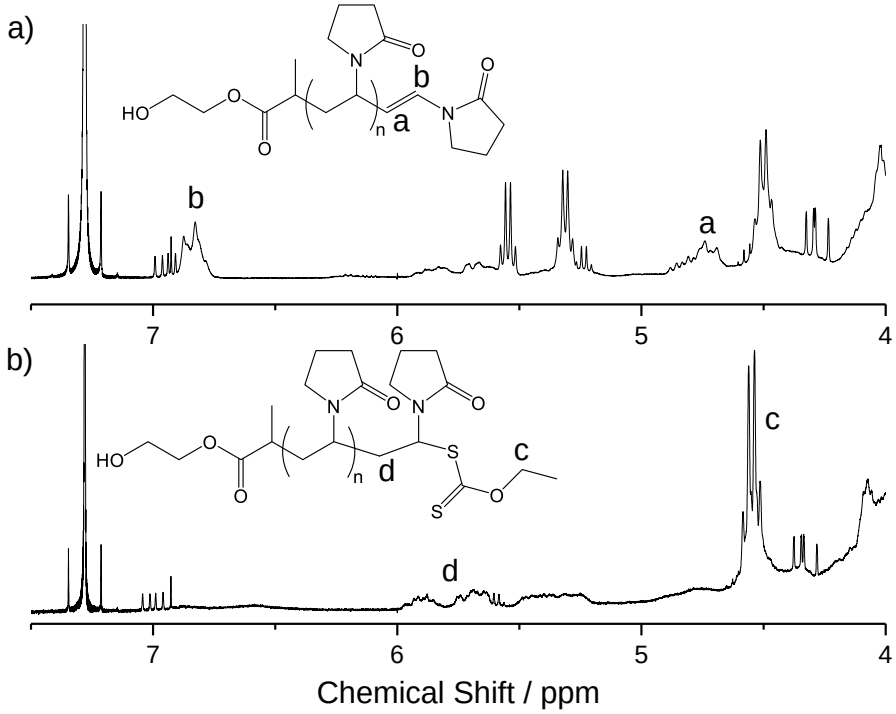

Figure 3.4 Depiction of unsaturated chain ends analysed by ^{1}H NMR spectroscopy. Spectra of (a): PVP synthesized using thermally initiated conventional RAFT–mediated polymerization (P3.8) and (b): PVP synthesized using redox initiated RAFT–mediated polymerization conditions (P3.7). Labels a and b indicate protons belonging to the unsaturated chain ends, while c and d indicate the protons present when the ω-end group is still present

It has been shown numerous times that aldehydes readily react with amine functionalities, such as those found in biological compounds, *e.g.* proteins and peptides. This occurs under mild reaction conditions using reductive amination via Schiff base formation. (57, 58) It has also been previously reported that it is possible to obtain α-aldehyde functionalized poly(2-hydroxyethyl methacrylate) by oxidizing the brush side chain hydroxyl groups (59) via the Albright-Goldman oxidation. (60, 61) This reaction employs a mixture of dimethyl sulfoxide and acetic acid in order to oxidize alcohols under mild reaction conditions. After aminolysis of **P3.7**, which was prepared using R3.2 and therefore contains a hydroxyl-functional α-chain end, the Albright-Goldman oxidation was employed. Although this oxidation is not as quantitative as, for example, the Swern oxidation, (62) it has no effect on the backbone of PVP. Figure 3.5 confirmed that the Albright-Goldman method converted some of the hydroxyl groups to aldehyde moieties. The observed aldehyde proton is characteristically

broad compared to aldehyde protons in small molecules, due to the slightly varying chemical environment inherent in polymeric systems. Although, the conversion efficiency was not quantified, this method is a very convenient protocol to obtain aldehyde functional PVP, underscored by the CTA synthesis being relatively straightforward and inexpensive.

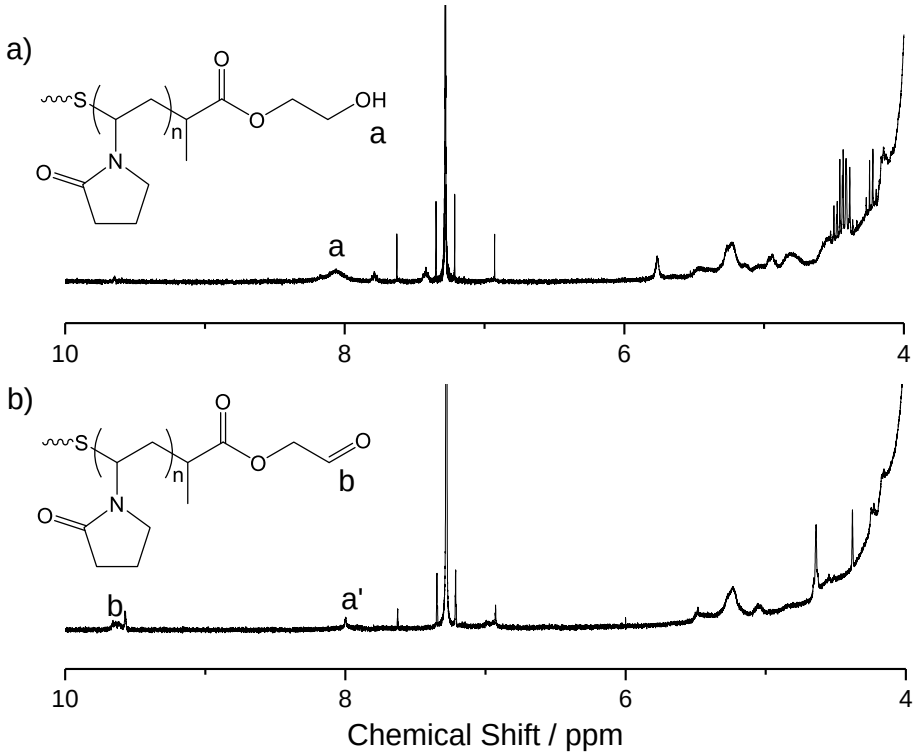

Figure 3.5 ^{1}H NMR spectra of (a): P3.7 after aminolysis with 2-aminoethan-1-ol, where it is possible to see the peak corresponding to the protons of the hydroxyl chain end, a, and (b): after oxidation via the Albright-Goldman method, where it is possible to see the peaks representing the aldehydic proton, b and residual hydroxyl protons a'.

Since this redox initiated method tolerated the use of unpurified *N*VP and the presence of protic functional groups, it was plausible to believe that it might also be more tolerant to the presence of a reactive moiety such as a benzaldehyde functional group. The redox method of polymerization of *N*VP using **R3.3** yielded PVP with good control over the molecular weight and its distribution (**P3.9**), while thermally initiated conventional RAFT–mediated polymerization with **R3.3** yielded no conversion of *N*VP. Using ^{1}H NMRit is possible to see that the benzaldehyde proton is present on the polymer, with no need for

further post-polymerization modification. However, the aldehyde proton peak in the spectrum looks slightly unusual since it is not one single, broad peak which is generally obtained for polymeric, aldehyde proton end-groups. This could be attributed to the isomeric forms of **R3.3**, and thus two different benzaldehyde proton chemical environments are present. It is also possible that some of the ω-chain end has been converted to an aldehyde moiety. However, more investigation in the future is necessary to further characterize this polymer, including through MALDI-TOF. It would also be interesting to further conjugate the aldehyde moiety with an amine via reductive amination followed by a Schiff base formation. In this case, it is expected that the aldehyde proton peak(s) would disappear.

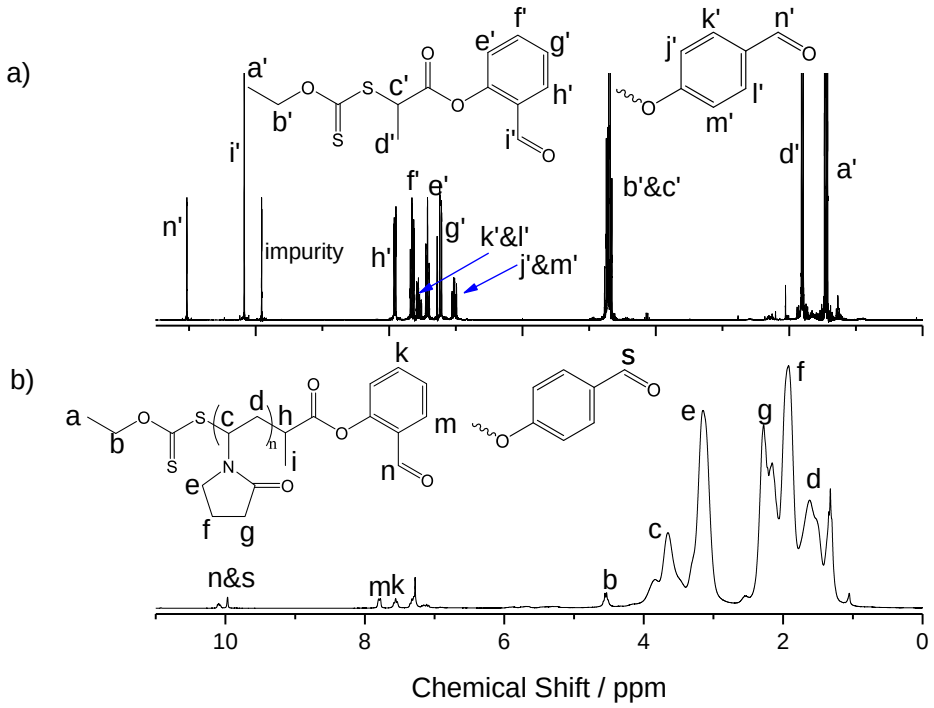

Figure 3.6 ^{1}H NMR spectrum of PVP polymerized with R3.3 using the redox method (P3.9)

Due to the nature of initiation, deactivation and re-initiation of RAFT–mediated polymerizations, it is expected that some initiator derived "I" end groups are formed in competition with the reinitiating leaving groups of the original CTA. However, the majority of the α–chain ends are usually derived from the original CTA's R group; therefore, making it

possible to quantify the ω–chain ends relative to the α–chain end to establish how many of the polymer chains are living, *i.e*. the fraction of chains carrying the RAFT chain end. For an ideal RAFT–mediated polymerization in which initiator–derived chains are neglected, the theoretical ratio of α– to ω–chain ends should be 1. (64, 65) Since the chemical shift of the protons belonging to the α– and ω–chain ends of **P3.9** are resolved, Figure 3.6, it was possible to compare the integrations corresponding to the ω–chain end protons (**b**) with those of the benzaldehyde protons on the α-chain end (**k**, **m**, and **n**). These results indicated that there was high chain-end fidelity, since the number of protons of the α– and ω– chain ends correlated to 0.96 relative to each other. Due to an overlay between the solvent peak ($CDCl_3$) and the peaks corresponding to **i** and **j**, these were not used for this correlation analysis.

This emphasizes the robust nature of the redox initiated polymerization in comparison to thermally initiated conventional RAFT–mediated polymerization. This means that long purification procedures during the synthesis of the CTA, for example column chromatography, are not necessary in order to gain control over the polymerization. Moreover, any impurities can be removed easily during the precipitation of the polymer. Most importantly, it opens new avenues for the production of telechelic PVP.

Further, we report an example whereby α,ω-heterotelechelic PVP was produced through facile post-polymerization functionalization of **P3.2**, seen in Scheme 3.3. This post-polymerization functionalization is only possible due to the tolerance for protic functional groups on the CTA. The xanthate was converted into an aldehyde moiety (**P3.10**) via the method previously published by Pound et al. (57) In short, the xanthate end group is converted to a hydroxyl group by hydrolysis, which was subsequently converted to an aldehyde functional group by heating at 120 ˚C under reduced pressure. Subsequently, the carboxylic acid on the α-chain end was reacted with 2-hydroxyethyl acrylate via a carbodiimide coupling using *N,N'*-dicyclohexylcarbodiimide (DCC) (**P3.11**).

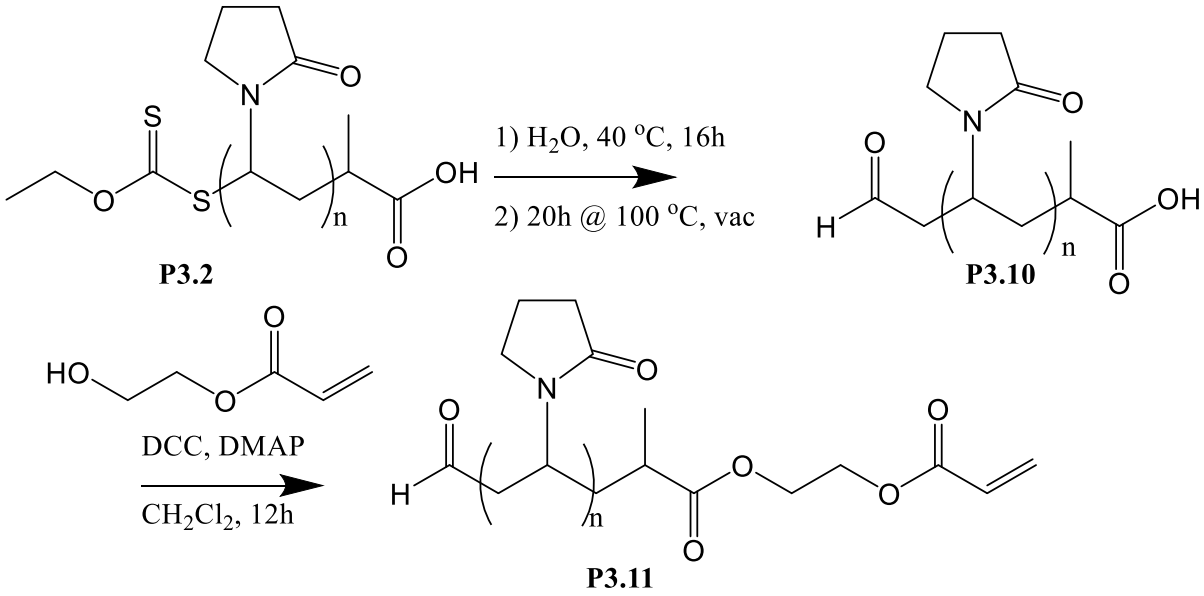

Scheme 3.3 Post-polymerization modification of P3.2's α-chain end into aldehyde end-groups and ω-chain end into an acrylate end group, ready for application as a α,ω-heterotelechelic polymer

Via ^{1}H NMR spectroscopic analysis, Figure 3.7, it was possible to quantify the ω–chain end functionality relative to that of the α–chain end of **P3.12**, in the same manner as **P3.9** above. High chain-end fidelity was retained as the proton integrations on the α–chain ends (**k** and **l** in Figure 3.7) and ω–chain ends (**f** in Figure 3.7) correspond to a ratio of 0.97. The peak corresponding to the aldehyde proton is characteristically broad for a polymeric system due to the slightly varying chemical environments. This example of post-polymerization functionalization further underscores the beneficial nature of the capability of this technique to accommodate CTAs containing reactive functional moieties in the production of α,ω–heterotelechelic PVP. **P3.11** is capable of reacting with bioactive compounds or biomacromolecules containing amine functional moieties on the ω-chain end, as well as via a Michael addition on the α-chain end. Thus, making it capable of orthogonal chain end functionalization reactions.

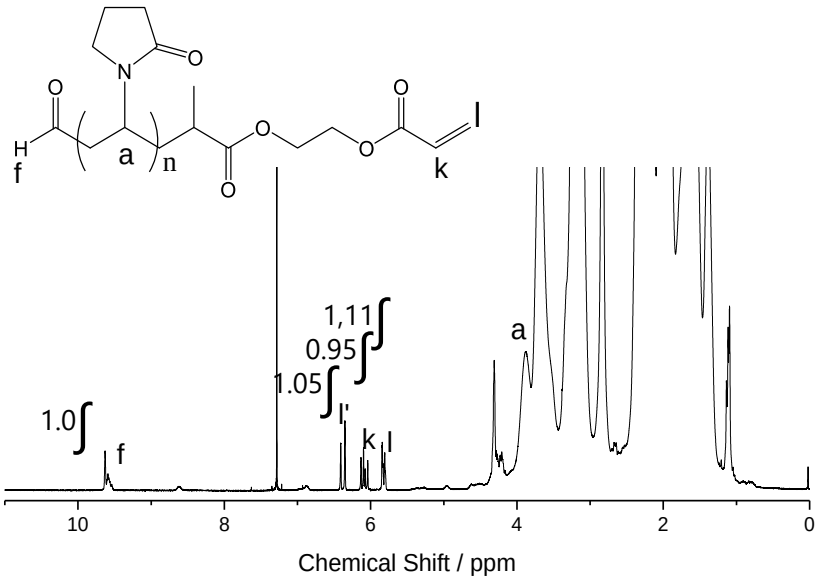

Figure 3.7 ^{1}H NMR spectrum of P3.12 after post-polymerization modification of α and ω-chain ends.

3.2.3 Polymerization of NVP using bromoxanthate CTAs and subsequent ATRP chain extension

As mentioned above, Matyjaszewski and co-workers showed that the use of a bromoxanthate CTA caused dimer formation during *N*VP polymerization. **R3.4** and **R3.5**, Figure 3.8, were synthesized according to literature, and the resulting structures were confirmed by ^{1}H NMR spectroscopy, which correlated well to literature. (44, 55) The CTAs were subsequently used for the polymerization of *N*VP using the redox initiation method.

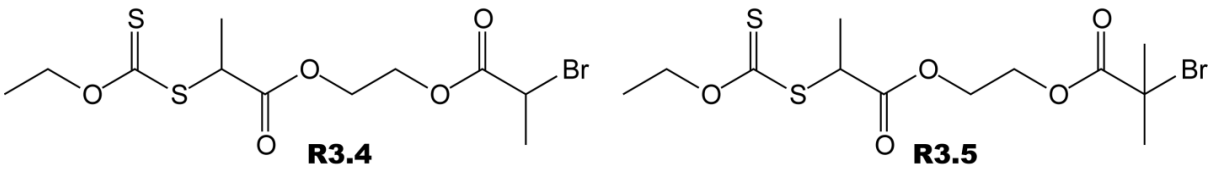

Figure 3.8 Chemical structures of bromoxanthate chain transfer agents, R3.4 and R3.5, used for the RAFT-mediated polymerization of NVP

The use of ascorbic acid/t-BuOOH resulted in low conversion of monomer; however when Na_2SO_3/t-BuOOH was employed instead, the polymerization yielded polymers (**P3.12** & **P3.13**) with good control over the molecular weight and dispersity (*Đ* = 1.3), especially in the

case where **R3.5** was used as the CTA, as summarized in Table 3.2. This means that it could be possible to chain extend these PVP macro-ATRP initiators with more active monomers, such as methyl methacrylate and styrene, etc. This will be further pursued in the near future.

Table 3.2 Tabulation of results from RAFT–mediated polymerization of NVP using R3.4-5

Entry	Solvent	Initiator	NVP	CTA	Temp (°C)	Time (h)	α‡ (%)	M_n (theo) (g·mol^{-1})	M_n§ (g·mol^{-1})	M_W§ (g·mol^{-1})	$Đ$§
P3.12	water	Na_2SO_3/ t-BuOOH	undistilled	R3.4	25	24	94	9400	13 300	17 300	1.3
P3.13	water	Na_2SO_3/ t-BuOOH	undistilled	R3.5	25	24	88	8800	8200	10 600	1.3

§ - Determined by SEC in DMAc relative to PMMA standards.
‡ - Conversion obtained through gravimetric analysis.

3.3 Conclusion

Based on the technique described by Destarac *et al*., we have been able to polymerize unpurified *N*VP in the presence of CTAs with functionalities that were previously deemed incompatible. With the availability of more reactive ω-end groups, we have proven that easy and valuable chain end modifications are possible, *e.g*. the introduction of an aldehyde functionality via the Albright-Goldman oxidation. Due to the robust nature of the redox initiated method, it was possible to polymerize *N*VP in the presence of an benzaldehyde functional CTA, thus, this method leads to facile production of α,ω-heterotelechelic PVP.

Furthermore, it was possible to use this method to polymerize *N*VP in the presence of bromoxanthate CTAs, thus producing a PVP-macroinitiator for ATRP chain extensions with active monomers. Due to previous difficulties in polymerizing PVP block copolymers of this nature, the field is almost uncharted. This method opens opportunities to produce PVP block copolymers that would be of particular interest for application in controlled drug delivery.

3.4 Supplementary

3.4.1 General Experimental Details

Unless stated otherwise, all of the chemicals used were purchased from commercial sources and used without further purification. 2,2'-Azobis(isobutyronitrile) (AIBN) (Riedel-de Haën) was recrystallized from methanol. Subsequently it was dried under vacuum at room temperature. Solvents and monomers were dried and distilled before use, unless stated otherwise. The progress of the reactions were monitored using thin layer chromatography (TLC) with Machery-Nagel Silica gel 60 plates with a UV 254 fluorescent indicator.

^{1}H and ^{13}C NMR spectra were measured on a Varian VXR-Unity (400 MHz) spectrometer and spectra were analyzed using MestreNova 9.0 and chemical shifts were reported in parts-per-million (ppm) which was referenced to the residual solvent protons. The samples were prepared in deuterated solvents (Cambridge Isotope Labs).

Size exclusion chromatography (SEC) was measured on a Shamdzu LC-10AT isocratic pump, a column fitted with a PSS guard column (50 x8 mm) in series with three PPS GRAM columns (300 x 8 mm, 10 µm, 2 x 3000 Å and 1 x 100 Å) kept at a constant temperature of 40 °C, a Waters 717+ auto-sampler, a Waters 2487 dual wavelength UV detector and a Waters 2414 differential refractive index (DRI) detector. The samples were measured in dimethylacetamide (DMAc) as the eluent stabilized with 0.05% BHT (*w*/*v*) and 0.03% LiCl (*w*/*v*), at a flow rate of 1 mL.min^{-1}. Sample preparation included filtering the sample solutions through a 0.45 µm GHP filter to remove impurities. The results were calibrated against PMMA standards (Polymer Laboratories) ranging from 690 to 1.2 x 10^{6} g.mol^{-1}. Data acquisition was performed using Millenium^{32} software, v4.

3.4.2 Experimental methods

*Synthesis of S-(2-propionic acid) O-ethyl xanthate (**R3.1**)*

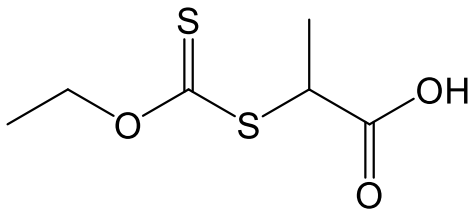

Method was followed according to procedure published by Pound *et al*. (33) In short, potassium ethyl xanthate (5.00 g, 31.2 mmol) was dissolved in water (15 mL) and NaOH (7.5 mL, 3.3M) was added while the solution was stirring. The solution was then cooled in an ice bath, and bromopropionic acid (4.34 g, 28.4 mmol) was added dropwise. The solution was stirred for 8 h. The pH was adjusted to pH 1 by the addition of HCl (1 M). The product was extracted with Et_2O (3 x 50 mL) and then with aq. Na_2CO_3 (3 x 50 mL). The pH was adjusted to pH 3 by the addition of HCl (1 M) and the product was extracted with Et_2O (3 x 100 mL) to yield **R3.1** as a white solid (4.4 g, 80%). ^{1}H NMR spectrum corresponded well to that in literature. (33)

^{1}H NMR (400 MHz, chloroform-d) δ 4.64 (qd, *J* = 7.1, 1.8 Hz, 2H), 4.41 (q, *J* = 7.4 Hz, 1H), 1.60 (d, *J* = 7.4 Hz, 3H), 1.41 (t, *J* = 7.1 Hz, 3H).

Synthesis of S-(4-hydroxyethyl(2-ethyl propionate)) O-ethyl xanthate (R3.2)

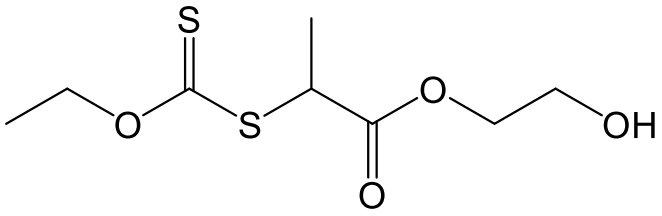

R3.1 (3.0 g, 15 mmol), ethylene glycol (1.12 mL, 77.2 mmol) and 4-dimethylaminopyridine (DMAP) (188.6 mg, 1.544 mmol) were dissolved in CH_2Cl_2 (50 mL) in a 100 mL RBF, and cooled to 0 °C in an ice bath. EDC (3.26 g, 17.0 mmol) was added portion-wise. The mixture was stirred for 12 hours, while reaching room temperature on its own accord. The solution was concentrated and re-dissolved in 100 mL EtOAc, and washed with (3 x 50 mL) water and (3 x 50 mL) brine. The organic layer was collected and dried over $MgSO_4$, and then filtered and concentrated. The crude product was purified via column chromatography (eluent: 10% EtOAC in pentane slowly increased to 40% EtOAc in pentane) (R_f = 0.2 in 40% EtOAc in pentane) to yield **R3.2** as a light yellow, oily liquid (2.3 g, 65%). ^{1}H NMR spectrum corresponded well to that in literature. (56)

^{1}H NMR (400 MHz, chloroform-d) δ 4.61 (q, *J* = 7.1 Hz, 2H), 4.39 (q, *J* = 7.4 Hz, 1H), 4.30 – 4.20 (m, 2H), 3.85 – 3.76 (m, 2H), 2.17 (s, 1H), 1.57 (d, *J* = 7.4 Hz, 3H), 1.39 (t, *J* = 7.1 Hz, 3H).

Synthesis of S-(2-salicylaldehyde propionate) O-ethyl xanthate (R3.3)

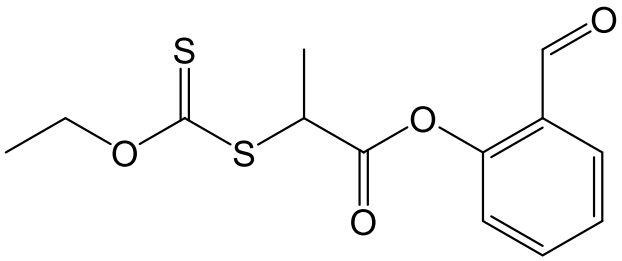

2-Hydroxylbenzaldehyde (0.63 g, 5.2 mmol) and **R3.1** (1.0 g, 5.2 mmol) were dissolved in CH_2Cl_2 (30 mL). DMAP (69.3 mg, 0.567 mmol) was added, and the solution was cooled to 0 °C in an ice bath. Thereafter, the solution was degassed with argon for 20 min. EDC (0.879 g, 5.67 mmol) was added portion-wise over 10 minutes. Solution was stirred for 8 hours, and allowed to reach rt on its own accord. Solvent was removed under vacuum. Crude product was re-dissolved in EtOAc (50 mL) and then washed with water (3 x 50 mL) and brine (3 x 50 mL). Combined organic fractions were dried over anhydrous $MgSO_4$, filtered and concentrated under vacuum. The RAFT agent was used without further purification. Its purity was determined to be 70% by ^{1}H NMR.

^{1}H NMR (300 MHz, chloroform-d) δ 11.03 (s, 0.3H), 10.17 (s, 1H), 9.92-9.90 (m, 0.2H, impurity), 7.91 (dd, *J* = 7.7, 1.8 Hz, 1H), 7.65 (tp, *J* = 8.1, 1.8 Hz, 1H), 7.60-7.50 (m, 0.6H) 7.42 (td, *J* = 8.2, 1.2 Hz, 1H), 7.23 (dd, *J* = 8.2, 1.2 Hz, 1H), 7.06-6.97 (m, 0.6H), 4.79 – 4.63 (m, 4H), 1.80 (dd, *J* = 7.1, 0.5 Hz, 3H), 1.45 (td, *J* = 7.1, 0.5 Hz, 3H).

^{13}C NMR (75 MHz, chloroform-d) δ 211.80, 196.61, 188.45, 169.78, 161.62, 151.61, 136.99, 135.32, 133.74, 130.71, 128.09, 126.72, 123.15, 119.85, 117.59, 70.71, 47.25, 16.50, 13.72.

*Synthesis of (**R3.4**) and (**R3.5**)*

Method modified from that described by Huang *et al*. (44) and Jumeaux *et al*. (55), as follows:

Synthesis of 2-hydroxyethyl 2'-bromopropionate

A solution of ethylene glycol (43 g, 0.69 mol) and triethylamine (8.4 g, 0.083 mol) in CH_2Cl_2 (250 mL) was placed in a two-neck round bottom flask equipped with a condenser. After cooling to 0 °C, 2-bromopropionyl bromide (15 g, 0.069 mol) in dry CH_2Cl_2 (50 mL) was added dropwise over 20 min under an inert argon atmosphere. The reaction mixture was

stirred at 25 °C under argon for 24 h. The reaction mixture was then filtered to remove any precipitate and the solvent was evaporated under reduced pressure. The mixture was dissolved in distilled water (100 mL) and extracted with chloroform (3 x 300 mL). The combined organic phases were dried over anhydrous $MgSO_4$, filtered and concentrated under vacuum. Pure 2-hydroxyethyl 2'-bromopropionate was isolated by vacuum distillation (bp 70 °C at 1.0 mmHg) (8.6 g, 63%). ^{1}H NMR spectrum corresponded well to that in literature. (44)

^{1}H NMR (600 MHz, chloroform-*d*) δ 4.37 (q, *J*= 7.0 Hz, 1H), 4.24 (t, *J*= 4.7 Hz, 2H), 3.88 (t, *J* = 4.7 Hz, 2H), 2.35 (s (broad), 1H), 1.78 (d, *J* = 7.0 Hz).

*Synthesis of S-[1-methyl-4-(6-bromopropionate)ethyl acetate] O-ethyl dithiocarbonate (**R3.4**)*

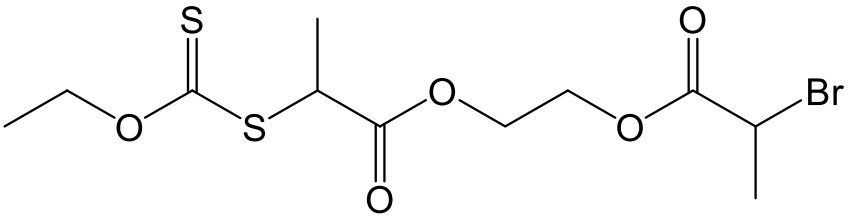

R3.2 (2.0 g, 8.8 mmol) and trimethylamine (0.934 mL, 6.70 mmol) were dissolved in dry THF (10 mL) under an inert argon atmosphere. The reaction mixture was cooled to 0 °C and a solution of 2-bromopropionyl bromide (1.1 mL, 11 mmol) in dry THF (5 mL) was added slowly while stirring. The mixture was stirred in the cooling bath for 1 h and then at 25 °C for 17 h. Excess 2-bromopropionyl bromide was neutralized with 0.1 mL of water and the reaction mixture was poured into a solution of hydrochloric acid (80 mL, pH 2), and extracted with CH_2Cl_2 (3 x 100 mL). The organic layers were combined and washed with a solution of sodium hydroxide (80 mL, 0.3 M) and (3 x 100 mL) brine, dried over anhydrous magnesium sulphate and concentrated under vacuum. The product was purified by column chromatography (eluent: hexane/ethyl acetate, 8:2) to yield **R3.4** as a yellow, viscous liquid (2.5 g, 76%). ^{1}H NMR spectrum corresponded well to that in literature. (44)

^{1}H NMR (400 MHz, chloroform-*d*) δ 4.63 (q, *J* = 7.1 Hz, 2H), 4.47 – 4.31 (overlapped m, 6H, 1.83 (d, *J* = 7.0 Hz, 3H), 1.58 (d, *J* = 7.4 Hz, 3H), 1.41 (t, *J* = 7.1 Hz).

*Synthesis of S-[1-methyl-4-(6-bromoisobutyrate)ethyl acetate] O-ethyl dithiocarbonate (**R3.5**)*

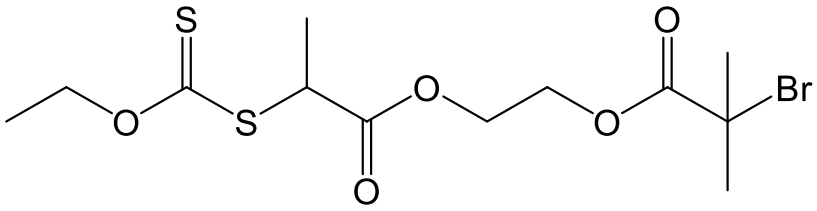

R3.2 (2.00 g, 8.80 mmol) and TEA (0.934 mL, 6.70 mmol) were dissolved in dry THF (10 mL) under an inert argon atmosphere. The reaction mixture was cooled to 0 °C and a solution of α-isobutyryl bromide (1.1 mL, 8.9 mmol) in dry THF (5 mL) was added slowly while stirring. The mixture was stirred in the cooling bath for 1 h and then at 25 °C for 17 h. Excess α-isobutyryl bromide was neutralized with 0.1 mL of water and the reaction mixture was poured into a solution of hydrochloric acid (80 mL, pH 2) and extracted with CH_2Cl_2 (3 x 100 mL). The organic layers were combined and washed with a solution of sodium hydroxide (80 mL, 0.3 M) and (3 x 100 mL) brine, dried over anhydrous magnesium sulphate and concentrated under vacuum. The product was purified by column chromatography (eluent: hexane/ethyl acetate, 8:2) to yield **R3.5** as a yellow viscous liquid (2.4 g, 70%). ^{1}H NMR spectrum corresponded well to that in literature. (44)

^{1}H NMR (400 MHz, chloroform-*d*) δ 4.64 (q, 2H, *J* = 7.4 Hz), 4.47 – 4.32 (overlapped m, 5H, 1.94 (s, 6H), 1.58 (d, *J* = 7.4 Hz, 3H), 1.42 (td, *J* = 7.1, 1.1 Hz, 3H).

A typical polymerization of undistilled NVP

Polymerization was altered from the procedure by Desterac *et al*. (52) *N*VP (straight from the bottle) (2.52 g, 22.7 mmol), water (1.83 g), R3.2 (0.1 g, 0.4 mmol) and *t*-BuOOH (15.38 mg, 0.1194 mmol) were added to a pear-shaped flask. Argon was bubbled through the solution for 20 minutes. Thereafter, ascorbic acid (19.28 mg, 0.1095 mmol) was added in one portion to the pear-shaped flask, with argon still flowing into the flask. The reaction solution was then stirred in a water bath, preheated to 25 °C, for 24 h, or until too viscous to continue stirring. Then, the solution was freeze-dried for 24 h, re-dissolved in chloroform (1 mL), and precipitated in cold Et_2O (45 mL) thrice. Finally, the polymer was re-dissolved in CH_2Cl_2 (1 mL) precipitated in Et_2O (45 mL) and centrifuged again. This process was repeated

twice. Finally, the polymer was dried under reduced pressure for 24 hours at room temperature to yield **P3.7**.

Conventional RAFT-mediated polymerization of NVP

Distilled *N*VP (2.56 g, 23.0 mmol), AIBN (8.446 mg, 0.052 mmol), R3.1 (0.1 g, 0.52 mmol) and 1,4 dioxane (2.6 mL) were added to a pear-shaped flask fitted with a Schlenk tap. The reaction flask underwent 3 freeze-pump-thaw cycles, and filled with argon. The flask was then immersed in an oil bath, preheated to 60 °C, in order to start the polymerization. When the polymerization was finished, the solution was precipitated into Et_2O (45 mL) and centrifuged. The precipitate was re-dissolved in CH_2Cl_2 (1 mL), precipitated in Et_2O (45 mL) and centrifuged again. This process was repeated twice. Finally, the polymer was dried under reduced pressure for 24 hours at room temperature. (57)

Xanthate end-group removal

PVP (0.5 g, 0.1 mmol) was dissolved in THF (10 mL) and 2-aminoethan-1-ol (61 mg, 1.0 mmol) was added drop-wise. The reaction mixture was stirred at room temperature for 24 hours, and then the solution was precipitated into Et_2O (150 mL) and centrifuged. The precipitate was re-dissolved in CH_2Cl_2 (1 mL), precipitated in Et_2O (45 mL) and centrifuged again. This process was repeated twice. Finally, the polymer was dried under reduced pressure in an oven for 24 hours at room temperature.

Albright-Goldman oxidation of PVP

The method was altered from literature. (59) PVP (200 mg) was dissolved in DMSO (1.5 mL) and stirred for 18 hours at room temperature. Solution was degassed with argon for 30 minutes. Acetic anhydride (1.5 mL) was added drop-wise and the mixture was stirred for a further 48 hours at room temperature. The polymer was precipitated in Et_2O and centrifuged. The precipitate was re-dissolved in CH_2Cl_2 (1 mL), precipitated in Et_2O (45 mL) and centrifuged again. This process was repeated twice. Finally, the polymer was dried under reduced pressure in an oven for 24 hours at room temperature.

3.5 References

1. Irving B. Nanoparticle drug delivery systems. Innov Pharm Technol. 2008;24:58-62.
2. Mudshinge SR, Deore AB, Patil S, Bhalgat CM. Nanoparticles: Emerging carriers for drug delivery. Saudi Pharm J. 2011;19(3):129-41.
3. Dikmen G, Genç L, Güney G. Advantage and disadvantage in drug delivery systems. J Mater Sci Eng. 2011;5(4):468-72.
4. Robinson DH, Mauger JW. Drug delivery systems. Am J Hosp Pharm. 1991;48(10 Suppl 1):S14-S23.
5. Roth PJ, Jochum FD, Zentel R, Theato P. Synthesis of hetero-telechelic α,ω bio-functionalized polymers. Biomacromolecules. 2010;11(1):238-44.
6. Heredia KL, Tao L, Grover GN, Maynard HD. Heterotelechelic polymers for capture and release of protein-polymer conjugates. Polym Chem. 2010;1(2):168-70.
7. Heredia KL, Grover GN, Tao L, Maynard HD. Synthesis of heterotelechelic polymers for conjugation of two different proteins. Macromolecules. 2009;42(7):2360-7.
8. Li M, De P, Gondi SR, Sumerlin BS. Responsive polymer-protein bioconjugates prepared by RAFT polymerization and copper-catalyzed azide-alkyne click chemistry. Macromol Rapid Commun. 2008;29(12-13):1172-6.
9. van Dijk M, van Nostrum CF, Hennink WE, Rijkers DTS, Liskamp RMJ. Synthesis and characterization of enzymatically biodegradable PEG and peptide-based hydrogels prepared by click chemistry. Biomacromolecules. 2010;11(6):1608-14.
10. Cobo I, Li M, Sumerlin BS, Perrier S. Smart hybrid materials by conjugation of responsive polymers to biomacromolecules. Nature Mater. 2014;14:143-59.
11. Canning SL, Smith GN, Armes SP. A critical appraisal of RAFT-mediated polymerization-induced self-assembly. Macromolecules. 2016;49(6):1985-2001.
12. Moad G, Chong YK, Postma A, Rizzardo E, Thang S. Advances in RAFT polymerization: The synthesis of polymers with defined end-groups. Polymer. 2013;46(11):8458-68.
13. Moad G. RAFT polymerization – then and now. Controlled radical polymerization: Mechanisms. ACS Symposium Series. 1187. Washington: American Chemical Society; 2015. p. 211-46.
14. Moad G, Rizzardo E, Thang SH. Living radical polymerization by the RAFT process. Aust J Chem. 2005;58(6):379-410.

15. Chiefari J, Chong YK, Ercole F, Krstina J, Jeffery J, Le TPT, Mayadunne RTA, Meijs GF, Moad CL, Moad G, Rizzardo E, Thang SH. Living free-radical polymerization by reversible addition−fragmentation chain transfer: The RAFT process. Macromolecules. 1998;31(16):5559-62.
16. Patten TE, Matyjaszewski K. Copper(I)-catalyzed atom transfer radical polymerization. Acc Chem Res. 1999;32(10):895-903.
17. Matyjaszewski K. Atom transfer radical polymerization (ATRP): Current status and future perspectives. Macromolecules. 2012;45(10):4015-39.
18. Perrier S, Takolpuckdee P. Macromolecular design via reversible addition–fragmentation chain transfer (RAFT)/xanthates (MADIX) polymerization. J Polym Sci, Part A: Polym Chem. 2005;43(22):5347-93.
19. Willcock H, O'Reilly RK. End group removal and modification of RAFT polymers. Polym Chem. 2010;1(2):149-57.
20. Chong YK, Moad G, Rizzardo E, Thang SH. Thiocarbonylthio end group removal from RAFT-synthesized polymers by radical-induced reduction. Macromolecules. 2007;40(13):4446-55.
21. Nair DP, Podgórski M, Chatani S, Gong T, Xi W, Fenoli CR, Bowman CN. The thiol-michael addition click reaction: A powerful and widely used tool in materials chemistry. Chem Mater. 2014;26(1):724-44.
22. Matsuoka S-i, Kamijo Y, Suzuki M. Post-polymerization modification of unsaturated polyesters by Michael addition of N-heterocyclic carbenes. Polym J. 2017;49:423-8.
23. Stenzel MH. Bioconjugation using thiols: Old chemistry rediscovered to connect polymers with nature's building blocks. ACS Macro Lett. 2013;2(1):14-8.
24. Mather BD, Viswanathan K, Miller KM, Long TE. Michael addition reactions in macromolecular design for emerging technologies. Prog Polym Sci. 2006;31(5):487-531.
25. Boyer C, Liu J, Bulmus V, Davis TP, Barner-Kowollik C, Stenzel MH. Direct synthesis of well-defined heterotelechelic polymers for bioconjugations. Macromolecules. 2008;41(15):5641-50.
26. Heredia KL, Nguyen TH, Chang C-W, Bulmus V, Davis TP, Maynard HD. Reversible siRNA-polymer conjugates by RAFT polymerization. Chem Commun. 2008(28):3245-7.

27. Bathfield M, D'Agosto F, Spitz R, Charreyre M-T, Delair T. Versatile precursors of functional RAFT agents. Application to the synthesis of bio-related end-functionalized polymers. J Am Chem Soc. 2006;128(8):2546-7.

28. Gondi SR, Vogt AP, Sumerlin BS. Versatile pathway to functional telechelics via RAFT polymerization and click chemistry. Macromolecules. 2007;40(3):474-81.

29. Pound G, McLeary JB, McKenzie JM, Lange RFM, Klumperman B. In-Situ NMR spectroscopy for probing the efficiency of RAFT/MADIX agents. Macromolecules. 2006;39(23):7796-7.

30. Postma A, Davis TP, Li G, Moad G, O'Shea MS. RAFT polymerization with phthalimidomethyl trithiocarbonates or xanthates. On the origin of bimodal molecular weight distributions in living radical polymerization. Macromolecules. 2006;39(16):5307-18.

31. Bilalis P, Pitsikalis M, Hadjichristidis N. Controlled nitroxide-mediated and reversible addition-fragmentation chain transfer polymerization of N-vinylpyrrolidone: Synthesis of block copolymers with styrene and 2-vinylpyridine. J Polym Sci, Part A: Polym Chem. 2006;44(1):659-65.

32. Nguyen TLU, Eagles K, Davis TP, Barner-Kowollik C, Stenzel MH. Investigation of the influence of the architectures of poly(vinyl pyrrolidone) polymers made via the reversible addition–fragmentation chain transfer/macromolecular design via the interchange of xanthates mechanism on the stabilization of suspension polymerizations. J Polym Sci, Part A: Polym Chem. 2006;44(15):4372-83.

33. Pound G, Eksteen Z, Pfukwa R, McKenzie JM, Lange RFM, Klumperman B. Unexpected reactions associated with the xanthate-mediated polymerization of *N*-vinylpyrrolidone. J Polym Sci, Part A: Polym Chem. 2008;46(19):6575-93.

34. Shimoni O, Postma A, Yan Y, Scott AM, Heath JK, Nice EC, Zelikin AN, Caruso F. Macromolecule functionalization of disulfide-bonded polymer hydrogel capsules and cancer cell targeting. ACS Nano. 2012;6(2):1463-72.

35. Zelikin AN, Such GK, Postma A, Caruso F. Poly(vinylpyrrolidone) for bioconjugation and surface ligand immobilization. Biomacromolecules. 2007;8(9):2950-3.

36. Reader PW, Pfukwa R, Jokonya S, Arnott GE, Klumperman B. Synthesis of α,ω-heterotelechelic PVP for bioconjugation, via a one-pot orthogonal end-group modification procedure. Polym Chem. 2016;7(42):6450-6.

37. Wan D, Satoh K, Kamigaito M, Okamoto Y. Xanthate-mediated radical polymerization of N-vinylpyrrolidone in fluoroalcohols for simultaneous control of molecular weight and tacticity. Macromolecules. 2005;38(25):10397-405.

38. Ilchev A, Pfukwa R, Hlalele L, Smit M, Klumperman B. Improved control through a semi-batch process in RAFT-mediated polymerization utilizing relatively poor leaving groups. Polym Chem. 2015;6(46):7945-8.

39. Hedir GG, Pitto-Barry A, Dove AP, O'Reilly RK. Amphiphilic block copolymer self-assemblies of poly(NVP)-b-poly(MDO-co-vinyl esters): Tunable dimensions and functionalities. J Polym Sci, Part A: Polym Chem. 2015;53(23):2699-710.

40. Zheng X, Zhang T, Song X, Zhang L, Zhang C, Jin S, Xing J, Liang X-J. Structural impact of graft and block copolymers based on poly(N-vinylpyrrolidone) and poly(2-dimethylaminoethyl methacrylate) in gene delivery. J Mater Chem B. 2015;3(19):4027-35.

41. Yamago S, Ray B, Iida K, Yoshida J-i, Tada T, Yoshizawa K, Kwak Y, Goto A, Fukuda T. Highly versatile organostibine mediators for living radical polymerization. J Am Chem Soc. 2004;126(43):13908-9.

42. Ray B, Kotani M, Yamago S. Highly controlled synthesis of poly(N-vinylpyrrolidone) and its block copolymers by organostibine-mediated living radical polymerization. Macromolecules. 2006;39(16):5259-65.

43. Benaglia M, Chiefari J, Chong YK, Moad G, Rizzardo E, Thang SH. Universal (switchable) RAFT agents. J Am Chem Soc. 2009;131(20):6914-5.

44. Huang C-F, Nicolaÿ R, Kwak Y, Chang F-C, Matyjaszewski K. Homopolymerization and block copolymerization of N-vinylpyrrolidone by ATRP and RAFT with haloxanthate inifers. Macromolecules. 2009;42(21):8198-210.

45. McDowall L, Stenzel MH. Disulfide bridge based conjugation of peptides to RAFT polymers. Polym Chem. 2014;5(5):1772-81.

46. Pound G, Klumperman B. Reversible addition fragmentation chain transfer (RAFT) mediated polymerization of N-vinylpyrrolidone (PhD). Stellenbosch: Stellenbosch University; 2008.

47. Yamago S, Kayahara E, Kotani M, Ray B, Kwak Y, Goto A, Fukuda T. Highly controlled living radical polymerization through dual activation of organobismuthines. Angew Chem Int Ed. 2007;46(8):1304-6.

48. Breitenbach JW. Polymerization and polymers of N-vinylpyrrolidone. J Polym Chem. 1957;23(104):949-53.

49. Kaupp G, Pogodda U, Schmeyers J. Gas/solid reactions with acetone. Chem Ber. 1994;127(11):2249-61.

50. Madl A, Spange S. On the importance of the amide-bonded hydrogen atom in the cationically induced oligomerization of N-vinylamides. Macromolecules. 2000;33(15):5325-35.

51. Zhuo J-C. Methyl (2E,4E)-5-Anilino-4-(methoxycarbonyl)penta-2,4-dienoate. Molecules. 1999;4(11):M118.

52. Guinaudeau A, Coutelier O, Sandeau A, Mazières S, Nguyen Thi HD, Le Drogo V, Wilson DJ, Destarac M. Facile access to poly(N-vinylpyrrolidone)-based double hydrophilic block copolymers by aqueous ambient RAFT/MADIX polymerization. Macromolecules. 2013;47(1):41-50.

53. Guinaudeau A, Mazières S, Wilson DJ, Destarac M. Aqueous RAFT/MADIX polymerisation of N-vinyl pyrrolidone at ambient temperature. Polym Chem. 2012;3(1):81-4.

54. Quemener D, Davis TP, Barner-Kowollik C, Stenzel MH. RAFT and click chemistry: A versatile approach to well-defined block copolymers. Chem Commun. 2006(48):5051-3.

55. Jumeaux C, Chapman R, Chandrawati R, Stevens MM. Synthesis and self-assembly of temperature-responsive copolymers based on N-vinylpyrrolidone and triethylene glycol methacrylate. Polym Chem. 2015;6(22):4116-22.

56. Pfukwa R, Klumperman B. Synthesis and characterization of telechelic hydroxyl functional poly(N-vinylpyrrolidone) (MSc). Stellenbosch: Stellenbosch University; 2008.

57. Pound G, McKenzie JM, Lange RF, Klumperman B. Polymer-protein conjugates from omega-aldehyde endfunctional poly(N-vinylpyrrolidone) synthesised via xanthate-mediated living radical polymerisation. Chem Commun. 2008;27:3193-5.

58. Gauthier MA, Klok HA. Peptide/protein-polymer conjugates: synthetic strategies and design concepts. Chem Commun. 2008(23):2591-611.

59. Bilgic T, Klok HA. Oligonucleotide Immobilization and Hybridization on Aldehyde-Functionalized Poly(2-hydroxyethyl methacrylate) Brushes. Biomacromolecules. 2015;16(11):3657-65.

60. Albright JD, Goldman L. Dimethyl sulfoxide-acid anhydride mixtures. New reagents for oxidation of alcohols. J Am Chem Soc. 1965;87(18):4214-6.

61. Albright JD, Goldman L. Dimethyl sulfoxide-acid anhydride mixtures for the oxidation of alcohols. J Am Chem Soc. 1967;89(10):2416-23.

62. Omura K, Swern D. Oxidation of alcohols by “activated” dimethyl sulfoxide. a preparative, steric and mechanistic study. Tetrahedron. 1978;34(11):1651-60.

63. Plummer R, Goh Y-K, Whittaker AK, Monteiro MJ. Effect of impurities in cumyl dithiobenzoate on RAFT-mediated polymerizations. Macromolecules. 2005;38(12):5352-5.

64. Vandenbergh J, Junkers T. Alpha and omega: Importance of the nonliving chain end in RAFT multiblock copolymerization. Macromolecules. 2014;47(15):5051-9.

65. Gody G, Maschmeyer T, Zetterlund PB, Perrier S. Rapid and quantitative one-pot synthesis of sequence-controlled polymers by radical polymerization. Nature Comm. 2013;4:2505-14.

Synopsis

Polymeric drug delivery systems containing "smart" responses based on physiological triggers have gained enormous interest recently due to their potential in solving the Achilles' heel of gene therapy: endosomal escape and cytoplasmic release of RNA therapeutics. In this chapter, a novel pH-sensitive diblock copolymer is reported as a potential gene delivery system. The synthesis and characterization of the diblock copolymer systems containing hydrolysable poly(2-(*N*,*N*-dimethylamino)ethyl acrylate) (pDMAEA) or non-hydrolysable poly(2-(*N*,*N*-dimethylamino)ethyl methacrylate) (pDMAEMA) conjugated to poly(*N*-vinylpyrrolidone) (PVP) via a β-thiopropionate linker, are described.

4.1 Introduction

As mentioned earlier in Chapter 2, applications of non-coding RNA therapeutics in gene therapy, *e.g*. short interfering RNA (siRNA) and microRNA (miRNA), are limited due to difficulties in their systemic and cellular delivery. (1) During systemic delivery, these naked RNAs are rapidly cleared via the kidneys. (2, 3) If these therapeutics do reach the cells, they are incapable of crossing the cellular membrane and do not undergo endosomal escape because of their small size and negative charge. (3, 4) This has led to many investigations towards developing systems that assist in gene delivery. As discussed in Chapter 2, polycations, *e.g*. polyethyleimine (PEI) (5-10) and pDMAEMA (11-15), have become a popular choice for such delivery systems due to their ability to condense the negatively charged RNAs. (3, 16, 17) However, because of the positive zeta potential of the polyplex systems, they possess inherent toxicity. They also readily aggregate and lack stability due to interactions with serum components. PEGylation, the addition of poly(ethylene glycol), has become a standard method of shielding the polyplexes of their positive charge, consequently reducing these negative traits and increasing the stealth behavior of the delivery systems as a whole. (18-22)

The PEGylated polyplexes have previously been shown to exhibit instability when applied *in vivo*, as they were seen to be cleared by the kidneys after disassembly at the glomerular basement membrane. (23, 24) The PEGylation only caused a small increase in the circulation time and a small improvement in bio-distribution compared to naked RNAs. Nelson *et al*. (25) developed polycationic systems with increased hydrophobicity by adding a hydrophobic comonomer component. They copolymerized 2-(*N*,*N*-dimethylamino)ethyl methacrylate (DMAEMA) and butyl methacrylate (BMA), optimizing the monomer feed ratio, and obtained an increase in polyplex circulation time *in vivo*, as well as improved endosomal escape (intracellular delivery) because of the pH dependent membrane disruption behavior.

In their study, they synthesized polycations composed of 0 – 75% BMA and found that the 75% BMA polyplexes displayed reduced RNA condensation properties, since only 38% of the siRNA was complexed by the 75% BMA at an N/P ratio of 10:1, while the 40 and 50% BMA polycations were able to fully condense the RNAs. (25)

While investigating the cellular uptake and transfection efficacy of the polyplex systems, Nelson *et al*. (25) reported that although the polyplexes with 0% BMA were most readily internalized by cells, and that polyplexes with 50% BMA showed the best transfection efficacy, with a 94% luciferase silencing compared to 20% silencing of 0% BMA. They proposed that this was due to the polyplexes containing 50% BMA being more capable of facilitating cellular membrane disruption, thus, enhancing the cytoplasmic release of the RNAs. This was substantiated with hemolysis experiments, where they found that 50% BMA provided the polyplexes with the optimal pH-responsive behavior at the pH corresponding to that of early and late endosomes, while remaining stable at physiological pH.

The greatest challenge in polyplex delivery has been narrowed down to endosomal escape and cytoplasmic release of RNAs. (26-28) The pH responsive behavior of p(DMAEMA-*co*-BMA) (50:50) addresses the endosomal escape; however, the cytoplasmic release remains a hurdle, thus, decreasing the efficacy of the systems. If the RNA is not released, it is unable to interact with the endoribonuclease DICER, and subsequently form part of the RNA-interfering silencing complex (RISC). (29-31) The use of polycation complexes is a double-edged sword, since the cationic nature is necessary for condensation and packaging of the RNAs; however, this electrostatic interaction also means that the RNAs have difficulties being released. (32, 33) Monteiro and coworkers developed hydrolytically degrading polyplexes from pDMAEA which de-cationized over time via hydrolysis of the ester linkage in aqueous medium into poly(acrylic acid) and *N*,*N*'-dimethylamino ethyl ethanol. (33) The advantage of this degradative behavior is that it does not depend on external cues or environmental changes within the cell, but is rather self-catalyzed, occurring after just 10 hours. They discovered a dependency of transfection on molecular weight, whereby higher molecular weight pDMAEA resulted in greater transfection efficiency. They further reported complexation occurring from N/P ratio of 10, although some smudging on the retardation gel indicated that partial complexation was occurring. In their various studies, they obtained improved transfection efficiencies, indicating that the hydrolytic degradation was allowing for RNA/oligo-DNA cytosolic release. Werfel *et al*. (34) further investigated these hydrolytic charge-reversing polyplexes by copolymerizing 2-(*N*,*N*-dimethylamino)ethyl acrylate (DMAEA) with BMA in order to obtain enhanced pH responsive behavior for endosomal escape, via PEGylation. They compared p(DMAEA-*co*-BMA)-*b*-PEG (50:50) to p(DMAEMA-*co*-

BMA)-*b*-PEG (50:50), and found that siRNA was delivered to the cytosol more completely for p(DMAEA-*co*-BMA)-*b*-PEG polyplexes than the non-charge–reversing p(DMAEMA-*co*-BMA)-*b*-PEG system, thus showing improved intracellular bioavailability produced from the de-cationizing system.

Although PEGylation imparts many positive characteristics in the polyplex delivery systems, it has been associated with a decreased endosomal release, impeding RNA bioavailability in the cell due to core stabilization. (35-37) Therefore, a number of studies have looked at reversible PEGylation, *e.g*. through reducible linkers, (38) biotin-triggered linkers, (39) acid-labile linkers (40-44) and matrix metalloproteinases (MMP)-cleavable peptides. (13, 45) The various studies that incorporate an acid-labile linker take advantage of the pH change between serum (pH 7.4) and endosomes (pH 5.0). (46, 47)

Although PEG is by far the most researched protecting polymer in gene therapy, there are a number of drawbacks associated with the use of PEG in drug delivery. It has been known since 1950s that non-specific interactions between PEG and blood, induced blood clotting. (48) PEG has also been shown to cause a non-specific response by the immune system, which in the case of polyplex systems could lead to an immune response after intravenous administration. (49) There are a number of alternatives to PEG, which are less well investigated for polyplex systems. One such alternative is poly(*N*-vinylpyrrolidone) (PVP). It is a commercially available polymer that is frequently used in cosmetic and pharmaceutical products. Its chemical structure allows for a highly hydrated polymer, suppressing any immune responses. (50-52) PVP is easily synthesized via RAFT–mediated polymerization, (53-57) which produces a polymer readily modified for further use in applications such as drug delivery and gene therapy. (58)

We investigated the effect of adding an acid-labile linker between p(DMAEA-*co*-BMA) (50:50) and PVPas well as between p(DMAEMA-*co*-BMA) (50:50) and PVP, Figure 4.1, to assess whether we can obtain improved endosomal escape, while comparing the hydrolysable and non-hydrolysable systems. Oishi *et al*. (44, 59) demonstrated the ability of β-thiopropionate to be hydrolyzed under mild acidic conditions. By taking advantage of the pH change within the endosome, the β-thiopropionate has been shown to break, while an orthogonal ester linker has been demonstrated to not be sensitive enough. (60)

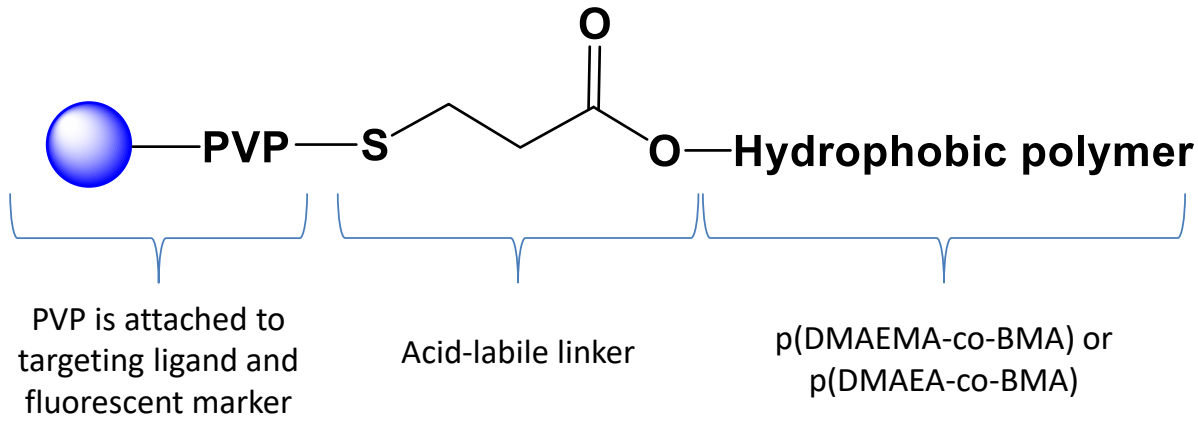

Figure 4.1 General structure of the diblock polymer system containing a hydrophobic polymer system, either p(DMAEMA-co-BMA) or p(DMAEA-co-BMA), capable of complexing with RNAs, conjugated via a β-thiopropionate linker to PVP. The PVP was pre-conjugated with targeting ligands and a fluorescent marker.

4.2 Results and discussion:

Figure 4.2 depicts the chemical structures of the reversible-addition fragmentation chain-transfer (RAFT) agents that have been utilized in the current study to prepare the respective polymer. RAFT agent **R4.1** was used to prepare well controlled PVP, while **R4.2** and **R4.3** were used to prepare p(DMAE(M)A-*co*-BMA). The details of the synthetic protocols and the choice of each RAFT agent are explained in more detail in Sections 4.2.1 and Section 4.2.2 for the hydrophilic block and hydrophobic blocks, respectively.

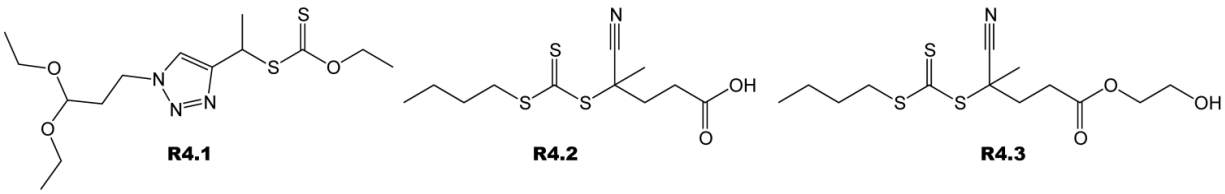

Figure 4.2 Chemical structures of chain transfer agents used within this chapter (R4.1-3)

Each block was separately synthesized and subsequently conjugated via a Michael addition (61-63) in order to obtain the β-thiopropionate linker in the manner seen in Scheme 4.1. Therefore, the synthesis and characterization of each block will be individually discussed below, as well as the subsequent conjugation experiments.

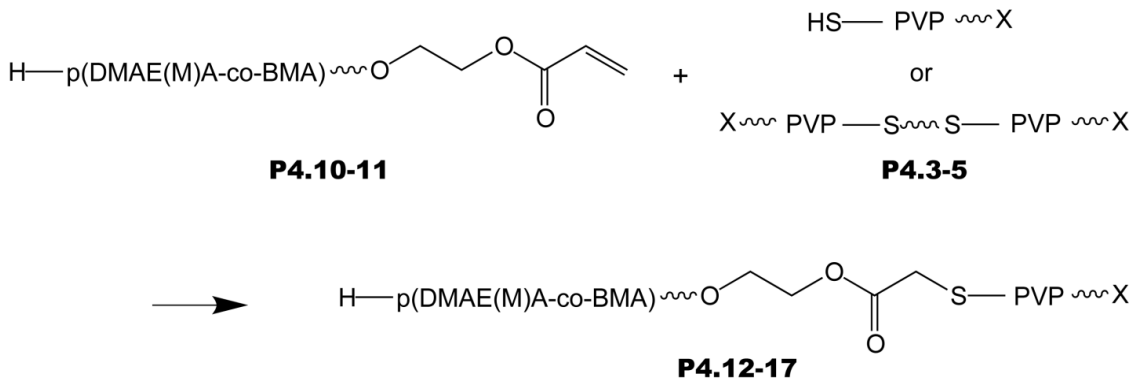

Scheme 4.1 Schematic representation of the reaction between the hydrophobic and hydrophilic polymer blocks via a Michael addition in order to obtain the pH-sensitive, diblock copolymer conjugates (P4.12-17)

4.2.1 Synthesis of the hydrophilic block: PVP

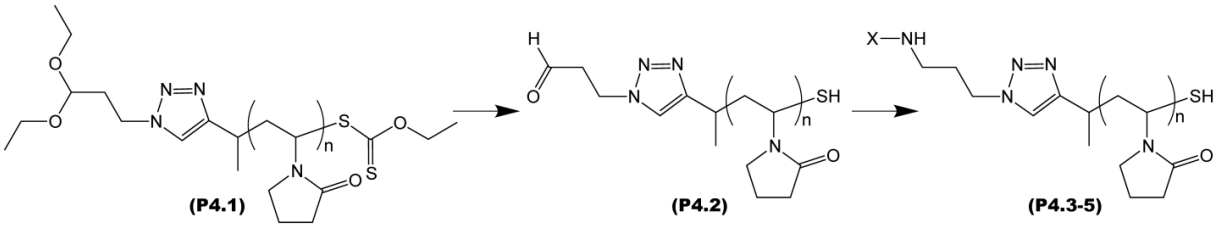

X – Targeting ligand or fluorescent marker or *n*-propylamine

Scheme 4.2 A schematic illustration of post-polymerization modification of PVP synthesized using R4.1 (See Figure 4.1); first the one-pot deprotection of the linear acetal into an aldehyde and a subsequent xanthate conversion to a thiol, followed by the conjugation of the aldehyde with an amine (targeting ligand, fluorescent marker, or *n*-propylamine quenching reagent) via reductive amination

A recent publication in our group described the RAFT–mediated polymerization of *N*VP using a xanthate as a chain transfer agent (CTA) (**R4.1**, Figure 4.2), containing a linear acetal leaving group functionality. The polymerization was shown to produce PVP with controlled molecular weight and low *Đ*. (64) The RAFT agent **R4.1** is a very convenient CTA for the polymerization of *N*VP, especially due to the ease with which α,ω-heterotelechelic polymer can be obtained via a one-pot, orthogonal end-group modification procedure. Thus, it is an ideal CTA for this study as it allows for the post-polymerization functionalization necessary

to link the PVP to the targeting ligand/fluorescent marker on the α-end group, and the acid-labile linker, connected to the hydrophobic polymer, on the ω-end group. **R4.1** was synthesized according to the method previously described by Reader *et al*. (64)

Table 4.1 Tabulation of results from RAFT–mediated polymerization of NVP using R4.1

Sample	M_n (target)	Temp (˚C)	CTA	Monomer	Initiator	Solvent	α‡ (%)	M_n§	M_W§	$Đ$§
P4.1	5000	25	**R4.1**	*N*VP	Ascorbic acid & *t*-BuOOH	water	60	4600	5500	1.2

§Determined by SEC in DMAc relative to PMMA standards.

‡Conversion obtained through gravimetric analysis.

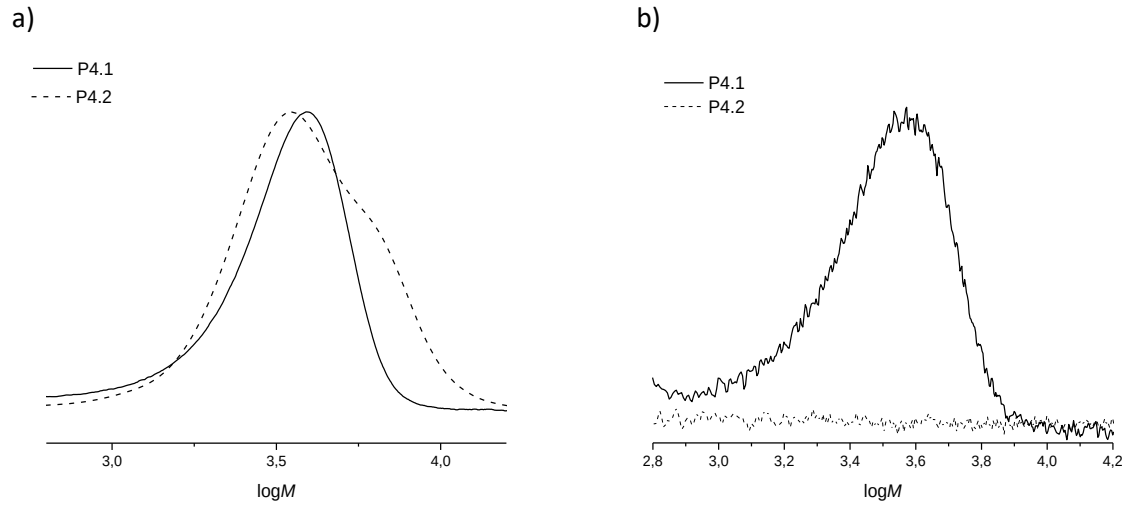

Figure 4.3 MMDs of RAFT–mediated polymerized PVP before (P4.1) and after (P4.2) the one-pot deprotection: (a): Molecular weight distribution (RI) of P4.1-2, whereby the bimodal distribution can be seen owing to the disulfide formation due to xanthate removal of P4.2. (b): UV-vis absorbance of the polymers at 290 nm with a disappearance of the absorbance due to xanthate end group removal of P4.2

Although conventional RAFT–mediated polymerization techniques, initiated with AIBN at 60 °C in 1,4-dioxane, using **R4.1** results in polymers with controlled molecular weight and molecular weight distribution, the AIBN:CTA ratio (1:4) needed in order to obtain 60% conversion of *N*VP was higher than desired. (64) The relatively high levels of AIBN mean that a higher fraction of chains than preferred will bear the AIBN fragment on the α-chain end, as

opposed to the leaving group of the chain transfer agent. In addition, the relatively high temperature leads to unsaturated chain ends. This of course, leads to a percentage of unmodifiable α- and ω-chain ends. Therefore, the aqueous redox method developed in Chapter 3 was used to polymerize *N*VP. Using this technique, PVP (**P4.1**) was obtained with good control over molecular weight and its distribution (*Đ* = 1.2), as seen in Table 4.1, while mitigating the chance of loss of xanthate end-groups. The one-pot method previously described (64) was used in order to simultaneously generate the deprotected aldehyde end-group and the thiol end-group to obtain the deprotected PVP (**P4.2**). The removal of the xanthate end-group was verified by both ^{1}H NMR spectroscopy and SEC analysis. Using ^{1}H NMR spectroscopy, the focus is on the disappearance of the protons belonging to the xanthate moiety (**f** in Figure 4.4a). While using SEC, Figure 4.3b, it is possible to see the disappearance of the UV-vis absorbance due to the xanthate group at 290 nm, as well as a bimodal distribution caused by the partial formation of disulfides, as previously described. (64) The aldehyde deprotection was confirmed by the appearance of a characteristic peak in the ^{1}H NMR spectrum at 9.7 ppm (**i** in Figure 4.4b), as well as the disappearance of the protons corresponding to the linear acetal protecting group (**h** in Figure 4.4a).

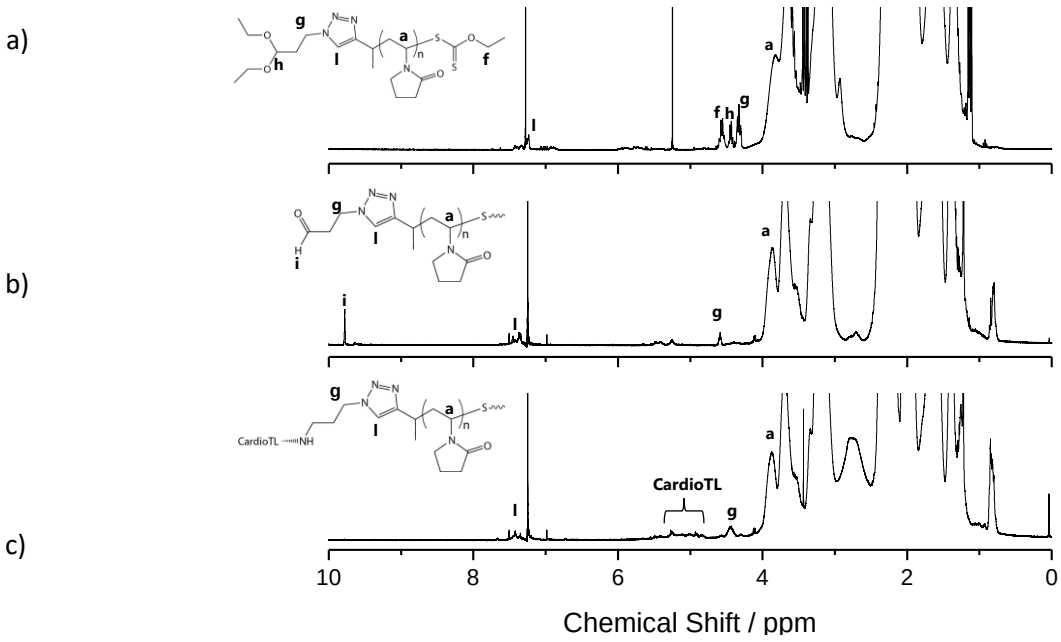

Figure 4.4 ^{1}H NMR spectra of (a): protected PVP (P4.1), (b): unprotected PVP (P4.2) and (c): CardioTL modified PVP (P4.4)

4.2.2 Targeting ligand modification of PVP

Next, the deprotected PVP was split up into three batches, two batches were modified with two targeting ligands (2% modification), ACDCRGDCFGG (hereafter referred to as RGD) (**P4.3**) and CSTSMLKAC (hereafter referred to as CardioTL) (**P4.4**), respectively, and the final batch was left without a targeting ligand modification (**P4.5**). Each batch containing the targeting ligand was also modified with amino-fluorescein (2% modification) and *n*-propyl amine (in excess) was used to quench the remaining aldehyde moieties in all three batches. These modifications were performed via a Schiff base formation and subsequent reductive amination to form secondary amines using sodium cyanoborohydride, as described in literature. (64) RGDs are known to assist with cellular uptake in a broad spectrum of cell types. (65, 66) Therefore, this targeting ligand was attached in order to obtain a more general polyplex system. In Chapter 5, the polymer conjugates will be used to complex anti-miR-214, which is known to regulate miRNA-214 expression, an inhibitor of angiogenesis via targeting Quaking and the reduction of angiogenic growth factor release. (67, 68) This will be discussed further in Chapter 5. However, due to the objective of targeting cardiovascular illnesses, and thus cardiovascular cell types, a known targeting ligand for cardiovascular cells, CardioTL, was attached to the PVP. The success of the Schiff base-reductive amination was confirmed via ^{1}H NMR spectroscopy, as seen in Figure 4.4c**,** with the disappearance of the representative aldehydic proton peak and a slight up-field shift of the protons belonging to **g**, due to the change in the protonic environment caused by the targeting ligands. Due to the low percentage of targeting ligand functionalization (2%) and amino-fluorescein (2%), and the comparatively large molecular weight of the PVP, it is not possible to precisely assign protons of these moieties. However, there are some small changes in the ^{1}H NMR spectra in the regions (4.8-5.3 ppm) where we expect protons corresponding to the targeting ligand, as well as in the region (7.25-7.5 ppm) in which we expect to find the targeting ligand's amide protons. Similarly, the protons corresponding to *n*-propyl amine overlap with the polymer's lactam protons, therefore, these peaks cannot be identified in the spectra. However, in order to confirm the fluorescence of the modified PVP, the samples were re-dissolved in water at a known concentration. Using a fluorescent plate reader, the samples were excited at 485 nm and the emission was measured at 535 nm. Figure 4.5 conclusively shows the strong emission of the amino-fluorescein modified polymers, while

the aldehyde precursor polymer does not show any fluorescence. This clearly indicates the successful attachment of the fluorescent marker via Schiff base-reductive amination.

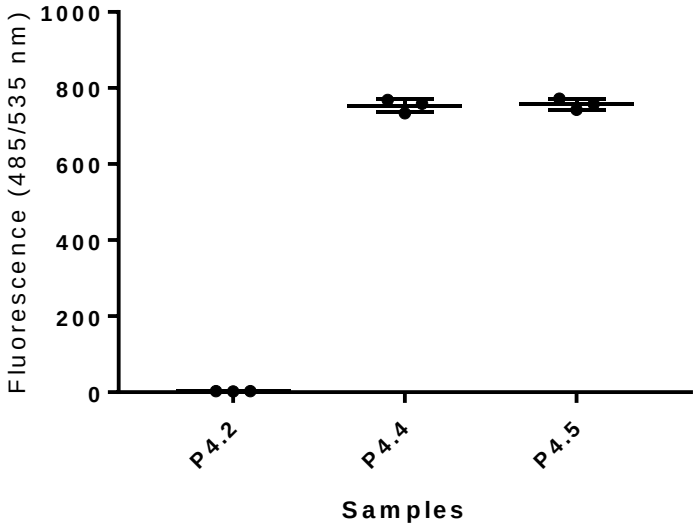

Figure 4.5 Fluorescence of amino-fluorescein modified and unmodified PVP at 485/535 nm

4.2.3 Synthesis of the hydrophobic blocks: p(DMAEMA-co-BMA) and p(DMAEA-co-BMA)

It was our desire to obtain a polycation block with an end group that could be functionalized post-polymerization to contain an acrylate moiety, with which the PVP could react via a Michael addition to obtain the β-thiopropionate acid-labile linkage. DMAEMA and DMAEA have been previously copolymerized with BMA using trithiocarbonate RAFT agents with good control over molecular weight and *Đ*. (25, 34) In order to stabilize the acid-labile linker, we used an ethylene glycol spacer between the carboxylic acid R-group and the potential β-thiopropionate acid-labile linkage. Therefore, we chose to synthesize 2-hydroxyethyl 4-{[(butylthio)carbonothioyl]thio}-4-cyanopentanoate (**R4.3,** Figure 4.2), with **R4.2** as an intermediate RAFT agent (the reaction is shown in Scheme S4.2). The synthesis was modified from a method previously described in literature. (69) The copolymerization and post-polymerization functionalization can be seen in Scheme 4.3 (a) and (b), respectively.

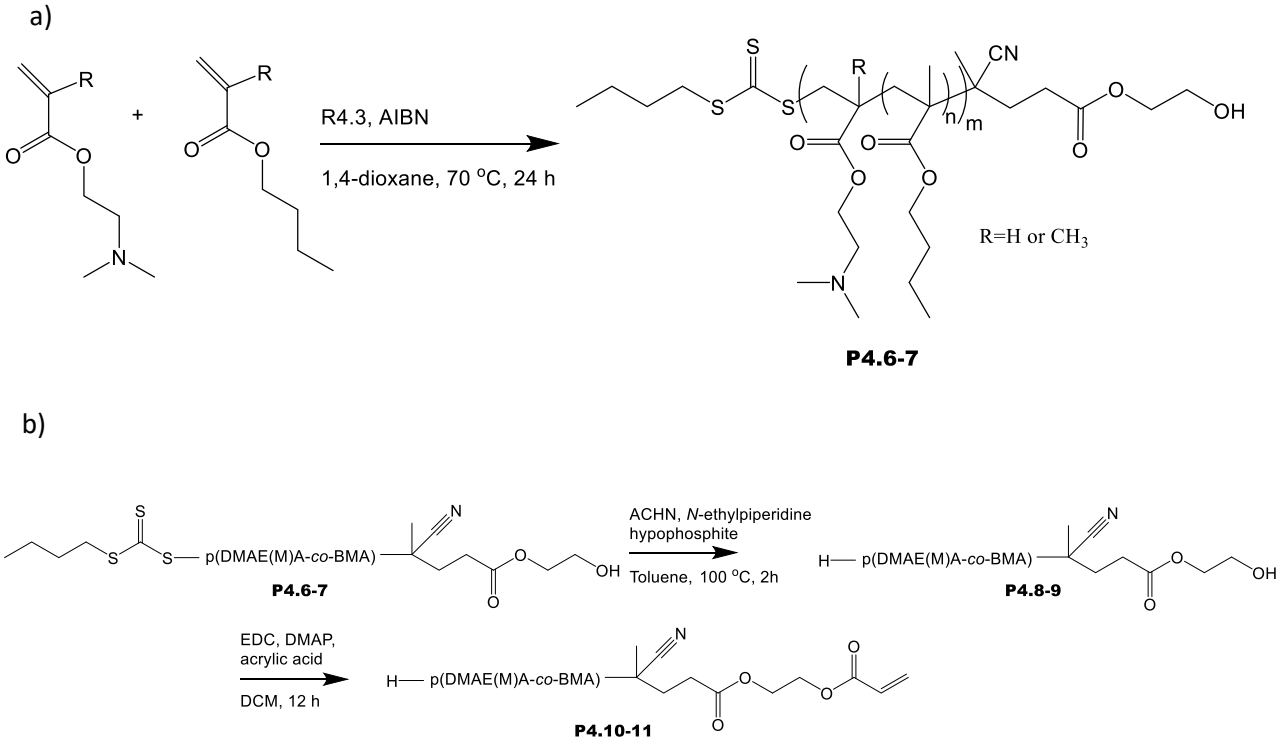

Scheme 4.3 (a): Copolymerization of DMAE(M)A and BMA, where R represents H (P4.6) or methyl (P4.7) moieties, (b): post-polymerization functionalization of end-groups on p(DMAE(M)A-*co*-BMA) in order to obtain an acrylate moiety for further conjugation via a Michael addition

As mentioned earlier in the chapter, the monomer feed ratio has previously been investigated, and a 1:1 ratio of DMAE(M)A:BMA seems to represent the best balance between the cationic nature of the copolymer for the complexation of RNAs and polyplex functionality, *e.g*. circulation time, pH-dependent membrane disruption leading to cellular uptake and enhanced endosomal escape. (25, 34) Therefore a 1:1 monomer feed ratio was chosen and using RAFT–mediated copolymerization of DMAEMA or DMAEA with BMA, p(DMAEMA-*co*-BMA) (**P4.6**) and p(DMAEA-*co*-BMA) (**P4.7**) were obtained with good control over the molecular weight and *Đ*, as seen in Table 4.2**.**

Table 4.2 Tabulation of results from RAFT–mediated copolymerization of DMAEMA and DMAEA with BMA

Sample	M_n (target)	Temp (˚C)	Monomer	CTA	AIBN:RAFT	Solvent	α‡ (%)	M_n§	M_W§	$Đ$§
P4.6	15 000	70	DMAEMA & BMA (1:1)	**R4.3**	1:7	1,4-Dioxane	95	16700	18700	1.1
P4.7	15 000	70	DMAEA & BMA (1:1)	**R4.3**	1:7	1,4-Dioxane	91	16800	19900	1.1

§Determined by SEC in DMAc relative to PMMA standards.
‡Conversion obtained through gravimetric analysis.

Post-polymerization modification of the copolymers was necessary in order to prepare them for the Michael addition to the PVP moieties. In order for this to be possible, Scheme 4.3 was followed, whereby the trithiocarbonate was first removed via a reaction with *N*-ethylpiperidine hypophosphite to form **P4.8-9**, according to literature. (70) The trithiocarbonate removal was confirmed by the disappearance of the characteristic trithiocarbonate UV-vis absorbance at 320 nm using SEC analysis, see Figure 4.6b and Figure 4.7b for p(DMAEMA-*co*-BMA) and p(PDMAEA-*co*-BMA), respectively. Subsequently, the acrylate moiety was added to the α-end group. At first, we tried to react the polymer with acryloyl chloride; however, this seemed to have an effect on the backbone of the p(DMAE(M)A-*co*-BMA). Thus, the acrylate was supplied via a 1-ethyl-3-(-3-dimethylaminopropyl) carbodiimide hydrochloride (EDC) coupling reaction between the polymer's hydroxyl end group and the carboxylic acid functional group of acrylic acid (**P4.10-11**). Confirming the success of this reaction was slightly problematic, since the molecular weights of the polymers were relatively high to rely on NMR or FT-IR spectroscopic analyses. The integrity of the polymer backbone was established using SEC analysis. However, no significant changes could be observed**,** Figure 4.6 (a) and Figure 4.7 (a), unlike after the previous method with acryloyl chloride. Therefore, we decided to continue with the Michael addition step. The Michael addition is completely dependent on the success of the EDC coupling; therefore, it could be quickly confirmed whether this was successful or not, through the realization of the diblock conjugation.

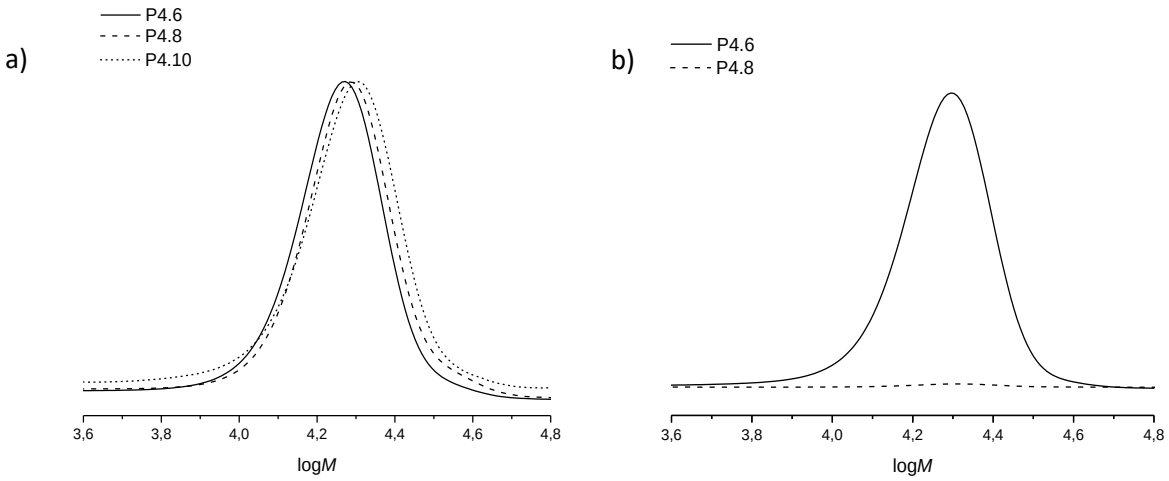

Figure 4.6 MMDs of p(DMAEMA-*co*-BMA) synthesized via RAFT–mediated polymerization before and after modification: Left: Molecular weight distribution (RI) of P4.6, P4.8 and P4.10. Right: UV-vis absorbance at 320 nm of P4.6 and P4.8 with a disappearance of the absorbance due to the trithiocarbonate-end group removal of P4.6

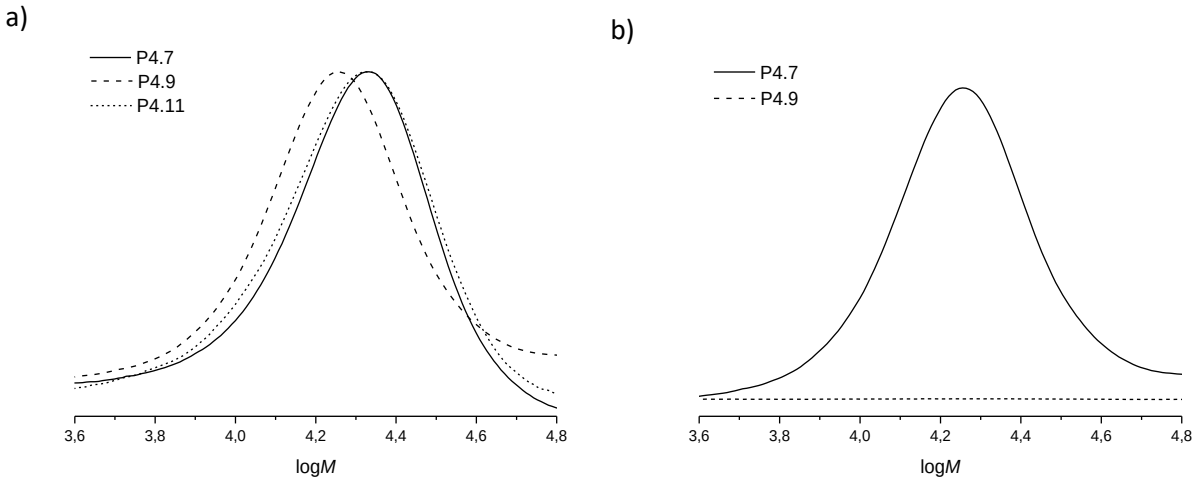

Figure 4.7 MMDs of p(DMAEA-*co*-BMA) synthesized via RAFT–mediated polymerization before and after modification: Left: Molecular weight distribution (RI) of P4.7, P4.9 and P4.11. Right: UV-vis absorbance at 320 nm of P4.7 and P4.9 with a disappearance of the absorbance due to the trithiocarbonate-end group removal of P4.7

4.2.4 Conjugation of PVP and p(DMAE(M)A-co-BMA) via the acid-labile linker

Table 4.3 Conjugation of p(DMAE(M)A-*co*-BMA) with three differently modified PVP blocks produced 6 conjugate diblock polymers

Conjugate	Hydrophobic block	Hydrophilic block
P4.12	p(DMAEMA-*co*-BMA) (**P4.10**)	PVP (**P4.3**)
P4.13	p(DMAEMA-*co*-BMA) (**P4.10**)	PVP-CardioTL (**P4.4**)
P4.14	p(DMAEMA-*co*-BMA) (**P4.10**)	PVP-RGD (**P4.5**)
P4.15	p(DMAEA-*co*-BMA) (**P4.11**)	PVP (**P4.3**)
P4.16	p(DMAEA-*co*-BMA) (**P4.11**)	PVP-CardioTL (**P4.4**)
P4.17	p(DMAEA-*co*-BMA) (**P4.11**)	PVP-RGF (**P4.5**)

PVP was added in a two-fold excess compared to p(DMAE(M)A-*co*-BMA)-acrylate. The Michael addition was performed by dissolving the variously modified PVPs (**P4.3-5**) and sodium borohydride in dry DMF under inert conditions. The sodium borohydride ensured that all of the PVP-disulfides are reduced to thiols. This was especially essential due to PVP's propensity towards disulfide formation after xanthate removal. The p(DMAE(M)A-*co*-BMA)-acrylate (**P4.10-11**) was separately dissolved in DMF and trimethylamine was added in catalytic amounts. The two solutions were then quickly added together and stirred for 12 hours, while maintaining inert conditions as to ensure disulfide formation was prevented. Six conjugates were obtained, as summarized in Table 4.3**:** p(DMAEMA-*co*-BMA)-*b*-PVP without a targeting ligand or fluorescent marker (**P4.12**), with a cardiovascular targeting ligand (CardioTL) and fluorescent marker (**P4.13**), and one with an RGD targeting ligand and fluorescent marker (**P4.14**); and then p(DMAEA-*co*-BMA)-*b*-PVP without a targeting ligand or fluorescent marker (**P4.15**), with a cardiovascular targeting ligand (CardioTL) and fluorescent marker (**P4.16**), and one with a RGD targeting ligand and fluorescent marker (**P4.17**). The conversion of the polymers into the conjugates was confirmed by a shift in the molecular weight distributions from SEC measurements in accordance to the sum of the molecular weights of the respective precursor blocks. This shift was observed for all 6 conjugates, refer to Figure 4.8. It is possible to see some residual, unconjugated PVP present in all of the samples. This is due to the excess of PVP used in the Michael addition. However, the shift of the molecular weight distribution of the precursor blocks towards higher molecular weight was sufficient evidence of the conjugation process.

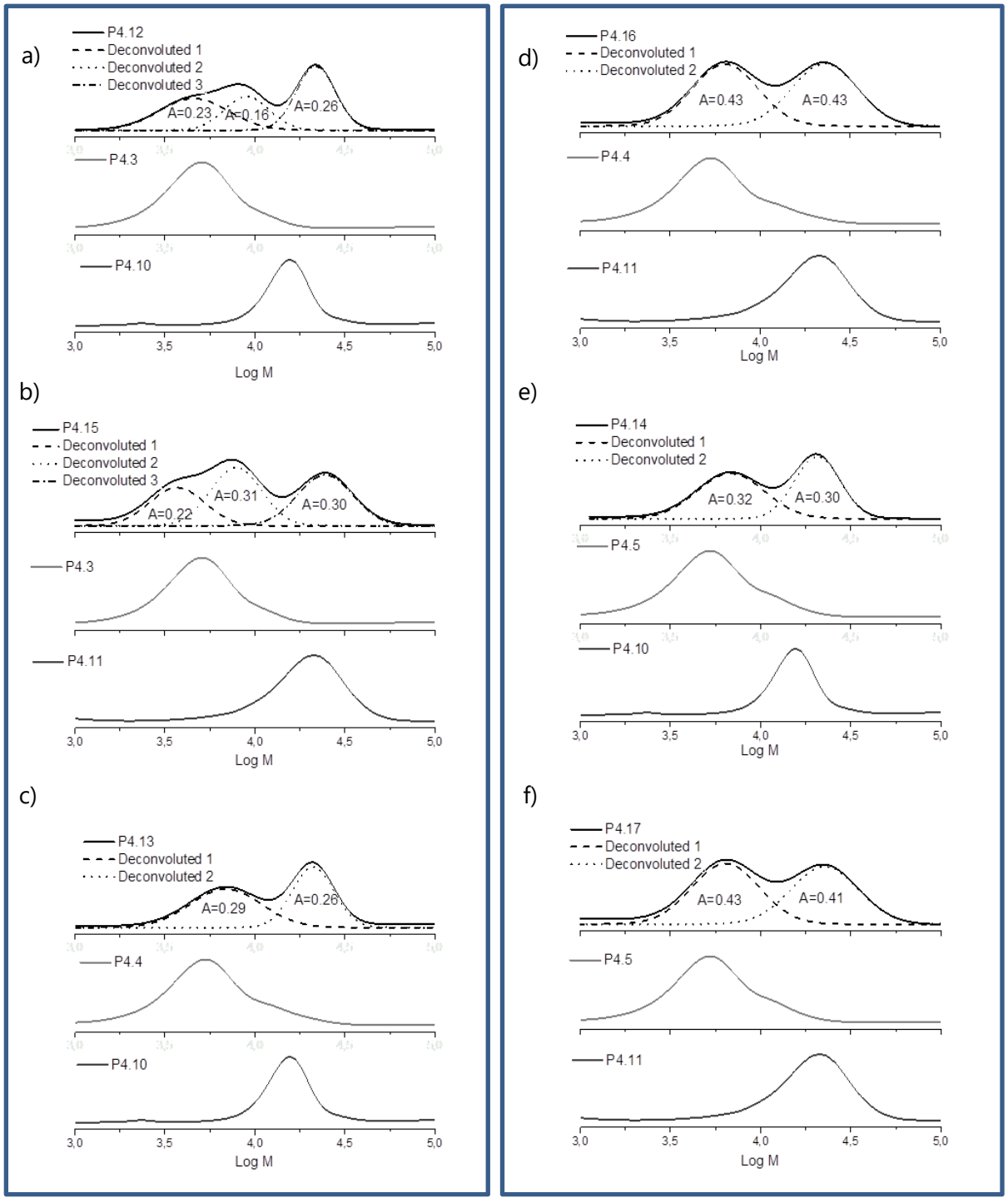

Figure 4.8 MMDs of p(DMAE(M)A-*co*-BMA)-*b*-PVP conjugates, where the conjugates contain (a): p(DMAEMA-*co*-BMA) and PVP without a targeting ligand (P4.12), (b): p(DMAEMA-*co*-BMA) and PVP with a cardiovascular targeting ligand (P4.13), (c): p(DMAEMA-co-BMA) and PVP with an RGD targeting ligand (P4.14), (d): p(DMAEA-*co*-BMA) and PVP without a targeting ligand (P4.15), (e): p(DMAEA-*co*-BMA) and PVP with a cardiovascular targeting ligand (P4.16) and (f): p(DMAEA-*co*-BMA) and PVP with an RGD targeting ligand (P4.17)

The efficiency of the conjugation process could not be evaluated from the current set of data, as the close proximity of the distribution of the precursor blocks and the resultant conjugate meant even the process of deconvolution of peaks would not provide conclusive evidence. For the purpose of the current study, the presence of either precursor block should not affect the formation of the polyplexes. Additionally, due to the sensitivity of the acid-labile, β-thiopropionate linker, we were cautious of further purification of the conjugates. Since the presence of free PVP in the samples should not affect the polyplex formation or function, it was decided to not pursue any further efforts towards purification of the conjugates.

4.3 Conclusion

α,ω-Heterotelechelic PVP was obtained by RAFT–mediated polymerization of NVP with the synthesized bifunctional CTA, **R4.1** via the polymerization technique developed in Chapter 3. A one-pot post-polymerization functionalization was then used to convert the protecting acetal into an aldehyde moiety, while the xanthate was converted to a thiol (disulfide). Thereafter, the PVP was split into three batches and reacted with various targeting ligands (2%), amino-fluorescein (2%), and finally quenched with *n*-propylamine.

p(DMAE(M)A-*co*-BMA) were prepared via RAFT–mediated polymerization with 2-hydroxyethyl 4-{[(butylthio)carbonothioyl]thio}-4-cyanopentanoate. After trithiocarbonate end-group removal, acrylate end-groups were added via an EDC-coupling between the hydroxyl α-end group of the polymer and acrylic acid.

The modified polymers were then conjugated together using a Michael addition, allowing for the incorporation of an acid-labile, β-thiopropionate linker between the two polymers. The success of the conjugation was confirmed using SEC analysis, and a shift in the molecular weight was observed. Due to the sensitivity of the acid-labile linker, no further purification techniques were used in order to purify the conjugates to rid them of excess free PVP. These conjugates were used for further experiments in Chapter 5.

4.4 Supplementary

4.4.1 General Experimental Details

Unless stated otherwise, all of the chemicals used were purchased from commercial sources and used without further purification. 2,2'-Azobis(isobutyronitrile) (AIBN) (Riedel-de Haën) was recrystallized from methanol. Subsequently it was dried under vacuum at room temperature. Solvents and monomers were dried and distilled before use, unless stated otherwise. The progress of the reactions were monitored using thin layer chromatography (TLC) with Machery-Nagel Silica gel 60 plates with a UV 254 fluorescent indicator.

^{1}H and ^{13}C NMR spectroscopy were measured on a Varian VXR-Unity (400 MHz) spectrometer and spectra were analyzed using MestreNova 9.0 and chemical shifts were reported in parts-per-million (ppm) which was referenced to the residual solvent protons. The samples were prepared in deuterated solvents (Cambridge Isotope Labs).

Size exclusion chromatography (SEC) was measured on a Shamdzu LC-10AT isocratic pump, a column fitted with a PSS guard column (50 x8 mm) in series with three PPS GRAM columns (300 x 8 mm, 10 µm, 2 x 3000 Å and 1 x 100 Å) kept at a constant temperature of 40 °C, a Waters 717+ auto-sampler, a Waters 2487 dual wavelength UV detector and a Waters 2414 differential refractive index (DRI) detector. The samples were measured in dimethylacetamide (DMAc) as the eluent stabilized with 0.05% BHT (*w*/*v*) and 0.03% LiCl (*w*/*v*), at a flow rate of 1 mL.min^{-1}. Sample preparation included filtering the sample solutions through a 0.45 µm GHP filter to remove impurities. The results were calibrated against PMMA standards (Polymer Laboratories) ranging from 690 to 1.2 x 10^{6} g.mol^{-1}. Data acquisition was performed using Millenium^{32} software, v4.

Fluorescent signal was measured using a SpectraMax M2 microplate-based multi-detector reader (Molecular Devices).

4.4.2 Experimental methods

*S-{1-[10(3,3-diethoxypropyl)-1H-1,2,3-triazol-4-yl]ethyl} O-ethyl carbonodithioate (**R4.1**)*

Method was followed according to procedure published by Reader *et al*. (64) ^{1}H NMR spectra for all steps corresponded well to that in literature. The synthesis steps were performed according to Scheme S4.1 and the methods are described in short below.

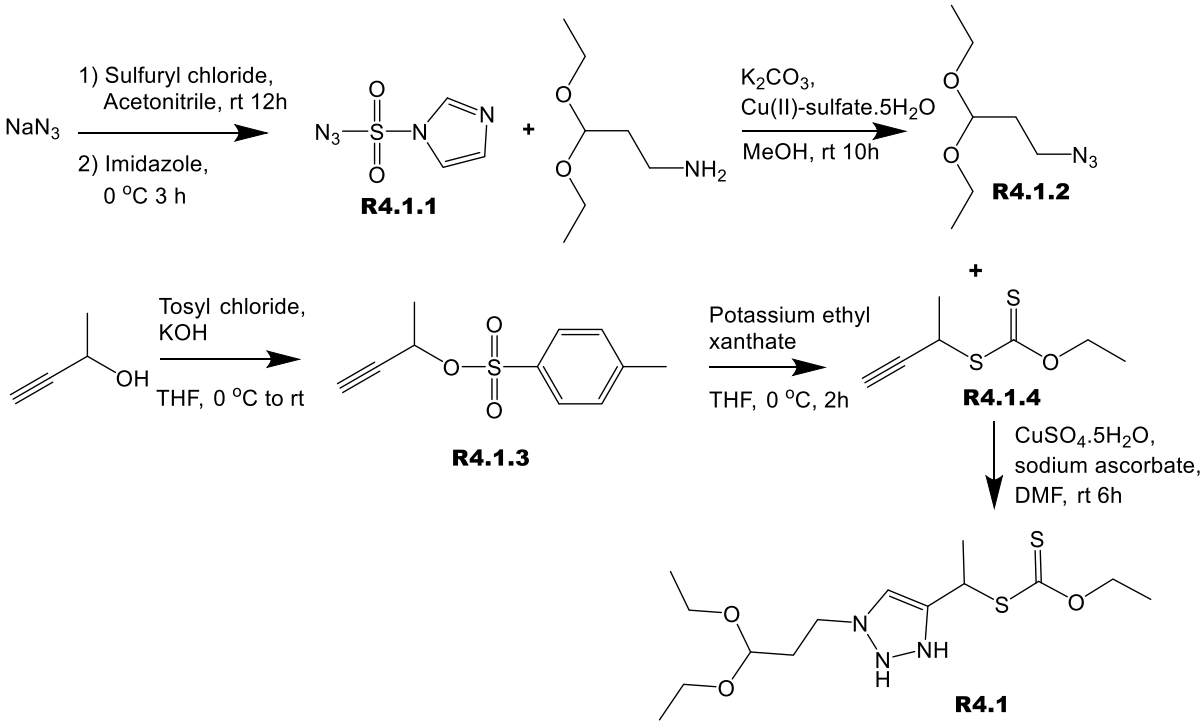

Scheme S4.1 schematic of synthetic pathway to obtain RAFT agents R4.1

*Step 1: Imidazole-1-sulfonyl azide hydrochloride (**R4.1.1**)*

Sulfuryl chloride (16.1 mL, 200 mmol) was added drop-wise to an ice-cooled suspension of sodium azide (13.0 g, 200 mmol) in dry acetonitrile (200 mL) and the mixture was stirred at rt for 12 h. The reaction mixture was cooled in an ice bath and imidazole (25.9 g, 380 mmol) added portion-wise and the resulting slurry was stirred for 3 h at rt. The reaction mixture was diluted with EtOAc (400 mL) and then washed with water (2 x 400 mL) and then with sat. $NaHCO_3$ (2 x 400 mL). The organic portion was isolated and dried over $MgSO_4$ and then filtered. A solution of HCl in ethyl acetate (4 M) (21.3 mL) was added drop-wise to the

filtrate while stirring in an ice bath. The precipitate was collected via filtration and washed with EtOAC (3 x 100 mL) to yield the activated azide product (**R4.1.1**) (23.4 g, 68%). Crude product used immediately in step 2 without any further purification.

*Step 2: 3-Azido-1,1-diethoxypropane (**R4.1.2**)*

1-amino-2,2-diethylpropane (5.00 g, 34.0 mmol), potassium carbonate (9.39 g, 68.0 mmol), Cu(II)-sulfate·$5H_2O$ (84.9 mg, 0.340 mmol) and MeOH (30 mL) were introduced into a RBF (100 mL). The activated azide (synthesized above) (8.50 g, 40.1 mmol) was dissolved in MeOH (20 mL) and added to the reaction mixture, and the solution was stirred for 10 h at rt. The mixture was then diluted with water (30 mL) and acidified to pH 6 using acetic acid and extracted with Et_2O (4 x 50 mL). The combined organic layers were washed with water (2 x 50 mL) and brine (2 x 50 mL), dried over anhydrous $MgSO_4$, filtered and concentrated to yield product as a dark yellow oil (**R4.1.2**) (3.8 g, 65%).

^{1}H NMR (400 MHz, $CDCl_3$) δ 4.61 (t, *J* = 5.6 Hz, 1H), 3.74 – 3.62 (m, 2H), 3.59 – 3.45 (m, 2H), 3.38 (t, *J* = 6.8 Hz, 2H), 1.89 (td, *J* = 6.8, 5.6 Hz, 2H), 1.28 – 1.17 (m, 6H).

*Step 3: O-(But-3-yn-2-yl) 4-methylbenzenesulfonate (**R4.1.3**)*

But-3-yn-2-ol (10.0 g, 142 mmol), Tosyl chloride (32.6 g, 171 mmol) and dry THF (100 mL) were added to a 250 mL RBF, and the mixture was cooled to 0 ˚C in a NaCl/ice bath. Potassium hydroxide (20.2 g, 360 mmol) was added portion-wise over 20 min, after which the suspension was stirred for 2 h, warming to rt on its own accord. The reaction mixture was filtered, washed with water (2 x 50 mL), dried over anhydrous MgSO4 and concentrated to yield crude, crystalline product **R4.1.3**. Product was used immediately in next step without further purification.

^{1}H NMR (400 MHz, DMSO-d_6) δ 7.78 (d, *J* = 7.7 Hz, 2H), 7.46 (d, *J* = 7.7 Hz, 2H), 5.23 (qd, *J* = 6.6, 2.1 Hz, 1H), 3.64 (d, *J* = 2.1 Hz, 1H), 2.40 (s, 3H), 1.40 (d, *J* = 6.6 Hz, 3H).

*Step 4: O-(But-3-yn-2-yl) O-ethyl carbonodithioate (**R4.1.4**)*

R4.1.3 (7.81g, 34.8 mmol) was dissolved in dry THF (100 mL) and cooled in an ice bath. Potassium ethyl xanthate (7.81 g, 48.7 mmol) was added portion-wise to the solution in an inert environment. The solution was stirred for 2 h in an ice bath. The mixture was filtered,

concentrated and purified via column chromatography (eluent: 100% pentane) to yield product as a light yellow oil (2.88 g, 47%).

^{1}H NMR (400 MHz, $CDCl_3$) δ 4.68 (q, *J* = 7.1 Hz, 2H), 4.49 (qd, *J* = 7.1, 2.5 Hz, 1H), 2.35 (d, *J* = 2.5 Hz, 1H), 1.64 (d, *J* = 7.1 Hz, 3H), 1.45 (t, *J* = 7.1 Hz, 3H).

*Step 5: O-(1-(1-(3,3-Diethoxypropyl)-1H-1,2,3-triazol-4-yl)ethyl) O-ethyl carbonodithioate (**R4.1**)*

R4.1.2 (1.0 g, 5.8 mmol), **R4.1.4** (1.51 g, 8.66 mmol), $CuSO_4 \cdot 5H_2O$ (144 mg, 0.577 mmol) and sodium ascorbate (285 mg, 1.44 mmol) were introduced into a small, pear-shaped flask (5 mL). Dry DMF (5 mL) was added and the solution was stirred at rt for 6 h. The solution was then filtered through celite and the filter was washed with CH_2Cl_2 (1 mL). The combined filtrate was purified via column chromatography (eluent: gradient eluent from 100 % hexane to 40 % EtOAc in Hexane) to yield product (**R4.1**) as a yellow oil (1.2 g, 3.48 mmol)

^{1}H NMR (400 MHz, $CDCl_3$) δ 7.52 (s, 1H), 5.08 (q, *J* = 7.2 Hz, 1H), 4.63 (q, *J* = 7.1 Hz, 2H), 4.47 (t, *J* = 5.4 Hz, 1H), 4.42 (t, *J* = 7.1 Hz, 2H), 3.71 – 3.60 (m, 2H), 3.53 – 3.40 (m, 2H), 2.20 (td, *J* = 7.0, 5.5 Hz, 2H), 1.81 (d, *J* = 7.2 Hz, 3H), 1.41 (t, *J* = 7.1 Hz, 3H), 1.20 (t, *J* = 7.0 Hz, 6H).

*Procedure for polymerizing NVP using **R4.1***

Method as described in Chapter 3.

One-pot removal of xanthate and aldehyde deprotection

Method was followed according to procedure published by Reader *et al.* (64)

In short, PVP (**P4.1**) (2.50 g, 0.543 mmol aldehyde), hexylamine (0.165 g, 1.63 mmol) and acetone (14 mL) were introduce into a RBF and the solution was stirred for 4h at rt. Thereafter, HCl in 1,4-dioxane (14 mL, 4M) was added dropwise. The solution was stirred for an additional 4 h at rt. The polymer was precipitated in Et_2O (3 x 200 mL) before redissolving in CH_2Cl_2 (5 mL) and purified via dialysis (3500 Da MWCO) against water/MeOH (1:1) for 2 days and then pure water for a further 2 days. The polymer was isolated as a white solid by freeze-drying it. End-group analysis was performed via ^{1}H NMR spectroscopy and SEC was performed in order to determine molar mass and dispersity.

Targeting ligand and amino-fluorescent functionalization of PVP

Method was followed according to procedure published by Reader *et al*. (64)

In short, deprotected PVP (1.00 g, 0.375 mmol aldehyde), Ala-Cys-Asp-Cys-Gly-Asp-Cys-Phe-Cys-Gly (8.6 mg, 0.0075 mmol), aminofluorescein (2.6 mg, 0.0075 mmol), $NaBH_3CN$ (235.65 mg, 3.75 mmol) and sodium borate buffer (5 mL, pH 10.4) were introduced into a pear-shaped flask. The solution was stirred at rt for 12 h and then purified via dialysis (3500 Da MWCO) against water for 2 days. The solution was then freeze-dried in order to obtain **P4.5** as a white powder. End-group analysis was performed via ^{1}H NMR spectroscopy.

Peptides used:

Cys-Ser-Thr-Ser-Met-Leu-Lys-Ala-Cys – Cardio TL

Ala-Cys-Asp-Cys-Gly-Asp-Cys-Phe-Cys-Gly – RGD TL

Synthesis of 2-hydroxyethyl 4-(((butylthio)carbonothioyl)thio)-4-cyanopentanoate (R4.3)

Synthesized according to method modified from a combination of *Eur. Polym. J.* **2015**, *66*, 543-557, (71) *Polymer* **2005**, *46*, 8458-8468 (72) and *Eur. Polym. J.* **2014**, *50*, 9-17. (69) The synthesis was performed according to Scheme S4.2 and the method is summarized below. ^{1}H NMR spectra for all steps corresponded well to that in literature.

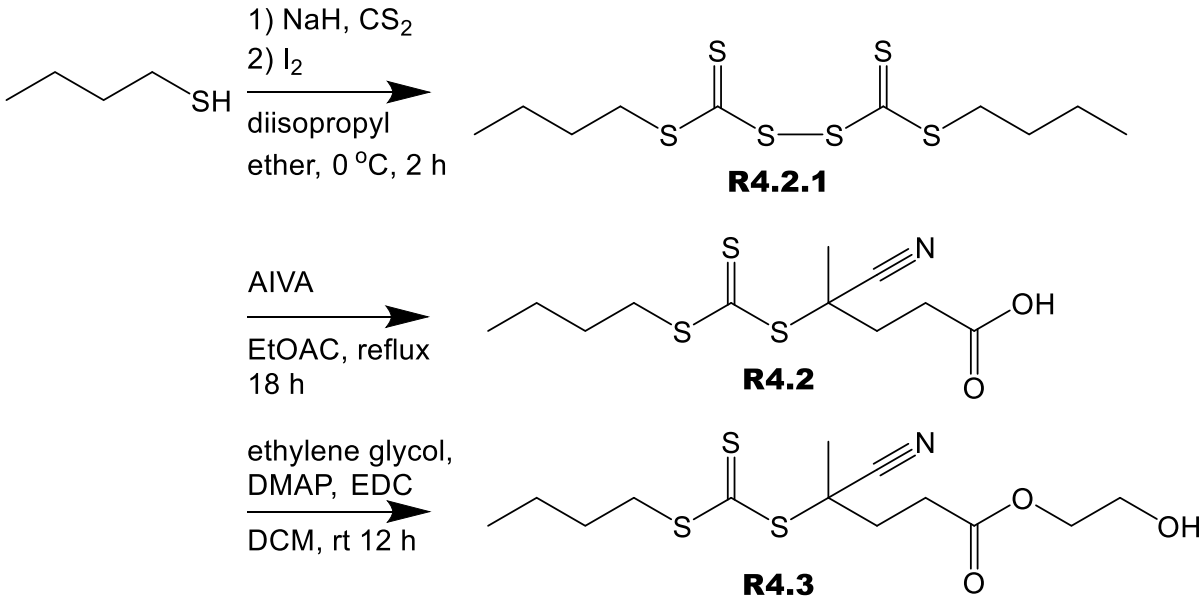

Scheme S4.2 schematic of synthetic pathway to obtain RAFT agents R4.2 and R4.3

*Synthesis of 4-cyano-4-(ethylthiocarbonothioylthio) pentanoic acid (**R4.2**)*

NaH (3.15 g, 79.0 mmol) was suspended in 100 mL diisopropyl ether (100 mL) at 0 ˚C. Butane thiol (6.84 g, 76.0 mmol) was added drop-wise over 10 min, and a white slurry formed. The solution was kept at 0 ˚C while CS_2 (6.0 g, 79 mmol) was added slowly and an orange/yellow precipitate formed. The precipitate was filtered and washed with diisopropyl ether (3 x 100 mL) and then resuspended in 100 mL diisopropyl ether (100 mL). Iodine (9.77 g, 38.8 mmol) was added and the solution was stirred for 1 h at rt. The solution was filtered and washed with 0.5 M aq. sodium thiosulphate solution, dried over anhydrous $MgSO_4$, filtered and concentrated to yield the corresponding disulphide as a yellow oil (**R4.2.1**), which was used for the next reaction without further purification.

R4.2.1 (7.0 g, 21 mmol) was redissolved in EtOAc (50 mL) and AIVA (8.90 g, 31.8 mmol) was added. The solution was refluxed for 18 h. Solution was concentrated and purified by column chromatography (eluent: 100% pentane gradient to 1:1 pentane: EtOAc) to yield **R4.2** as a yellow oil (5.45 g, 89%).

^{1}H NMR (300 MHz, $CDCl_3$) δ 3.36 (t, *J* = 7.2 Hz, 2H), 2.74 – 2.66 (m, 2H), 2.62 – 2.34 (m, 2H), 1.90 (s, 3H), 1.78 – 1.62 (m, 2H), 1.52 – 1.36 (m, 2H), 0.95 (t, *J* = 7.3 Hz, 3H)

*Step 2: 2-hydroxyethyl 4-{[(butylthio)carbonothioyl]thio}-4-cyanopentanoate (**R4.3**)*

R4.2 (8.45 g, 29.0 mmol), ethylene glycol (8.11 mL, 145 mmol) and DMAP (0.35 g, 2.9 mmol) were dissolved in CH_2Cl_2 (50 mL) and cooled to 0 ˚C. EDC (6.11 g, 31.9 mmol) was added portion-wise at 0 ˚C. The solution was stirred for 12 hours and allowed to reach rt on its own accord. The solution was concentrated under vacuum and redissolved in EtOAc (150 mL). Solution was washed with water (3 x 100 mL) and brine (3 x 100 mL), dried over $MgSO_4$, filtered and concentrated under vaccum. The crude product was purified by column chromatography (eluent: 1:1 EtOAc:pentane gradient to 100% EtOAc) to yield **R4.3** as an orange oil (7.9 g, 81%).

^{1}H NMR (300 MHz, $CDCl_3$) δ 4.30 – 4.21 (m, 2H), 3.89 – 3.79 (m, 2H), 3.41 – 3.29 (m, 2H), 2.73 – 2.65 (m, 2H), 2.64 – 2.33 (m, 2H), 1.89 (s, 3H), 1.74 – 1.60 (m, 2H), 1.51 – 1.37 (m, 2H), 0.95 (t, *J* = 7.3 Hz, 3H)

General procedure for synthesis of p(DMAEMA-co-BMA) and p(DMAEA-co-BMA):

DMAEMA (9.4 g, 59 mmol), BMA (8.5 g, 59 mmol), R4.3 (0.455 g, 1.19 mmol) and AIBN (28 mg, 0.17 mmol) were dissolved in 1,4-dioxane (17.88 mL). The solution was degassed with argon for 30 min and placed in a preheated bath at 70 ˚C. The reaction mixture was stirred for 24 h. The reaction was terminated by exposing it to oxygen, and the resulting polymer was precipitated in cold 1:1 pentane:diisopropyl ether (200 mL). After redissolving the polymer in CH_2Cl_2 (5 mL), it was again precipitated in 1:1 pentane:diisopropyl ether (200 mL). This was repeated twice to yield the polymer as a yellow solid (**P4.6**).

General procedure for removal of trithiocarbonate end group of p(DMEA(M)A-co-BMA):

p(DMAEMA-*co*-BMA) (**P4.6**) (2.0 g), ACHN (10.4, 0.043 mmol) and *N*-ethylpiperidine hypophosphite (0.120 g, 0.667 mmol) were dissolved in toluene (3 mL) and the solution was degassed with argon for 20 min. It was then heat to 100 ˚C for 2 h. The polymer was precipitated in cold 1:1 pentane:diisopropyl ether (3 x 200 mL) to obtain p(DMAEMA-*co*-BMA)-H (**P4.8**) (1.9 g).

General procedure for end-group functionalization of polymer with acrylic acid:

p(DMAEMA-*co*-BMA)-H (**P4.8**) (1.35 g), acrylic acid (69 mg, 0.96 mmol), DMAP (12 mg, 0.096 mmol) were dissolved in CH_2Cl_2 (5 mL) and cooled to 0 °C. EDC (277 mg, 1.45 mmol) was added portion-wise. Mixture was stirred at 0 °C for 30 minutes and then at rt for a further 12 hours. Precipitated in pentane and re-dissolved in MeOH. Solution was dialyzed against MeOH/water (1:1) for 2 days. MeOH was removed on the rotor evaporator under vacuum, and the remaining water was removed using the freeze dryer in order to obtain p(DMAEMA-*co*-BMA)-acrylate (**P4.10**) (1.3 g).

General procedure for conjugation of hydrophobic and hydrophilic blocks:

PVP-RGD (**P4.4**) (100 mg, 0.0217 mmol, 2 eq) and $NaBH_4$ (15 mg) were dissolved in DMF (2 mL) and degassed for 20 minutes. p(DMAEMA-*co*-BMA)-acrylate (**P4.10**) (190 mg, 0.0114

mmol, 1 eq) was dissolved in 2 mL DMF and TEA (60 mg) was added. The solution was added in one shot to the PVP solution. The resulting mixture was stirred for 12 hours. Water was added to the solution and then freeze dried to remove the water and DMF mixture in order to obtain the conjugate (**P4.14**) (202 mg).

4.5 References

1. Wang J, Lu Z, Wientjes MG, Au JLS. Delivery of siRNA therapeutics: Barriers and carriers. AAPS J. 2010;12(4):492-503.
2. Bartlett DW, Davis ME. Effect of siRNA nuclease stability on the in vitro and in vivo kinetics of siRNA-mediated gene silencing. Biotechnol Bioeng. 2007;97(4):909-21.
3. Whitehead KA, Langer R, Anderson DG. Knocking down barriers: advances in siRNA delivery. Nat Rev Drug Discov. 2009;8(2):129-38.
4. Kanasty R, Dorkin JR, Vegas A, Anderson D. Delivery materials for siRNA therapeutics. Nat Mater. 2013;12(11):967-77.
5. Biswal BK, Debata NB, Verma RS. Development of a targeted siRNA delivery system using FOL-PEG-PEI conjugate. Mol Biol Rep. 2010;37(6):2919-26.
6. Gosselin MA, Guo W, Lee RJ. Efficient gene transfer using reversibly cross-linked low molecular weight polyethylenimine. Bioconj Chem. 2001;12(6):989-94.
7. Liu Y, Samsonova O, Sproat B, Merkel O, Kissel T. Biophysical characterization of hyper-branched polyethylenimine-graft- polycaprolactone-block-mono-methoxyl-poly(ethylene glycol) copolymers (hy-PEI-PCL-mPEG) for siRNA delivery. J Control Release. 2011;153(3):262-8.
8. Wiseman JW, Goddard CA, McLelland D, Colledge WH. A comparison of linear and branched polyethylenimine (PEI) with DCChol/DOPE liposomes for gene delivery to epithelial cells in vitro and in vivo. Gene Ther. 2003;10:1654-62.
9. Raof NA, Rajamani D, Chu H-C, Gurav A, Johnson JM, LoGerfo FW, Bhasin M, Pradhan-Nabzdyk L. The effects of transfection reagent polyethyleneimine (PEI) and non-targeting control siRNAs on global gene expression in human aortic smooth muscle cells. BMC Genomics. 2016;17(20):1-13.
10. Peng H, Yang H, Song L, Zhou Z, Sun J, Du Y, Lu K, Li T, Yin A, Xu J, Wei S. Sustained delivery of siRNA/PEI complex from in situ forming hydrogels potently inhibits the proliferation of gastric cancer. J Exp Clin Cancer Res. 2016;35(57):1-9.
11. Verbaan FJ, Oussoren C, Snel CJ, Crommelin DJA, Hennink WE, Storm G. Steric stabilization of poly(2-(dimethylamino)ethyl methacrylate)-based polyplexes mediates prolonged circulation and tumor targeting in mice. J Gene Med. 2004;6(1):64-75.

12. Agarwal S, Zhang Y, Maji S, Greiner A. PDMAEMA based gene delivery materials. Mater Today. 2012;15(9):388-93.
13. Song Y, Zhang T, Song X, Zhang L, Zhang C, Xing J, Liang X-J. Polycations with excellent gene transfection ability based on PVP-g-PDMAEMA with random coil and micelle structures as non-viral gene vectors. J Mater Chem B. 2015;3(5):911-8.
14. Bitoque DB, Simão S, Oliveira AV, Machado S, Duran MR, Lopes E, da Costa AMR, Silva GA. Efficiency of RAFT-synthesized PDMAEMA in gene transfer to the retina. J Tissue Eng Regen M. 2017;11(1):265-75.
15. Synatschke CV, Schallon A, Jérôme V, Freitag R, Müller AHE. Influence of polymer architecture and molecular weight of poly(2-(dimethylamino)ethyl methacrylate) polycations on transfection efficiency and cell viability in gene delivery. Biomacromolecules. 2011;12(12):4247-55.
16. Pack DW, Hoffman AS, Pun S, Stayton PS. Design and development of polymers for gene delivery. Nat Rev Drug Discov. 2005;4(7):581-93.
17. Gary DJ, Puri N, Won Y-Y. Polymer-based siRNA delivery: Perspectives on the fundamental and phenomenological distinctions from polymer-based DNA delivery. J Control Release. 2007;121(1):64-73.
18. Mishra S, Webster P, Davis ME. PEGylation significantly affects cellular uptake and intracellular trafficking of non-viral gene delivery particles. Eur J Cell Biol. 2004;83(3):97-111.
19. Venkataraman S, Ong WL, Ong ZY, Joachim Loo SC, Rachel Ee PL, Yang YY. The role of PEG architecture and molecular weight in the gene transfection performance of PEGylated poly(dimethylaminoethyl methacrylate) based cationic polymers. Biomaterials. 2011;32(9):2369-78.
20. Sato A, Choi SW, Hirai M, Yamayoshi A, Moriyama R, Yamano T, Takagi M, Kano A, Shimamoto A, Maruyama A. Polymer brush-stabilized polyplex for a siRNA carrier with long circulatory half-life. J Control Release. 2007;122(3):209-16.
21. Davis ME, Zuckerman JE, Choi CHJ, Seligson D, Tolcher A, Alabi CA, Yen Y, Heidel JD, Ribas A. Evidence of RNAi in humans from systemically administered siRNA via targeted nanoparticles. Nature. 2010;464(7291):1067-70.
22. Zuckerman JE, Gritli I, Tolcher A, Heidel JD, Lim D, Morgan R, Chmielowski B, Ribas A, Davis ME, Yen Y. Correlating animal and human phase Ia/Ib clinical data with CALAA-

01, a targeted, polymer-based nanoparticle containing siRNA. P Natl Acad Sci. 2014;111(31):11449-54.

23. Zuckerman JE, Choi CHJ, Han H, Davis ME. Polycation-siRNA nanoparticles can disassemble at the kidney glomerular basement membrane. P Natl Acad Sci. 2012;109(8):3137-42.

24. Naeye B, Deschout H, Caveliers V, Descamps B, Braeckmans K, Vanhove C, Demeester J, Lahoutte T, De Smedt SC, Raemdonck K. In vivo disassembly of IV administered siRNA matrix nanoparticles at the renal filtration barrier. Biomaterials. 2013;34(9):2350-8.

25. Nelson CE, Kintzing JR, Hanna A, Shannon JM, Gupta MK, Duvall CL. Balancing cationic and hydrophobic content of PEGylated siRNA polyplexes enhances endosome escape, stability, blood circulation time, and bioactivity in vivo. ACS Nano. 2013;7(10):8870-80.

26. Shete HK, Prabhu RH, Patravale VB. Endosomal escape: a bottleneck in intracellular delivery. J Nanosci Nanotechnol. 2014;14(1):460-74.

27. Jhaveri A, Torchilin V. Intracellular delivery of nanocarriers and targeting to subcellular organelles. Expert Opin Drug Discov. 2016;13(1):49-70.

28. Lönn P, Kacsinta AD, Cui X-S, Hamil AS, Kaulich M, Gogoi K, Dowdy SF. Enhancing endosomal escape for intracellular delivery of macromolecular biologic therapeutics. Sci Rep. 2016;6(32301):1-9.

29. Ichim TE, Li M, Qian H, Popov IA, Rycerz K, Zheng X, White D, Zhong R, Min W-P. RNA interference: A potent tool for gene-specific therapeutics. Am J Transplant. 2004;4(8):1227-36.

30. Kurreck J. RNA interference: From basic research to therapeutic applications. Angew Chem Int Ed. 2009;48(8):1378-98.

31. Bumcrot D, Manoharan M, Koteliansky V, Sah DWY. RNAi therapeutics: a potential new class of pharmaceutical drugs. Nat Chem Biol. 2006;2:711-9.

32. Schaffer DV, Fidelman NA, Dan N, Lauffenburger DA. Vector unpacking as a potential barrier for receptor-mediated polyplex gene delivery. Biotechnol Bioeng. 2000;67(5):598-606.

33. Gu W, Jia Z, Truong NP, Prasadam I, Xiao Y, Monteiro MJ. Polymer nanocarrier system for endosome escape and timed release of siRNA with complete gene silencing and cell death in cancer cells. Biomacromolecules. 2013;14(10):3386-9.

34. Werfel TA, Swain C, Nelson CE, Kilchrist KV, Evans BC, Miteva M, Duvall CL. Hydrolytic charge-reversal of PEGylated polyplexes enhances intracellular un-packaging and activity of siRNA. J Biomed Mater Res Part A. 2016;104(4):917-27.

35. Nguyen H, Lemieux P, Vinogradov S, Gebhart C, Guérin N, Paradis G, Bronich T, Alakhov V, Kabanov A. Evaluation of polyether-polyethyleneimine graft copolymers as gene transfer agents. Gene Ther. 2000;7(2):126-38.

36. Choi YH, Liu F, Kim J-S, Choi YK, Jong Sang P, Kim SW. Polyethylene glycol-grafted poly-L-lysine as polymeric gene carrier. J Control Release. 1998;54(1):39-48.

37. Oupicky D, Ogris M, Howard KA, Dash PR, Ulbrich K, Seymour LW. Importance of lateral and steric stabilization of polyelectrolyte gene delivery vectors for extended systemic circulation. Mol Ther. 2002;5(4):463-72.

38. Carlisle RC, Etrych T, Briggs SS, Preece JA, Ulbrich K, Seymour LW. Polymer-coated polyethylenimine/DNA complexes designed for triggered activation by intracellular reduction. J Gene Med. 2004;6(3):337-44.

39. Xiong MP, Forrest ML, Karls AL, Kwon GS. Biotin-triggered release of poly(ethylene glycol)−avidin from biotinylated polyethylenimine enhances in vitro gene expression. Bioconj Chem. 2007;18(3):746-53.

40. Walker GF, Fella C, Pelisek J, Fahrmeir J, Boeckle S, Ogris M, Wagner E. Toward synthetic viruses: Endosomal pH-triggered deshielding of targeted polyplexes greatly enhances gene transfer in vitro and in vivo. Mol Ther. 2005;11(3):418-25.

41. Knorr V, Allmendinger L, Walker GF, Paintner FF, Wagner E. An acetal-based PEGylation reagent for pH-sensitive shielding of DNA polyplexes. Bioconj Chem. 2007;18(4):1218-25.

42. Chan C-L, Majzoub RN, Shirazi RS, Ewert KK, Chen Y-J, Liang KS, Safinya CR. Endosomal escape and transfection efficiency of PEGylated cationic liposome–DNA complexes prepared with an acid-labile PEG-lipid. Biomaterials. 2012;33(19):4928-35.

43. Chen K, Chen Q, Wang K, Zhu J, Li W, Li W, Qiu L, Guan G, Qiao M, Zhao X, Hu H, Chen D. Synthesis and characterization of a PAMAM-OH derivative containing an acid-labile β-thiopropionate bond for gene delivery. Int J Pharm. 2016;509(1):314-27.

44. Oishi M, Sasaki S, Nagasaki Y, Kataoka K. pH-responsive oligodeoxynucleotide (ODN)−poly(ethylene glycol) conjugate through acid-labile β-thiopropionate linkage: Preparation and polyion complex micelle formation. Biomacromolecules. 2003;4(5):1426-32.

45. Li H, Yu SS, Miteva M, Nelson CE, Werfel T, Giorgio TD, Duvall CL. Matrix metalloproteinase responsive, proximity-activated polymeric nanoparticles for siRNA delivery. Adv Funct Mater. 2013;23(24):3040-52.

46. Binauld S, Stenzel MH. Acid-degradable polymers for drug delivery: a decade of innovation. Chem Commun. 2013;49(21):2082-102.

47. Tannock IF, Rotin D. Acid pH in tumors and its potential for therapeutic exploitation. Cancer Res. 1989;49(16):4373-84.

48. Smyth HF, Carpenter CP, Weil CS. The toxicology of the polyethylene glycols. J Am Pharm Assoc Sci. 1950;39(6):349-54.

49. Knop K, Hoogenboom R, Fischer D, Schubert US. Poly(ethylene glycol) in drug delivery: Pros and cons as well as potential alternatives. Angew Chem Int Ed. 2010;49(36):6288-308.

50. Ouimet MA, Fogaça R, Snyder SS, Sathaye S, Catalani LH, Pochan DJ, Uhrich KE. Poly(anhydride-ester) and poly(N-vinyl-2-pyrrolidone) blends: salicylic acid-releasing blends with hydrogel-like properties that reduce inflammation. Macromol Biosci. 2015;15(3):342-50.

51. Lopérgolo LC, Lugão AB, Catalani LH. Direct UV photocrosslinking of poly(N-vinyl-2-pyrrolidone) (PVP) to produce hydrogels. Polymer. 2003;44(20):6217-22.

52. Payne MS, Horbett TA. Complement activation by hydroxyethylmethacrylate-ethylmethacrylate copolymers. J Biomed Mater Res. 1987;21(7):843-59.

53. Barner-Kowollik C, Davis TP, Stenzel MH. Synthesis of star polymers using RAFT polymerization: What is possible? Aust J Chem. 2006;59(10):719-27.

54. Boyer C, Bulmus V, Davis TP, Ladmiral V, Liu J, Perrier S. Bioapplications of RAFT polymerization. Chem Rev. 2009;109(11):5402-36.

55. Harrisson S, Liu X, Ollagnier J-N, Coutelier O, Marty J-D, Destarac M. RAFT polymerization of vinyl esters: Synthesis and applications. Polymer. 2014;6(5):1437-88.

56. Patel VK, Mishra AK, Vishwakarma NK, Biswas CS, Ray B. (*S*)-2-(Ethyl propionate)-(O-ethyl xanthate) and (*S*)-2-(ethyl isobutyrate)-(O-ethyl xanthate)-mediated RAFT polymerization of N-vinylpyrrolidone. Polym Bull. 2010;65(2):97-110.

57. Stenzel MH. RAFT polymerization: an avenue to functional polymeric micelles for drug delivery. Chem Commun. 2008(30):3486-503.

58. Hamidi M, Azadi A, Rafiei P. Hydrogel nanoparticles in drug delivery. Adv Drug Del Rev. 2008;60(15):1638-49.

59. Oishi M, Nagasaki Y, Itaka K, Nishiyama N, Kataoka K. Lactosylated poly(ethylene glycol)-siRNA conjugate through acid-labile β-thiopropionate linkage to construct pH-sensitive polyion complex micelles achieving enhanced gene silencing in hepatoma cells. J Am Chem Soc. 2005;127(6):1624-5.

60. Lin S, Du F, Wang Y, Ji S, Liang D, Yu L, Li Z. An acid-labile block copolymer of PDMAEMA and PEG as potential carrier for intelligent gene delivery systems. Biomacromolecules. 2008;9(1):109-15.

61. Nair DP, Podgórski M, Chatani S, Gong T, Xi W, Fenoli CR, Bowman CN. The thiol-michael addition click reaction: A powerful and widely used tool in materials chemistry. Chem Mater. 2014;26(1):724-44.

62. Matsuoka S-i, Kamijo Y, Suzuki M. Post-polymerization modification of unsaturated polyesters by Michael addition of N-heterocyclic carbenes. Polym J. 2017;49(5):423-8.

63. Mather BD, Viswanathan K, Miller KM, Long TE. Michael addition reactions in macromolecular design for emerging technologies. Prog Polym Sci. 2006;31(5):487-531.

64. Reader PW, Pfukwa R, Jokonya S, Arnott GE, Klumperman B. Synthesis of α,ω-heterotelechelic PVP for bioconjugation, via a one-pot orthogonal end-group modification procedure. Polym Chem. 2016;7(42):6450-6.

65. Bellis SL. Advantages of RGD peptides for directing cell association with biomaterials. Biomaterials. 2011;32(18):4205-10.

66. Zhou Q-H, You Y-Z, Wu C, Huang YI, OupickÝ D. Cyclic RGD-targeting of reversibly-stabilized DNA nanoparticles enhances cell uptake and transfection in vitro. J Drug Target. 2009;17(5):364-73.

67. van Mil A, Grundmann S, Goumans M-J, Lei Z, Oerlemans MI, Jaksani S, Doevendans PA, Sluijter JPG. MicroRNA-214 inhibits angiogenesis by targeting Quaking and reducing angiogenic growth factor release. Cardiovasc Res. 2012;93(4):655-65.

68. Wu Y, Li Z, Yang M, Dai B, Hu F, Yang F, Zhu J, Chen T, Zhang L. MicroRNA-214 regulates smooth muscle cell differentiation from stem cells by targeting RNA-binding protein QKI. Oncotarget. 2017;8(12):19866-78.

69. Liu J, Cui L, Kong N, Barrow CJ, Yang W. RAFT controlled synthesis of graphene/polymer hydrogel with enhanced mechanical property for pH-controlled drug release. Eur Polym J. 2014;50(Supplement C):9-17.

70. Chong YK, Moad G, Rizzardo E, Thang SH. Thiocarbonylthio end group removal from RAFT-synthesized polymers by radical-induced reduction. Macromolecules. 2007;40(13):4446-55.

71. Krivorotova T, Radzevicius P, Makuska R. Synthesis and characterization of anionic pentablock brush copolymers bearing poly(acrylic acid) side chains on the brush blocks separated by linear poly(butyl methacrylate) blocks. Eur Polym J. 2015;66(Supplement C):543-57.

72. Moad G, Chong YK, Postma A, Rizzardo E, Thang SH. Advances in RAFT polymerization: the synthesis of polymers with defined end-groups. Polymer. 2005;46(19):8458-68.

Synopsis

pH-responsive polyplexes have been reported for their use as carriers in modulation of gene regulation through improved facilitation of endosomal escape. In this study, the use of novel PVPylated pDMAEMA and pDMAEA conjugates, linked via a β-thiopropionate linker were tested for complexation efficiency with anti-microRNA (miRNA) therapeutics, their cytotoxicity and serum and blood stability, cellular uptake and finally efficiency regulation in luciferase expression.

5.1 Introduction

New blood vessels, crucial for embryonic organ development and adult tissue repair, are formed from pre-existing endothelium during angiogenesis as a response to angiogenic stimuli. Lack of control over the growth of blood vessels is a side-effect of several disorders, and can either be in the form of an excessive increase or decrease in angiogenesis. Examples of overexpressed angiogenesis can lead to cancer, diabetic blindness or age-related macular degeneration, while endothelial dysfunction can lead to coronary artery disease and strokes. (1) Non-coding microRNAs (miRNAs) are known to play an important role in regulating gene expression by inhibiting or degrading messenger RNAs (mRNAs). One miRNA has been seen to be capable of targeting numerous mRNA with similar functions or within related pathways, thus, making them master regulators of gene expression. (2-4) Research into microRNA-214 has linked it to the inhibition of angiogenesis. It does this by directly targeting a protein that is critical for vascular development and remodeling, Quaking (QKI), probably by regulating the secretion of growth factors such as VEGF, bFGF and PDGF. (5) QKI has been identified as an RNA-binding protein, which has an impact on vasculature development and remodeling. (6-8)

When a disease originates from abnormal inhibition of mRNAs triggered by an overexpression of miRNAs, it is possible to use synthetically designed, complementary anti-miRNAs in order to inhibit the expression of the miRNA through direct binding. (9) Anti-miRNAs can be modified with e.g. 2'O methyl, phosphorothioate linkages and 3'cholesterol, for enhanced stability, nuclease resistance and cellular uptake, as well as improved binding affinity to target miRNAs, and are then known as antagomiRs, see Figure 5.1. (10) Antagomirs and anti-miRNAs are thought to be powerful therapeutic tools for the silencing of miRNAs in disease. (9) Van Mil *et al*. (5) showed that anti-miRNA-214 can be used in the downregulation of miRNA-214, and thus, is a possible therapeutic in the upregulation of QKI.

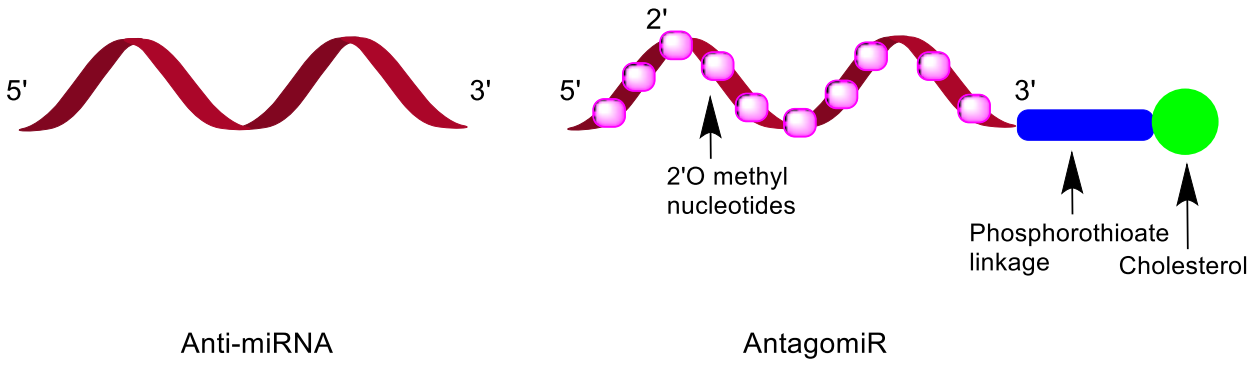

Figure 5.1 Schematic representation of anti-miRNA and antagomiR structures and the chemical modifications of antagomiRs which provide stability and protection against nucleases

However, the challenge of the therapeutic applications of anti-miRNAs remains in their specific targeted delivery. They face the same problems with stability, circulation time and uptake as miRNAs and siRNAs, unless in their modified, antagomiR form. However, antagomiRs are only plausible for local delivery. Since anti-miRNAs share the same basic properties, including small size and negative charge, with miRNA and siRNA, the previously provided extensive research into their delivery, discussed in Chapter 2 and 4, can also be applied to anti-miRNAs.

In this chapter, we have used the di-block polymeric system designed in Chapter 4 to test its feasibility as a delivery vehicle for anti-miRNA-214. In order to do this, the complexation ability, cytotoxicity, cellular uptake and transfection efficiency of the polyplex systems were tested.

5.2 Results and Discussion

5.2.1 Polyplex formation and characterization

The block copolymer conjugates synthesized in Chapter 4 and anti-miRNA-214/antagomiR-214 were combined to form polyplexes at different N/P ratios. The successful complexation with Cy3-labelled antagomiR-214 was confirmed by agarose gel electrophoresis, as seen in Figure 5.2. Complexation of the antagomiR with all polymer combinations (no targeting ligand, CSTSMLKAC-cardiovascular targeting ligand (**CardioTL**) (11, 12) and the integrin targeting peptide ACDCRGDCFGG (**RGD**) (13, 14)) was tested. Complexed RNA is unable to move through the gel, whereas free RNA moves from the negative electrode towards the

positive due to its negative charge and smaller size. Therefore, the free RNA is close to the positive electrode (right hand side), while the formation of polyplexes can be visualized by the RNA not moving towards the positive electrode, and instead remaining in the wells where it was plated (left hand side). Since, antagomiR-214 is single stranded, ethidium bromide, a DNA interchelator and a common staining technique cannot be used to visualize it. Therefore, a fluorescent scanner was used in order to visualize the Cy-3 fluorescent label attached to antagomiR-214. All polymers are seen to condense antagomiR-214 at N/P ratios as low as 3, with no free RNA molecules present. These complexation N/P ratios are somewhat lower than those previously reported for pDMAEA polyplexes. (15) In Figure 5.2, it is possible to see an increase in the complexation efficiency from a low N/P ratio towards a higher N/P ratio by the increase in the fluorescent signal at higher N/P ratios.

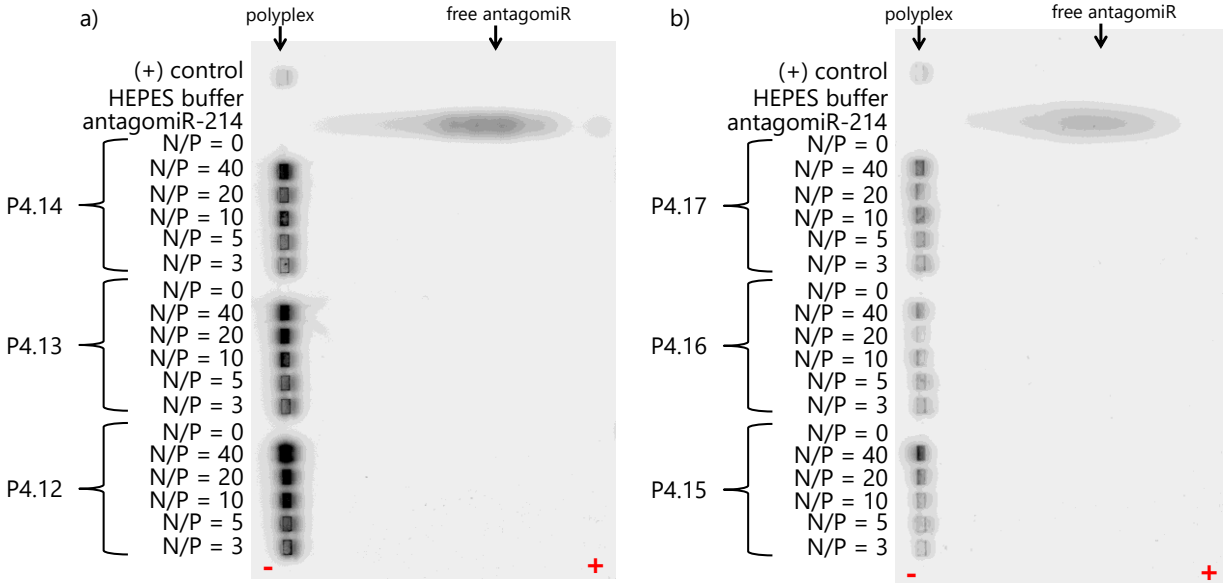

Figure 5.2 Agarose gel retardation of polyplexes containing Cy3-labeled antagomiR-214 at different N/P ratios, where a) shows complexes composed of p(DMAEMA-co-BMA)-*b*-PVP (P4.12-P4.14) and b) shows complexes composed of p(DMAEA-co-BMA)-*b*-PVP (P4.15-P4.17). Successful complexation can be observed at all N/P ratios for all six polymer systems.

As discussed in Chapter 4, pDMAEA is known to hydrolyze to nontoxic poly(acrylic acid) in aqueous environments over a few hours without any influence from triggers such as a change in pH, as seen in Scheme 5.1. As this decationizing degradation is favourable, since it

allows for the release of the RNA payload, we wanted to ensure that it was not inhibited in anyway by the PVPylation or presence of the acid-labile linker. Thus, the polyplexes were incubated in HEPES buffer for 2 days and subsequently agarose gel electrophoresis was employed to visualize the complexation efficiency, see Figure 5.3. The polyplexes formed from p(DMAEMA-*co*-BMA)-*b*-PVP are stable after 2 days of incubation in an aqueous environment, whereas those polyplexes formed from p(DMAEA-*co*-BMA)-*b*-PVP had released some of the RNAs, observed by the presence of free RNA on the positive region of the gel. The fluorescent intensity of the agarose gels in Figure 5.3 is somewhat lower than that in Figure 5.2, which is most probably due to the time-frame of the experiment causing the fluorescent marker to exhibit lower emission.

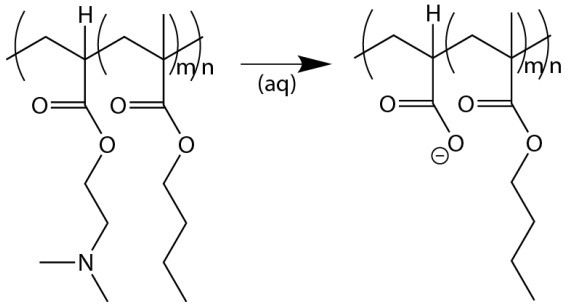

Scheme 5.1 Hydrolysis of pDMAEA into poly(acrylic acid), causing decationization of the polymer block.

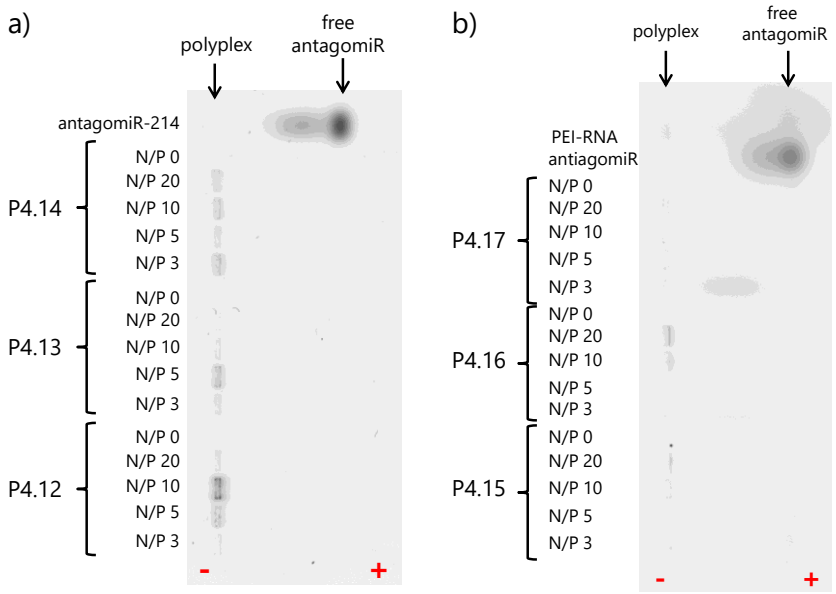

Figure 5.3 Agarose gel retardation of polyplexes after 2 days of incubation in HEPES buffer. The polyplexes composed of a) p(DMAEMA-*co*-BMA)-*b*-PVP remain stable with antagomiR complexed,

while polyplexes composed of b) p(DMAEA-*co*-BMA)-*b*-PVP are starting to decompose releasing some of the antagomiRs

p(DMAEMA-*co*-BMA)-*b*-PVP polyplexes were then incubated for a period of 5 days, and it was observed that some antagomiR was starting to be released from the polyplex, indicating some possible polyplex degradation, seen in Figure 5.4.

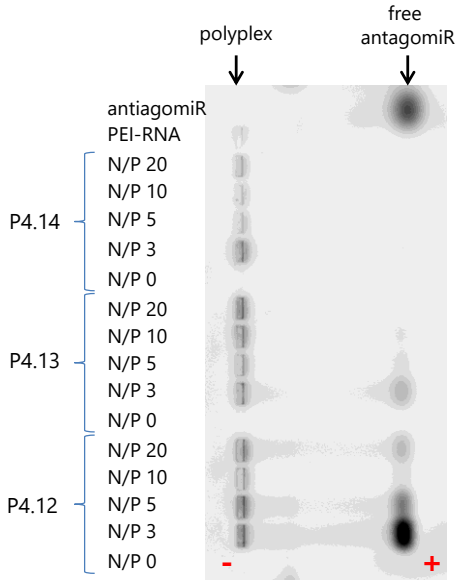

Figure 5.4 After 5 days of incubation in HEPES buffer, the polyplexes containing P(DMAEMA-co-BMA)-b-PVP are also starting to release some of the RNAs

Nanoparticle tracking analysis (NTA) was employed to determine the mean size of the polyplexes at N/P ratios of 10 and 20. As expected, the size is inversely proportional to the N/P ratio, with N/P ratios of 20 producing marginally smaller polyplexes. All polyplexes are between 44 and 58 nm in size with narrow dispersities, as can be seen in Table 5.1.

Table 5.1 Complex size measured by NTA reported in nm. Results are shown as mean ± SD where n=3.

Polyplex polymer	N/P 10	N/P 20
p(DMAEMA-co-BMA)-*b*-PVP	51.4 ± 1.1	46.7 ± 2.2
p(DMAEA-co-BMA))-*b*-PVP	49.9 ± 0.3	45.8 ± 0.9

To subsequently visualize the polyplexes we used TEM, however, a large amount of aggregation was observed in the obtained images, see Figure 5.5. Uranyl acetate, frequently used to stain TEM samples, was employed during the sample preparation. As the staining solution has a pH below 6, it is possible that the acid-labile linker hydrolyzed during the staining procedure. Polyplexes without a hydrophilic block are known to aggregate, while the PEGylation of polyplexes is reported to decrease this aggregation. (16) The aggregation in the TEM results was not consistent with the results obtained via nanoparticle tracker analysis (NTA). A different, neutral stain, methylamine tungstate, was attempted; however, this resulted in micrographs with poor contrast (results not shown).

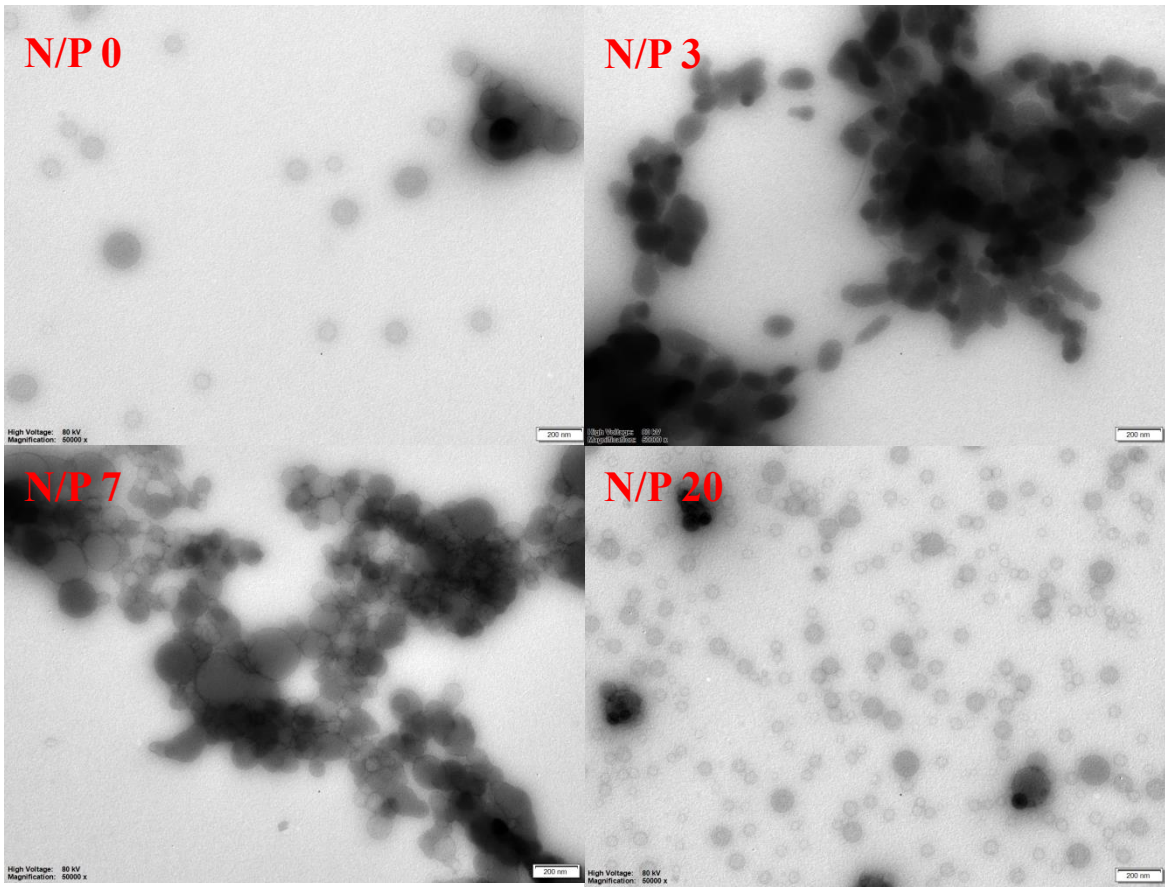

Figure 5.5 Transmission electron micrographs of polyplexes composed of P4.12 and anti-miRNA-214 at various N/P ratios. Samples were stained with uranyl acetate.

The zeta-potential (ζ-potential) of the polyplexes was measured at N/P 10, 20 and 40 with a linear relationship observed between ζ-potential and N/P ratio for all of the polyplexes, see

Figure 5.6. The obtained results show that, in general, the complexes containing p(DMAEMA-*co*-BMA)-*b*-PVP (**P4.12-14**) contain a higher negative charge at N/P 10 than those containing p(DMAEA-*co*-BMA)-*b*-PVP (**P4.15-17**). However at an N/P ratio of 40, the complexes also contained a similar higher positive charge than the p(DMAEA-*co*-BMA)-*b*-PVP complexes.

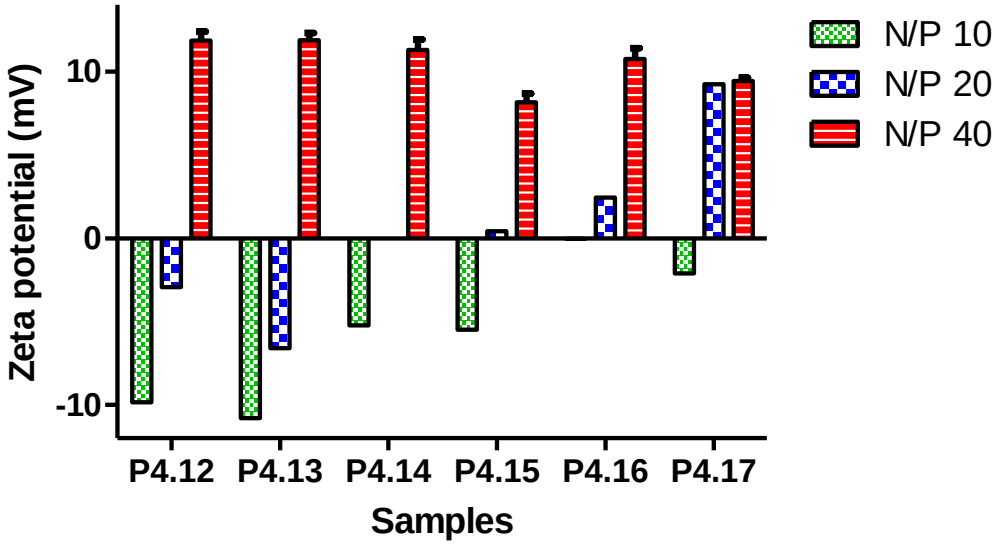

Figure 5.6 Zeta potential measured in polyplexes at different N/P ratios. Results are shown as mean ± SD where n=3.

5.2.2 Serum stability

When the polyplexes are used intravenously, they will be exposed to blood, where it is possible for them to interact with serum proteins, erythrocytes and other blood cells. This can cause aggregation which would ultimately lead to polyplex clearance by the reticulo-endothelial system (RES) as well as to cellular toxicity. (17) The instability of polyplexes in the presence of serum is a rather large setback in most polyplex systems. It has been shown that conjugation of the polyplexes with PEG improves biocompatibility and stability. (16) The stability of PVPylated polyplexes at N/P 10 and N/P 20 was determined by incubating them in the presence of varying concentrations of fetal bovine serum (FBS) for 4 hours, and subsequently running agarose gel electrophoresis, see Figure 5.7**.** No significant polyplex

degradation was observed as evidenced by the strong bands in the agarose gel corresponding to undamaged polyplexes. An additional band can be observed, which is characteristic of the presence of serum. Therefore, the polyplexes exhibit excellent serum stability in these conditions, which indicates that the presence of PVP on the surface of the polyplexes prevent nonspecific protein adsorption. Interestingly, the polyplexes containing p(DMAEA-*co*-BMA)-*b*-PVP incubated in the absence of FBS, see Figure 5.7 (b), exhibit some decomplexation probably due to decationization via hydrolysis in the aqueous medium. However, in the presence of FBS, this decationization is reduced. Consequently, decationizing polyplexes will potentially show enhanced stability in the presence of serum, *i.e.* during systemic circulation, which would improve their half-life and passive targeting, while after cellular uptake they provide a mechanism to release their payload. Further, *in vivo* investigations will be necessary to confirm this.

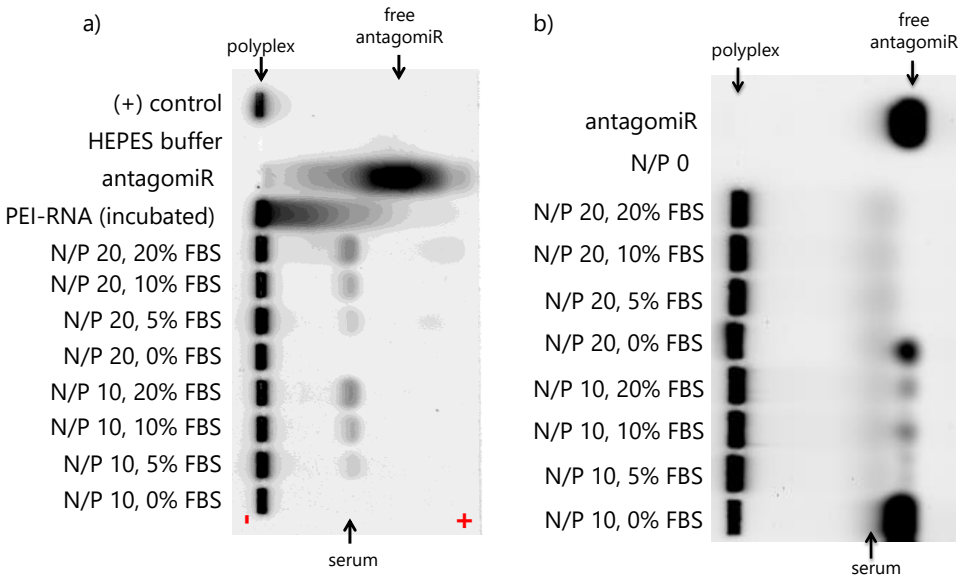

Figure 5.7 Agarose gel retardation of polyplexes incubated in the presence of varying concentrations of fetal bovine serum, where polyplexes are composed of a) P4.13 and b) P4.15

Erythrocytes are negatively charged blood cells and have previously been shown to interact with polyplexes. Ultimately, this leads to aggregate formation and systemic toxicity. (18) In order to predict the possibility of erythrocyte hemolysis induced by the polyplexes, erythrocytes were isolated from human blood and incubated in the presence of polyplexes

(N/P 10, 20, 40, 100 and 500) for 1 hour at 37 °C. Subsequently, the concentration of released haemoglobin in the supernatant after centrifugation was measured by UV-vis absorbance at 550 nm, see Figure 5.8. The pellet was redissolved in PBS and visualized for aggregation under the microscope, Figure 5.9.

The hemolysis caused by polyplexes was compared to the hemolysis effect caused by Lipofectamine and PEI, Figure 5.8. It is clear that polyplexes from p(DMAEA-*co*-BMA)-*b*-PVP (**P4.15-17**) induce hemolysis to a greater extent than those from p(DMAEMA-*co*-BMA)-*b*-PVP (**P4.12-14**). The N/P ratio also impacts the hemolysis, with higher N/P ratios causing more hemolysis. Lipofectamine 2000 induced a large degree of hemolysis, only surpassed by the polyplexes investigated in this study at extremely high N/P ratios (>100).

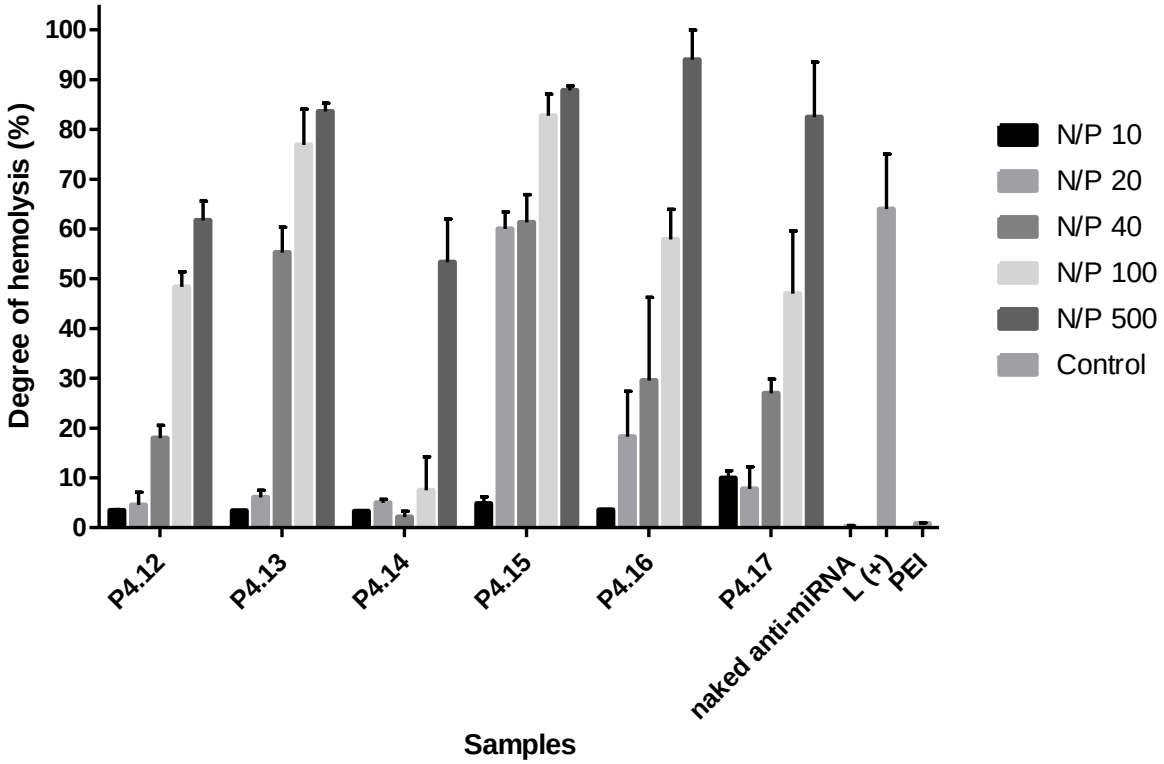

Figure 5.8 Polyplex-induced erythrocyte hemolysis. Polyplexes were incubated with erythrocytes for 1 hour at 37 °C. PEI polyplex and Lipofectamine 2000 were used as controls. The graph represents the degree of erythrocyte hemolysis determined by absorbance detection at 550 nm. Results are shown as mean ± SD where n=3.

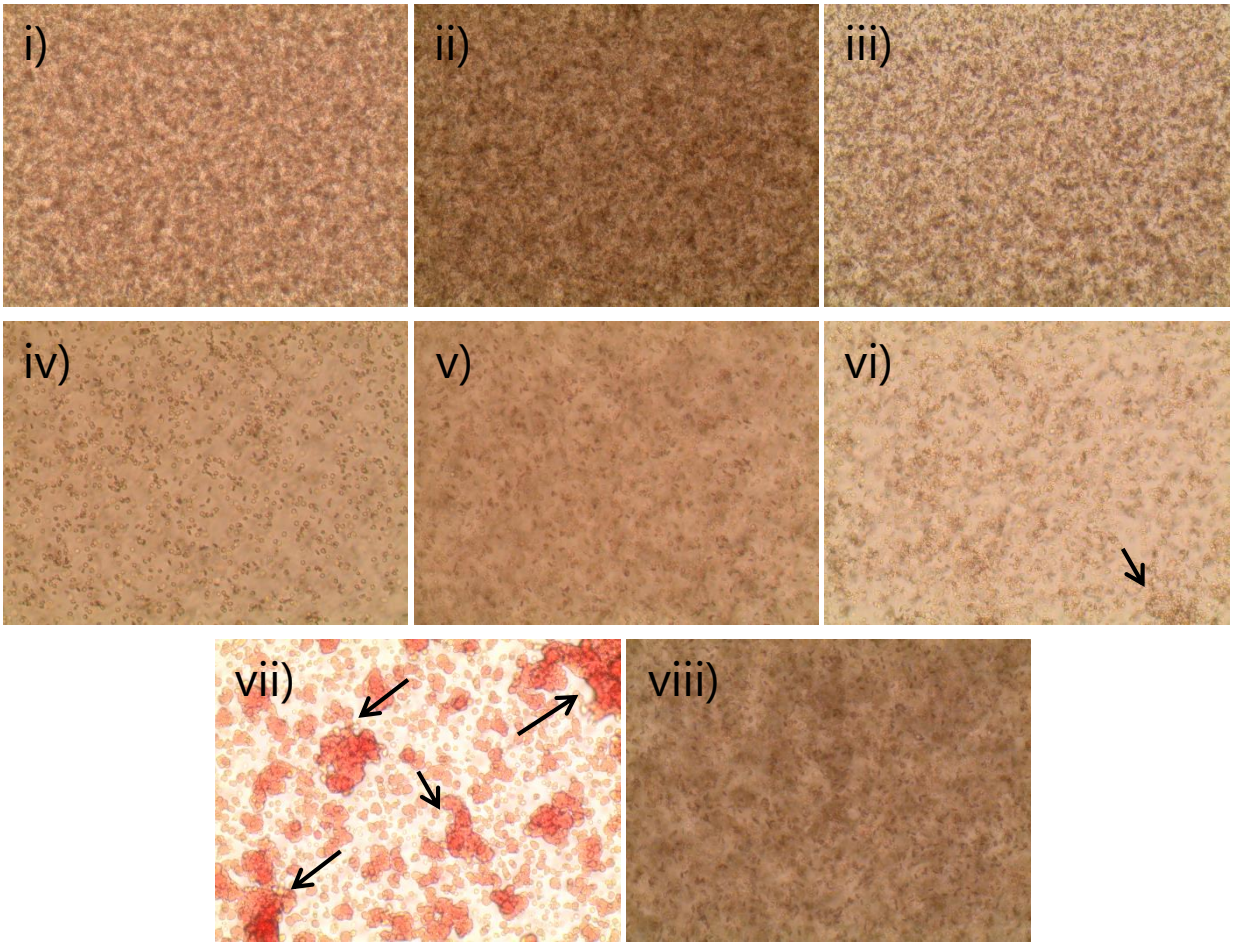

Figure 5.9 Polyplex-induced erythrocyte aggregation. Polyplexes were incubated with erythrocytes for 1 hour at 37 °C. PEI polyplex and naked anti-miRNAs were used as controls. Representative microscopic images of erythrocyte aggregation, whereby aggregates are indicated using arrows. Erythrocytes were incubated with anti-miRNA-214 polyplexes composed of i) P4.12, ii) P4.13, iii) P4.14, iv) P4.15, v) P4.16, vi) P4.17, all at N/P 40, vii) PEI and finally with viii) naked anti-miRNA-214.

Although it can be observed in Figure 5.8, that PEI causes very small degrees of hemolysis, it causes extremely large degrees of erythrocyte aggregation, see Figure 5.9. Conversely, the polyplexes composed of the p(DMAEMA-*co*-BMA)-*b*-PVP (**P4.12-14**), Figure 5.9 (i-iii), and p(DMAEA-*co*-BMA)-*b*-PVP (**P4.15-17**), Figure 5.9 (iv-vi), did not cause high degrees of aggregation at N/P ratios as high as 40. Only P4.17 shows a slight amount of erythrocyte clustering. However, there are fewer erythrocytes visible for samples incubated with pDMAEA polyplexes (**P4.15-17**) correlating to the higher degrees of hemolysis.

5.2.3 Cytotoxicity

The *in vitro* cytotoxicity was assessed using Annexin V and Sytox® blue. Annexin V is an intracellular protein, which binds to phosphatidylerine. In healthy cells, phosphatidylerine is located on the intracellular leaflet of the plasma membrane, however, during early apoptosis, or cell stress, the membrane loses its asymmetry and the phosphatidylerine can also be seen on the external leaflet. When present on the external leaflet, Annexin V is able to bind to the phosphatidylerine, and when it is labelled with a fluorophore, it can be used to detect early apoptotic cells through flow cytometry. Since cells are capable of recovering from early apoptosis, it is also important to detect dead cells. This was performed using Sytox® blue, which is a stain with a high affinity for nucleic acids. When cell membranes are compromised, *i.e*. the cells are dead, the stain is able to penetrate the cell membrane and reach the nucleic acids. However, when the cells are still viable, the stain is unable to cross the cell membrane. Therefore, only dead cells are stained with Sytox® blue.

Cardiomyocyte progenitor cells (CMPCs) were exposed to polyplexes at various N/P ratios at a constant concentration of Cy3-labelled antagomiRs. The results are summarized in Figure 5.10. No significant signs of cell death are observed. Only at N/P 40 for RGD-labeled polyplexes, some apoptosis is observed indicating some cell stress. However, it is notable that the pDMAEA complexes (**P4.15-17**) cause slightly higher cytotoxicity than the pDMAEMA complexes (**P4.12-14**).

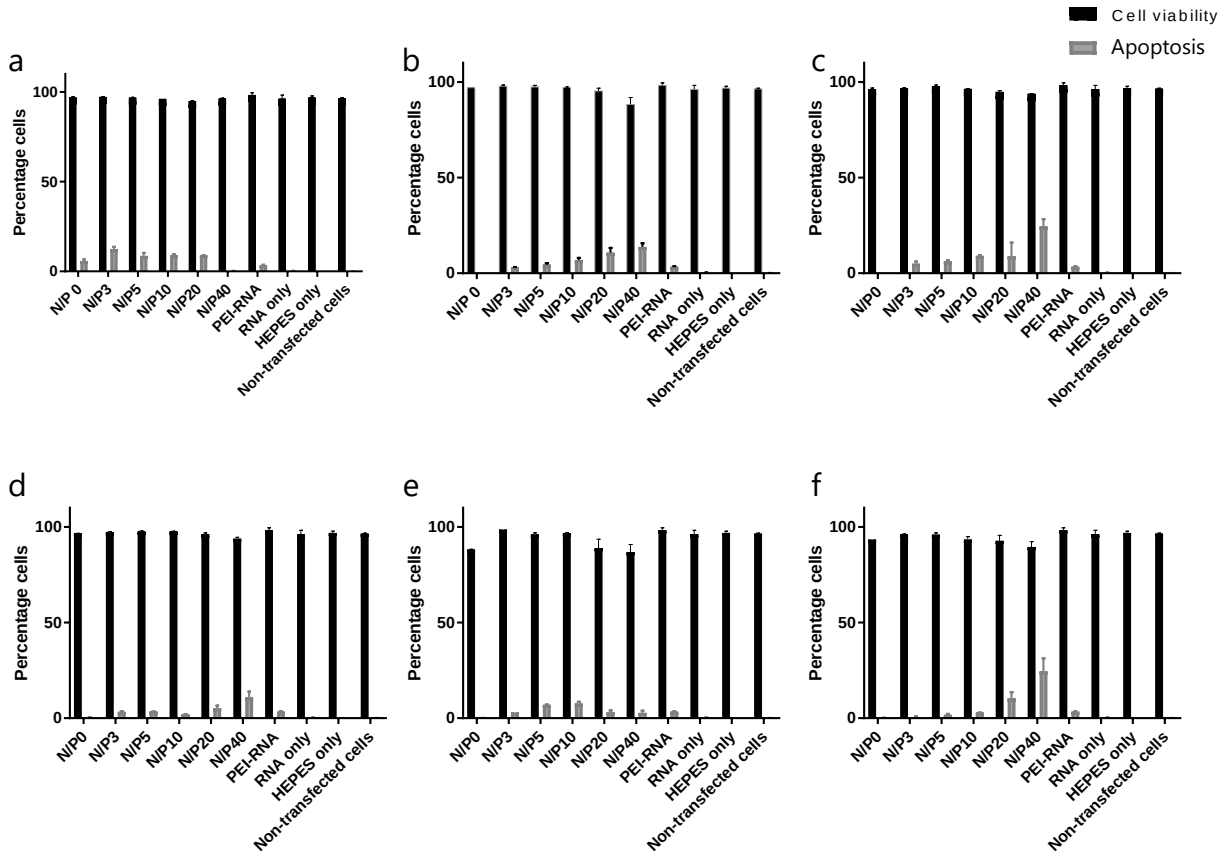

Figure 5.10 CMPC viability and induced apoptosis after transfection with polyplexes at various N/P ratios composed of a)P4.12, b) P4.13, c)P4.14, d) P4.15, e) P4.16, f)4.17. Controls included cells transfected with PEI, naked Cy5-labelled antagomiR, HEPES buffer and non-transfected cells. Results are shown as mean ± SD where n=3.

5.2.4 Cellular uptake and transfection efficiency

The cellular uptake of polyplexes is a crucial step for gene delivery, and therefore, it is important to evaluate the cellular uptake efficiency for these polymer systems. CMPCs were thus transfected with polyplexes formulated with Cy3-labelled antagomiR-214. The medium was changed after four hours. After further incubation for 24 hours, the cells were harvested and cellular uptake was quantified by flow cytometry. The results are summarized in Figure 5.11.

The polyplexes were efficiently taken up by the cells at all N/P ratios. A proportional correlation between N/P ratio and uptake is expected, since it is well known that higher N/P ratios of polyplexes facilitate greater uptake in cells. This relationship was not observed. However, this method for determining cellular uptake is known to give contradictory

estimations of the cellular uptake due to quenching effects at higher N/P ratios. (19). This means that the tight complexation of the polycations with the RNA at high N/P ratios shields the RNA's fluorescent signal; consequently, generating results that do not always correlate to a proportional increase in uptake corresponding to an increased N/P ratio.

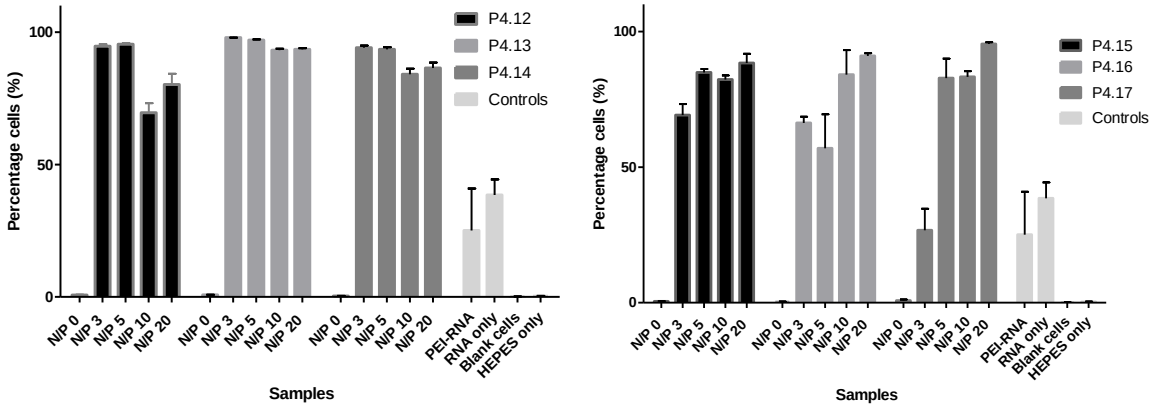

Figure 5.11 Determination of cellular uptake by flow cytometry. Where complexes composed of a) p(DMAEMA-co-BMA)-*b*-PVP b) p(DMAEA-co-BMA)-*b*-PVP. Results are shown as mean ± SD where n=3.

To further investigate whether this inconsistency of N/P ratio versus uptake was indeed due to shielding effects of the polycations, cell lysis and polyplex decomplexation experiments were performed before measuring the fluorescent signal, as described previously by Vader *et al*. (19) In short, CMPCs were exposed to polyplexes, and after numerous washing steps, the cells were lysed and the polyplexes were disrupted with 2% sodium dodecyl sulfate (SDS) in order to release the antagomiR, and subsequently the lysates were centrifuged. The fluorescent signal of the supernatant was measured in order to calculate the relative quantity of fluorescently-labelled antagomiR. These results have been summarized in Figure 5.12. From these analyses, it is evident that the cellular uptake of polyplexes is directly proportional to the N/P ratio, with an increase in N/P ratio leading to an increase in the cellular uptake. It can also be noticed that the uptake is greater for polyplexes that are functionalized with the cardioTL (**P4.13** and **P4.16**) than those with RGD (**P4.14** and **P4.17**), probably since the tested cell line being of cardiovascular origin. Lastly, polyplexes without any targeting ligand are seen to be least efficiently taken up by the cells. Further suggesting

the importance of targeting ligands on the surface of polyplexes for enhanced receptor-mediated uptake. It should be noted that the uptake of polyplexes formulated from p(DMAEA-*co*-BMA)-*b*-PVP (**P4.15-17**) show slightly higher uptake than the polyplexes from p(DMAEMA-*co*-BMA)-*b*-PVP (**P4.12-14**).

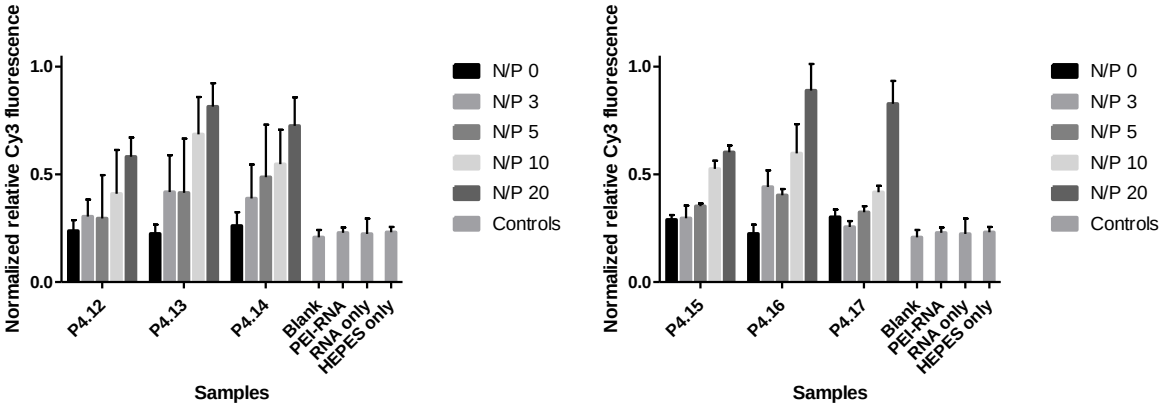

Figure 5.12 Determination of cellular uptake by measuring the fluorescent signal in the supernatant of cell lysates. Fluorescent values were corrected for the protein content. Where complexes were formulated from a) p(DMAEMA-*co*-BMA)-*b*-PVP b) p(DMAEA-*co*-BMA)-*b*-PVP. Results are shown as mean ± SD where n=3.

Confocal microscopy was used as the third method for determining the cellular uptake of the polyplexes. Human microvascular endothelial cells (HMECs) exposed to complexes formulated from **P4.13-14** or **P4.16-17** and Cy3-labelled antagomiR-214 were observed under the confocal microscope after being stained with Lysotracker and Hoechst. The images can be seen in Figure 5.13 where (i) shows the signal from the Hoechst stain, (ii) shows the signal from lysotracker, (iii) shows the signal from the Cy3-labelled antagomiR and (iv) is a merged image from all three signals. Hoechst is a common stain for DNA, *i.e*. it allows for visualization of the nucleus. Lysotracker is a highly selective dye for acidic organelles, thus it is specific for visualization of late endosomes and lysosomes. The microscope images again suggest that p(DMAEA-*co*-BMA)-*b*-PVP (**P4.16-17**) polyplexes, Figure 5.13 (c) and (d), were taken up more readily by the cells than p(DMAEMA-*co*-BMA)-*b*-PVP polyplexes (**P4.13-14**), Figure 5.13 (a) and (b).

As discussed in Chapter 2, endosomal entrapment is a very serious problem for many non-viral gene delivery systems. (20, 21) This causes problems in gene regulation, since the payload does not reach the cytoplasm, where the RNA therapeutics must perform its end-application. Therefore, by staining with lysotracker, it was possible to see whether or not the complexes were trapped within the endosomal/lysosomal compartment. In Figure 5.13, it can be observed that although the majority of the complexes are still within the endosome/lysosome, there is some endosomal escape occurring. This escape can be seen when the Lysotracker signal, Figure 5.13 (ii), does not overlap with the Cy3 signal from the antagomiR, Figure 5.13 (iii). The mechanism of escape does not seem to be very efficient, even with the presence of the pH-labile linker between the two polymer blocks. However, to fully establish and understand the extent of polyplex delivery and cytoplasmic release of the payload, the efficiency of gene expression was investigated.

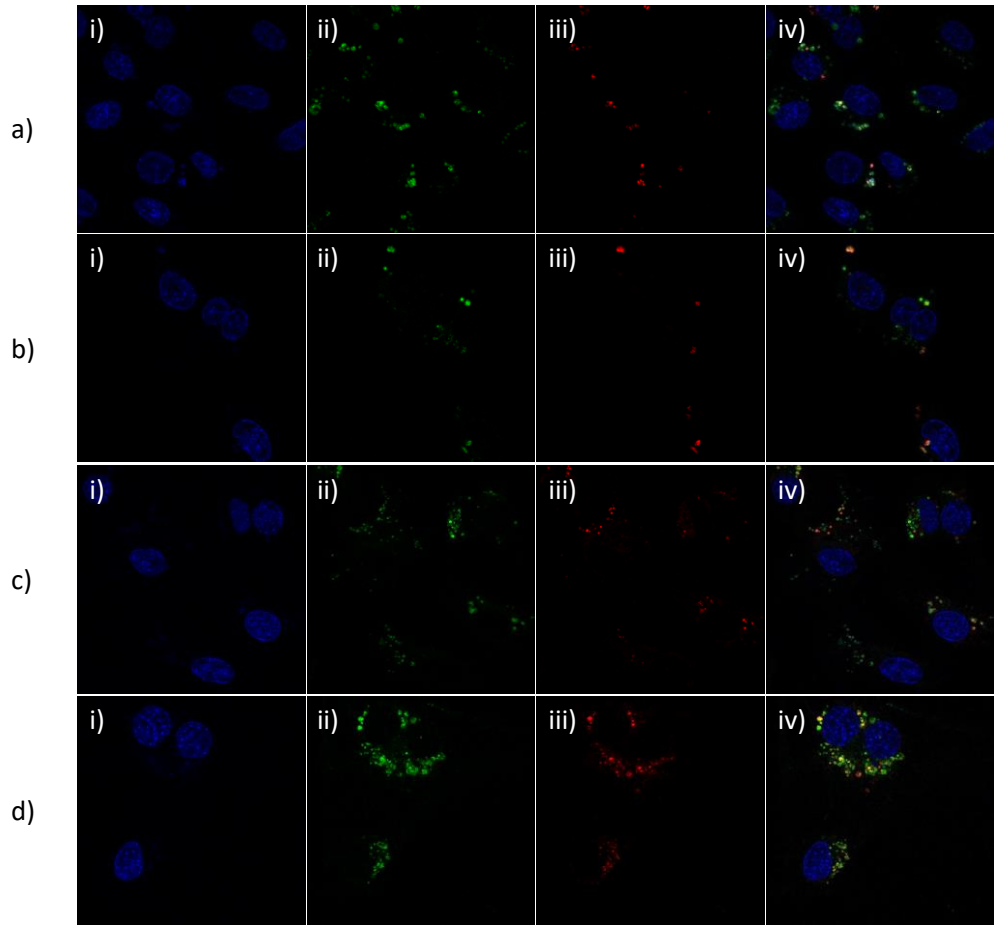

Figure 5.13 Localization of Cy5-labelled antagomiR-214 48 hours after treatment with a) P4.13, b) P4.14, c) P4.16 and d) P4.17 complexes, characterized by microscope analysis. Nuclei were stained with Hoechst are shown in blue (i) Lysosomal marker, Lysotracker, is shown in green (ii), Cy5 signal is shown in red (iii), and the images were finally merged (iv)

5.2.5 Gene regulation efficiency

Luciferase reporter assays are a common tool utilized to determine the gene expression at a cellular level because they provide an easy, inexpensive and quantitative method of quantifying the end-function of delivered gene therapeutics. In this way, it is possible to assess the efficiency of the gene delivery vehicle.

pMIR-QKI-3'UTR reporter, a miRNA-214 reporter that expresses luciferase; however in the presence of miRNA-214, this expression is inhibited. If anti-miR-214 is present, it is able to inhibit miRNA-214 from blocking the luciferase expression, *i.e*. luciferase expression can be detected. HEK293 cells were co-transfected with pMIR-QKI-3'UTR reporter and pMIR-Report β-gal control plasmid. The β-gal control plasmid was transfected as an internal control to establish the transfection efficiency, and normalize the luciferase expression results. The cells were also transfected with pre-miRNA-214 (**pre-miRNA-214**), a nonsense miRNA (**neg control**), a scrambled miRNA (**scrambled RNA**), or no miRNA (**Luc**). The following day, the cells transfected with pre-miRNA-214 were further exposed to polyplexes containing anti-miR-214, as well as a number of controls: naked anti-miRNA-214 (**naked anti-miR**), Lipofectamine 2000-anti-miR-214 (**L(+)**), Lipfectamine 2000-nonsense miRNA (**L(-)**) or PEI-anti-miR-214 (**PEI**). After incubation for 48 hours, the cells were lysed and the luciferase activity was assessed, see Figure 5.14. Lipofectamine 2000 is known to have an extremely high transfection efficiency *in vitro* and therefore served as a posiive control. The pMIR-QKI-3'UTR reporter (**Luc**) expresses luciferase and upon the addition of pre-miRNA-214, this expression should decrease. If anti-miRNA-214 is effectively transported into the cell, the miRNA-214 will be inhibited, re-establishing the luciferase signal. As expected, the Lipofectamine transported anti-miR-214 (**L(+)**) almost completely re-established the luciferase expression. A trend in the gene regulation efficiency can be observed for all of the polyplexes, except **P4.17**, whereby the efficiency increases with an increase in the N/P ratio. All of the complexes were equivalent to or out-performed the 'gold standard', PEI. Interestingly, the p(DMAEA-*co*-BMA) (**P4.15**) containing no targeting ligand out-performed all of the other conjugates, while in general the p(DMAEMA-*co*-BMA) systems (**P4.12-14**) performed better than the p(DMAEA-*co*-BMA) conjugates with targeting ligands (**P4.16** and **P4.17**).

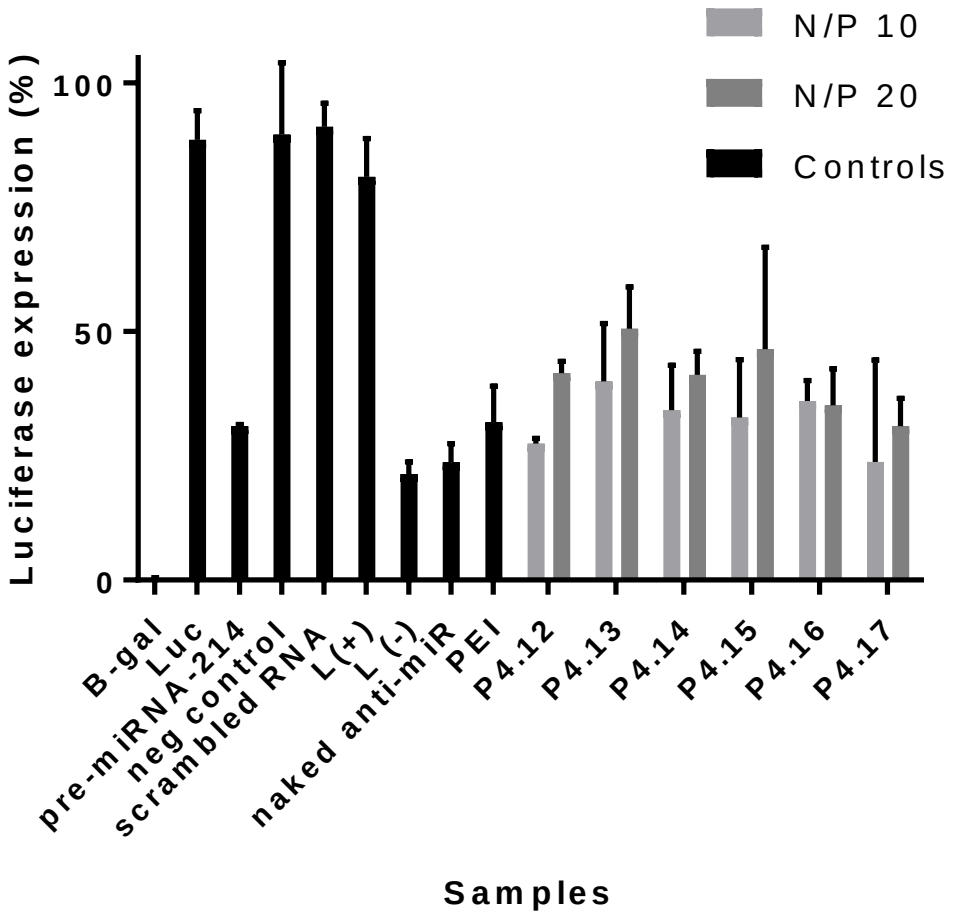

Figure 5.14 Gene silencing activity of P4.12-17 complexes. Luciferase expression of QKI-3'UTR reporter transfected in HEK 293 cells was determined 48 hours after transfection. Complexes were prepared using 50 nM anti-miRNA-214 concentration. Lipofectamine 2000 and PEI were used as controls. Results shown as mean ±SD for n=3.

In order to ascertain whether it is possible to further re-establish the luciferase signal, a higher concentration of anti-miRNA-214 was loaded into the polyplexes, and a higher N/P ratio was compared to N/P 20 complexes, seen in the previous experiment to be more efficient that N/P 10. The results are summarized in Figure 5.15.

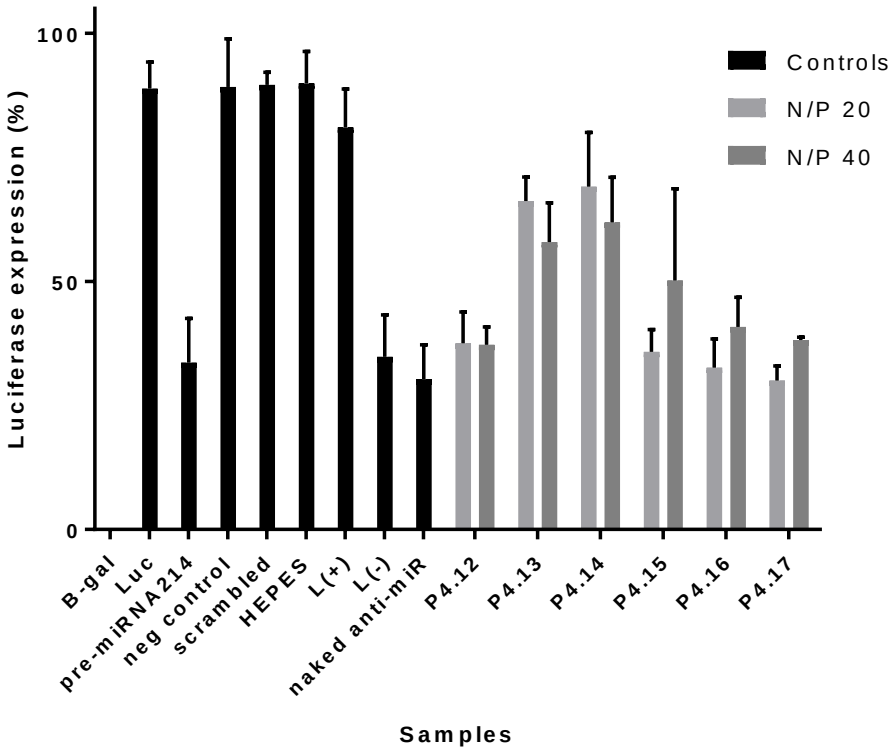

Figure 5.15 Gene silencing activity of P4.12-17 complexes. Luciferase expression of QKI-3'UTR reporter transfected in HEK 293 cells was determined 48 hours after transfection. Complexes were prepared using 100 nM anti-miRNA-214 concentration. Lipofectamine 2000 and PEI were used as controls. Results shown as mean ±SD for n=3.

An increased signal was obtained, especially for **P4.13** and **P4.14**, where almost 50% of the signal was re-established. Very little difference was seen in the extent of re-established signal between the other complexes and the previously obtain results. The most notable result is that the pDMAEMA-containing complexes (**P4.12-14**) show higher expression in Figure 5.15 than the de-cationizing pDMAEA-containing complexes (**P4.15-17**). These results contradict previous reports of pDMAEA versus pDMAEMA complexes. (22) Additionally, while the p(DMAEMA-*co*-BMA) conjugates with targeting ligands (**P4.13-14**) perform better than those without targeting ligands (**P4.12**), the opposite is true for the p(DMAEA-*co*-BMA) system (**P4.15** and **P4.16-17**). This will be discussed further below.

To further explore the versatility of the gene delivery systems, the diblock conjugates were complexed with siRNA-luc. Cells genetically modified to express luciferase, Human Epithelial firefly luciferase (FaDu Fluc) cells, were transfected. After lysis, the luciferase expression was

measured. In this case, the delivered siRNA-luc causes a knockdown effect on the luciferase expression. Therefore, successful delivery is seen by a decrease in the luciferase expression measured compared to cells without siRNA delivery. The results are summarized in Figure 5.16.

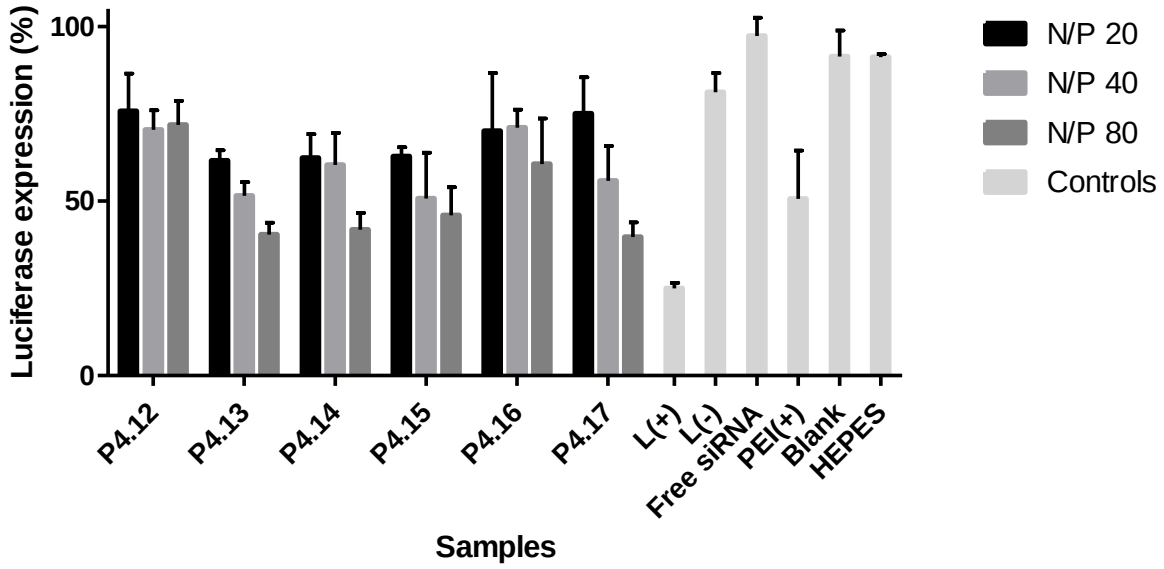

Figure 5.16 Gene silencing activity of P4.12-17 complexes. Luciferase expression of FADU-Fluc cells determined 48 hours after transfection. Complexes were prepared using 8 pmol siRNA. Lipofectamine 2000 and PEI were used as controls. Results shown as mean ±SD for n=3.

The conjugates were successfully able to deliver siRNA to the cells for luciferase knockdown to be observed. As described for the anti-miRNA system, the luciferase knockdown was proportional to the N/P ratio, and in general p(DMAEMA-*co*-BMA) polyplexes (**P4.12-14**) were more efficient in gene regulation than the p(DMAEA-*co*-BMA) polyplexes (**P4.15-17**). Both systems showed similar knockdown efficiency to PEI. Interestingly, it was hypothesized that the RGD targeting ligands would elicit the highest knockdown effect; however, no significant difference between knockdown efficiency was seen for the RGD-functionalized systems. It was again noticed that the p(DMAEMA-*co*-BMA) conjugates without targeting ligand (**P4.12**) performed the worst within the p(DMAEMA-*co*-BMA) group (**P4.12-14**), whereas the opposite was seen for the p(DMAEA-*co*-BMA) conjugates (**P4.15-17**). As the same effect was seen for the anti-miRNA-214 luciferase expression results, Figure 5.15, it seemed to be a significant observation. Therefore, it is possible that the targeting ligands

have an effect on the efficiency of the p(DMAEA-*co*-BMA) system (**P4.16-17**). If this is the case, then it is also possible that the shielding presence of PVP plays a role in lower gene regulation efficiency of the p(DMAEA-*co*-BMA) (**P4.15-4.17**). It is possible that the contradictory results obtained in this study compared to those reported in literature for the gene regulation efficiency of pDMAEA versus pDMAEMA is linked to the presence of the targeting ligand and/or the PVP. However, further investigation would be necessary to test this hypothesis, and elucidate the reasoning behind it.

In order to assess whether great knockdown efficiency could be obtained by increasing the quantity of siRNA delivered to the cells, a siRNA concentration gradient was performed, whereby 4, 8 and 32 pmol siRNA were complexed with non-targeted p(DMAEMA-*co*-BMA)-*b*-PVP (**P4.12)** and p(DMAEA-*co*-BMA)-*b*-PVP (**P4.15**) at N/P ratio of 20. The results are summarized in Figure 5.17. It was seen that as the amount of siRNA-luc complexed with the diblock conjugates increases, the knockdown effect also increases.

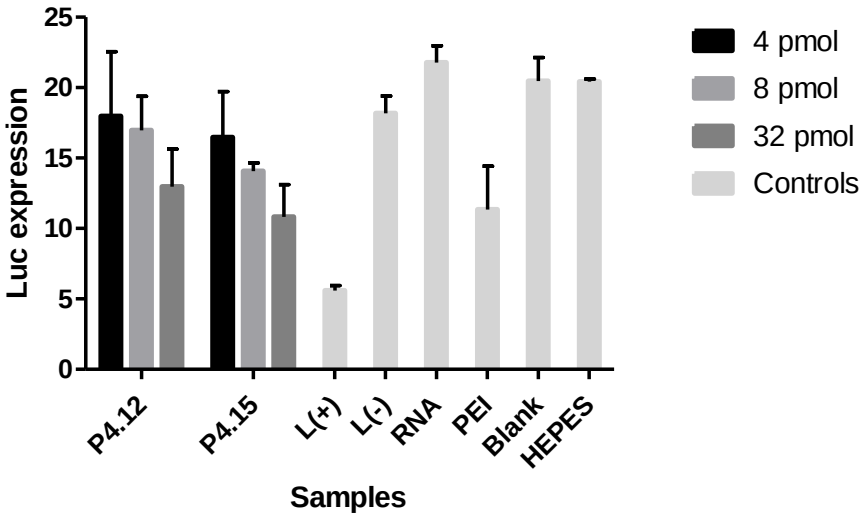

Figure 5.17 Gene silencing activity of P4.12 and P4.15 complexes containing various concentrations of siRNA-luc. Luciferase expression of FADU-Fluc cells determined 48 hours after transfection. Lipofectamine 2000 and PEI were used as controls. Results shown as mean ±SD for n=3.

5.3 Conclusion

The conjugates synthesized in Chapter 4 were investigated as possible gene delivery vectors. Their anti-miRNA binding efficiency was established, and all of the conjugates were seen to efficiently condense the RNA therapeutics, even at N/P ratios as low as 3. The polyplexes were shown to not cause high degrees of erythrocyte aggregation, with the aggregation increasing proportional to the N/P ratio. The complexes containing p(DMAEA-*co*-BMA) (**P4.15-17**) caused more hemolysis than those formulated from p(DMAEMA-*co*-BMA) (**P4.12-14**). No significant cytotoxicity was observed for the complexes, although some signs of apoptosis were observed.

Furthermore, the complexes were seen to facilitate cellular uptake, with uptake increasing proportionally to the N/P ratios. The incorporation of targeting ligands improved the cellular internalization of complexes, and p(DMAEA-*co*-BMA) (**P4.15-17**) was seemingly more efficient at enabling uptake. Conversely, the p(DMAEMA-*co*-BMA) complexes (**P4.15-17**) stimulated higher luciferase expression regulation than p(DMAEA-*co*-BMA) complexes (**P4.15-17**) and inverse results with regards to the presence of targeting ligands and luciferase regulation were observed for p(DMAEMA-*co*-BMA) (**P4.15-17**) compared to p(DMAEA-*co*-BMA) complexes (**P4.15-17**). Further investigation will be needed to resolve why the presence of the targeting ligand, and possibly PVP, decreases the gene regulation modulation effect of p(DMAEA-*co*-BMA) (**P4.15-17**). That said, both systems elicit gene regulation efficiency that is equal to or greater than PEI, and thus, these conjugates show potential as possible gene delivery vectors. *In vivo* studies will be conducted in the near future in order to investigate the systemic stability, biodistribution and *in vivo* gene regulation efficiency.

5.4 Supplementary

5.4.1 General experimental details

Unless stated otherwise, all of the chemicals used were purchased from commercial sources and used without further purification.

ζ-potential was measured on Malvern Zetasizer Nano Z. The samples were exposed to 3 V maz, and 3 measurement of 100 scans were obtained per sample. Complex size distribution was measured using nanoparticle tracking analysis (NTA) with a Nanosight NS500 nanoparticle analyser (Malvern Instruments) which was equipped with a 405 nm laser. The camera level was set to 16 and all post-acquisition settings were set to automatic, except for the detection threshold, which was set at 5. Three 30 s videos were recorder per sample using the script control function.

Flow cytometry was carried out on a CytoFLEX Flow Cytometer (Beckman Coulter). Data was analyzed using Kaluza Analysis 1.5a.

5.4.2 Experimental methods

Complex formation

Polymers were dissolved in DMSO and mixed with anti-miRNA-214 at various N/P ratios and diluted in HEPES buffer (pH 6.7). The solution was incubated at 37 °C for 1 hour. Complexes were used immediately.

Complex characterization

Complexes containing 550 pmol Cy3-labelled antagomiR-214 with a final volume of 25 µL were prepared for agarose gel retardation. 6 µL 6 x loading dye was added to the samples prior to loading. 2% agarose gel was prepared and the electrophoresis was performed at 140 V for 45 min. The gels were then imaged using the Typhoon 9410 Variable Mode Imager [Amersham, Biosciences).

RNA sequences

hsa-miR-214 ACAGCAGGCACAGACAGGCAGU

antagomiR-214: (Cy3)-5'-ACTGCCTGTCTGTGCCTGCTGT-3'-CHOLESTEROL

Cell culture

Human Epithelial firefly luciferase (FaDu-Fluc) cells and Human embryonic kidney 293 cells (HEK 293) were cultured in Dulbecco's modified Eagle's medium (DMEM) (Introgen, Carlsbad, CA) supplemented with 10% fetal bovine serum (FBS) and 10% Penicillin Streptomycin solution (P/S). Fetal cardiomyocyte progenitor cells (CMPCs) were cultivated on 0.1% gelatin in SP++ medium (1 part endothelial cell growth medium-2 (EGM-2), 3 parts Medium199 (M199) supplemented with 1% P/S, 1% non-essential amino acids (NEAA) and 10% FBS). Human microvascular endothelial cells (HMECs) were cultivated on 0.1% gelatin in EGM-2.

Cellular uptake (flow cytometry)

CMPCs were seeded in 12 well plates and incubated for 24 hours. Medium was removed and replaced with 500 µL OptiMem. Cells were transfected with complexes at various N/P ratios formulated with 5.5 nmol Cy3 labelled antagomiR-214. After 4 hours, the OptiMem was replaced with SP++ medium and cells were incubated for 48 hours. Cells were washed twice with PBS buffer to remove non-internalized polyplexes. Cells were harvested using Trypsin and centrifuged (350·g, 5 min) and supernatant was aspirated. The cells were resuspended in 500 µL PBS buffer containing 10% FBS. Again cells were centrifuged (350·g, 5 min) and supernatant was aspirated. The cells were resuspended in 500 µL PBS and after a final centrifugation step, the cells were resuspended in PBS buffer with 2% FBS (FACS medium). The samples were then analyzed on the CytoFLEX flow cytometer.

Cellular uptake (lysis)

CMPCs were seeded in 12 well plates and incubated for 24 hours. Medium was removed and replaced with 500 µL OptiMem. Cells were transfected with complexes at various N/P ratios formulated with 15 nmol Cy3-labelled antagomiR-214. After 4 hours, the OptiMem was replaced with SP++ medium and cells were incubated for 48 hours. Cell lysis and uptake

measurement was performed according to literature. (19) Method was as follows: Cells were washed twice with PBS buffer to remove non-internalized polyplexes. 200 µL lysis buffer (2% SDS, 1% Triton X-100 in PBS) was added and the cells were incubated on ice for 1 hour. Lysates were then centrifuged (14000·g, 15 min, 4 °C) in order to remove the cell debris. 100 µL of the supernatant was transferred to a 96-well plate to measure the fluorescence using a SpectraMax M2 (Molecular Devices). Data was acquired with SoftMax Pro (v5.4.5). The mean fluorescence intensity was normalized to the amount of protein present in the sample. The amount of protein was determined using a Micro BCA™ protein assay kit (ThermoFisher Scientific), protocol was followed according to manufacturer.

Cytotoxicity studies

CMPCs were seeded in 12 well plates and incubated for 24 hours. Medium was removed and replaced with 500 µL OptiMem. Cells were transfected with complexes at various N/P ratios formulated with 5.5 nmol antagomiR-214. After 4 hours, the OptiMem was replaced with SP++ medium and cells were incubated for 48 hours. Annexin V, Alexa Fluor™ 647 conjugate (Invitrogen) and Sytox Blue (Invitrogen) was used for cytotoxicity assay. Protocol was followed according to manufacturer. The cells were analyzed by flow cytometry on CytoFLEX Flow Cytometer (Beckman Coulter) directly after staining. Data was analyzed using Kaluza Analysis 1.5a.

Erythrocyte aggregation and hemolysis

Method was modified from literature. (16) In short, erythrocytes were obtained from 5 mL whole human blood by multiple centrifugation steps (1000·g, 10 min, 4 °C), followed by aspiration of supernatant and resuspension in PBS buffer until the supernatant was clear. Approximately 4 steps were required. 100 µL of the pellet was resuspended in 4 mL PBS. 160 µL of the final erythrocyte suspension was added to 40 µL polyplex solution with an anti-miRNA concentration of 1 µM. Triton X-100 (1%) in PBS and HEPES (pH 7.2) were used as reference samples of 100% lysis and 0% lysis respectively. Samples were incubated for 1 hour at 37 °C. After a further centrifugation step (1000g, 10 min), the absorbance at 550 nm was measured of 150 µL of the supernatant to ascertain the degree of hemolysis. The pellet was resuspended in 50 µL PBS and observed under the microscope to evaluate degree of erythrocyte aggregation.

Confocal microscopy

HMECs were seeded in an 8-well flow chamber and incubated for 24 hours. The medium was aspirated and replaced with 150 µL OptiMem. Cells were transfected with complexes (N/P 20) with a final antagomiR-214 concentration of 3 µM. After 4 hours, the OptiMem was replaced by EGM-2 medium and the cells were incubated for 48 hours. The medium was then replaced to medium containing 1:10000 Lysotracker Red and incubated for 2 hours. The medium was then replaced with medium containing Hoechst solution (1 µg/mL) and the cells were incubated for 10 minutes. The medium was aspirated and the cells were washed twice with EGM-2 medium. 150 µL of EGM-2 was added to the wells and the cells were imaged on a ZEISS LSM 700 confocal microscope (Carl Zeiss).

Luciferase Assay (anti-miRNA-214)

The method was modified from literature. (5) The conserved miRNA-214-binding sequences in the QKI 3' untranslated region (UTR) were cloned into pMIR-Reporter vector (Ambion). HEK293 cells were seeded in 48-well plates and incubated for 24 hours. The medium was replaced with OptiMem. The cells were co-transfected with 200 ng of pMIR-Reporter-QKI-3'UTR Luciferase vector and pMIR-Report β-gal control plasmid. The latter was used to assess the transfection efficiency. In addition, 50 nM pre-miRNA-214, ctrl-miRNA or scrambled miRNA were also transfected. The transfection was carried out by using Lipofectamine 2000 (Invitrogen). After 4 hours, the medium was replaced with DMEM supplemented with 10% FBS. After 24 hours of incubation, the medium was replaced with OptiMem, and cells were transfected with complexes containing 50 nM anti-miRNA-214 at different N/P ratios, or Lipofectamine with either anti-miRNA-214 or ctrl-miRNA, PEI-anti-miRNA-214 polyplexes or naked anti-miRNA-214. After 4 hours, the medium was replaced. The cells were incubated for 48 hours. They were then washed with PBS and lysed with 150 µL 1 x Luciferase lysis buffer. The cells were incubated for 15 minutes. 10 µL of the supernatant was transferred to a white 96-well plate, and the luciferase activity was assessed with Luciferase Assay System (Promega). 25 µL of the cell lysis supernatant was transferred to a 96-well plate and 25 µL β-galactosidase Enzyme Assay buffer. After incubation at 37 °C for 1 hour, the absorbance at 405 nm and 570 nm was measured.

Luciferase assay (siRNA-luc)

FADU-Fluc cells were seeded in 48-well plates and incubated for 24 hours. The medium was replaced with OptiMem and the cells were transfected with polyplexes containing 4, 8, 16 or 32 pmol siRNA. After 4 hours, the medium was replaced and the cells were incubated for a further 48 hours. The cells were washed with PBS buffer and lysed with luciferase assay buffer (ThermoFischer Scientific). After incubation at room temperature for 20 minutes, 10 µL of the supernatant was transferred to a white 96-well plate, and the luciferase activity was assessed with Luciferase Assay System (Promega) on a Fluoroskan Ascent FL (ThermoScientific). Data was acquired with Ascent Software (v 2.6). 50 µL of the supernatant was used to assess the protein content using a Micro BCA™ protein assay kit (ThermoFisher Scientific), protocol was followed according to manufacturer.

5.5 References

1. Carmeliet P. Angiogenesis in life, disease and medicine. Nature. 2005;438:932-6.
2. Bartel DP. MicroRNAs: Genomics, biogenesis, mechanism, and function. Cell. 2004;116(2):281-97.
3. Ambros V. The functions of animal microRNAs. Nature. 2004;431:350-5.
4. Dorn G, Patel S, Wotherspoon G, Hemmings-Mieszczak M, Barclay J, Natt FJC, Martin P, Bevan S, Fox A, Ganju P, Wishart W, Hall J. siRNA relieves chronic neuropathic pain. Nucleic Acids Res. 2004;32(5):e49-e.
5. van Mil A, Grundmann S, Goumans M-J, Lei Z, Oerlemans MI, Jaksani S, Doevendans PA, Sluijter JPG. MicroRNA-214 inhibits angiogenesis by targeting Quaking and reducing angiogenic growth factor release. Cardiovasc Res. 2012;93(4):655-65.
6. Noveroske JK, Lai L, Gaussin V, Northrop JL, Nakamura H, Hirschi KK, Justice MJ. Quaking is essential for blood vessel development. Genesis. 2002;32(3):218-30.
7. Li Z, Takakura N, Oike Y, Imanaka T, Araki K, Suda T, Kaname T, Kondo T, Abe K, Yamamura K-i. Defective smooth muscle development in qkI-deficient mice. Dev Growth Differ. 2003;45(5-6):449-62.
8. Bohnsack BL, Lai L, Northrop JL, Justice MJ, Hirschi KK. Visceral endoderm function is regulated by quaking and required for vascular development. Genesis. 2006;44(2):93-104.
9. Weiler J, Hunziker J, Hall J. Anti-miRNA oligonucleotides (AMOs): ammunition to target miRNAs implicated in human disease? Gene Ther. 2005;13(6):496-502.
10. Krützfeldt J, Rajewsky N, Braich R, Rajeev KG, Tuschl T, Manoharan M, Stoffel M. Silencing of microRNAs in vivo with 'antagomirs'. Nature. 2005;685-689:685.
11. Gray BP, Brown KC. Combinatorial Peptide Libraries: Mining for Cell-Binding Peptides. Chem Rev. 2014;114(2):1020-81.
12. Kanki S, Jaalouk DE, Lee S, Yu AYC, Gannon J, Lee RT. Identification of targeting peptides for ischemic myocardium by in vivo phage display. J Mol Cell Cardiol. 2011;50(5):841-8.
13. Pierschbacher MD, Ruoslahti E. Cell attachment activity of fibronectin can be duplicated by small synthetic fragments of the molecule. Nature. 1984;309:30-3.

14. Arap W, Pasqualini R, Ruoslahti E. Cancer treatment by targeted drug delivery to tumour vasculature in a mouse model. Science. 1998;279:377-80.

15. Truong NP, Jia Z, Burges M, McMillan NAJ, Monteiro MJ. Self-catalyzed degradation of linear cationic poly(2-dimethylaminoethyl acrylate) in water. Biomacromolecules. 2011;12(5):1876-82.

16. Vader P, van der Aa LJ, Engbersen JFJ, Storm G, Schiffelers RM. Physicochemical and biological evaluation of siRNA polyplexes based on PEGylated poly(amido amine)s. Pharm Res. 2012;29(2):352-61.

17. Verbaan FJ, Oussoren C, van Dam IM, Takakura Y, Hashida M, Crommelin DJA, Hennink WE, Storm G. The fate of poly(2-dimethyl amino ethyl)methacrylate-based polyplexes after intravenous administration. Int J Pharm. 2001;214(1):99-101.

18. Kircheis R, Wightman L, Schreiber A, Robitza B, Rössler V, Kursa M, Wagner E. Polyethylenimine/DNA complexes shielded by transferrin target gene expression to tumors after systemic application. Gene Ther. 2001;8:28-40.

19. Vader P, van der Aa LJ, Engbersen JFJ, Storm G, Schiffelers RM. A method for quantifying cellular uptake of fluorescently labeled siRNA. J Control Release. 2010;148(1):106-9.

20. Liang W, Lam JKW. Endosomal escape pathways for non-viral nucleic acid delivery systems. In: Ceresa B, editor. Molecular regulation of endocytosis. Rijeka: InTech; 2012. p. Ch. 17.

21. Dominska M, Dykxhoorn DM. Breaking down the barriers: siRNA delivery and endosome escape. J Cell Sci. 2010;123(8):1183-9.

22. Werfel TA, Swain C, Nelson CE, Kilchrist KV, Evans BC, Miteva M, Duvall CL. Hydrolytic charge-reversal of PEGylated polyplexes enhances intracellular un-packaging and activity of siRNA. J Biomed Mater Res Part A. 2016;104(4):917-27.

Chapter 6: Zwitterionic poly(styrene-co-maleic anhydride) copolymer derivatives for application in gene therapy

Synopsis

Zwitterionic polymers are increasingly being studied as gene delivery vectors, as they contain the necessary positive charge for gene complexation, while their negative charge acts to balance the charge. Hereby, a significant decrease in the cytotoxicity and aggregation behaviour is observed compared to their cationic counterparts. In this study, novel poly(styrene-*co*-maleic anhydride) (SMA)-derivatives were investigated for their efficiency as non-viral vectors in anti-miRNA-214 delivery. After complexation, targeted cells did not exhibit significant toxicity, hemolysis or aggregation. Their mechanism of cellular uptake was investigated and, although active transport is involved, they do not follow the usual clathrin–or caveolae–mediated endocytic pathways. The exhibited gene delivery efficiency of these SMA-complexes was equivalent to or greater than that of the current gold standard, poly(ethylamine) (PEI).

6.1 Introduction

Zwitterionic polymers are macromolecules that contain both positive and negative charge. These polymers have emerged as a new possibility for non-viral, gene delivery vectors, which exhibit characteristics of both cationic polymers and liposomes, while maintaining a lower cytotoxicity than their polycation analogues. (1, 2) This lowered cytotoxicity is most probably due to their closer-to-neutral zeta-potential (ζ-potential) when complexed to nucleotides, brought about by their balance in charge. This lower ζ-potential also resists non-specific interactions with blood plasma and serum, a known problem for polycation based delivery systems. (3)

A common amphiphilic polymer employed in biomedical applications is ring-opened poly(styrene-*co*-maleic anhydride) (SMA). SMA is very easy to modify due to maleic anhydride's reactivity towards hydroxyl, sulfhydryl and amine groups. (4-8) When the pH decreases, for example upon entering the endosome, the carboxylic acid moiety is protonated, which induces a change in the polymer from hydrophilic to more hydrophobic. (9) This change in state previously caused the endosomal membrane to destabilize, facilitating endosomal escape of the polymer and its payload. (10)

Although highly used in drug delivery, (11-14) SMA has not been extensively explored for gene delivery applications. Stayton and co-workers (15) mentioned the possibility of using SMA modified with alkyl amines for gene delivery due to their pH responsive nature. However, the first example where SMA was employed as a vector in gene delivery was carried out by Duan *et al*. (16) where they conjugated SMA with low molecular weight PEI (800 Da). The SMA-PEI complexes condensed DNA more efficiently than the unconjugated, low molecular weight PEI analogue, while the zeta potential of the SMA-PEI-DNA complexes was significantly lower than that of high molecular weight PEI (25 kDa) polyplexes. This lowered zeta-potential was due to the neutralizing effect of carboxylic acids on the SMA block. Hereby, a higher transfection efficiency and cellular uptake for SMA-PEI complexes was observed than for high molecular weight PEI. They hypothesized that this was due to the presence of phenyl groups on the SMA which can form π-π stacking interactions with the nucleotide base-pairs. Furthermore, the improved cellular interaction was correlated to

the amphiphilic nature of the polymer. No results were shown, however, regarding gene expression regulation.

More recently, Alex *et al*. (9) created a small library of low molecular weight SMA (2:1) grafts containing cationic amine functional groups, including spermine, L-arginine, aromatic (isonicotinic acid), aliphatic (glycidyl trimethylammonium chloride) and cyclo aliphatic 1-(2-aminoethyl)piperazine. The side-chains on the last three SMA-derivatives were quaternized in order to infer cationic charge to the system. Interestingly, the L-arginine and spermine grafted SMA-derivatives showed enhanced endosomal escape characteristics, while also condensing the DNA more efficiently; whereas, the quaternized amine-modified SMAs displayed varying positive and negative attributes. The aromatic group on the (isonicotinic acid)-modified SMA increased hydrophobicity of the system, which in turn enhanced the endosomal rupturing capabilities of the complexes. However, their hydrophobicity caused issues in their protection against DNase at physiological pH. Although the aliphatic (glycidyl trimethylammonium chloride)-modified SMAs were able to effectively protect against DNase, they caused high levels of cytotoxicity. Finally the cyclo aliphatic (1-(2-aminoethyl) piperazine-modified SMAs were unable to effectively complex DNA.

In the present study, 3-(*N*,*N*-dimethylamino)propyl-1-amine (DMAPA)-modified SMA was investigated as a possible candidate vector for non-viral gene delivery, see Scheme 6.1. The ring-opened analogue is zwitterionic and highly water soluble, which is highly desirable since it avoids disruption of the cellular environment caused by insoluble complexes. (2) In order to evaluate the effect that the amphiphilic and zwitterionic nature imparts, the DMAPA-modified SMA was also ring-closed to form poly(styrene-*co*-*N*-(3-(*N'*,*N'*-dimethylamino)propyl)-maleimide) (DMAP-SMI), and the two forms were compared with each other in terms of complexation efficiency, cellular cytotoxicity, uptake and transfection efficiency.

6.2 Results and discussion

6.2.1 Polymer synthesis, modification and characterization

Figure 6.1 depicts the chemical structure of the reversible-addition fragmentation chain-transfer (RAFT) agent (**R6.1**) that was utilized in the current study to prepare poly(styrene-*co*-maleic anhydride) (**P6.1**). The RAFT agent was synthesized according to literature, and

the ^{1}H NMR corresponded to literature values. **(17)** The details of the synthetic protocol of the RAFT agent synthesis and polymerization are summarized in Section 6.4.

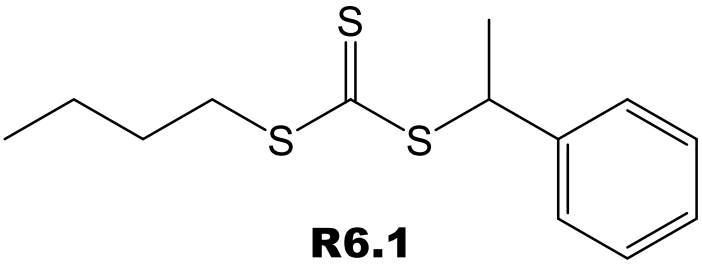

R6.1

Figure 6.1 Structure of butyl 1-phenylethyl trithiocarbonate (R6.1)

Table 6.1 summarizes the results from the RAFT–mediated polymerization to prepare poly(styrene-*co*-maleic anhydride), **P6.1**. **P6.1** was obtained with control over molecular weight and its distribution (Đ = 1.1). A polymer with an M_n of 12800 g.mol^{-1} was obtained.

Table 6.1 Tabulation of results from the RAFT-mediated polymerization of maleic anhydride and styrene

Sample	M_n (target)	Temp (˚C)	CTA	Monomers	Initiator	Solvent	α‡ (%)	M_n*	M_n§	M_W§	Đ§
P6.1	11000	70	R6.1	Sty:MAnh (1:1)	AIBN	MEK	58	12800	12600	14300	1.1

§Determined by SEC in DMAc relative to PMMA standards.
*Determined via ^{1}H NMR
‡Conversion obtained through gravimetric analysis.

Amidation of the SMA was performed post-polymerization in order to obtain DMAP-SMI (**P6.2**), as depicted in Scheme 6.1.

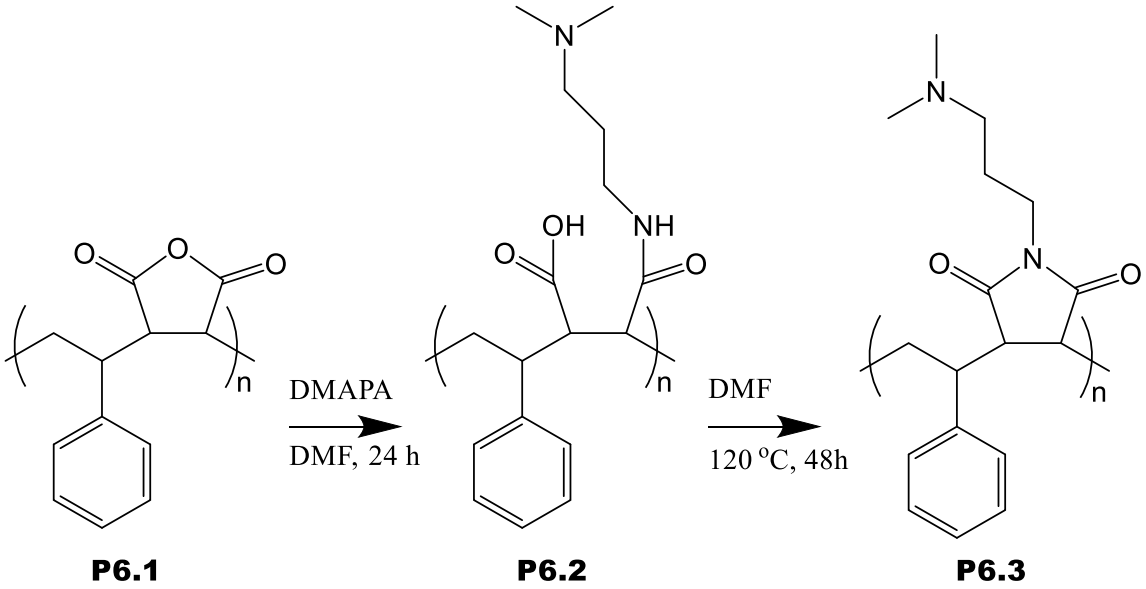

Scheme 6.1 Amidation of P6.1 with DMAPA to obtain ring-open amine-modified SMA (P6.2) and subsequent thermally induced ring-closing reaction to obtain P6.3

The success of the modification was confirmed through Fourier transform infrared (FT-IR) spectroscopy, as previously reported in our group, see Figure 6.2. (18) In short, the band attributed to the carbonyl groups (1858 and 1774 cm^{-1}) and C-O-C stretching bands (between 903 and 1220 cm^{-1}) of carbonyl anhydride in **P6.1** disappeared upon amidation, and the carboxylic acid C=O stretch (1690 cm^{-1}), carboxylic acid O-H stretch (3664-3126 cm^{-1}) and the two amine peaks (1559 and 1356 cm^{-1}) appeared in **P6.2**. A portion of **P6.2** was then subjected to thermally induced ring-closure to obtain **P6.3**. Again, the success of the ring-closure could be confirmed via FT-IR (19) by the disappearance of the carboxylic acid C=O peak (1695 cm^{-1}) and carboxylic acid O-H stretch (3000-2500 cm^{-1}), as well as a shift in the C=O carbonyl anhydride peaks seen for **P6.1** to 1769 and 1690 cm^{-1}, as indicated by the dotted blue line in Figure 6.2.

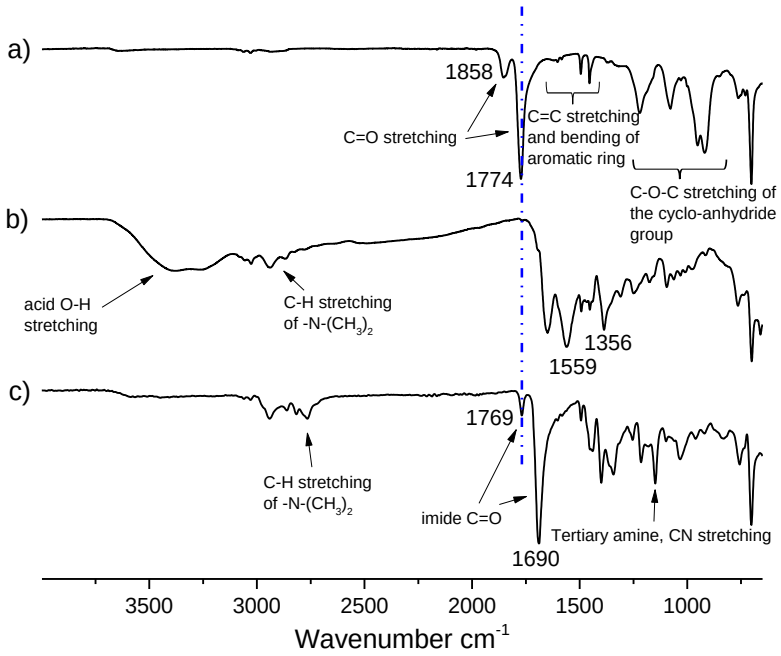

Figure 6.2 ATR–FTIR spectra of a)poly(styrene-*co*-maleic anhydride) (P6.1), b) ring-opened, DMAPA-modified poly(styrene-*co*-maleic anhydride (P6.2) and c) ring-closed, DMAPA-modified poly(styrene-*co*-maleimide (P6.3). The blue dotted line indicates the shift in the carbonyl anhydride bands due to imidation.

6.2.2 Complex characterization

For complexation to be possible, **P6.2** and **P6.3** were dissolved in sodium acetate/acetic acid buffer (pH 4.2) in order for the tertiary amine functional groups to be positively charged which enables them to condense the negatively charged anti-miRNA-214 and Cy3-labelled antagomiR-214. If **P6.2** is in its zwitterionic state, the overall positive charge of the system will be lower than **P6.3**, since **P6.3** has no propensity for zwitterionic properties. Thereby **P6.3 is** potentially more capable of condensing the RNAs. It is also possible that any negative charge present on **P6.2** could repel the negatively charged RNAs, thus decreasing the complexation efficiency. The complexation efficiency of **P6.2** and **P6.3** was assessed using gel electrophoresis at various Nitrogen-to-Phosphorus charge (N/P) ratios, as seen in Figure 6.3. It was observed that **P6.3** was more efficient in complexing with the antagomiR-214 than **P6.2**. However, neither of the two systems are very effective at condensing the RNA molecule as a significant portion of free RNA is seen running towards the positive electrode. Only at an N/P ratio of 100, can **P6.3** efficiently complex the RNA. Further investigations would be necessary to optimize the systems to increase the complexation efficiency. It

would be very useful to measure the pk_a values and perhaps investigate the effect of molecular weight on the RNA complexation.

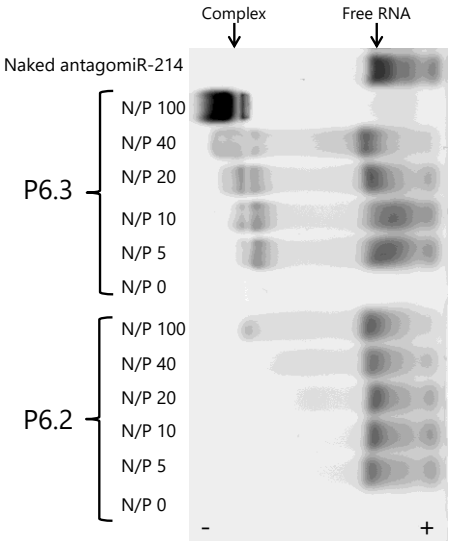

Figure 6.3 Agarose gel electrophoresis of Cy3-antagomiR-214 complexes from P6.2 and P6.3 at different N/P ratios.

The complex size distribution was measured using nanoparticle tracking analysis (NTA). The results are summarized in Table 6.2. The mean size of the generated particles is relatively large compared to that of common polyplex systems which usually range between 40 and 100 nm. This is possibly due to the low complexation efficiency imparted by the SMA-derivatives. Additionally, the polymers do not contain amphiphilic properties which promote self-assembly; therefore, it is possible that no secondary structures, e.g. micelles, are displayed by the complexes.

Table 6.2 Complex size measured by NTA reported in nm. Results are shown as mean ± SD where n=3.

N/P ratio	10	20	50	100	200
P6.2	346.6 ± 115.7	161.2 ± 32.4	96.8 ± 27.3	119.6 ± 27.7	126.3 ± 14.6
P6.3	226 ± 59.4	148.1 ± 12.4	154.9 ± 43.5	129.9 ± 24.7	110.4 ± 21.7

The ζ-potential of polyplexes containing **P6.2** and **P6.3** at different N/P ratios were measured in sodium acetate/acetic acid buffer, see Figure 6.4. An anticipated linear relationship between ζ-potential and N/P ratio was observed, since the concentration of positively charged moieties increases with an increase in the polymer concentration. The ring-closed, DMAP-SMI produce polyplexes with higher ζ-potential, which is comprehensible since it is conceivable that these polymers contain an overall higher positive charge compared to the zwitterionic, ring-opened analogue.

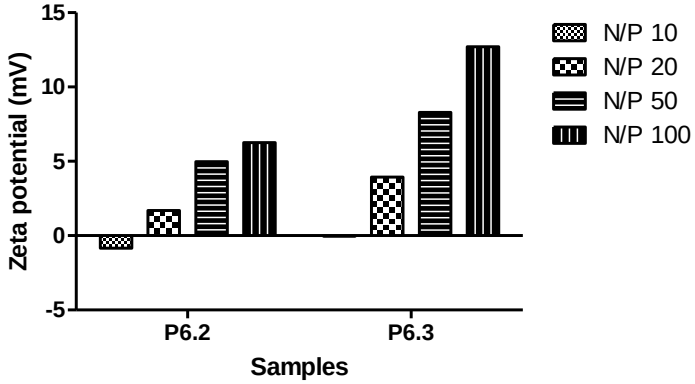

Figure 6.4 Zeta potential of complexes containing P6.2 and P6.3 at different N/P ratios.

6.2.3 Erythrocyte hemolysis and aggregation

For a successful application in gene delivery, formed polyplexes should minimally interact with serum proteins, erythrocytes or other blood cells. This interaction can, for example, induce erythrocyte aggregation, leading to clearance by the reticulo-endothelial system (RES), and hemolysis. After incubation of DMAPA-modified SMA polymers with freshly isolated red blood cells for one hour, human full-blood derived erythrocytes were pelleted via centrifugation and observed under a microscope, see Figure 6.5 (a), while the supernatant was used to measure the degree of hemolysis, Figure 6.5 (b).

PEI complexes are known to stimulate blood components, as indicated in Figure 6.5 (a) (i), and are indeed inducing erythrocyte aggregation. As indicated in Figure 6.5 (a) (ii), the exposure of red blood cells to naked anti-miRNA, or the complexes composed of **P6.2** and **P6.3**, Figure 6.5 (a) (iii) and (iv), respectively, did not cause aggregation, even at N/P ratios as high as 100.

However, as indicated in Figure 6.5 (b), **P6.3** complexes formed some degree of red blood cell hemolysis; however, even at N/P ratio of 100, the degree of hemolysis is below 4%, which is remarkably lower than the hemolysis in common cationic polyplex systems, like Lipofectamine. The slightly higher degree of hemolysis for **P6.3** compared to **P6.2** is most probably due to the more cationic nature of **P6.3** due to the ring-closed configuration, which lacks the charge neutralization from the zwitterionic properties in the ring-open analogue.

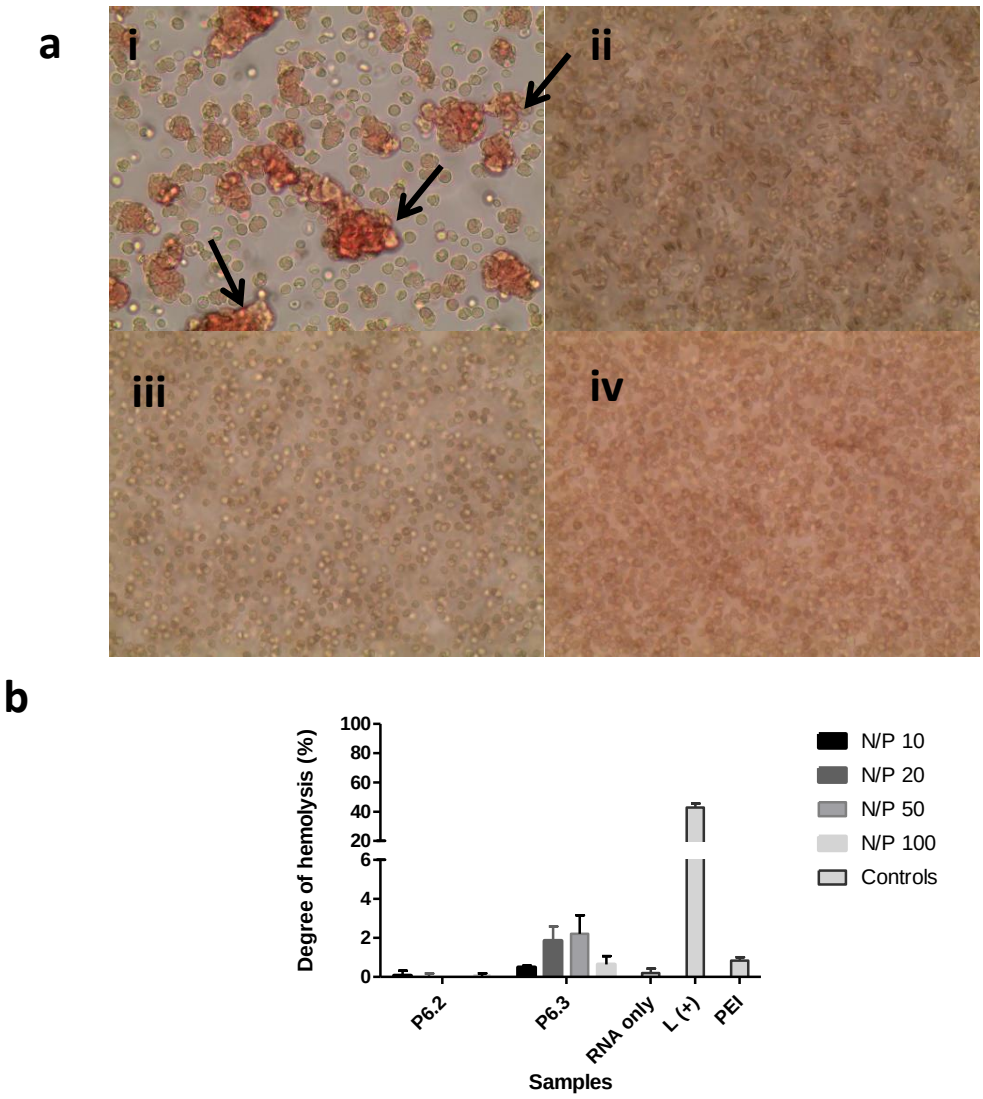

Figure 6.5 Polyplex-induced erythrocyte aggregation and hemolysis. Polyplexes were incubated with erythrocytes for 1 hour at 37 °C. PEI polyplex and Lipofectamine 2000 were used as controls. a) Microscopic images of erythrocyte aggregation, whereby aggregates are indicated using arrows. i) PEI, ii) naked anti-miRNA, iii) complexes with P6.2 and iv) complexes with P6.3. b) graph representing the degree of erythrocyte hemolysis determined by absorbance detection at 550 nm. Results are shown as mean ± SD where n=3.

6.2.4 In vitro cytotoxicity assay

The *in vitro* cytotoxicity caused by exposing fetal-derived cardiomyocyte progenitor cells (CMPCs) to the nanoparticles at various N/P ratios was tested using Annexin V and 7-amino-actinomycin D (7-AAD) (apoptotic and necrotic cells, respectively). Flow cytometry was used to determine the degree of incorporation of the fluorescent signals within the cells, and hence the cellular cytotoxicity caused by the polyplexes. The results of these assays can be seen in Figure 6.6 (a) and (b) for complexes containing **P6.2** and **P6.3**, respectively. While transfection with Lipofectamine 2000 caused significant apoptosis and necrosis, no cytotoxicity was caused by transfection with the SMA-derived complexes, at any of the N/P ratios, as detected via apoptosis or necrosis.

a)

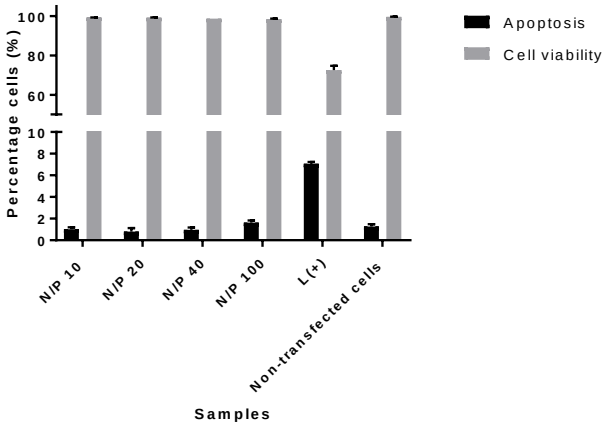

b)

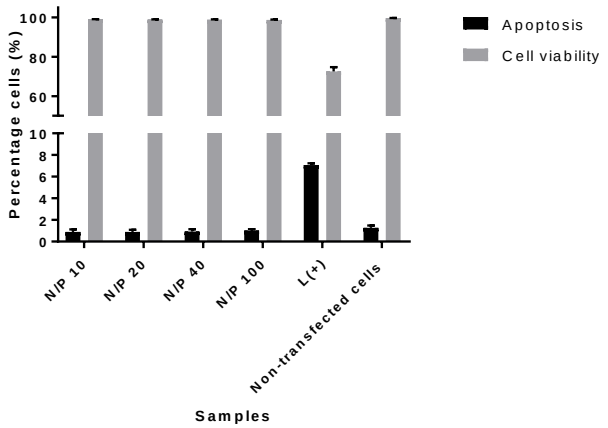

Figure 6.6 Cell viability and degree of apoptosis of CMPCs determined for complexes composed of a) P6.2 and b) P6.3 at different N/P ratios determined using Annexin V and 7-AAD staining. Lipofectamine was used as a control (L(+)). Results are shown as mean ± SD where n=3

6.2.5 Cellular uptake and transfection efficiency

The cellular uptake of the complexes is of utmost importance to facilitate gene delivery. This was investigated by transfecting cells with complexes containing Cy3-labelled antagomiR-214 and thereafter quantified their uptake by flow cytometry and confocal microscopy.

In the first experiment, Cy5-labelled antagomiR was complexed with **P6.2** and **P6.3** and transfected into CMPCs. After incubation for 48 hours, CMPCs were analysed by flow cytometry in order to ascertain the uptake efficiency (summarized in Figure 6.7). Lipofectamine 2000 was used as a control. A slightly higher cellular uptake was observed for complexes composed of **P6.3** compared to those of **P6.2**, probably due to the cationic charge of polycations and a higher ζ-potential which have been reported to induce cellular uptake.

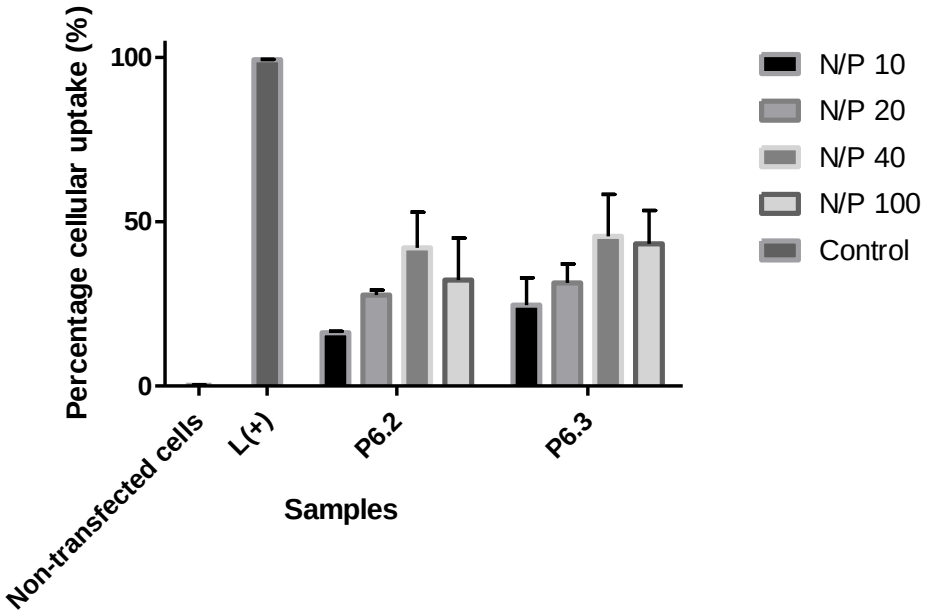

Figure 6.7 Cellular uptake determined by flow cytometry. Results are shown as mean ± SD where n=3.

An overall trend in increased cellular uptake was observed for higher N/P ratios. It is commonly accepted that as the N/P ratio increases, the complexation efficiency improves. As reported by Vader *et al*., (20) this causes an increase in the polymer shielding of RNA-labelled fluorescence, which in turn quenches the fluorescence signal at higher N/P ratios.

Thus, as the N/P ratio increases, a linear trend is not seen in the flow cytometry results, observed for N/P 100 in Figure 6.7. It was ascertained using agarose gel electrophoresis, Figure 6.3, that at N/P 100 for both **P6.2** and **P6.3**, the complexation efficiency was higher than for lower N/P ratios. Therefore, it is very possible that the increased binding efficiency at N/P 100 is inducing this shielding phenomenon, and decreasing the observed cellular uptake.

Human microvascular endothelial cells (HMECs) were subsequently transfected with complexes containing fluorescently labelled antagomiR-214 and observed under the confocal microscope after co-staining with Lysotracker, see Figure 6.8. Lysotracker is a dye which is highly selective for acidic organelles, *i.e*. late endosomes and lysosomes. As discussed in Chapter 2, endosomal entrapment is a very serious problem for many non-viral gene delivery systems, (21, 22) since the payload does not reach its target site. As indicated in the micrographs in Figure 6.8, polyplexes were taken up by the cells but more importantly, some of the antagomiR's fluorescent signal, Figure 6.8 (iii), does not overlap with the Lysotracker signal, Figure 6.8 (ii). This suggests that some of the internalized polyplexes have escaped into the cytoplasm.

Upon closer examination of the micrographs, interestingly, some of the complexes formed with **P6.3** remained within the lysosomal compartment, while the fluorescent signal from the Cy3-labelled antagomiR delivered by **P6.2** did not overlap with the Lysotracker signal at all. Therefore, it was hypothesized that either the ring open, DMAPA-modified SMA polyplexes were immediately escaping the endosome after endocytosis, or being taken up by the cells in a manner different to endocytosis. Based on the zwitterionic properties of **P6.2**, both of these hypotheses are plausible. As the plasma membrane is a bilipid membrane, the ring-opened analogue is possibly less repelled by the membrane, and therefore, it is possible that the ring-opened polyplexes facilitate direct diffusion through the membrane. Since, the mechanism of uptake is a very important aspect for designing the delivery vector, it is relevant to investigate this further.

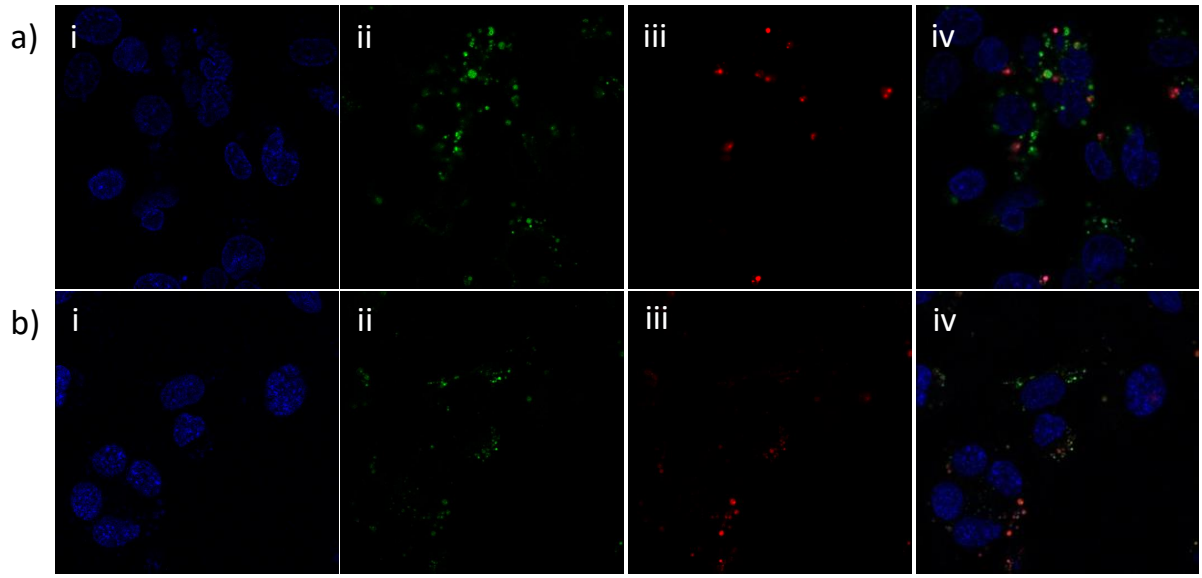

Figure 6.8 Localization of Cy5-labelled antagomiR-214, 48 hours after treatment with a) P6.2 and b) P6.3 complexes, characterized by microscope analysis. Nuclei were stained with Hoechst are shown in blue (i) Lysosomal marker, Lysotracker, is shown in green (ii), Cy5 signal is shown in red (iii), and the images were finally merged (iv)

6.2.6 Mechanism of cellular uptake

To study the mechanism of cellular uptake, clathrin–mediated and caveolae–mediated endocytosis were inhibited, as they are reported to be the major pathways through which polyplexes are taken up. (23, 24) Chloropromazine has been used in the past to inhibit clathrin–mediated endocytosis, since clathrin and its adapter proteins are translocated from the plasma membrane to the intracellular vesicles. Clathrin-coated pits are therefore inhibited from forming on the surface of the cell. (25) Genistein is a turosine kinase inhibitor known to inhibit caveolae–mediated endocytosis by disrupting the actin network at the site of endocytosis, while also inhibiting the enlistment of dynamin II. (26-28) CMPCs were thus transfected with **P6.2** complexes, in the presence and absence of Genistein and chloropromazine. As a reference, cells were also transfected with unformulated (free) Cy3-labelled antagomiR, Lipofectamine 2000 and only Genistein and chlorpromazine. The cells were then analysed by flow cytometry to determine the quantity of cellular uptake (summarized in Figure 6.9).

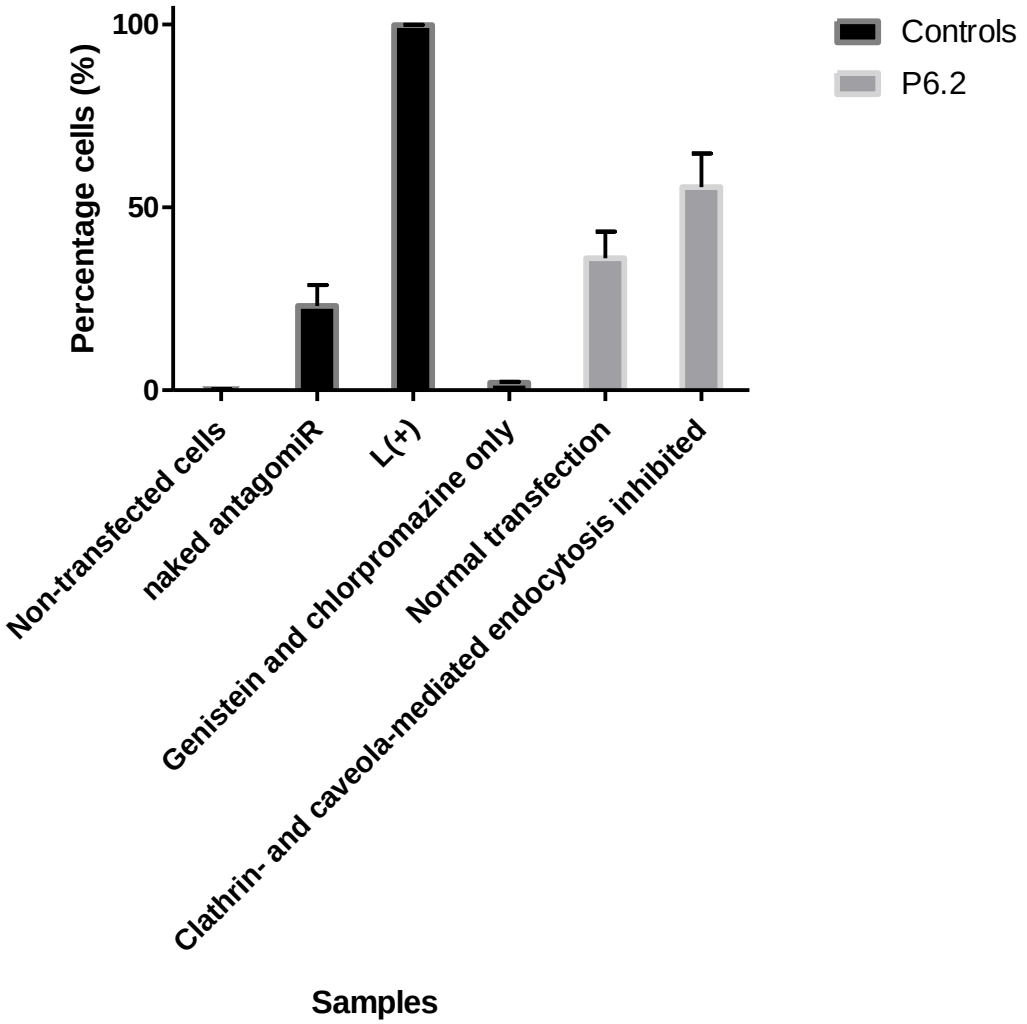

Figure 6.9 Investigation of mechanism of cellular uptake by inhibiting the clathrin- and caveaolae-mediated endocytic pathways compared to uptake for uninhibited cells, determined by flow cytometry. Control cells were treated with unformulated antagomiR, Lipofectamine 2000, endocytic inhibitor (Genistein and chlorpromazine). 3.5 nmol of antagomiR was used for polyplex formation. Results are shown as mean ± SD where n=3

Interestingly, the addition of clathrin– and caveolae–mediated endocytic pathway inhibitors did not hinder the cellular uptake of **P6.2** complexes, but rather enhanced cellular uptake. As Genistein (29) and chloropromazine (30) are known to interact and disrupt the plasma membranes, it is plausible that while they inhibit endocytic pathways, they may also make the membrane more permeable. Another possibility is that the uptake was enhanced due to cross-regulation, (31) *i.e*. by changing the clathrin– and caveolae–mediated endocytic pathway activity, other pathways are enhanced in order to compensate for the cellular change.

The lack of uptake inhibition suggests that the complexes are not taken up via the two main endocytic pathways known to be the predominant pathways for polyplex uptake. (21, 23) Although it does not exclude the possibility that they are taken up by another endocytic pathway, it is more probable that there is a different mechanism by which the complexes enter cells. A possible other hypothesis is that the zwitterionic nature of **P6.2** allow the complexes to pass through the plasma membrane via direct diffusion, without the need for endocytosis, which has been described previously for amphiphathic phospholipid polymers. (32) Additionally, the complexes might penetrate the cell through pore formation, described previously for poly(amidoamine) dendrimers. (33) However, further exploration of the cellular uptake is necessary.

To further investigate the mechanism by which the complexes are taken up, more inhibition pathway experiments were performed. Since active cellular uptake pathways, such as endocytosis and macropinocytosis, require energy (*e.g.* ATRP), a manner in which to see whether cellular uptake is occurring via a passive mechanisms is to perform the cellular uptake studies at 4 ˚C. (34) As indicated in Figure 6.10, no uptake occurred at 4 ˚C which means that cellular uptake of these polyplexes is occurring via an active pathway and not via direct diffusion.

Methyl β-cyclodextrin is a common inhibitor which affects the structure and function of cholesterol-rich membrane domains. (35) In addition, 5-(*N*-ethyl-*N*-isopropyl)amirolide (EIPA) inhibits Na^+/H^+ exchange which in turn lowers the sub-membranous pH causing an inhibition of macropinocytosis. (36) These two chemicals were separately added to the cell medium 30 minutes prior to transfection. In Figure 6.10, it can be seen that the number of cells transfected increased in the presence of methyl β-cyclodextrin. This means cellular uptake of these polyplexes is independent of cholesterol activity. (35) Inversely, the presence of EIPA significantly decreased the cellular uptake which thereby suggests that macropinocytos is important in the cellular uptake of these complexes. (36) As uptake via micropinocytosis still requires escape from the endocytic pathway, it is possible that the ring-open polyplexes are very efficient at escaping macropinosome into the cytoplasm due to their zwitterionic properties. A further transfection was performed where Genistein, chlorpromazine, EIPA and methyl β-cyclodextrin were added to the cell culture medium. In this experiment, the cellular uptake decreased slightly; however, uptake was still observed

(Figure 6.10). All together, these experiments suggest that there is another active pathway by which the polyplexes are transported into the cells, which will require further investigation in the future.

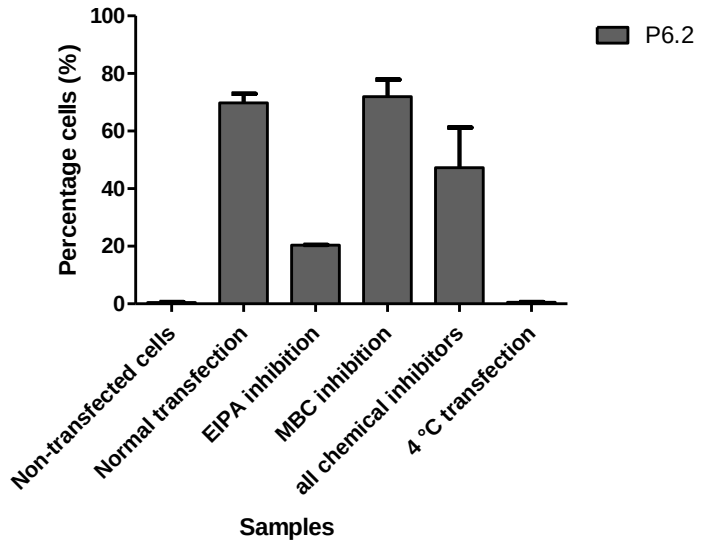

Figure 6.10 Investigation of mechanism of cellular uptake by inhibiting the macropiniocytotic pathway and cholesterol and compared to uptake for uninhibited cells, determined by flow cytometry. Control cells were treated with unformulated antagomiR. 5.5 nmol of antagomiR was used for polyplex formation. Results are shown as mean ± SD where n=3

6.2.7 Gene regulation efficiency

As in Chapter 5, the pMIR-QKI-3'UTR reporter was used to determine the luciferase expression at a cellular level. Again, HEK293 cells were co-transfected with pMIR-QKI-3'UTR reporter and pMIR-Report β-gal control plasmid. In the same way as in Chapter 5, the HEK cells were transfected with pre-miRNA-214 (**pre-mir-214**), a nonsense miRNA (**neg control**), a scrambled miRNA (**scrambled control)**, or no miRNA (**QK-pmiR**). The following day, cells transfected with pre-miRNA-214 were further exposed to **P6.2**– and **P6.3**–anti-miR-214 complexes as well as controls: Lipofectamine 2000-anti-miR-214 (**L(+)**), Lipfectamine 2000-nonsense miRNA (**L(-)**) or PEI-anti-miR-214 (**PEI**). After 48 hours incubation, the luciferase activity was assessed. The results from the luciferase assay are summarized in Figure 6.11. Upon the addition of pre-miRNA-214, the luciferase expression decreased if anti-miRNA-214 is effectively transported into the cell. As expected, the Lipofectamine transported anti-

miR-214 (**L(+)**) almost completely re-established the luciferase expression. A trend in the gene regulation efficiency can be seen for both **P6.2** and **P6.3** complexes, whereby the efficiency increases with an increase in N/P ratio. Furthermore, the ring-opened analogues (**P6.2**) outperform the ring-closed polymer (**P6.3**) which is probably attributed to the amphiphilic nature of the ring-open analogue. This improved transfection also correlated to their proficiency in intracellular delivery, as discussed above. All of the complexes were equivalent to or out-performed the 'gold standard', PEI.

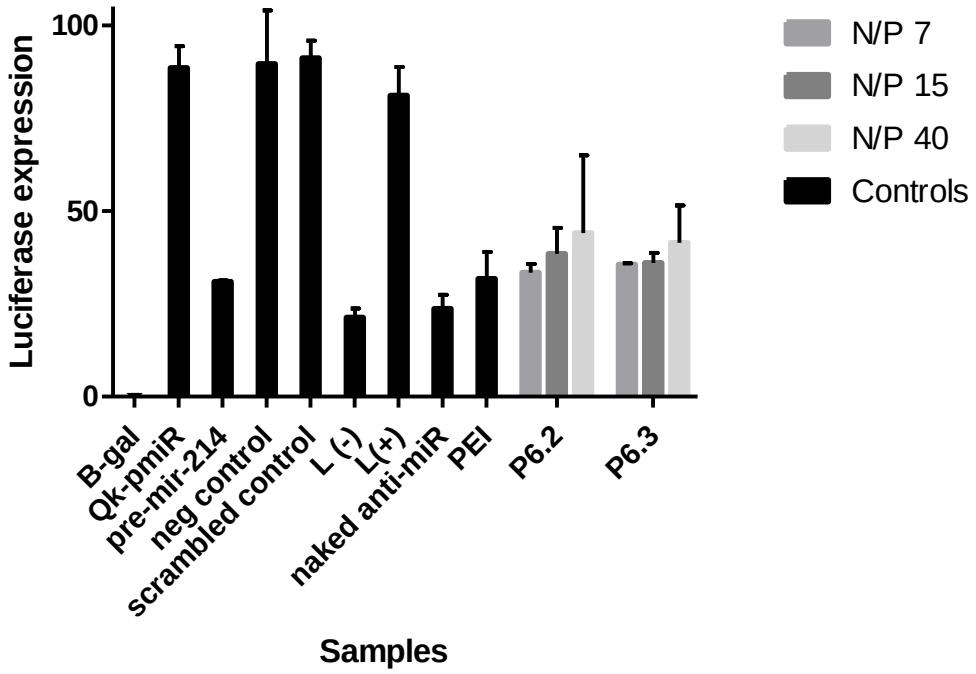

Figure 6.11 Gene silencing activity of P6.2 and P6.3 complexes. Luciferase expression of QKI-3'UTR reporter transfected in HEK 293 cells was determined 48 hours after transfection. Complexes were prepared using 50 nM anti-miRNA-214 concentration. Lipofectamine 2000 and PEI were used as controls. Results shown as mean ±SD for n=3.

6.3 Conclusion

SMA was successfully synthesized using RAFT-mediated polymerization. The polymer was modified in order to obtain ring-open DMAPA-modified SMA and ring-closed DMAP-SMI. These modified polymers were complexed with anti-miRNA-214 and antagomir-214 and they did not cause any cell apoptosis, cell necrosis, erythrocyte aggregation or hemolysis.

The cellular uptake was investigated by flow cytometry and confocal microscopy. Using Lysotracker, it was possible to visualize the transport of the Cy3-labelled antagomiR to the cytoplasm, with the ring-open analogue facilitating a greater concentration of RNA to the cytoplasm. The mechanism of uptake was investigated by inhibiting the caveaolae- and clathrin-mediated endocytic pathways, and it was found that **P6.2** complexes are not transported into the cell through either of these mechanisms. A cellular uptake study at 4 ˚C revealed that the complexes are taken up by active transport. Further inhibition studies using methyl β-cyclodextrin and EIPA indicated that while cholesterol activity does not impact uptake, the inhibition of Na^+/H^+ exchange, important in macropinocytosis, does affect cellular uptake. This indicates that the ring-open polyplexes are efficient at escaping the macropinosome/lysosome. However, further investigation regarding the uptake mechanism is necessary, as cellular uptake was still observed upon the combined inhibition of all the active pathways described above.

The gene regulation efficiency was then investigated via a luciferase experiment. Although the **P6.2** and **P6.3** complexes were not as efficient at restoring luciferase expression as Lipofectamine 2000, they performed better than or equal to PEI polyplexes.

These SMA analogues represent a novel, zwitterionic gene delivery vector. Future studies will include investigating the effect of molecular weight, polymer structure, modifications and copolymerization on RNA binding efficiency, cellular uptake and gene regulation efficiency. Furthermore, in the near future, *in vivo* studies will be conducted in order to assess the stability, biodistribution and efficacy of these gene therapy vectors.

6.4 Supplementary

6.4.1 General experimental details

Unless stated otherwise, all of the chemicals used were purchased from commercial sources and used without further purification. 2,2'-Azobis(isobutyronitrile) (AIBN) (Riedel-de Haën) was recrystallized from methanol. Subsequently it was dried under vacuum at room temperature. Solvents and monomers were dried and distilled before use, unless stated otherwise. The progress of the reactions were monitored using thin layer chromatography (TLC) with Machery-Nagel Silica gel 60 plates with a UV 254 fluorescent indicator.

^{1}H and ^{13}C NMR spectra were measured on a Varian VXR-Unity (400 MHz) spectrometer and spectra were analyzed using MestreNova 9.0 and chemical shifts were reported in parts-per-million (ppm) which was referenced to the residual solvent protons. The samples were prepared in deuterated solvents (Cambridge Isotope Labs).

FT-IR spectroscopy was measured using Thermo Nicolet iS10 FT-IR spectrometer, and data was acquired using Omnic software (version 6.0a). 32 scans were performed per sample, between 650 and 4100 cm^{-1}.

Size exclusion chromatography (SEC) was measured on a Shamdzu LC-10AT isocratic pump, a column fitted with a PSS guard column (50 x8 mm) in series with three PPS GRAM columns (300 x 8 mm, 10 µm, 2 x 3000 Å and 1 x 100 Å) kept at a constant temperature of 40 °C, a Waters 717+ auto-sampler, a Waters 2487 dual wavelength UV detector and a Waters 2414 differential refractive index (DRI) detector. The samples were measured in dimethylacetamide (DMAc) as the eluent stabilized with 0.05% BHT (*w*/*v*) and 0.03% LiCl (*w*/*v*), at a flow rate of 1 $mL.min^{-1}$. Sample preparation included filtering the sample solutions through a 0.45 µm GHP filter to remove impurities. The results were calibrated against PMMA standards (Polymer Laboratories) ranging from 690 to 1.2 x 10^{6} $g.mol^{-1}$. Data acquisition was performed using Millenium[32] software, v4.

ζ-potential was measured on Malvern Zetasizer Nano Z. The samples were exposed to 3 V maz, and 3 measurement of 100 scans were obtained per sample. Complex size distribution was measured using nanoparticle tracking analysis (NTA) with a Nanosight NS500 nanoparticle analyser (Malvern Instruments) which was equipped with a 405 nm laser. The

camera level was set to 16 and all post-acquisition settings were set to automatic, except for the detection threshold, which was set at 5. Three 30 s videos were recorder per sample using the script control function.

Flow cytometry was carried out on a CytoFLEX Flow Cytometer (Beckman Coulter). Data was analyzed using Kaluza Analysis 1.5a.

6.4.2 Experimental methods

*Butyl 1-phenylethyl trithiocarbonate synthesis (**R6.1**)*

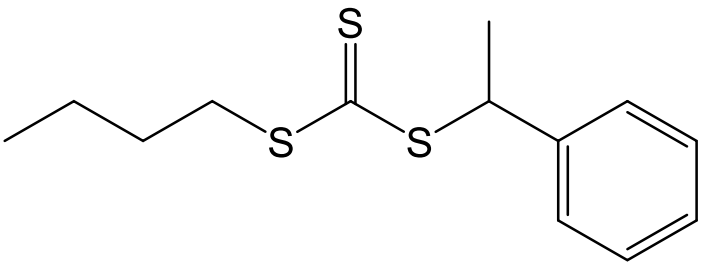

Synthesized according to a protocol described in literature. (17) In short, triethyl amine (11.2 g, 111 mmol) was added dropwise to a solution of 1-butanethiol (5.00 g, 55.5 mmol) and carbon disulfide (8.45 g, 111 mmol) in chloroform (35 mL) with stirring at rt. The solution was stirred for 3 h at rt. (1-Bromoethyl)-benzene (10.1 g, 54.4 mmol) was added dropwise to the solution and the mixture was stirred for 12 h at rt. Mixture was diluted with with chloroform (20 mL) and washed with water (3 x 50 mL), 2 M H_2SO_4 (aq) (3 x 50 mL), water (3 x 50 mL) and brine (3 x 50 mL). Organic layer was dried over anhydrous $MgSO_4$, filtered and concentrated to give **R6.1** as a yellow oil (14.39 g, 98%). The ^{1}H NMR spectrum corresponds well to that in literature. (17)

^{1}H NMR (300 MHz, Benzene-d_6) δ 7.20 – 7.11 (m, 3H), 7.06 – 6.91 (m, 2H), 5.41 (q, J = 7.1 Hz, 1H), 3.08 (t, J = 7.2 Hz, 2H), 1.52 (d, J = 7.1 Hz, 3H), 1.37 – 1.27 (m, 2H), 1.14 – 1.00 (m, 2H) 0.64 (t, J = 7.2 Hz, 3H).

*General co-polymerization of styrene and maleic anhydride (**P6.1**)*

Styrene (2.00 g, 0.0192 mol), maleic anhydride (1.9 g, 0.019 mol), **R6.1** (0.224 g, 0.821 mmol) and AIBN (0.027 g, 0.16 mmol) were accurately weighed off and transferred to a Schlenk flask along with MEK (5 mL) and a magnetic stirrer bar. The solution was thoroughly

degassed with argon gas for one hour prior to the start of the reaction. The flask was immersed in a preheated oil bath at 70 °C for 24 hours and **P6.1** was retrieved by precipitation in diethyl ether (200 mL). **P6.1** was allowed to dry in a vacuum oven at room temperature for 24 hours.

FT-IR 3044 (C-H, aromatic), 2928 (C-H, aliphatic), 1858 (C=O), 1774 (C=O), 1495 (C=C, aromatic), 1452 (C=C, aromatic), 1220 (C-O-C, cyclo-anhydride), 1081 (C-O-C, cyclo-anhydride), 959 (C-O-C, cyclo-anhydride), 903 (C-O-C, cyclo-anhydride), 700 (C-H, aromatic)

*Ring-opened DMAPA-modified poly(styrene-co-maleic anhydride) (**P6.2**)*

For functionalization of the polymers with DMAPA, **P6.1** (2 g) was dissolved in a minimum amount of DMF (3 mL). DMAPA (1.5 eq. to the maleic anhydride incorporated in the polymer backbone) was added dropwise to the polymer solution. **P6.2** was retrieved by precipitation in Et_2O (150 mL). **P6.2** was dried in a vacuum oven at room temperature for 24 hours.

FT-IR 3664-3126 (O-H, carboxylic acid), 3126-2814 ((C-H, -N-$(CH_3)_2$), 1659 (C=O, carboxylic acid), 1559 (NH), 1356 (NH), 700 (C-H, aromatic)

*Ring-closed DMAPA-modified poly(styrene-co-maleimide) (**P6.3**)*

P6.2 (1.0 g) was dissolved in DMF (20 mL) and heated to 120 °C for 24 hours. After cooling, it was dialysed against a solution of water and methanol (1:1) for 2 days and a further 2 days against 100% water. **P6.3** (1.3 g) was isolated by freeze-drying for 24 hours.

FT-IR 2996-2707 ((C-H, -N-$(CH_3)_2$), 1769 (C=O, imide), 1690 (C=O, imide), 1149 (CN), 700 (C-H, aromatic)

RNA sequences

hsa-miR-214 ACAGCAGGCACAGACAGGCAGU

antagomiR-214: (Cy3)-5'-ACTGCCTGTCTGTGCCTGCTGT-3'-Cholesterol

Complex synthesis

P6.2/**P6.3** were dissolved in sodium ascorbate buffer (pH 4.2) (40 mg/mL) and mixed with anti-miRNA-214 (4 mg/mL) at various N/P ratios. The concentration of anti-miRNA was kept constant, but concentration varied depending on the experiment in question. The polymer-anti-miRNA solution was incubated at 37 °C for 1 hour. Complexes were used immediately.

Complex characterization

Complexes containing 550 pmol Cy3-labelled antagomiR-214 with a final volume of 25 µL were prepared for agarose gel retardation. 6 µL 6 x loading dye was added to the samples prior to loading. 2% agarose gel was prepared and the electrophoresis was performed at 140 V for 45 min. The gels were then imaged using the Typhoon 9410 Variable Mode Imager [Amersham, Biosciences).

Cell culture

Human embryonic kidney 293 cells (HEK 293) were cultured in Dulbecco's modified Eagle's medium (DMEM) (Introgen, Carlsbad, CA) supplemented with 10% fetal bovine serum (FBS) and 10% penicillin streptomycin solution (P/S). Fetal cardiomyocyte progenitor cells (CMPCs) were cultivated on 0.1% gelatin in SP++ medium (1 part endothelial cell growth medium-2 (EGM-2), 3 parts Medium199 (M199) supplemented with 1% P/S, 1% non-essential amino acids (NEAA) and 10% FBS). Human microvascular endothelial cells (HMECs) were cultivated on 0.1% gelatin in EGM-2.

Cellular uptake (flow cytometry)

CMPCs were seeded in 12 well plates and incubated for 24 hours. Medium was removed and replaced with 500 µL OptiMem. Cells were transfected with complexes at various N/P ratios formulated with 1.5 µM Cy3 labelled antagomiR-214. After 4 hours, the OptiMem was replaced with SP++ medium and cells were incubated for 48 hours. Cells were washed twice with PBS buffer to remove non-internalized polyplexes. Cells were harvested using Trypsin and centrifuged (350·g, 5 min) and supernatant was aspirated. The cells were resuspended in 500 µL PBS buffer containing 10% FBS. Again cells were centrifuged (350·g, 5 min) and supernatant was aspirated. The cells were resuspended in 500 µL PBS and after a final

centrifugation step, the cells were resuspended in PBS buffer with 2% FBS (FACS medium). The samples were then analysed on the CytoFLEX flow cytometer (Beckman Coulter). Data was analysed using Kaluza Analysis 1.5a.

In order to inhibit endocytosis, 10 µM final concentration chlorpromazine, 200 µM final concentration Genistein, 2 mM or 200 µM methyl β-cyclodextrin or 10 µM EIPA were added to the cell medium 30 min prior to transfection. Quantifying cellular uptake by flow cytometry was carried out in the manner described above.

Cytotoxicity studies

CMPCs were seeded in 12 well plates and incubated for 24 hours. Medium was removed and replaced with 500 µL OptiMem. Cells were transfected with complexes at various N/P ratios formulated with 5.5 µM anti-miRNA-214. After 4 hours, the OptiMem was replaced with SP++ medium and cells were incubated for 48 hours. APC Annexin V Apoptosis Detection Kit with 7-AAD purchased from BioLegend was used for cytotoxicity assay. Protocol was followed according to manufacturer. The cells were analysed by flow cytometry on CytoFLEX Flow Cytometer (Beckman Coulter) directly after staining. Data was analysed using Kaluza Analysis 1.5a.

Erythrocyte aggregation and hemolysis

The method for investigating erythrocyte aggregation and hemolysis was modified from literature. (3) In short, erythrocytes were obtained from 5 mL whole human blood by multiple centrifugation steps (1000·g, 10 min, 4 °C), followed by aspiration of supernatant and resuspension in PBS buffer until the supernatant was clear, where approximately 4 steps were required. 100 µL of the pellet was resuspended in 4 mL PBS. 160 µL of the final erythrocyte suspension was added to 40 µL polyplex solution with an anti-miRNA concentration of 1 µM. Triton X-100 (1%) in PBS and HEPES (pH 7.2) were used as reference samples of 100% lysis and 0% lysis respectively. Samples were incubated for 1 hour at 37 °C. After a further centrifugation step (1000·g, 10 min), the absorbance at 550 nm was measured of 150 µL of the supernatant to ascertain the degree of hemolysis. The pellet was resuspended in 50 µL PBS and observed under the microscope to evaluate the degree of erythrocyte aggregation.

Confocal microscopy

HMECs were seeded in an 8-well flow chamber and incubated for 24 hours. The medium was aspirated and replaced with 150 µL OptiMem. Cells were transfected with complexes (N/P 40) with a final antagomiR-214 concentration of 3 µM. After 4 hours, the OptiMem was replaced by EGM-2 medium and the cells were incubated for 48 hours. The medium was then replaced by medium containing 1:10000 Lysotracker Red and incubated for 2 hours. The medium was then replaced with medium containing Hoechst solution (1 µg/mL) and the cells were incubated for 10 minutes. The medium was aspirated and the cells were washed twice with EGM-2 medium. 150 µL of EGM-2 was added to the wells and the cells were imaged on a ZEISS LSM 700 confocal microscope (Carl Zeiss).

Luciferase Assay

The method was modified from literature. (37) The conserved miRNA-214-binding sequences in the QKI 3' untranslated region (UTR) were cloned into pMIR-Reporter vector (Ambion). HEK293 cells were seeded in 48-well plates and incubated for 24 hours. The medium was replaced with OptiMem. The cells were co-transfected with 200 ng of pMIR-Reporter-QKI-3'UTR Luciferase vector and pMIR-Report β-gal control plasmid. The latter was used to assess the transfection efficiency. In addition, 50 nM pre-miRNA-214, ctrl-miRNA or scrambled miRNA were also transfected. The transfection was carried out by using Lipofectamine 2000 (Invitrogen). After 4 hours, the medium was replaced with DMEM supplemented with 10% FBS. After 24 hours of incubation, the medium was replaced with OptiMem, and cells were transfected with complexes containing 50 nM anti-miRNA-214 at different N/P ratios, or Lipofectamine with either anti-miRNA-214 or ctrl-miRNA, PEI-anti-miRNA-214 polyplexes or naked anti-miRNA-214. After 4 hours, the medium was replaced. The cells were incubated for 48 hours. They were then washed with PBS and lysed with 150 µL 1 x Luciferase lysis buffer. The cells were incubated for 15 minutes. 10 µL of the supernatant was transferred to a white 96-well plate, and the luciferase activity was assessed with Luciferase Assay System (Promega). 25 µL of the cell lysis supernatant was transferred to a 96-well plate and 25 µL β-galactosidase Enzyme Assay buffer. After incubation at 37 °C for 1 hour, the absorbance at 405 nm and 570 nm was measured.

6.5 References

1. Cao Z, Yu Q, Xue H, Cheng G, Jiang S. Nanoparticles for drug delivery prepared from amphiphilic PLGA zwitterionic block copolymers with sharp contrast in polarity between two blocks. Angew Chem Int Ed. 2010;49(22):3771-6.
2. Lin X, Ishihara K. Water-soluble polymers bearing phosphorylcholine group and other zwitterionic groups for carrying DNA derivatives. J Biomater Sci Polym Ed. 2014;25(14-15):1461-78.
3. Vader P, van der Aa LJ, Engbersen JFJ, Storm G, Schiffelers RM. Physicochemical and biological evaluation of siRNA polyplexes based on PEGylated poly(amido amine)s. Pharm Res. 2012;29(2):352-61.
4. Hu GH, Lindt JT. Amidification of poly(styrene-co-maleic anhydride) with amines in tetrahydrofuran solution: A kinetic study. Polym Bull. 1992;29(3):357-63.
5. Rietman EA, Kaplan ML. Single-ion conductivity in comblike polymers. J Polym Sci Part C: Polym Lett. 1990;28(6):187-91.
6. Dérand H, Wesslén B. Synthesis and characterization of anionic graft copolymers containing poly(ethylene oxide) grafts. J Polym Sci Part A: Polym Chem. 1995;33(3):571-9.
7. Wittgren B, Wahlund K-G, Dérand H, Wesslén B. Aggregation behavior of an amphiphilic graft copolymer in aqueous medium studied by asymmetrical flow field-flow fractionation. Macromolecules. 1996;29(1):268-76.
8. Dérand H, Wesslén B, Wittgren B, Wahlund K-G. Poly(ethylene glycol) graft copolymers containing carboxylic acid groups: aggregation and viscometric properties in aqueous solution. Macromolecules. 1996;29(27):8770-5.
9. Aji Alex MR, Nagpal N, Kulshreshtha R, Koul V. Synthesis and evaluation of cationically modified poly(styrene-alt-maleic anhydride) nanocarriers for intracellular gene delivery. RSC Adv. 2015;5(28):21931-44.
10. Lackey CA, Press OW, Hoffman AS, Stayton PS. A biomimetic pH-responsive polymer directs endosomal release and intracellular delivery of an endocytosed antibody complex. Bioconj Chem. 2002;13(5):996-1001.

11. Richard R, Schwarz M, Chan K, Teigen N, Boden M. Controlled delivery of paclitaxel from stent coatings using novel styrene maleic anhydride copolymer formulations. J Biomed Mater Res Part A. 2009;90A(2):522-32.
12. Bacu E, Chitanu GC, Couture A, Grandclaudon P, Singurel G, Carpov A. Potential drug delivery systems from maleic anhydride copolymers and phenothiazine derivatives. Eur Polym J. 2002;38(8):1509-13.
13. Saisyo A, Nakamura H, Fang J, Tsukigawa K, Greish K, Furukawa H, Maeda H. pH-sensitive polymeric cisplatin-ion complex with styrene-maleic acid copolymer exhibits tumor-selective drug delivery and antitumor activity as a result of the enhanced permeability and retention effect. Colloids Surf B Biointerfaces. 2016;138(Supplement C):128-37.
14. Khazaei A, Saednia S, Saien J, Kazem-Rostami M, Sadeghpour M, Borazjani MK, Abbasi F. Grafting amino drugs to poly(styrene-alt-maleic anhydride) as a potential method for drug release. J Braz Chem Soc. 2013;24:1109-15.
15. Henry SM, El-Sayed MEH, Pirie CM, Hoffman AS, Stayton PS. pH-responsive poly(styrene-alt-maleic anhydride) alkylamide copolymers for intracellular drug delivery. Biomacromolecules. 2006;7(8):2407-14.
16. Duan X, Xiao J, Yin Q, Zhang Z, Mao S, Li Y. Amphiphilic graft copolymer based on poly(styrene-co-maleic anhydride) with low molecular weight polyethylenimine for efficient gene delivery. Int J Nanomedicine. 2012;7:4961-72.
17. Postma A, Davis TP, Evans RA, Li G, Moad G, O'Shea MS. Synthesis of well-defined polystyrene with primary amine end groups through the use of phthalimido-functional RAFT agents. Macromolecules. 2006;39(16):5293-306.
18. Bshena O, Klumperman B. Synthesis of permanent non-leaching antimicrobial polymer nanofibers (PhD). Stellenbosch: Stellenbosch University; 2012.
19. Bshena O, Klumperman B. Synthesis of Permanent Non-Leaching Antimicrobial Polymer Nanofibers. Stellenbosch: Stellenbosch University; 2012.
20. Vader P, van der Aa LJ, Engbersen JFJ, Storm G, Schiffelers RM. A method for quantifying cellular uptake of fluorescently labeled siRNA. J Control Release. 2010;148(1):106-9.

21. Liang W, Lam JKW. Endosomal escape pathways for non-viral nucleic acid delivery systems. In: Ceresa B, editor. Molecular regulation of endocytosis. Rijeka: InTech; 2012.

22. Dominska M, Dykxhoorn DM. Breaking down the barriers: siRNA delivery and endosome escape. J Cell Sci. 2010;123(8):1183-9.

23. Rejman J, Bragonzi A, Conese M. Role of clathrin- and caveolae-mediated endocytosis in gene transfer mediated by lipo- and polyplexes. Mol Ther. 2005;12(3):468-74.

24. Vercauteren D, Vandenbroucke RE, Jones AT, Rejman J, Demeester J, De Smedt SC, Sanders NN, Braeckmans K. The use of inhibitors to study endocytic pathways of gene carriers: optimization and pitfalls. Mol Ther. 2010;18(3):561-9.

25. Ivanov AI. Pharmacological inhibition of endocytic pathways: Is it specific enough to be useful? In: Ivanov AI, editor. Exocytosis and endocytosis. Totowa: Humana Press; 2008. p. 15-33.

26. Thors L, Alajakku K, Fowler CJ. The ‘specific' tyrosine kinase inhibitor genistein inhibits the enzymic hydrolysis of anandamide: implications for anandamide uptake. Br J Pharmacol. 2007;150(7):951-60.

27. Nabi IR, Le PU. Caveolae/raft-dependent endocytosis. J Cell Biol. 2003;161(4):673-7.

28. Parton RG, Joggerst B, Simons K. Regulated internalization of caveolae. J Cell Biol. 1994;127(5):1199-215.

29. Pawlikowska-Pawlęga B, Misiak LE, Jarosz-Wilkołazka A, Zarzyka B, Paduch R, Gawron A, Gruszecki WI. Biophysical characterization of genistein–membrane interaction and its correlation with biological effect on cells — The case of EYPC liposomes and human erythrocyte membranes. Biochim Biophys Acta. 2014;1838(8):2127-38.

30. Eisenberg S, Giehl K, Henis YI, Ehrlich M. Differential interference of chlorpromazine with the membrane interactions of oncogenic K-Ras and its effects on cell growth. J Biol Chem. 2008;283:27279-88.

31. Mayor S, Pagano RE. Pathways of clathrin-independent endocytosis. Nat Rev Mol Cell Biol. 2007;8:603-12.

32. Goda T, Goto Y, Ishihara K. Cell-penetrating macromolecules: Direct penetration of amphipathic phospholipid polymers across plasma membrane of living cells. Biomaterials. 2010;31(8):2380-7.

33. Hong S, Bielinska AU, Mecke A, Keszler B, Beals JL, Shi X, Balogh L, Orr BG, Baker JR, Banaszak Holl MM. Interaction of poly(amidoamine) dendrimers with supported lipid bilayers and cells: Hole formation and the relation to transport. Bioconj Chem. 2004;15(4):774-82.

34. dos Santos T, Varela J, Lynch I, Salvati A, Dawson KA. Effects of transport inhibitors on the cellular uptake of carboxylated polystyrene nanoparticles in different cell lines. PLoS One. 2011;6(9):e24438:1-10.

35. Ivanov AI. Pharmacological inhibition of endocytic pathways: is it specific enough to be useful? Methods Mol Biol. 2008;440:15-33.

36. Koivusalo M, Welch C, Hayashi H, Scott CC, Kim M, Alexander T, Touret N, Hahn KM, Grinstein S. Amiloride inhibits macropinocytosis by lowering submembranous pH and preventing Rac1 and Cdc42 signaling. J Cell Biol. 2010;188:547-63.

37. van Mil A, Grundmann S, Goumans M-J, Lei Z, Oerlemans MI, Jaksani S, Doevendans PA, Sluijter JPG. MicroRNA-214 inhibits angiogenesis by targeting Quaking and reducing angiogenic growth factor release. Cardiovasc Res. 2012;93(4):655-65.

Chapter 7 Epilogue

7.1 General conclusions

This dissertation focused on the production of non-viral, polymeric gene delivery systems. A facile method of producing α,ω-heterotelechelic poly(*N*-vinylpyrrolidone) (PVP) for the incorporation in such systems was described. Thereafter, two types of delivery systems were synthesized and *in vitro* studies were conducted in order to assess their success within the gene delivery application.

In Chapter 1, a general introduction was provided to the pathway a cationic delivery system follows in order to deliver its payload to the cell. This discussion included the hurdles that delivery systems must overcome in order to successfully encourage gene regulation. Thereafter, Chapter 2 gave a more in depth discussion of reported polymeric delivery systems, as well as their advantages and disadvantages. It elaborated on the obstacles that have been overcome, especially with the advent of reversible-deactivation radical polymerization, and those which still need to be addressed, *e.g.* cytotoxicity, endosomal escape and cytoplasmic release.

In Chapter 3, a new method for synthesizing α,ω-heterotelechelic PVP was described. Using this method, PVP with high chain-end fidelity was obtained, which is superior for application in biological systems since a greater percentage of the polymer is able to be functionalized. Moreover, the synthetic technique allows for RAFT-agents with more reactive leaving groups than previously reported, leading to easier post-polymerization modification. An added benefit of the system is that *N*VP can be polymerized without prior purification. Different examples of chain end modifications were shown, including the inclusion of aldehyde moieties.

Chapter 4 described the development of a diblock system containing a hydrophobic copolymer, either p(DMAEMA-*co*-BMA) or p(DMAEA-*co*-BMA), and hydrophilic PVP linked via an acid-labile linker to facilitate endosomal escape. The PVP was synthesized using the method developed in Chapter 3 facilitated by a xanthate RAFT agent with a linear acetal leaving group. PVP of approximately 4600 $g{\cdot}mol^{-1}$ ($Đ$ = 1.2) was obtained. Using a one-pot post-polymerization functionalization, the PVP end-groups were converted into an aldehyde functional group, for further modification with a RGD or cardiovascular targeting ligand and

amino-fluorescein, and a thiol end-group, for later conjugation to the hydrophobic polymer via a Michael addition.

The p(DMAE(M)A-*co*-BMA) blocks were synthesized via RAFT-mediated polymerization using 2-hydroxyethyl 4-{[(butylthio)carbonothioyl]thio}-4-cyanopentanoate as the RAFT-agent. Polymers of approximately 16500 $g \cdot mol^{-1}$ ($Đ$ = 1.1) were obtained for both copolymers, and the trithiocarbonate was removed post-polymerization. Subsequently, the hydroxyl α-chain end was reacted with acrylic acid via a 1-ethyl-3-(-3-dimethylaminopropyl) carbodiimide hydrochloride (EDC) coupling reaction, supplying the final acrylate end group for the Michael addition with PVP. After the Michael addition, the conjugated diblocks were characterized by size exclusion chromatography.

Chapter 5 explored the use of the conjugates synthesized in Chapter 4 as gene delivery vehicles. The complexation efficiency of the conjugates with Cy3-labelled RNA was investigated by means of agarose gel retardation, and it was seen that complexation occurred at N/P ratios as low as 3. The complex size decreased with increasing N/P ratio, and they were shown to be stable in the presence of 20% fetal bovine serum. The p(DMAEMA-*co*-BMA) containing blocks caused less hemolysis than the p(DMAEA-*co*-BMA) containing blocks, although both remained at acceptable levels of hemolysis at N/P ratio of 20 and below, except **P4.15**. No significant cytotoxicity was observed for cardiomyocyte progenitor cells after transfection for any of the blocks, and their cellular uptake was seen to be directly proportional to the N/P ratio. Furthermore, it was seen that the p(DMAEA-*co*-BMA) was taken up slightly more than the p(DMAEMA-*co*-BMA), and the presence of the cardiovascular targeting ligand facilitated the highest uptake. Luciferase expression was seen to be restored by the diblock conjugates more efficiently than by PEI-polyplexes, although not as efficiently as by Lipofectamine 2000. P(DMAEA-*co*-BMA) without targeting ligand was the most effective polyplex at a concentration of 50 nM anti-miRNA-214, however, when this concentration was doubled, the p(DMAEMA-*co*-BMA) polyplexes showed higher efficiency. These results are contradictory to those previously reported for comparative studies between pDMAEMA and pDMAEA polyplex systems. (1) A hypothesis was drawn as a result of the observed results that the presence of targeting ligand and/or PVP negatively affects the gene regulation efficiency of pDMAEA polyplexes. However, further investigation would be necessary in order to endorse this hypothesis.

Chapter 6 investigated the synthesis and use of ring-open and ring-closed 3-(*N*,*N*-dimethylamino)propyl-1-amine (DMAPA)-modified poly(styrene-*co*-maleic anhydride) (SMA) as gene delivery vectors. SMA was synthesized using butyl 1-phenylethyl trithiocarbonate as a RAFT-agent, yielding polymer with a number average molecular weight of approximately 12800 g·mol^{-1} ($Đ$ = 1.1). The SMA was functionalized with DMAPA using an amidation reaction, and a portion of this was thermally ring-closed. The DMAPA modification, ring-opened and ring-closed structures were confirmed via FT-IR analysis. The complexation efficiency was assessed via agarose gel retardation, and it was seen that the ring-closed analogue was more efficiently able to complex the RNAs; however, both polymers did not show as high complexation efficiency as the diblock conjugate system described in Chapter 5. The toxicity profiles of both analogues were pristine, with no significant cytotoxicity, hemolysis or erythrocyte aggregation detected at any N/P ratio. Although negligible, the ring-closed analogue caused slightly higher hemolysis than the ring-open version. This is probably due to the slightly higher cationic charge on the ring-closed polymer, since the positive charge is offset by the zwitterionic nature of the ring-opened polymer. The cellular uptake was measured by flow cytometry, and confocal microscopy was used to track whether the polymers were delivering the Cy3-labelled RNA to the cytoplasm or whether it was getting trapped within the endosome. It was seen that both analogues delivered the RNA to the cytoplasm, although the ring-open polymer was more efficient in this. A question arose about the mode through which the ring-open analogue was being taken up by the cells, since the RNA's fluorescent signal was not overlapping with the Lysotracker signal, *i.e*. the RNA was not found within the endosome or lysosome to any significant extent. Therefore, some experiments were conducted in which clathrin- and caveolae-mediated endocytosis were inhibited. Cellular uptake was still observed, and thus, it was concluded that the usual route for polyplexes to be taken up by the cells, clathrin- and caveaolae-mediated endocytosis, were not employed in the case of the ring-open SMA derivative. Further experiments revealed that the polyplexes are taken up by active transport. While it was observed that the cellular uptake is independent of the cholesterol activity of cell membranes, transfection in the presence of 5-(*N*-ethyl-*N*-isopropyl)amirolide (EIPA) revealed that the polyplexes are somewhat transported via macropinocytosis. However, since significant uptake was still present after inhibition of all of the abovementioned

pathways, further investigation is necessary to elucidate the exact mechanism employed in cellular uptake of these polyplexes.

The ring-opened (**P6.2**) and ring-closed (**P6.3**) polymer complexes were then tested for their efficiency in regulating luciferase expression. A linear relationship was observed between the regulation efficiency and the N/P ratio. Furthermore, even though the ring-closed construct (**P6.3**) was more efficiently able to condense the RNAs, the ring-opened polymer showed higher regulation efficieny. This was correlated to the zwitterionic nature of the ring-open analogue (**P6.2**), which means that more of the polymer is delivered to the cytoplasm than with the ring-closed polycation. Therefore, it is hypothesized that the different mechanism of cellular uptake is the driving factor for enhanced regulation.

When comparing the two different gene delivery systems that were investigated in this dissertation, it is prudent to keep in mind that results obtain in *in vitro* studies do not directly translate to *in vivo* studies. Systems that have shown high gene regulation within the *in vitro* setting have gone on to show no results *in vivo*, and vice versa. That said, the cytotoxicity profile of the SMA-derivatives shows great promise. Although the pDMAE(M)A systems described in Chapter 5 do not cause worrisome levels of toxicity, the SMA complexes are far superior in this aspect, especially at high N/P ratios.
Furthermore, the mode of uptake for the ring-open SMA system is very exciting, since it is possible that the obstacle of endosomal escape could be circumvented. That said, the RNA complexation efficiency and cellular uptake of the diblock conjugate systems was far superior to that of the SMA derivatives. This is most probably due to the higher charge contained within the pDMAE(M)A systems. It is possible that this could be improved in the SMA systems by increasing the positive charge. This will be discussed further in Section 7.2.

7.2 Future perspectives

Ethical clearance has been obtained for *in vivo* studies on mice for both gene delivery systems reported in this dissertation, and these studies will begin shortly.

It would be worth-while studying the impact that the molecular weight of PVP has on the diblock conjugate system. It is hypothesized that this, like PEG, might have a threshold point

between improving the toxicity profile and too much shielding causing a decrease in cellular uptake. Furthermore, it would be interesting to study the conjugation of PVP to other hydrophobic polycations, via acid-labile linkers. PVPylation has not been extensively investigated in gene therapy, but it holds potential for an improved delivery system compared to poly(ethylene glycol) (PEG) because of its biocompatibility and the ease with which it can be made while maintaining complete control over molecular weight, molecular weight distribution, architecture and end-group functionality.

As metioned above, SMA has not been extensively studied as a polymer for gene delivery. Therefore, it would be of interest to study the impact that the molecular weight and architecture has on its gene delivery application. Furthermore, amidation with different cationic compounds would be interesting, including the use of moieties that can be decationized in a similar manner to DMAEA. It would also be on point to investigate the effect of co-amidation with different side chains and studying the use of different percentages of side-chain funtionalization.

The incorporation of both hydrophobic blocks, *e.g*. styrene, and hydrophilic blocks, such as PVP, would be interesting. Recently in our group, sequence-controlled styrene-styrene-maleic anhydride polymers have been synthesized successfully. A study investigating the different effect that such a hydrophobic block would have on gene delivery compared to more random styrene block lengths would be interesting. For example, as the sequence controlled polymer still contains some maleic anhydride, the hydrophobic block would retain some of the zwitterionic properties. While the hydrophobic character would enable amphiphilic self-assembly, the retained zwitterionic character may act to enhance gene delivery, compared to a homopolymeric styrene block.

Due to the exciting results with regards to the mechanism of uptake of the ring-open SMA derivative, it would also be of utmost importance to conduct a full study on the uptake mechanism. Furthermore, it would be interesting to also see what effect the inclusion of hydrophobic and hydrophilic blocks would have on this mechanism.

Within our group, SMA derived particles have been synthesized via surfactant-free dispersion polymerization with divinylbenzene as the crosslinking monomer. It might be of interest to exchange the divinyl benzene with a reducible, disulphide crosslinker, such as the

one used within Zentel's group. (2) These crosslinkers contain amines for RNA complexation. The use of such SMA-derived particles is interesting because they are potentially taken up by cells via a non-endocytic mechanism. Therefore, this would, like the ring-open SMA-derivative, render them able to bypass the obstacles associated with endosomal escape. The reducible bond would allow the system to release the RNAs within the cytoplasm for gene regulation to take place.

7.3 References

1. Nelson CE, Kintzing JR, Hanna A, Shannon JM, Gupta MK, Duvall CL. Balancing cationic and hydrophobic content of PEGylated siRNA polyplexes enhances endosome escape, stability, blood circulation time, and bioactivity in vivo. ACS Nano. 2013;7(10):8870-80.
2. Leber N, Kaps L, Aslam M, Schupp J, Brose A, Schäffel D, Fischer K, Diken M, Strand D, Koynov K, Tuettenberg A, Nuhn L, Zentel R, Schuppan D. SiRNA-mediated in vivo gene knockdown by acid-degradable cationic nanohydrogel particles. J Control Release. 2017;248(Supplement C):10-23.